Affinity-based profiling of the adenosine receptors

Beerkens, B.L.H.

Cover design and Thesis lay-out: Bert Beerkens and Ridderprint

Printing: Ridderprint | www.ridderprint.nl

ISBN: 978-94-6483-381-2

Affinity-Based Profiling of the Adenosine Receptors

Proefschrift

ter verkrijging van

de graad van doctor aan de Universiteit Leiden,

op gezag van rector magnificus prof.dr.ir. H. Bijl,

volgens besluit van het college voor promoties

te verdedigen op donderdag 9 november 2023

klokke 13:45 uur

door

Bert Leonardus Hendrikus Beerkens

geboren te Venray, Nederland

in 1993

Promotor: Prof. dr. A.P. IJzerman

Co-promotor: Dr. D. van der Es

Promotiecommissie:

Prof. dr. H. Irth

Prof. dr. E.C.M. de Lange

Prof. dr. M. van der Stelt

Dr. K.A. Jacobson (National Institutes of Health, Bethesda, USA)

Dr. K.M. Bonger (Radboud University Nijmegen)

The research described in this thesis was performed at the division of drug discovery and safety of the Leiden Academic Centre for Drug Research (LACDR), Leiden University (Leiden, The Netherlands).

Table of Contents

Chapter 1

General Introduction

Caffeine and the Adenosine Receptors

Caffeine is a substance present in coffee, tea and chocolate, among other food and beverages, consumed widely across the world. Caffeine is well-known because of its effects upon consumption, resulting in a decreased feeling of tiredness for the consumer.[1] The molecular mechanisms behind the stimulatory effects have been elucidated about fifty years ago, when caffeine was found to block **adenosine-responsive receptors**.[2–4] In other words, caffeine prevents the molecule adenosine from binding to and stimulating 'its' receptor, thereby impairing the natural feeling of drowsiness caused by receptor activation. Up to today, four subtypes of adenosine receptor have been characterized: the **A_1**, **A_{2A}**, **A_{2B}** and **A_3 receptors** (coined A_1AR, A_{2A}AR, A_{2B}AR and A_3AR throughout this dissertation).[5] These subtypes vary in their molecular structure, induced effects upon activation and expression levels in certain cell- and tissue types.[5–7] All four subtypes share similar structural characteristics, as well as a mode of action that involves Guanine Nucleotide Binding Protein (G Protein) signaling, making them part of the so-called **G Protein-Coupled Receptor** (GPCR) family of proteins.[8]

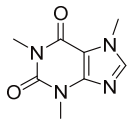

Caffeine was first isolated as a pure substance in 1819 by the German Friedlieb Ferdinand Runge and termed 'Kaffeebase'. The molecule was later independently discovered by the French Pierre-Joseph Pelletier, who gave the substance the name 'caffeine'. Both names are derived from the word 'coffee'.

G Protein-Coupled Receptors (GPCRs)

Proteins within the family of GPCRs share several characteristics. Considering structure, GPCRs have an extracellular N-terminus, seven transmembrane helices and an intracellular C-terminus.[9] Upon activation, GPCRs change their conformation, resulting in the dissociation of the intracellularly bound G Protein.[10] In turn, the G Protein is able to induce various intracellular pathways, of which cyclic adenosine monophosphate (cAMP) generation is the most well-studied (Figure 1).[11] Next to G Proteins, GPCRs have been found to bind arrestin, a signaling protein that induces internalization of the receptor from the membrane into the cell.[12–15] These "classical" and fundamental GPCR pathways have been known for a couple of decades. Nowadays, however, it is becoming clear that there are more factors that influence the fate of GPCRs and their signaling pathways.[16–19]

One of the factors that influences the outcome GPCR signaling pathways is the ability of the GPCR to form **protein-protein interactions** (PPIs) with other proteins. Next to the well-known interactions with subtypes of G Protein and arrestin, PPIs between GPCRs and multiple other proteins have been discovered. Possible interactions partners are the same GPCR (homodimer formation), a different GPCR (heterodimer formation), other membrane proteins (e.g. adenylyl cyclase), or intracellular proteins (e.g. G protein-coupled receptor kinases (GRKs)).[16] A second factor of influence is the presence or absence of certain **post-translational modifications** (PTMs): covalent reversible modifications onto the protein that are not encoded within their DNA.[17,18] GPCR **signaling from other cellular compartments** has also been observed, e.g. from organelles and vesicles. Cellular localization of GPCRs is thus a third factor that influences GPCR signaling. All of these factors, PPIs, PTMs and cellular localization, are highly intertwined, thereby complicating the outcome of the induced signaling pathways.[16–19]

Knowledge of all different aspects of GPCR signaling is highly valuable when targeting a GPCR for medicinal purposes. In fact, GPCRs are one of the most popular drug targets, as roughly one third of all marketed drugs is targeting a specific GPCR, directly or indirectly.[23,24] The reason for their popularity is the important role of GPCR signaling in a wide range of physiological and pathological conditions. This is also true for all four of the adenosine receptors, that are involved in multiple pathophysiological conditions, ranging from immune regulation to cancer.[25]

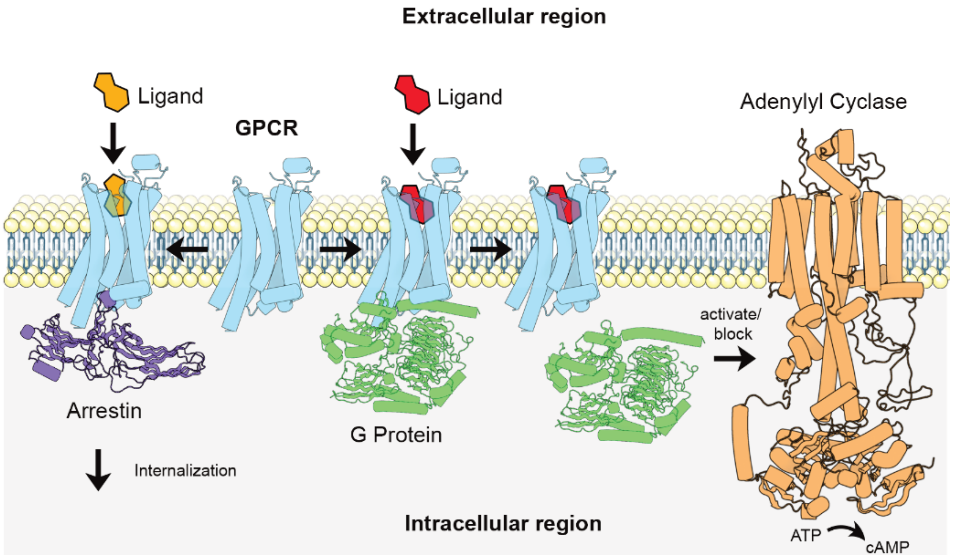

Figure 1. Activation of GPCRs results in intracellular signal transduction pathways, of which G protein-dependent stimulation or inhibition of adenylyl cyclase (right-hand side) and arrestin-mediated internalization (left-hand side) are the most well studied. Adenylyl cyclase in turn produces cAMP from adenosine triphosphate (ATP). This figure was partly created using Protein Imager,[20] using the structures of the A_{2A}AR (PDB: 7ARO), modified G_S Protein (PDB: 8HDO), β-Arrestin1 (PDB: 7SRS) and predicted structure of Adenylyl Cyclase type 6 (Alphafold: AF-043306-F1).[21,22]

Adenosine Receptors as Drug Target

Although the adenosine receptors are a target for caffeine, the receptors are named after their endogenous ligand: adenosine (Figure 2).[5] Adenosine is a signaling molecule that is formed, next to other biosynthetic pathways, through the breakdown of extracellular ATP.[6] ATP functions as energy carrier of the cell. Hence, a high extracellular concentration of adenosine indicates high levels of ATP consumption. Increased concentrations of adenosine have been found in various pathological conditions, for example during inflammation, hypoxia and in the tumor microenvironment.[26,27] Cells respond to this adenosine-rich environment via binding of adenosine to one or more of the four adenosine receptors (ARs), most often leading to an immunosuppressive response. Targeting the adenosine receptors is therefore an interesting strategy to modulate immune responses in a variety of pathologies, as further outlined below.

The **adenosine A_1 receptor** (A_1AR) is expressed in several brain regions (cortex, cerebellum, hippocampus), the heart (cardiomyocytes) and fat tissue (adipocytes), among other tissue types.[5] Activation of the receptor results in, for example, analgesic effects, reduction of ischemic injury or induction of lipolysis, however, this is highly dependent on cell- and tissue type.[30–32] Clinical trials of A_1AR-targeting drugs have mostly been focused on reducing and preventing heart damage, using either (partial) agonists or antagonists for the A_1AR.[30] More recent studies reveal a reduction of nociception upon treatment with an A_1AR allosteric modulator, implying novel therapeutic pathways for the treatment of pain.[32]

The **adenosine A_{2A} receptor** (A_{2A}AR) is expressed in multiple brain regions (a high A_{2A}AR receptor density is found in the basal ganglia), as well as on immune cells (granulocytes and lymphocytes, among other cells).[7] The stimulatory effects of caffeine are mostly caused by inhibition of A_1ARs and A_{2A}ARs in the brain.[33] Next to that, antagonism of A_{2A}ARs in brain regions dampens the effects of neurodegenerative diseases, such as Parkinson's and Alzheimer's, leading to FDA approval of the A_{2A}AR antagonist Istradefylline as therapy for Parkinson's disease.[34–36]

The **adenosine A_{2B} receptor** (A_{2B}AR) is expressed on smooth muscle cells, endothelial cells and immune cells (macrophages, dendritic cells and antigen-presenting cells, among other immune cells). Like the A_{2A}AR, activation of A_{2B}ARs leads to local immune suppression.[37] Pathways involving both A_{2A}ARs and A_{2B}ARs have been found beneficial for the proliferation of cancerous cells within the tumor micro-environment.[26,27,37] Therefore, multiple clinical trials are currently ongoing using antagonists to block A_{2A}ARs and A_{2B}ARs in certain types of cancer.[7]

Lastly, the **adenosine A_3 receptor** (A_3AR), is expressed on immune cells (granulocytes), various cancerous cell lines and in testes and lungs, among other tissue types.[5] Activation of the A_3AR can lead to various immunomodulatory effects, depending on cell and tissue type, and ranges from the release of immune mediators to chemotaxis.[38–40] Altering immune signaling through the activation or inhibition of A_3ARs is currently being investigated as treatment of rheumatoid arthritis, COVID-19 and psoriasis.[7]

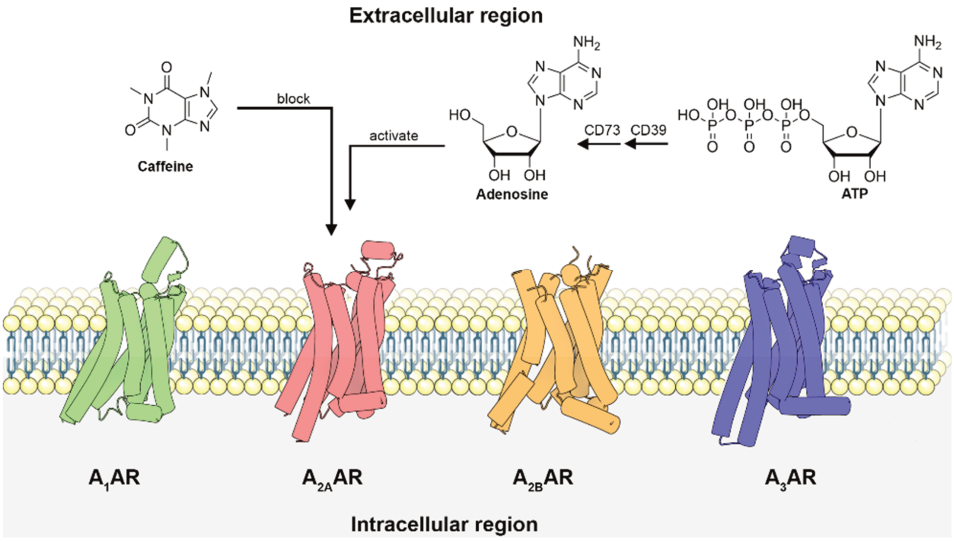

Figure 2. The four adenosine receptors are activated by their endogenous ligand adenosine and blocked by caffeine, although with differences in binding affinity between receptors, experiments and species.[7,28,29] ATP is a source of extracellular adenosine and is dephosphorylated by the membrane enzymes CD39 and CD73. This figure was partly created with Protein Imager,[20] using the structures of the A_1AR (PDB: 7LD4), A_{2A}AR (PDB: 7ARO), A_{2B}AR (PDB: 8HDO) and predicted structure of the A_3AR (Alphafold: AF-P0DMS8-F1).[21,22]

Challenges in Studying Adenosine Receptors

As evident from the examples above, the adenosine receptors are widely expressed throughout the human body. Consequently, activation of the adenosine receptors can cause a variety of downstream effects, dependent on cell type and cellular environment. Using the adenosine receptors to modulate immune responses in heart diseases, neurodegenerative diseases, cancers and immune disorders are interesting new strategies for drug discovery programs. Nevertheless, caution must be taken upon targeting the ARs, as the multitasking role of the receptors might cause unwanted side effects.[41] It is therefore of great importance to investigate the ARs and decipher all aspects of AR signaling, prior to the introduction of new drug candidates.

Studying the ARs, however, has many challenges. Being part of the GPCR family of proteins, ARs have various structural features that make them difficult to detect in standard biochemical assays. First of all, the seven hydrophobic transmembrane domains cause **poor solubility** of the receptors, thus requiring adjusted buffers and assay conditions.[9,42,43] This initially hampered the progress in crystallization studies of GPCRs but has become less of an issue with the rise of cryo-EM techniques.[43] Nevertheless, other biochemical assay types, for example chemical proteomics, still suffer from the poor solubility of GPCRs under standard assay conditions.[44]

Next to that, **low endogenous expression levels** of ARs (not to be confused with the wide expression on various cell types) hinder detection of ARs on endogenous cells, while low levels are still of physiological importance.[6,42,44] Most studies towards AR detection have therefore been carried out on AR-overexpressing cell lines, purified membrane fractions or purified receptors.

Lastly, the factors that influence GPCR signaling, as discussed above, also increase the **complexity of AR signaling**. These include PPIs, PTMs and (sub)cellular localization. All the ARs interact with other proteins, contain multiple PTM sites and partake in internalization pathways after agonist-induced activation.[45] The A_{2A}AR has been the most extensively studied, resulting in the discovery of PPIs with multiple other proteins, such as members of the subfamilies of cannabinoid and dopamine receptors.[46–48] Next to the A_2AR, homo- and/or heteromeric PPIs have been observed for the A_1AR, A_{2B}AR and A_3AR, although the physiological relevance of these PPIs has yet to be understood.[49,50]

Fortunately, various chemical and biochemical tools are being developed to aid the detection of ARs, as well as AR-induced signaling pathways. These include genetic alterations of the receptor, e.g. incorporation of FRET- and BRET-based proteins or tags, the development of antibodies, and the development of chemical probe molecules.[51,52] Of these tools, genetic incorporation of fluorescent sensors is not possible when looking at endogenous AR expression in native systems. Next to that, GPCR antibodies are often hindered by their low selectivity.[53,54] Therefore, this thesis focuses on the development and use of selective chemical probes to target and study the adenosine receptors.

Targeting the Adenosine Receptors with Chemical Probes

Over the past decades, various types of chemical probes have been developed to target the adenosine receptors.[51] Practically, these chemical probes can be divided into two categories: reversible and covalent probes. Reversible chemical probes bind to ARs in a similar manner as adenosine and caffeine: through intermolecular forces in the binding pocket of the receptor. Reversible probes can leave the receptor binding pocket after binding, thereby generating an equilibrium between bound and unbound receptor (Figure 3A). Reversible probes for adenosine receptors include ligands that have been functionalized with radioactive isotopes (radioligands) or fluorophores (fluorescent ligands).[51,55,56]

Covalent probes on the other hand, contain an electrophilic or photoreactive group that reacts with an amino acid residue near the probe binding pocket, inducing a covalent bond between probe and receptor (Figure 3B).[57] Covalent probes have an 'infinite' residence time and therefore show a time-dependent increase in receptor occupancy. Ligands functionalized with an electrophilic or photoreactive group (covalent ligands) have been used as tool to permanently block the adenosine receptors. A summary of most of the previously (before 2020) developed radioligands, fluorescent ligands and covalent ligands can be found in a recent review paper.[51]

Building upon this, covalent ligands have been functionalized with reporter groups, such as radioactive isotopes, fluorophores and biotin moieties. Contrary to the reversible radioligands and fluorescent ligands, these reporter groups are attached to the receptor in a covalent manner, allowing detection of ARs in assay types that require thorough washing steps or the use of denaturing conditions. Different strategies to covalently functionalize GPCRs with small molecular probes are reviewed in chapter 2. In case of the ARs, two different types of functionalized covalent probes have been developed: affinity-based probes and ligand-directed probes.

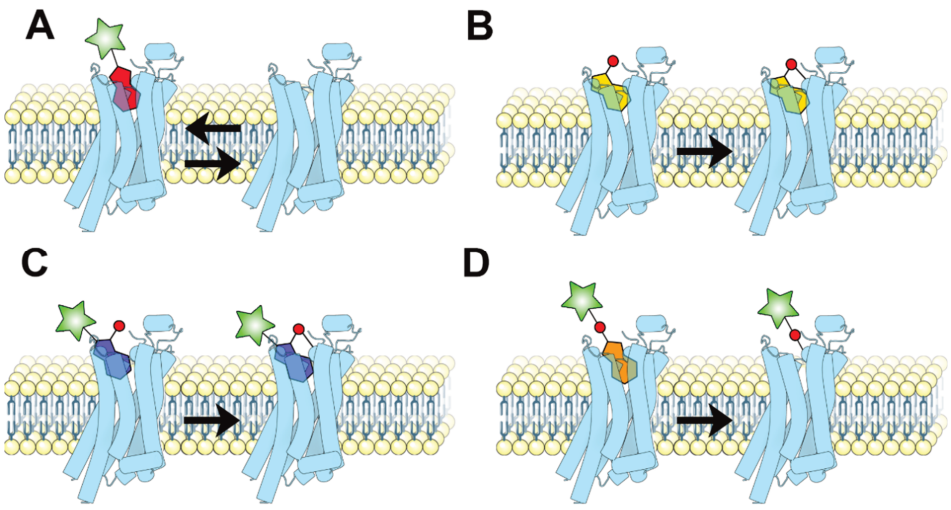

Figure 3. Schematic overview of the types of probes that have been developed for the adenosine receptors. (A) Reversible probes; (B) Covalent ligands; (C) Affinity-based probes; (D) Ligand-directed probes. This figure was partly created with Protein Imager,[20] using the structure of the A_{2A}AR (PDB: 7ARO).

Affinity-based probes are covalent ligands functionalized with reporter groups and consist of three parts: a high affinity ligand to induce selectivity; an electrophilic or photoreactive group ('warhead') that ensures covalent bond formation between probe and receptor; and a reporter group that allows detection of the probe-bound receptor in biochemical assays (Figure 3C). Early examples of affinity-based probes for ARs contain a radioisotope that is directly conjugated to the molecular scaffold (one-step probes),[58–60] while more recent examples of affinity-based probes use click chemistry to 'click' detection moieties onto the probe-bound receptors *in situ* (two-step probes).[61–64]

Ligand-directed probes consist of the same three parts as affinity-based probes: a high affinity ligand to induce selectivity; an electrophilic group that reacts with a nearby amino acid residue; and a reporter group that allows detection of all probe-bound receptors. However, ligand-directed probes use a different type of electrophile: upon binding covalently to the receptor, the high affinity-ligand acts as leaving group (Figure 3D). This means that the binding pocket of the receptor is 'free' to bind other ligands, which allows studies towards receptor activation upon binding to various (partial) agonists. Both one-step and two-step ligand-directed probes have been developed for the ARs.[65,66]

Aim and Outline of This Thesis

The adenosine receptors are interesting protein targets from a drug discovery perspective. However, targeting specific AR pathways is hampered by the wide expression of ARs and their multitude of functionalities. Besides that, the inherent properties of being GPCRs, such as poor solubility, low expression levels, PPIs, PTMs and subcellar localization, all add extra layers of complexity to AR behavior. Therefore, in this thesis, we aim to develop new chemical probes that allow the detection of ARs in a broad range of assay types, in order to both overcome and study the abovementioned complexities. These chemical probes include covalent ligands, affinity-based probes and ligand-directed probes.

Chapter 2 provides an overview of all the small molecular probes that have been developed to covalently functionalize the whole family of GPCRs. Various types of probes are discussed, as well as their potential applications in GPCR research. **Chapter 3** describes the development of a covalent ligand for the adenosine A_{2B} receptor. A set of potential covalent ligands for the A_{2B}AR was synthesized and the effect of location and type of electrophile ('warhead') is evaluated in this chapter. In **Chapter 4** the development of an affinity-based probe for the adenosine A_1 receptor is reported. The synthesis of the probe is described, as well as the evaluation of the probe in radioligand binding assays. Furthermore, utilization of the affinity-based probe in SDS-PAGE, pull-down proteomics and microscopy experiments is described. **Chapter 5** reports the development of an affinity-based probe for the adenosine A_3 receptor. Likewise, synthesis and pharmacological evaluation of the affinity-based probe are reported. This chapter also shows the application of the affinity-based probe in SDS-PAGE, microscopy and flow cytometry experiments to detect both overexpressed and endogenous A_3AR. **Chapter 6** builds onto the work of chapter 3 and describes the development of a ligand-directed probe based on the aforementioned A_{2B}AR covalent ligand. Reactivity, selectivity and functionality of the ligand-directed probe are evaluated in this chapter. Finally, **Chapter 7** gives an overview of the developed probes and their use in various types of biochemical assays. In conclusion, future applications of the herein presented probe types are this discussed in this chapter.

References

[1] B. B. Fredholm, K. Bättig, J. Holmén, A. Nehlig, E. E. Zvartau, *Pharmacol Rev* **1999**, *51*, 83–133.

[2] T. de Gubareff, W. Jr. Sleator, *J Pharmacol Exp Ther* **1965**, *148*, 202–214.

[3] H. Shimizu, J. W. Daly, C. R. Creveling, *J Neurochem* **1969**, *16*, 1609–1619.

[4] A. Sattin, T. W. Hall, *Mol Pharmacol* **1970**, *6*, 13–23.

[5] B. B. Fredholm, A. P. IJzerman, K. A. Jacobson, K.-N. Klotz, J. Linden, *Pharmacol Rev* **2001**, *53*, 527–552.

[6] B. B. Fredholm, A. P. IJzerman, K. A. Jacobson, J. Linden, C. E. Müller, *Pharmacol Rev* **2011**, *63*, 1–34.

[7] A. P. IJzerman, K. A. Jacobson, C. E. Müller, B. N. Cronstein, R. A. Cunha, *Pharmacol Rev* **2022**, *74*, 340–372.

[8] S. M. Foord, T. I. Bonner, R. R. Neubig, E. M. Rosser, J. P. Pin, A. P. Davenport, M. Spedding, A. J. Harmar, *Pharmacol Rev* **2005**, *57*, 279–288.

[9] D. M. Rosenbaum, S. G. F. Rasmussen, B. K. Kobilka, *Nature* **2009**, *459*, 356–363.

[10] M. M. Papasergi-Scott, G. Pérez-Hernández, H. Batebi, Y. Gao, G. Eskici, A. B. Seven, O. Panova, D. Hilger, M. Casiraghi, F. He, L. Maul, P. Gmeiner, B. K. Kobilka, P. W. Hildebrand, G. Skiniotis, *bioRxiv* **2023**, 2023.03.20.533387.

[11] N. Wettschureck, S. Offermanns, *Physiol Rev* **2005**, *85*, 1159–1204.

[12] H. Kühn, U. Wilden, *Journal of Receptors and Signal Transduction* **1987**, *7*, 283–298.

[13] J. L. Benovic, H. Kchnt, I. Weyandt, J. Codinat, M. G. Caron, R. J. Lefkowitz, *Proceedings of the National Academy of Sciences* **1987**, *84*, 8879–8882.

[14] M. J. Lohse, J. L. Benovic, J. Codina, M. G. Caron, R. J. Lefkowitz, *Science (1979)* **1990**, *248*, 1547–1550.

[15] S. K. Shenoy, R. J. Lefkowitz, *Trends Pharmacol Sci* **2011**, *32*, 521–533.

[16] D. Wootten, A. Christopoulos, M. Marti-Solano, M. M. Babu, P. M. Sexton, *Nat Rev Mol Cell Biol* **2018**, *19*, 638–653.

[17] C. K. Goth, U. E. Petäjä-Repo, M. M. Rosenkilde, *ACS Pharmacol Transl Sci* **2020**, *3*, 237–245.

[18] A. Patwardhan, N. Cheng, J. Trejo, *Pharmacol Rev* **2021**, *73*, 120–151.

[19] M. Ali, M. Nezhady, J. C. Rivera, S. Chemtob, *iScience* **2020**, *23*, 101643.

[20] G. Tomasello, I. Armenia, G. Molla, *Bioinformatics* **2020**, *36*, 2909–2911.

[21] J. Jumper, R. Evans, A. Pritzel, T. Green, M. Figurnov, O. Ronneberger, K. Tunyasuvunakool, R. Bates, A. Žídek, A. Potapenko, A. Bridgland, C. Meyer, S. A. A. Kohl, A. J. Ballard, A. Cowie, B. Romera-Paredes, S. Nikolov, R. Jain, J. Adler, T. Back, S. Petersen, D. Reiman, E. Clancy, M. Zielinski, M. Steinegger, M. Pacholska, T. Berghammer, S. Bodenstein, D. Silver, O. Vinyals, A. W. Senior, K. Kavukcuoglu, P. Kohli, D. Hassabis, *Nature* **2021**, *596*, 583–589.

[22] M. Varadi, S. Anyango, M. Deshpande, S. Nair, C. Natassia, G. Yordanova, D. Yuan, O. Stroe, G. Wood, A. Laydon, A. Žídek, T. Green, K. Tunyasuvunakool, S. Petersen, J. Jumper, E. Clancy, R. Green, A. Vora, M. Lutfi, M. Figurnov, A. Cowie, N. Hobbs, P. Kohli, G. Kleywegt, E. Birney, D. Hassabis, S. Velankar, *Nucleic Acids Res* **2022**, *50*, D439–D444.

[23] A. S. Hauser, M. M. Attwood, M. Rask-Andersen, H. B. Schiöth, D. E. Gloriam, *Nat Rev Drug Discov* **2017**, *16*, 829–842.

[24] D. Yang, Q. Zhou, V. Labroska, S. Qin, S. Darbalaei, Y. Wu, E. Yuliantie, L. Xie, H. Tao, J. Cheng, Q. Liu, S. Zhao, W. Shui, Y. Jiang, M. W. Wang, *Signal Transduct Target Ther* **2021**, *6*, 7.

[25] P. A. Borea, S. Gessi, S. Merighi, F. Vincenzi, K. Varani, *Physiol Rev* **2018**, *98*, 1591–1625.

[26] C. Cekic, J. Linden, *Nat Rev Immunol* **2016**, *16*, 177–192.

[27] B. Allard, D. Allard, L. Buisseret, J. Stagg, *Nat Rev Clin Oncol* **2020**, *17*, 611–629.

[28] P. J. M. Van Galen, A. H. Van Bergen, C. Gallo-Rodriguez, N. Melman, M. E. Olah, A. P. IJzerman, G. L. Stiles, K. A. Jacobson, *Mol Pharmacol* **1994**, *45*, 1101–1111.

[29] K. A. Jacobson, A. P. IJzerman, J. Linden, *Drug Dev Res* **1999**, *47*, 45–53.

[30] D. Meibom, B. Albrecht-Küpper, N. Diedrichs, W. Hübsch, R. Kast, T. Krämer, U. Krenz, H. G. Lerchen, J. Mittendorf, P. G. Nell, F. Süssmeier, A. Vakalopoulos, K. Zimmermann, *ChemMedChem* **2017**, *12*, 728–737.

[31] Y. Yun, J. Chen, R. Liu, W. Chen, C. Liu, R. Wang, Z. Hou, Z. Yu, Y. Sun, A. P. IJzerman, L. H. Heitman, X. Yin, D. Guo, *Biochem Pharmacol* **2019**, *164*, 45–52.

[32] C. J. Draper-Joyce, R. Bhola, J. Wang, A. Bhattarai, A. T. N. Nguyen, I. Cowie-Kent, K. O'Sullivan, L. Y. Chia, H. Venugopal, C. Valant, D. M. Thal, D. Wootten, N. Panel, J. Carlsson, M. J. Christie, P. J. White, P. Scammells, L. T. May, P. M. Sexton, R. Danev, Y. Miao, A. Glukhova, W. L. Imlach, A. Christopoulos, *Nature* **2021**, *597*, 571–576.

[33] G. Faudone, S. Arifi, D. Merk, *J Med Chem* **2021**, *64*, 7156–7178.

[34] M. A. Schwarzschild, L. Agnati, K. Fuxe, J. F. Chen, M. Morelli, *Trends Neurosci* **2006**, *29*, 647–654.

[35] J. F. Chen, R. A. Cunha, *Purinergic Signal* **2020**, *16*, 167–174.

[36] S. V. Da Silva, M. G. Haberl, P. Zhang, P. Bethge, C. Lemos, N. Gonçalves, A. Gorlewicz, M. Malezieux, F. Q. Gonçalves, N. Grosjean, C. Blanchet, A. Frick, U. V. Nägerl, R. A. Cunha, C. Mulle, *Nat Commun* **2016**, *7*, 11915.

[37] Z. G. Gao, K. A. Jacobson, *Int J Mol Sci* **2019**, *20*, 5139.

[38] Y. Chen, R. Corriden, Y. Inoue, L. Yip, N. Hashiguchi, A. Zinkernagel, V. Nizet, P. A. Insel, W. G. Junger, *Science (1979)* **2006**, *314*, 1792–1795.

[39] R. Corriden, T. Self, K. Akong-Moore, V. Nizet, B. Kellam, S. J. Briddon, S. J. Hill, *EMBO Rep* **2013**, *14*, 726–732.

[40] K. A. Jacobson, S. Merighi, K. Varani, P. A. Borea, S. Baraldi, M. Aghazadeh Tabrizi, R. Romagnoli, P. G. Baraldi, A. Ciancetta, D. K. Tosh, Z.-G. Gao, S. Gessi, *Med Res Rev* **2018**, *38*, 1031–1072.

[41] J.-F. Chen, H. K. Eltzschig, B. B. Fredholm, *Nat Rev Drug Discov* **2013**, *12*, 265–286.

[42] A. O. Helbig, A. J. R. Heck, M. Slijper, *J Proteomics* **2010**, *73*, 868–878.

[43] S. J. Piper, R. M. Johnson, D. Wootten, P. M. Sexton, *Chem Rev* **2022**, *122*, 13989–14017.

[44] O. Vit, J. Petrak, *J Proteomics* **2017**, *153*, 8–20.

[45] E. C. Klaasse, A. P. IJzerman, W. J. de Grip, M. W. Beukers, *Purinergic Signal* **2008**, *4*, 21–37.

[46] P. Carriba, G. Navarro, F. Ciruela, S. Ferré, V. Casadó, L. Agnati, A. Cortés, J. Mallol, K. Fuxe, E. I. Canela, C. Lluís, R. Franco, *Nat Methods* **2008**, *5*, 727–733.

[47] G. Navarro, P. Carriba, J. Gandía, F. Ciruela, V. Casadó, A. Cortés, J. Mallol, E. I. Canela, C. Lluis, R. Franco, *ScientificWorldJournal* **2008**, *8*, 1088–1097.

[48] S. Ferré, F. Ciruela, *J Caffeine Adenosine Res* **2019**, *9*, 89–97.

[49] C. T. Lauren May, E. A. Vecchio, J.-A. Baltos, A. T. N Nguyen, A. Christopoulos, P. J. White, L. T. May, E. Vecchio, J. Baltos, *Br J Pharmacol* **2018**, *175*, 4036.

[50] R. Franco, A. Cordomí, C. Llinas del Torrent, A. Lillo, J. Serrano-Marín, G. Navarro, L. Pardo, *Cellular and Molecular Life Sciences* **2021**, *78*, 3957–3968.

[51] X. Yang, L. H. Heitman, A. P. IJzerman, D. van der Es, *Purinergic Signal* **2021**, *17*, 85–108.

[52] M. Soave, L. A. Stoddart, C. W. White, L. E. Kilpatrick, J. Goulding, S. J. Briddon, S. J. Hill, *FEBS Journal* **2021**, *288*, 2585–2601.

[53] M. Jo, S. T. Jung, *Exp Mol Med* **2016**, *48*, e207.

[54] L. Dahl, I. B. Kotliar, A. Bendes, T. Dodig-Crnković, S. Fromm, A. Elofsson, M. Uhlén, T. P. Sakmar, J. M. Schwenk, *bioRxiv* **2022**, 2022.11.24.517810.

[55] E. Kozma, P. Suresh Jayasekara, L. Squarcialupi, S. Paoletta, S. Moro, S. Federico, G. Spalluto, K. A. Jacobson, *Bioorg Med Chem Lett* **2013**, *23*, 26–36.

[56] S. Federico, L. Lassiani, G. Spalluto, *Pharmaceuticals* **2019**, *12*, 168.

[57] D. Weichert, P. Gmeiner, *ACS Chem Biol* **2015**, *10*, 1376–1386.

[58] A. Patel, R. H. Craig, S. M. Daluge, J. Linden, T. Burroughs, *Mol Pharmacol* **1988**, *33*, 585–591.

[59] W. W. Barrington, K. A. Jacobson, G. L. Stiles, *Mol Pharmacol* **1990**, *38*, 177–183.

[60] D. R. Luthin, K. S. Lee, D. Okonkwo, P. Zhang, J. Linden, *J Neurochem* **1995**, *65*, 2072–2079.

[61] X. Yang, T. J. M. Michiels, C. de Jong, M. Soethoudt, N. Dekker, E. Gordon, M. van der Stelt, L. H. Heitman, D. van der Es, A. P. IJzerman, *J Med Chem* **2018**, *61*, 7892–7901.

[62] P. N. H. Trinh, D. J. W. Chong, K. Leach, S. J. Hill, J. D. A. Tyndall, L. T. May, A. J. Vernall, K. J. Gregory, *J Med Chem* **2021**, *64*, 8161–8178.

[63] B. L. H. Beerkens, Ç. Koç, R. Liu, B. I. Florea, S. E. Le Dévédec, L. H. Heitman, A. P. IJzerman, D. van der Es, *ACS Chem Biol* **2022**, *17*, 3131–3139.

[64] B. L. H. Beerkens, I. M. Snijders, J. Snoeck, R. Liu, A. T. J. Tool, S. E. Le Dévédec, W. Jespers, T. W. Kuijpers, G. J. P. van Westen, L. H. Heitman, A. P. IJzerman, D. van der Es, *ChemRxiv* **2023**, DOI 10.26434/chemrxiv-2023-6g59z.

[65] S. M. Moss, P. S. Jayasekara, S. Paoletta, Z. G. Gao, K. A. Jacobson, *ACS Med Chem Lett* **2014**, *5*, 1043–1048.

[66] L. A. Stoddart, N. D. Kindon, O. Otun, C. R. Harwood, F. Patera, D. B. Veprintsev, J. Woolard, S. J. Briddon, H. A. Franks, S. J. Hill, B. Kellam, *Commun Biol* **2020**, *3*, 722.

Chapter 2

Covalent Functionalization of G Protein-Coupled Receptors by Small Molecular Probes

Bert L.H. Beerkens, Adriaan P. IJzerman and Daan van der Es.

Abstract
Roughly one third of all marketed drugs act via binding to one or multiple of the >800 human GPCRs, mostly through activation or inhibition via the orthosteric binding site. Next to that, novel strategies to alter GPCR functioning are being developed, including allosteric, biased and covalently binding ligands. Molecular probes play an important role to verify such drug molecules with new modes of action and provide information on all factors involved in GPCR-signaling. Various flavors of molecular probes have been developed, ranging from small molecules to antibodies, each bearing its own advantages and disadvantages. In this mini-review, a closer look is taken at small molecular probes that functionalize GPCRs in a covalent manner, e.g. through conjugation of reporter groups such as a fluorophore or biotin. Covalently bound reporter groups allow the investigation of GPCRs in an increasing amount of biochemical assay types, yielding new information on GPCR-signaling pathways. Here, a broad range of recently developed 'functionalized covalent probes' is summarized. Furthermore, the use of these probes in biochemical assays, as well as their applications in the field of GPCR research are discussed. Lastly, a view on possible future applications of these types of small molecular probes is provided.

1. Introduction

G protein-coupled receptors (GPCRs) are transmembrane proteins that share the same structural features: seven trans-membrane helices, three extra- and three intracellular loops, an extracellular N-terminus and an intracellular C-terminus. The human family of GPCRs comprises >800 members, divided over multiple subfamilies classified by their ligand binding partners.[1] Upon binding to extracellular stimuli, GPCRs undergo conformational changes, in turn inducing a cascade of intracellular signaling events. GPCRs thus allow cells to respond to molecules in the extracellular environment. Signaling pathways that originate from GPCRs can have a major influence on the physiology of the cell, and many pathophysiological conditions have been linked to the activation or malfunctioning of GPCRs.[2] Such findings have led to a surge in GPCR drug discovery at the end of the 20th century, resulting in a high amount (>500) of currently marketed drugs targeting GPCRs.[3] Besides the development of 'classical' orthosteric ligands, current strategies to modulate GPCR functioning include new types of small molecules, examples being biased, allosteric, bitopic and covalent ligands.[4] To take advantage of these novel modulation strategies, it is important to study these ligands and understand their molecular mechanisms of action.

Studying GPCRs however, has many challenges that share some common grounds. Firstly, most GPCRs have a relatively low basal expression level on native cells, as compared to e.g. cytosolic proteins, hindering purification and characterization.[5] Secondly, most GPCRs are believed to contain multiple post-translational modifications (PTMs), such as extracellular glycan modifications, intracellular phosphorylated residues and an intracellular palmitoyl modification, all of which add another dimension of complexity to structure-based and functional studies.[6,7] Thirdly, having seven transmembrane helices, GPCRs contain a large portion of hydrophobic amino acids that hamper solubilization and require additional surfactants in conventional assay buffers.[5,8,9] Additionally, other factors, such as cellular localization, protein-protein interactions (PPIs) and proteolytic cleavage all influence the fate of a GPCR in its cellular context.[7,10] Fortunately, a plethora of chemical and biological probes has been developed as tools to aid the molecular and pharmacological characterizations of GPCRs.[11–14] Utilization of the right type of probe can help overcome and even study the challenges mentioned above.

Radioactive chemical probes have historically been a primary source for GPCR characterization.[15] β-emitting radioligands are being used to precisely determine the binding affinity of putative ligands, while positron-emitting radioligands are being used to trace GPCR distribution *in vivo*. Radiolabeled chemical probes, however, require the use of radioactive material and specialized labs. Therefore, in addition to radioligands, fluorescent ligands have been and are being developed as chemical probes for GPCRs.[13,14] Besides compound screening and visualizing GPCR distribution, fluorescent ligands aid in determining subcellular localization and cellular expression levels of GCPRs, using modern confocal microscopes and flow cytometry techniques, respectively. Next to that, GPCR-targeting antibodies are being developed as biological probes. The use of GPCR antibodies, however, is not without challenges.[13] While some antibodies have shown successful applications,[16,17] other antibodies suffer from low selectivity towards their target GPCR.[17–19] One reason for the lack of selectivity is the low number of possible unique epitopes: the extracellular portion of a GPCR 'merely' consist of an N-terminus and three extracellular loops. Length of these extracellular domains, and thus the ability to be selectively targeted by an antibody, differs greatly per GPCR. Altogether, there is a broad overlap between the applications of radioligands, fluorescent ligands and antibodies.

The chemical and biological probes mentioned above mostly bind in a reversible fashion. A different strategy to study GPCRs is through covalent functionalization, in which the GPCR is

covalently functionalized with a detection group of interest, such as a fluorophore, biotin moiety or 'click' handle. A big advantage of covalent functionalization is the robustness of the bond between GPCR and detection group, allowing the use of washing steps, reductants, oxidants, surfactants and other chemicals in biochemical assays. This allows the investigation of GPCRs in an expanded set of experiment types, for instance SDS-PAGE and pull-down proteomics.

In this mini-review, we will discuss the recently reported small molecular probes that are able to covalently functionalize GPCRs. As the term 'covalent probes' is already used to describe covalent ligands, we will use the term 'functionalized covalent probes' or 'functionalized covalent ligands' throughout this mini-review. As such, we hope to put emphasis on both the reactive groups and the reporter groups. Although covalent GPCR functionalization might also be done through genetic or metabolic alterations,[12,13] these strategies are not applicable to *native* GPCRs and are therefore beyond the scope of this review. Here, we list most if not all recently developed small molecular probes that covalently functionalize GPCRs. Additionally, we will briefly discuss their applications.

2. Types of Probes

In the next paragraphs, four different types of functionalized covalent probes are being discussed: affinity-based probes (AfBPs) (Figure 1A), ligand-directed probes (LD probes) (Figure 1B), glycan-targeting probes (Figure 1C) and metabolic probes (Figure 1D). Each of these probes label target GPCRs in their own specific manner.

2.1. Affinity-based probes

AfBPs are tool compounds that consist of three functional moieties: (1) a high affinity ligand that promotes selective binding to the protein target of interest, hence the term 'affinity-based'; (2) a reactive group ('warhead') that induces covalent binding to the protein target; (3) a reporter group that allows detection of the probe-bound protein in biochemical assays (Figure 1A). Although such probes have been synthesized for GPCRs for over three decades, the recent term 'affinity-based probes' is a derivation of the term 'activity-based probes', as first coined by Cravatt and coworkers.[21] Activity-based probes are similar tool compounds but differ in reactivity, as their warheads target nucleophilic amino acid residues within the active site of enzymes. GPCRs on the other hand, do not have such an active site nucleophile that can be targeted. Therefore AfBPs for GPCRs require relatively more reactive warheads.

Two types of warheads can be distinguished: photoreactive groups and electrophilic groups. AfBPs with photoreactive groups, also named 'photo-affinity probes', covalently bind their target GPCR upon irradiation at specific wavelengths. Dependent on the type of photoreactive group, carbene or nitrene species are generated that will insert into neighboring hydrogen-heteroatom bonds.[22] Due to this broad reactivity, most photo-affinity probes do not require a particularly reactive amino acid residue to be present in the binding pocket of the receptor. However, the broad reactivity might also cause an increased amount of off-target labeling. Electrophilic AfBPs on the other hand, covalently bind their target GPCR through attack of a proximate nucleophilic amino acid residue. Here, specific labeling of the target GPCR requires a balanced electrophile: reactive enough to be attacked by the weakly nucleophilic amino acid, but not randomly attacked by any amino acid residue in the proteome.[23]

Considering the third functional moiety of AfBPs, the reporter group, a distinction can be made between 'one-step' and 'two-step' probes.[24–26] In case of one-step AfBPs, the reporter group, e.g. a fluorophore or biotin moiety, is directly conjugated to the probe. Two-step AfBPs on the other hand, contain a bio-orthogonal group (click handle) that can be functionalized after covalent binding to the target GPCR. Multiple probes have been developed that contain either an alkyne or an azide group that can be functionalized using click chemistry. The advantage

of two-step AfBPs is the lack of bulky reporter groups that might strongly influence the affinity towards the target GPCR. Disadvantages are the introduction of an extra 'click' step in the assay protocol, as well as possible use of cytotoxic reagents such as copper. In the next paragraphs, the most recent advancements will be discussed considering the development of one- and two-step, photo-affinity and electrophilic AfBPs for GPCRs.

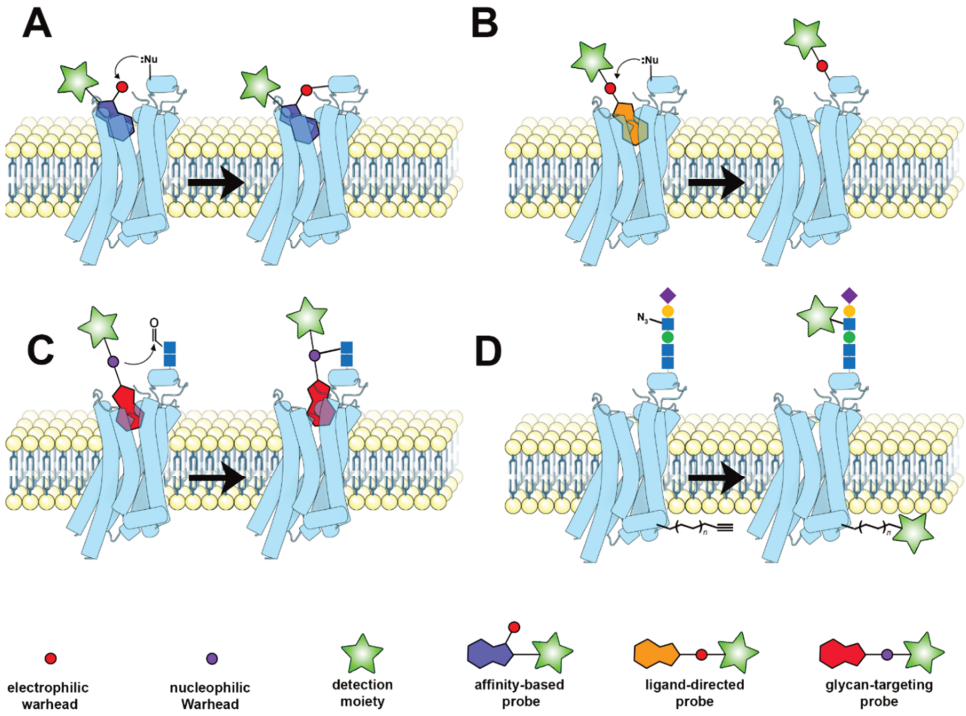

Figure 1. Schematic overview of the various functionalized covalent probes described in this review. (A) Affinity-based probes (AfBPs). After reversible binding of an AfBP to the target GPCR, a nearby nucleophilic residue attacks the electrophilic warhead, resulting in a covalently bound AfBP; (B) Ligand-directed probes (LD probes). Upon reversible binding of an LD probe to the target GPCR, a nearby nucleophilic residue attacks the electrophilic warhead, resulting in intramolecular bond cleavage and subsequent donation of the reporter group to the GPCR; (C) Glycan-targeting probes. First, aldehydes are generated through oxidation of the extracellular glycan chain of the GPCR. Next, the glycan-targeting probe binds reversibly to the GPCR and the nucleophilic warhead attacks the generated aldehyde, resulting in covalently bound glycan-targeting probe; (D) Metabolically incorporated probes. First, fatty acids or sugar molecules derivatized with click groups are added to the cell culture medium. These molecules are then post-translationally incorporated in the GPCR structure, allowing functionalization of the GPCR via click chemistry. This figure was partly generated with Protein Imager,[20] using the structure of the adenosine A_{2A} receptor (PDB: 7ARO).

2.1.1. One-step photo-affinity probes

The introduction of photoreactive groups in the molecular structure of GPCR ligands has a long history, as photo-affinity ligands have been widely used to decipher the location of binding pockets in GPCRs.[27] In some cases, these photo-affinity ligands have been equipped with reporter groups, such as a fluorophore, biotin, or a radioisotope, to allow detection of the probe-bound residues by SDS-PAGE and MS-techniques. Technological advances in the fields of

microscopy and MS-based proteomics have led to new approaches to use photo-affinity ligands to study GPCRs, resulting in the recent development of novel one-step photo-affinity probes (Figure 2).[28–34] While initially most photo-affinity probes were equipped with benzophenone and aryl azide groups, most modern probes contain a diazirine as photoreactive group. The reasons for this are the relatively small size, favorable absorption range and improved synthetic accessibility.[22] On the other hand, Hayashi *et al.* implemented multiple photoreactive groups into the scaffold of a known Dopamine D_2 Receptor (D_2R) ligand, including diazirines, and found the 2-aryl 5-carboxytetrazole-contaning probe (**4**) to bind less off-targets in proteomic studies.[31] Thus, the right balance needs to be found between size and reactivity of the photoreactive group.

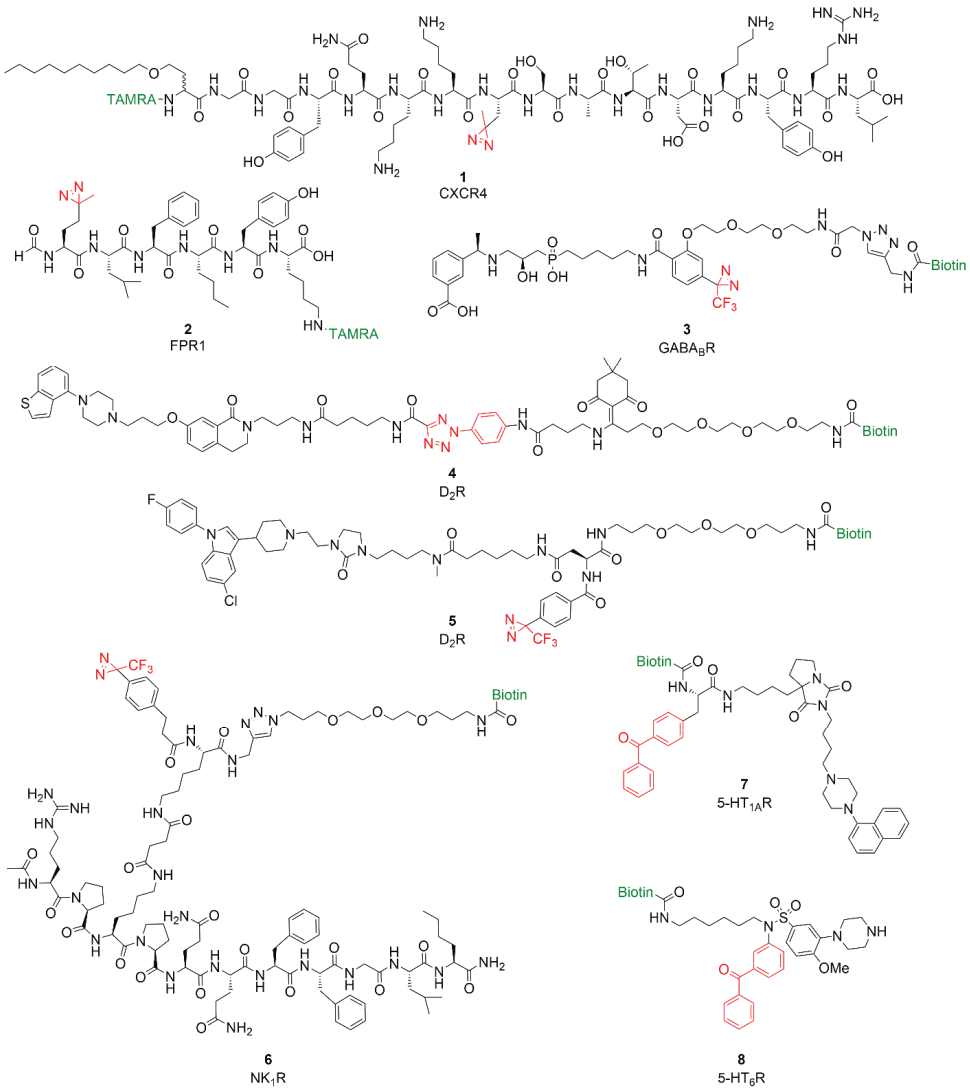

Figure 2. Molecular structures of one-step photo-affinity probes and their target GPCRs. Show in in red are the electrophilic groups and in green the reporter groups.

One-step photo-affinity probes functionalized with a fluorophore for confocal imaging have been developed for the C-X-C chemokine receptor type 4 (CXCR4)[28] and the Formyl Peptide Receptor 1 (FPR1).[29] Both probes **1** and **2** were able to visualize agonist-induced internalization upon binding their target GPCR. One-step photo-affinity probes functionalized with biotin for proteomic pull-down (receptor capture) experiments have been developed for the $GABA_B$ receptor ($GABA_BR$),[30] D_2R,[31,32] Neurokinin 1 receptor (NK_1R),[33] 5-HT_{1A} receptor (5-$HT_{1A}R$) and 5-HT_6 receptor (5-HT_6R).[34] Of these one-step photo-affinity probes, **3** ($GABA_BR$) has been used to elucidate PPIs within the $GABA_BR$ signaling complex, while **5** (D_2R), **7** (5-$HT_{1A}R$) and **8** (5-HT_6R) have been used to profile the protein interactome of their respective molecular scaffolds.

2.1.2. Two-step photo-affinity probes

Most of the reported two-step photo-affinity probes were developed using a strategy that combines the photoreactive group and the click handle onto the same 'R' group, substituted at a location on the pharmacological scaffold that does not impair binding to the target GPCR (Figure 3). However, having this option is strongly dependent on both the molecular scaffold and GPCR binding pocket. The diazirine and benzophenone groups are the most popular warheads among the two-step photo-affinity probes, but phenyl azide and acetophenone groups have also been reported.[34–41] Two-step photo-affinity probes do not only avoid the use of bulky reporter groups, as mentioned above, but also allow functionalization of the probe-bound GPCR by any detection moiety of interest. This is reflected in the wide variety of assays that have been performed, i.e. two-step photo-affinity probes **9**-**12** have been used in SDS-PAGE experiments to detect the 5-$HT_{1A}R$,[34] 5-HT_6R,[34] metabotropic glutamate receptor 2 ($mGlu_2R$)[35] and metabotropic glutamate receptor 5 ($mGlu_5R$)[36]; **13** in flow cytometry experiments to investigate cannabinoid receptor type 2 (CB_2R)[37] expression on lymphocytes; **14**-**16** in target identification experiments to identify GPR39,[38] GPR75[39] and GPRC5A[40] as their respective protein targets; and **17** in pull-down experiments to map possible PPIs of the D_2R.[41]

2.1.3. Two-step electrophilic affinity-based probes

As general interest in covalent ligands is currently emerging, more and more electrophilic covalent ligands are being developed to target GPCRs. Covalent ligands for GPCRs and their wide variety of warheads are extensively reviewed elsewhere.[42] To the best of our knowledge no one-step electrophilic AfBP for GPCRs has recently been developed. In case of the two-step electrophilic AfBPs, the fluorosulfonyl group is the most popular warhead, reacting through an S_N2 mechanism with a lysine or tyrosine residue on the target GPCR.[43–46] Next to that, thiocyanate and acrylamide groups have been implemented in AfBPs to target cysteine residues, reacting through reductive disulfide formation or a Michael addition, respectively (Figure 4).[47] In general, the strategy for the development of electrophilic AfBPs has been substitution of a click handle, with or without extra linker, onto the scaffold of an existing covalent ligand. Two-step probes provide the advantage of being used in a wide variety of assay types due to 'click' functionalization *in situ*. This has resulted in the use of electrophilic AfBPs in a broad range of assay types, such as SDS-PAGE, confocal microscopy, flow cytometry and proteomic pull-down experiments, as has been showcased for the adenosine A_1, A_{2A} and A_3 receptors (A_1AR, $A_{2A}AR$ and A_3AR)[43–46] and the chemokine receptor subtype 2 (CCR2).[47] Of these electrophilic AfBPs, **18**, **20** and **22** have been used to study *N*-glycosylation of the A_1AR, A_3AR and CCR2, respectively; **18** to observe internalization of the A_1AR; and **20** to detect endogenously expressed A_3AR on human primary cells.

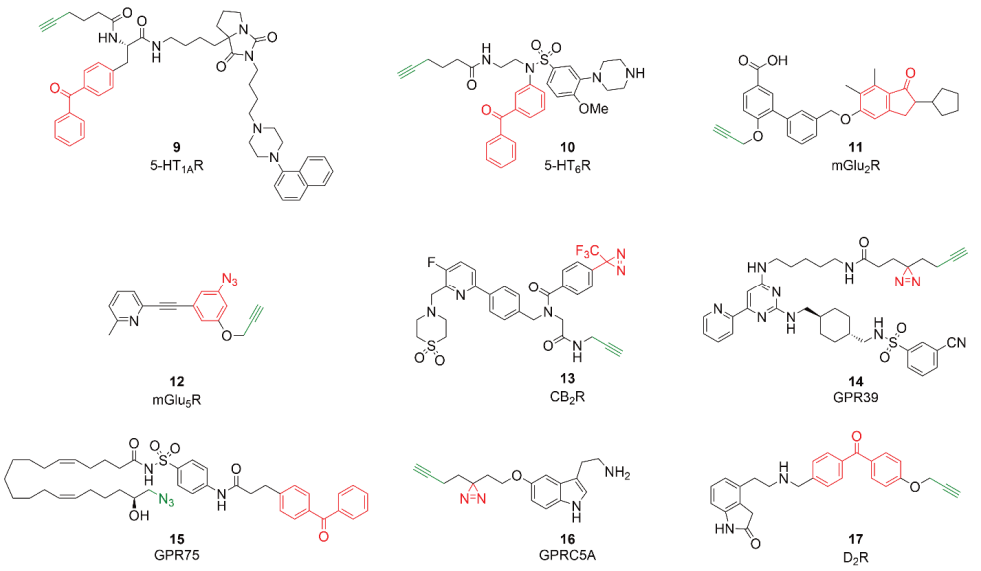

Figure 3. Molecular structures of two-step photo-affinity probes and their target GPCRs. Shown in red are the photoreactive groups, shown in green are the click handles for functionalization.

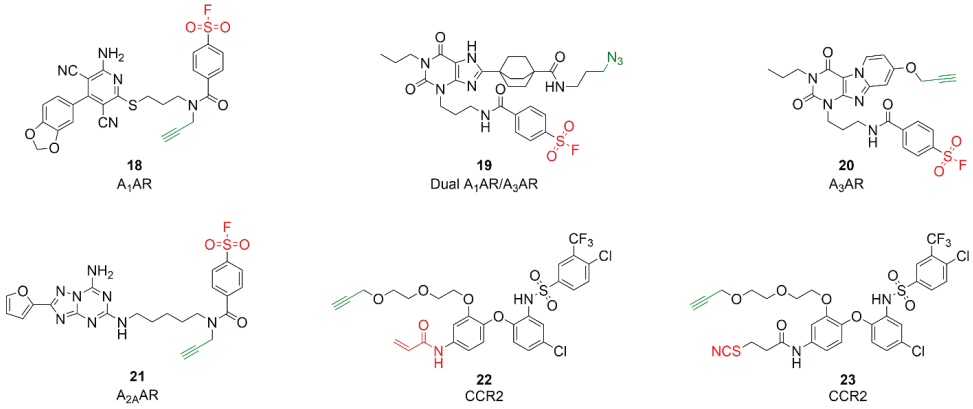

Figure 4. Molecular structures of electrophilic affinity-based probes and their target GPCRs. Shown in red are the electrophiles, shown in green are the click handles for functionalization.

2.1.4. Broad-spectrum affinity-based probes

Besides targeting one specific GPCR, a (sub)family of GPCRs might also be targeted by a 'broad-spectrum' AfBP. Broad-spectrum activity-based probes have already found their widespread use in proteomic studies towards various families of enzymes, such as hydrolases, proteases and kinases. In case of GPCRs, the 'high affinity' moiety of the probe should be a molecular scaffold that binds to multiple GPCRs. Steroids are a good example, as these molecules have shown to allosterically bind GPCRs in crystallization studies. In fact, both cholesterol and bile acid have been transformed in broad spectrum photo-affinity probes **24** and **25** for proteomics studies.[48,49] Next to that, the Δ8/9-Tetrahydrocannabinol (THC)-based

probes **26** and **27** have been developed for the investigation of all THC-binding proteins besides their target cannabinoid receptors (Figure 5).[50,51] However, the number of GPCRs detected by these broad-spectrum probes is still smaller than expected, presumably due to low expression levels of GPCRs as compared to other proteins binders. For example, C-X-C motif chemokine receptor 4 (CXCR4) is one of the GPCRs detected by utilization of probe **24**, though presumably picked up due to its relatively high expression levels in the cell line used.[52] Improvements to the enrichment of GPCRs, e.g. during protein solubilization steps,[53] is therefore necessary for the future detection of GPCRs with broad-spectrum AfBPs.

2.2. Ligand-directed probes

LD probes are very similar to AfBPs as they also consist of three functional moieties, (1) a high affinity-ligand that induces selectivity, (2) an electrophilic group that reacts with a nucleophilic amino acid residue, and (3) a reporter group for detection in chemical biological assays. The main difference between AfBPs and LD probes is the electrophilic group. Upon reacting with a nucleophilic amino acid residue, the electrophilic group of an LD probe induces bond cleavage between the high affinity ligand and the reporter group (Figure 1B), allowing the high affinity-ligand to leave the binding pocket after donation of the reporter group to the protein. LD probes are therefore interesting new tools to label native GPCRs, without occupying the GPCR ligand binding pockets.

The idea of LD probes has been developed by Hamachi and coworkers, where multiple electrophilic groups have been investigated for their use in LD chemistry, examples being the tosyl, dibromo benzoate, acyl imidazole and *N*-acyl, *N*-alkyl sulfonamide groups.[54–57] An important note is that the right balance should be found between selectivity and reactivity of the electrophile, to prevent off-target labeling of the LD probe. The same team also provided evidence for the first LD probe capable of tagging a GPCR.[55,58] Over the past decade, multiple research groups have followed, resulting in a in a recent increase in LD probes as tools to study GPCRs. Also in case of LD probes, one-step and two-step probes have been developed. These will be discussed in the paragraphs below.

2.2.1. One-step ligand-directed probes

Early examples of one-step LD probes use the acyl imidazole group as electrophile,[55,59] while more recent one-step LD probes have also implemented 2-nitrophenyl esters, 2-fluorophenyl esters and *N*-acyl, *N*-alkyl sulfonamides as electrophilic groups (Figure 6).[60–62] An interesting strategy is the use of the *O*-nitrobenzoxadiazole moiety as both the electrophile and the fluorophore in LD probes **35** and **36**.[62,63] Upon nucleophilic attack by a proximal lysine residue, the moiety becomes fluorescent, resulting in a measurable 'turn-on' signal upon receptor binding. Besides the nitrobenzoxadiazole group, one-step LD probes have been conjugated to biotin and fluorophore moieties and used in SDS-PAGE, flow cytometry and confocal microscopy experiments. One-step LD probes have been developed for the bradykinin B_2 receptor (B_2R),[64] $A_{2A}AR$,[60,61] metabotropic glutamate receptor 1 ($mGlu_1R$),[65] μ opioid receptor (MOR),[59], dopamine D1 receptor (D_1R),[66] CB_2R,[62] and smoothened receptor (SMOR).[63] Of these one-step LD probes, **30** has been used to selectively target endogenous A_{2A}ARs on breast cancer cells; and one-step LD Probes **31** and **32** have been used to selectively label endogenously expressed mGlu1R and MOR, respectively, in brain slices derived from rodents.[59,65]

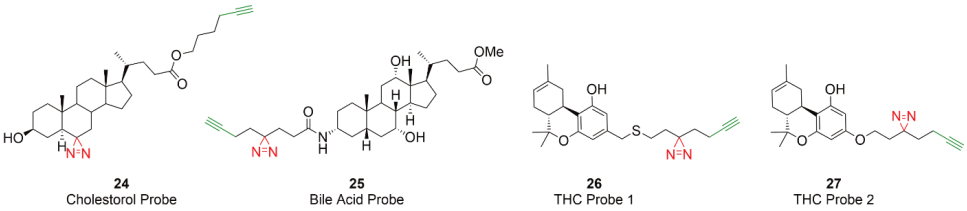

Figure 5. Molecular structures of broad-spectrum affinity-based probes and the names of their parent molecules. Shown in red are the photoreactive groups, shown in green are the click handles for functionalization.

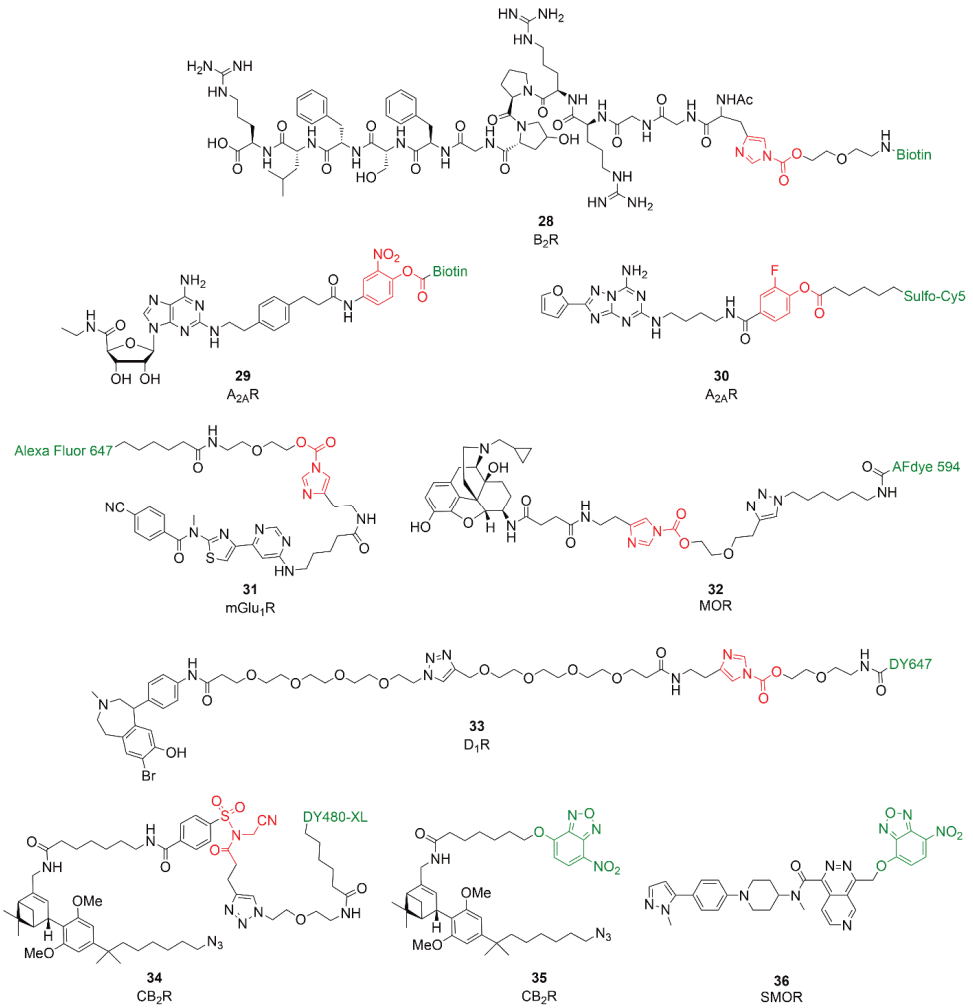

Figure 6. Molecular structures of one-step ligand-directed probes and their GPCR targets. Show in in red are the electrophilic groups and in green the reporter groups.

2.2.2. Two-step ligand-directed probes

Incorporation of a click handle increases the versatility of the LD probe, however also demands the implementation of an additional 'click' step during labeling assays. The latter might hamper the use of LD probes in cellular environments. The first two-step LD probes for GPCRs were based on a catalytic mode of action: a high-affinity ligand was conjugated to a catalytic group, e.g. a dimethyl aminopyridine (DMAP) or pyridinium oxide (PyrOx) moiety, that catalyzes the reaction of the reporter molecule with a nearby nucleophilic amino acid residue (Figure 7).[58,67] This strategy has been used to substitute fluorophores onto the B_2R, among other protein targets,[58] and allowed receptor labeling in SDS-PAGE and confocal microscopy experiments. These reactions however, are not specific between two functional groups and might therefore result in unwanted off-target labeling. Instead, a click handle has been implemented in the recently developed two-step LD probe **38** for the adenosine A_{2B} receptor ($A_{2B}AR$) (chapter 6). This LD probe incorporated an *N*-acyl, *N*-alkyl sulfonamide group as electrophile for donation of a clickable terminal alkyne group to the $A_{2B}AR$, as observed in SDS-PAGE experiments.

2.3. Glycan-targeting probes

Glycosylation is a PTM expected to be present on all cell surface GPCRs.[6] A strategy has been developed that makes use of glycosylation to covalently label all cell surface proteins, including GPCRs.[68,69] First, the oligosaccharides within the glycan chain are mildly oxidized to generate aldehyde groups that function as electrophiles. Next, a trifunctional probe is added, again containing three functional moieties, (1) a high affinity ligand; (2) a nucleophilic group; and (3) a reporter group for detection. The trifunctional probe binds to the target GPCR and subsequently forms a covalent bond with an aldehyde of a proximal glycan chain (Figure 1C), allowing detection of the GPCR in biochemical assays. The first glycan-targeting probe (coined 'TRICEPS') implemented trifluoroacetylated hydrazine as nucleophile, while later probes implemented aminooxy groups ('ASB' probe) and acetone protected hydrazine groups ('HATRIC' probe) (Figure 8).[68–71] Noteworthy, all the reported glycan-targeting probes need to be 'pre-coupled' to a GPCR ligand prior to their utilization in biochemical assays. Pre-coupling is carried out via the electrophilic *N*-hydroxy succinimide ester or the nucleophilic thiol group. Biotin has been the reporter moiety of choice in all these examples. Of these glycan-targeting probes, **39** has been used in target identification experiments, leading to the detection and identification of the Apelin Receptor (APLNR)[68] and Latrophilin 2 receptor (LPHN2R)[72] via pull-down proteomics.

2.4. Metabolic incorporation of two-step probes

Huge efforts have been performed in the labs of Lin and Sakmar on the incorporation of unnatural amino acids into the peptide sequence of GPCRs.[12,73] These include amino acids that contain photoreactive or clickable groups. Although these probes are beyond the scope of this review, there are two interesting strategies that metabolically incorporate probes without altering the genetic code of the GPCR (Figure 1D). First, clickable oligosaccharide **42** has been incorporated in the glycan chains of the Histamine H3 Receptor (H_3R) (Figure 9). This has led to the detection of the H_3R in FRET-based assays.[74] Secondly, clickable variants of palmitic acid **43** and **44** have been metabolically incorporated as S-palmitoyl groups. This allowed identification of the palmitoylation sites at the α_1 adrenergic receptor (α_1R),[75] β_1 and β_2 adrenergic receptors (β_1R and β_2R),[76,77] MOR[78] and D_2R[79] through SDS-PAGE and western blot experiments.

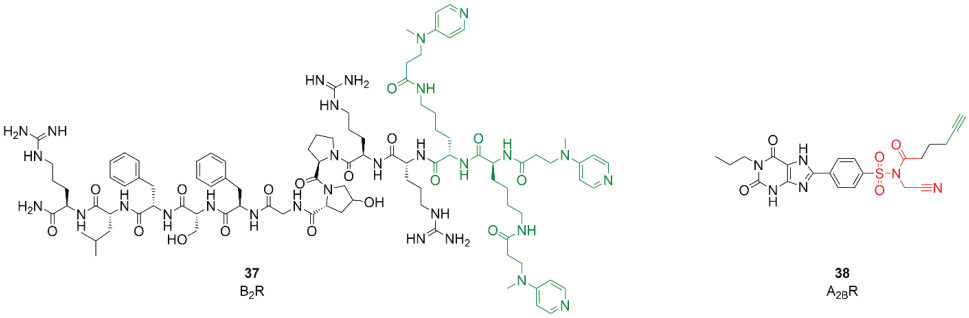

Figure 7. Molecular structures of two-step ligand directed probes and their GPCR targets. Shown in green are the chemical groups that allow functionalization of the receptor, show in red are the electrophilic groups.

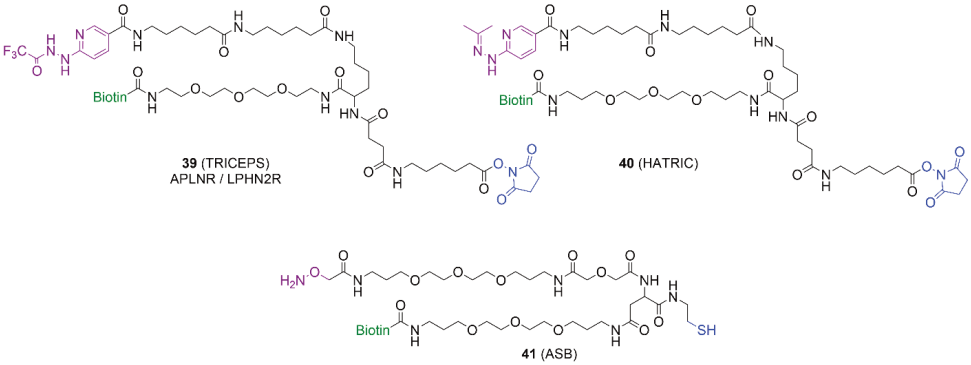

Figure 8. Molecular structures of glycan-targeting probes and their GPCR targets. Shown in purple are the nucleophiles responsible for glycan binding, show in green are the detection moieties and shown in blue are the chemical groups that allow ligand incorporation.

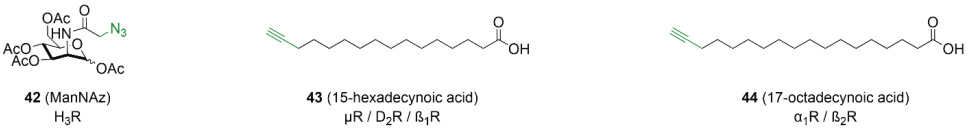

Figure 9. Molecular structures of two-step probes for metabolic incorporation and their target GPCRs. Shown in green are the click handles for functionalization.

3. Concluding Remarks

Over the past decade a modest set of roughly 40 small molecular probes has been developed for the covalent functionalization of GPCRs (Table 1). These include affinity-based probes, ligand-directed probes, glycan-targeting probes and metabolic probes, using either a one- or two-step labeling strategy. Depending on the envisioned assay setup, a specific type of probe might be preferable, e.g. one-step probes might be suitable for live-cell imaging experiments, while ligand-directed probes might be used to track receptors upon ligand binding.

Thus far, most of the reported functionalized covalent probes have been used to detect the presence of the receptor using overexpressing cell lines, although in some studies receptor expression was assessed in human blood cells,[37,45] mouse adipocytes,[43] or brain slices from rats and mice.[59,65] Similar studies on GPCR expression have also been carried out using reversible ligands, either fluorescent or radiolabeled, and are therefore not a specific application of covalent probes. However, functionalized covalent probes can be used to track GPCR localization inside the cell without possible loss of reversibly bound detection moieties. This is exemplified in literature by the detection of agonist-induced internalization.[28,29,43,64]

Next to that, covalent functionalization of GPCRs has also revealed the presence of several PTMs, of which *N*-glycosylation has been the most evident.[29,37,43,45,58,64]. Glycan-targeting and clickable sugar moieties are based on the idea of receptor glycosylation.[68–71,74] Nevertheless, many questions remain regarding location and sequence of *N*- and *O*-glycosylation, as well as their regulatory effects on receptor functioning.[6,7,80] *S*-palmitoylation as a PTM has been studied with two-step metabolic fatty acid probes to investigate agonist-induced internalization,[76] receptor stability and trafficking for their respective GPCRs.[77,79]

Furthermore, covalent probes have shown to be elegant tools for the target identification of bioactive molecules using pull-down proteomics.[40,48–50,72] Yet, such proteomic strategies have not always yielded a detectable signal of the target GPCR.[39,41,81] Careful examination of multiple variables, e.g. expression level, solubilization and digestion methods, is therefore of great importance in target identification studies.[8,32,43,53,70] Further complicating, GPCRs also form signaling complexes, interacting with both membrane and cytosolic proteins. Several of the aforementioned probes have already identified potential interaction partners of GPCRs.[30,32,34,39,41] However, in such experiments, careful analysis is necessary to distinguish between off-target proteins and true PPI partners.

4. Outlook

For future studies, the toolbox with functionalized covalent probes will aid thorough investigations of GPCRs. Example studies in the near future can be: (i) covalently tagging GPCRs with fluorophores to track GPCRs intracellularly, investigating possible signaling activity on intracellular organelles.[10] (ii) Covalently tagging GPCRs with biotin to perform pull-down proteomics and subsequent MS experiments, identifying PTMs through sophisticated MS analysis software.[6,82] (iii) Covalently tagging GPCRs with fluorophores or biotin to detect protein interaction partners, using cross-linking chemistry (pull-down proteomics) or counterstaining (fluorescent microscopy) methods.[83,84]

Altogether, there are many possibilities to make smart use of functionalized covalent probes. However, it must be noted that these probes do not replace reversible probes, genetic techniques or metabolic techniques to functionalize receptors. Instead, these techniques are complementary towards one another, all yielding their own subset of information. In the future, this combined toolbox filled with reversible, covalent, genetic and metabolic probes will therefore be of great use in answering fundamental questions regarding GPCRs.

Table 1. List of functionalized covalent probes for GPCRs, sorted by GPCR name.

Target GPCR	Probe	Name	Type of probe	Electrophile	Reporter	Detection Methods	Ref
5-HT_{1A}R	**7**	**5**	one-step photo-affinity	benzophenone	biotin	mass spectrometry	[34]
5-HT_{1A}R	**9**	**7**	two-step photo-affinity	benzophenone	alkyne	SDS-PAGE	[34]
5-HT_6R	**8**	**16**	one-step photo-affinity	benzophenone	biotin	mass spectrometry	[34]
5-HT_6R	**10**	**18**	two-step photo-affinity	benzophenone	alkyne	SDS-PAGE	[34]
A_1AR	**18**	LUF7909	two-step electrophilic	fluorosulfonyl	alkyne	SDS-PAGE, microscopy, mass spectrometry	[43]
A_1AR, A_3AR	**19**	UODC9	two-step electrophilic	fluorosulfonyl	alkyne	SDS-PAGE	[44]
A_{2A}AR	**30**	**1**	one-step ligand-directed	2-fluorophenyl ester	Cy5	SDS-PAGE, TR-FRET, microscopy	[61]
A_{2A}AR	**29**	**3c**	one-step ligand-directed	2-nitrophenyl ester	biotin	-	[60]
A_{2A}AR	**21**	LUF7487	two-step electrophilic	fluorosulfonyl	alkyne	SDS-PAGE	[46]
A_{2B}AR	**38**	LUF8019	two-step ligand-directed	*N*-acyl, *N*-alkyl sulfonamide	alkyne	SDS-PAGE	-
A_3AR	**20**	LUF7960	two-step electrophilic	fluorosulfonyl	alkyne	SDS-PAGE, flow cytometry, microscopy	[45]
B_2R	**28**	**3**	one-step ligand-directed	Acyl imidazole	biotin	SDS-PAGE, microscopy	[64]
B_2R	**37**	**9**	two-step ligand-directed	-	tri-DMAP	SDS-PAGE, microscopy	[58]
CB_2R	**34**	**15**	one-step ligand-directed	*N*-acyl, *N*-alkyl sulfonamide	DY-480XL	Imaging flow cytometry, microscopy	[62]
CB_2R	**35**	**2b**	one-step ligand-directed	*O*-nitro benzoxa diazole	*O*-nitro benzoxa diazole	TR-FRET	[62]
CB_2R	**13**	LEI121	two-step photo-affinity	diazirine	alkyne	SDS-PAGE, flow cytometry, mass spectrometry	[37]
CCR2	**22**	LUF7834	two-step electrophilic	acrylamide	alkyne	SDS-PAGE, mass spectrometry	[47]

CCR2	**23**	LUF7835	two-step electrophilic	thiocyanate	Alkyne	SDS-PAGE, mass spectrometry	[47]
CXCR4	**1**	ATI-2766	one-step photo-affinity	diazirine	TAMRA	SDS-PAGE, microscopy	[28]
D_1R	**33**	**5h**	one-step ligand-directed	acyl imidazole	DY647	TR-FRET, microscopy	[66]
D_2R	**17**	**5**	two-step photo-affinity	benzophenone	alkyne	SDS-PAGE, flow cytometry, microscopy, mass spectrometry	[41]
D_2R	**5**	CPT-00031	one-step photo-affinity	diazirine	biotin	SDS-PAGE, mass spectrometry	[32]
D_2R	**4**	Probe 7	one-step photo-affinity	2-aryl, 5-carboxy tetrazole	biotin	mass spectrometry	[31]
FPR1	**2**	Probe-TAMRA	one-step photo-affinity	diazirine	TAMRA	SDS-PAGE, flow cytometry, microscopy	[29]
$GABA_B$	**3**	CGP 64213^B	one-step photo-affinity	diazirine	biotin	SDS-PAGE	[30]
GPR39	**14**	**1A**	two-step photo-affinity	diazirine	alkyne	mass spectrometry	[38]
GPR75	**15**	20-ApheDa	two-step photo-affinity	benzophenone	azide	SDS-PAGE, mass spectrometry	[39]
GPRC5A	**16**	x-alk-TA	two-step photo-affinity	diazirine	alkyne	SDS-PAGE, microscopy, mass spectrometry	[40]
$mGlu_1R$	**31**	CmGlu1M	one-step ligand-directed	acyl imidazole	Alexa Fluor 647	SDS-PAGE, microscopy	[65]
$mGlu_2R$	**11**	(±)**-14**	two-step photo-affinity	acetophenone	alkyne	SDS-PAGE, microscopy	[35]
$mGlu_5R$	**12**	**8**	two-step photo-affinity	phenyl azide	alkyne	SDS-PAGE	[36]
MOR	**32**	NAI-A594	one-step ligand-directed	acyl imidazole	Alexa 594	SDS-PAGE, flow cytometry, microscopy	[59]
NK_1R	**6**	Ac-Nle-SP-probe	one-step photo-affinity	diazirine	biotin	SDS-PAGE, microscopy, mass spectrometry	[33]
SMOR	**36**	**9**	one-step ligand-directed	*O*-nitro benzoxadiazole	*O*-nitro benzoxadiazole	SDS-PAGE	[63]

[a] Nucleophilic group that reacts with oxidized glycan chains.

References

[1] S. M. Foord, T. I. Bonner, R. R. Neubig, E. M. Rosser, J. P. Pin, A. P. Davenport, M. Spedding, A. J. Harmar, *Pharmacol Rev* **2005**, *57*, 279–288.

[2] T. Schöneberg, I. Liebscher, *Pharmacol Rev* **2021**, *73*, 89–119.

[3] D. Yang, Q. Zhou, V. Labroska, S. Qin, S. Darbalaei, Y. Wu, E. Yuliantie, L. Xie, H. Tao, J. Cheng, Q. Liu, S. Zhao, W. Shui, Y. Jiang, M. W. Wang, *Signal Transduct Target Ther* **2021**, *6*, 7.

[4] K. A. Jacobson, *Biochem Pharmacol* **2015**, *98*, 541–555.

[5] D. M. Rosenbaum, S. G. F. Rasmussen, B. K. Kobilka, *Nature* **2009**, *459*, 356–363.

[6] A. Patwardhan, N. Cheng, J. Trejo, *Pharmacol Rev* **2021**, *73*, 120–151.

[7] C. K. Goth, U. E. Petäjä-Repo, M. M. Rosenkilde, *ACS Pharmacol Transl Sci* **2020**, *3*, 237–245.

[8] A. O. Helbig, A. J. R. Heck, M. Slijper, *J Proteomics* **2010**, *73*, 868–878.

[9] S. Elschenbroich, Y. Kim, J. A. Medin, T. Kislinger, *Expert Rev Proteomics* **2010**, *7*, 141–154.

[10] M. Ali, M. Nezhady, J. C. Rivera, S. Chemtob, *iScience* **2020**, *23*, 101643.

[11] M. M. Shchepinova, A. C. Hanyaloglu, G. S. Frost, E. W. Tate, *Curr Opin Chem Biol* **2020**, *56*, 98–110.

[12] T. Huber, T. P. Sakmar, *Chem Biol* **2014**, *21*, 1224–1237.

[13] M. Soave, L. A. Stoddart, C. W. White, L. E. Kilpatrick, J. Goulding, S. J. Briddon, S. J. Hill, *FEBS Journal* **2021**, *288*, 2585–2601.

[14] Y. Wu, B. Zhang, H. Xu, M. He, X. Deng, L. Zhang, Q. Dang, J. Fan, Y. Guan, X. Peng, W. Sun, *Coord Chem Rev* **2023**, *480*, 215040.

[15] C. A. Flanagan, *Methods Cell Biol* **2016**, *132*, 191–215.

[16] C. J. Hutchings, M. Koglin, W. C. Olson, F. H. Marshall, *Nat Rev Drug Discov* **2017**, *16*, 787–810.

[17] L. Dahl, I. B. Kotliar, A. Bendes, T. Dodig-Crnković, S. Fromm, A. Elofsson, M. Uhlén, T. P. Sakmar, J. M. Schwenk, *bioRxiv* **2022**, 2022.11.24.517810.

[18] H. Cernecka, P. Ochodnicky, W. H. Lamers, M. C. Michel, *Naunyn Schmiedebergs Arch Pharmacol* **2012**, *385*, 875–882.

[19] Y. Marchalant, P. W. Brownjohn, A. Bonnet, T. Kleffmann, J. C. Ashton, *Journal of Histochemistry and Cytochemistry* **2014**, *62*, 395–404.

[20] G. Tomasello, I. Armenia, G. Molla, *Bioinformatics* **2020**, *36*, 2909–2911.

[21] Y. Liu, M. P. Patricelli, B. F. Cravatt, *PNAS* **1999**, *96*, 14694–14699.

[22] P. P. Geurink, L. M. Prely, G. A. Van Der Marel, R. Bischoff, H. S. Overkleeft, *Top Curr Chem* **2012**, *324*, 85–113.

[23] M. Gehringer, S. A. Laufer, *J Med Chem* **2019**, *62*, 5673–5724.

[24] H. Ovaa, P. F. Van Swieten, B. M. Kessler, M. A. Leeuwenburgh, E. Fiebiger, A. M. C. H. Van den Nieuwendijk, P. J. Galardy, G. A. Van der Marel, H. L. Ploegh, H. S. Overkleeft, *Angew Chem Int Ed* **2003**, *42*, 3626–3629.

[25] A. E. Speers, G. C. Adam, B. F. Cravatt, *J Am Chem Soc* **2003**, *125*, 4686–4687.

[26] J. A. Prescher, C. R. Bertozzi, *Nat Chem Biol* **2005**, *1*, 13–21.

[27] A. Grunbeck, T. P. Sakmar, *Biochemistry* **2013**, *52*, 8625–8632.

[28] J. M. Janz, Y. Ren, R. Looby, M. A. Kazmi, P. Sachdev, A. Grunbeck, L. Haggis, D. Chinnapen, A. Y. Lin, C. Seibert, T. McMurry, K. E. Carlson, T. W. Muir, S. Hunt, T. P. Sakmar, *J Am Chem Soc* **2011**, *133*, 15878–15881.

[29] D. H. Field, J. S. White, S. L. Warriner, M. H. Wright, *RSC Chem Biol* **2023**, *4*, 216–222.

[30] X. Lin, X. Li, M. Jiang, L. Chen, C. Xu, W. Zhang, H. Zhao, B. Sun, X. Xu, F. Nan, J. Liu, *Biochemical Journal* **2012**, *443*, 627–634.

[31] R. Miyajima, K. Sakai, Y. Otani, T. Wadatsu, Y. Sakata, Y. Nishikawa, M. Tanaka, Y. Yamashita, M. Hayashi, K. Kondo, T. Hayashi, *ACS Chem Biol* **2020**, *15*, 2364–2373.

[32] C. Blex, S. Michaelis, A. K. Schrey, J. Furkert, J. Eichhorst, K. Bartho, F. Gyapon Quast, A. Marais, M. Hakelberg, U. Gruber, S. Niquet, O. Popp, F. Kroll, M. Sefkow, R. Schülein, M. Dreger, H. Köster, *ChemBioChem* **2017**, *18*, 1639–1649.

[33] F. M. Müskens, R. J. Ward, D. Herkt, H. van de Langemheen, A. B. Tobin, R. M. J. Liskamp, G. Milligan, *Mol Pharmacol* **2019**, *95*, 196–209.

[34] A. M. Gamo, J. A. González-Vera, A. Rueda-Zubiaurre, D. Alonso, H. Vázquez-Villa, L. Martín-Couce, Ó. Palomares, J. A. Lõpez, M. Martín-Fontecha, B. Benhamú, M. L. Lõpez-Rodríguez, S. Ortega-Gutiérrez, *Chemistry - A European Journal* **2016**, *22*, 1313–1321.

[35] S. D. Hellyer, S. Aggarwal, A. N. Y. Chen, K. Leach, D. J. Lapinsky, K. J. Gregory, *ACS Chem Neurosci* **2020**, *11*, 1597–1609.

[36] K. J. Gregory, R. Velagaleti, D. M. Thal, R. M. Brady, A. Christopoulos, P. J. Conn, D. J. Lapinsky, *ACS Chem Biol* **2016**, *11*, 1870–1879.

[37] M. Soethoudt, S. C. Stolze, M. V. Westphal, L. van Stralen, A. Martella, E. J. van Rooden, W. Guba, Z. V. Varga, H. Deng, S. I. van Kasteren, U. Grether, A. P. IJzerman, P. Pacher, E. M. Carreira, H. S. Overkleeft, A. Ioan-Facsinay, L. H. Heitman, M. van der Stelt, *J Am Chem Soc* **2018**, *140*, 6067–6075.

[38] J. R. Thomas, S. M. Brittain, J. Lipps, L. Llamas, R. K. Jain, M. Schirle, in *Proteomics for Drug Discovery: Methods and Protocols* (Eds.: I.M. Lazar, M. Kontoyianni, A.C. Lazar), Springer New York, New York, NY, **2017**, pp. 1–18.

[39] V. Garcia, A. Gilani, B. Shkolnik, V. Pandey, F. F. Zhang, R. Dakarapu, S. K. Gandham, N. R. Reddy, J. P. Graves, A. Gruzdev, D. C. Zeldin, J. H. Capdevila, J. R. Falck, M. L. Schwartzman, *Circ Res* **2017**, *120*, 1776–1788.

[40] X. Zhao, K. R. Stein, V. Chen, M. E. Griffin, H. C. Hang, *bioRxiv* **2021**, 2021.12.16.472979.

[41] S. T. Kim, E. J. Doukmak, R. G. Flax, D. J. Gray, V. N. Zirimu, E. De Jong, R. C. Steinhardt, *ACS Chem Neurosci* **2022**, *13*, 3008–3022.

[42] D. Weichert, P. Gmeiner, *ACS Chem Biol* **2015**, *10*, 1376–1386.

[43] B. L. H. Beerkens, Ç. Koç, R. Liu, B. I. Florea, S. E. Le Dévédec, L. H. Heitman, A. P. IJzerman, D. van der Es, *ACS Chem Biol* **2022**, *17*, 3131–3139.

[44] P. N. H. Trinh, D. J. W. Chong, K. Leach, S. J. Hill, J. D. A. Tyndall, L. T. May, A. J. Vernall, K. J. Gregory, *J Med Chem* **2021**, *64*, 8161–8178.

[45] B. L. H. Beerkens, I. M. Snijders, J. Snoeck, R. Liu, A. T. J. Tool, S. E. Le Dévédec, W. Jespers, T. W. Kuijpers, G. J. P. van Westen, L. H. Heitman, A. P. IJzerman, D. van der Es, *ChemRxiv* **2023**, DOI 10.26434/chemrxiv-2023-6g59z.

[46] X. Yang, T. J. M. Michiels, C. de Jong, M. Soethoudt, N. Dekker, E. Gordon, M. van der Stelt, L. H. Heitman, D. van der Es, A. P. IJzerman, *J Med Chem* **2018**, *61*, 7892–7901.

[47] L. S. den Hollander, S. Dekkers, B. L. H. Beerkens, J. P. D. van Veldhoven, N. V. O. Ortiz-Zacharías, C. van der Horst, I. Sieders, B. de Valk, J. Wang, A. P. IJzerman, D. van der Es, L. H. Heitman, *manuscript in preparation* **n.d.**

[48] J. J. Hulce, A. B. Cognetta, M. J. Niphakis, S. E. Tully, B. F. Cravatt, *Nat Methods* **2013**, *10*, 259–264.

[49] S. Zhuang, Q. Li, L. Cai, C. Wang, X. Lei, *ACS Cent Sci* **2017**, *3*, 501–509.

[50] M. Soethoudt, G. Alachouzos, E. J. Van Rooden, M. D. Moya-Garzón, R. J. B. H. N. Van Den Berg, L. H. Heitman, M. Van Der Stelt, *Cannabis Cannabinoid Res* **2018**, *3*, 136–151.

[51] Y.-J. Lim, G. Tang, Z. Ye, C.-J. Zhang, J. Wu, S. Q. Yao, *Chemistry – A European Journal* **2023**, e202300531.

[52] C. Park, J. W. Lee, K. Kim, D. S. Seen, J. Y. Jeong, W. K. Huh, *Sci Rep* **2023**, *13*, 1894.

[53] J. S. Behnke, L. H. Urner, *Anal Bioanal Chem* **2023**, DOI 10.1007/s00216-023-04584-z.

[54] S. Tsukiji, M. Miyagawa, Y. Takaoka, T. Tamura, I. Hamachi, *Nat Chem Biol* **2009**, *5*, 341–343.

[55] S. H. Fujishima, R. Yasui, T. Miki, A. Ojida, I. Hamachi, *J Am Chem Soc* **2012**, *134*, 3961–3964.

[56] Y. Takaoka, Y. Nishikawa, Y. Hashimoto, K. Sasaki, I. Hamachi, *Chem Sci* **2015**, *6*, 3217–3224.

[57] T. Tamura, T. Ueda, T. Goto, T. Tsukidate, Y. Shapira, Y. Nishikawa, A. Fujisawa, I. Hamachi, *Nat Commun* **2018**, *9*, 1870.

[58] H. Wang, Y. Koshi, D. Minato, H. Nonaka, S. Kiyonaka, Y. Mori, S. Tsukiji, I. Hamachi, *J Am Chem Soc* **2011**, *133*, 12220–12228.

[59] S. Arttamangkul, A. Plazek, E. J. Platt, H. Jin, T. F. Murray, W. T. Birdsong, K. C. Rice, D. L. Farrens, J. T. Williams, *Elife* **2019**, *8*, e49319.

[60] S. M. Moss, P. S. Jayasekara, S. Paoletta, Z. G. Gao, K. A. Jacobson, *ACS Med Chem Lett* **2014**, *5*, 1043–1048.

[61] L. A. Stoddart, N. D. Kindon, O. Otun, C. R. Harwood, F. Patera, D. B. Veprintsev, J. Woolard, S. J. Briddon, H. A. Franks, S. J. Hill, B. Kellam, *Commun Biol* **2020**, *3*, 722.

[62] M. Kosar, D. A. Sykes, A. E. G. Viray,] Rosa, M. Vitale, R. C. Sarott, R. L. Ganzoni, D. Onion, J. M. Tobias, P. Leippe, C. Ullmer, E. A. Zirwes, W. Guba, U. Grether, J. A. Frank, D. B. Veprintsev, E. M. Carreira, *ChemRxiv* **2022**, DOI 10.26434/chemrxiv-2022-z58fd.

[63] D. Xue, L. Ye, J. Zheng, Y. Wu, X. Zhang, Y. Xu, T. Li, R. C. Stevens, F. Xu, M. Zhuang, S. Zhao, F. Zhao, H. Tao, *Org Biomol Chem* **2019**, *17*, 6136–6142.

[64] T. Miki, S. H. Fujishima, K. Komatsu, K. Kuwata, S. Kiyonaka, I. Hamachi, *Chem Biol* **2014**, *21*, 1013–1022.

[65] H. Nonaka, S. Sakamoto, K. Shiraiwa, M. Ishikawa, T. Tamura, K. Okuno, S. Kiyonaka, E. A. Susaki, C. Shimizu, H. R. Ueda, W. Kakegawa, I. Arai, I. Hamachi, *bioRxiv* **2023**, 2023.01.16.524180.

[66] X. Gómez-Santacana, M. Boutonnet, C. Martínez-Juvés, J. L. Catena, E. Moutin, T. Roux, E. Trinquet, L. Lamarque, J. Perroy, L. Prézeau, J. M. Zwier, J.-P. Pin, A. Llebaria, *ChemRxiv* **2022**, DOI 10.26434/chemrxiv-2022-mqqtz-v2.

[67] T. Tamura, Z. Song, K. Amaike, S. Lee, S. Yin, S. Kiyonaka, I. Hamachi, *J Am Chem Soc* **2017**, *139*, 14181–14191.

[68] A. P. Frei, O. Y. Jeon, S. Kilcher, H. Moest, L. M. Henning, C. Jost, A. Plückthun, J. Mercer, R. Aebersold, E. M. Carreira, B. Wollscheid, *Nat Biotechnol* **2012**, *30*, 997–1001.

[69] A. P. Frei, H. Moest, K. Novy, B. Wollscheid, *Nat Protoc* **2013**, *8*, 1321–1336.

[70] T. L. Tremblay, J. J. Hill, *Sci Rep* **2017**, *7*, 46574.

[71] N. Sobotzki, M. A. Schafroth, A. Rudnicka, A. Koetemann, F. Marty, S. Goetze, Y. Yamauchi, E. M. Carreira, B. Wollscheid, *Nat Commun* **2018**, *9*, 1519.

[72] G. N. Yin, D. K. Kim, J. I. Kang, Y. Im, D. S. Lee, A. reum Han, J. Ock, M. J. Choi, M. H. Kwon, A. Limanjaya, S. B. Jung, J. Yang, K. W. Min, J. Yun, Y. Koh, J. E. Park, D. Hwang, J. K. Suh, J. K. Ryu, H. M. Kim, *Exp Mol Med* **2022**, *54*, 626–638.

[73] S. K. Gangam, Q. Lin, in *Methods Enzymol*, Academic Press Inc., **2020**, pp. 95–111.

[74] H. Stockmann, V. Todorovic, P. L. Richardson, V. Marin, V. Scott, C. Gerstein, M. Lake, L. Wang, R. Sadhukhan, A. Vasudevan, *J Am Chem Soc* **2017**, *139*, 16822–16829.

[75] E. P. Marin, L. Jozsef, A. di Lorenzo, K. F. Held, A. K. Luciano, J. Melendez, L. M. Milstone, H. Velazquez, W. C. Sessa, *Arterioscler Thromb Vasc Biol* **2016**, *36*, 370–379.

[76] D. M. Zuckerman, S. W. Hicks, G. Charron, H. C. Hang, C. E. Machamer, *Journal of Biological Chemistry* **2011**, *286*, 19014–19023.

[77] N. Adachi, D. T. Hess, P. McLaughlin, J. S. Stamler, *Journal of Biological Chemistry* **2016**, *291*, 20232–20246.

[78] B. Ebersole, J. Petko, R. Levenson, *Anal Biochem* **2014**, *451*, 25–27.

[79] B. Ebersole, J. Petko, M. Woll, S. Murakami, K. Sokolina, V. Wong, I. Stagljar, B. Lüscher, R. Levenson, *PLoS One* **2015**, *10*, e0140661.

[80] L. Verhallen, J. J. Lackman, R. Wendt, M. Gustavsson, Z. Yang, Y. Narimatsu, D. M. Sørensen, K. Mac Lafferty, M. Gouwy, P. E. Marques, G. M. Hjortø, M. M. Rosenkilde, P. Proost, C. K. Goth, *Cellular and Molecular Life Sciences* **2023**, *80*, 55.

[81] A. Garelli, F. Heredia, A. P. Casimiro, A. Macedo, C. Nunes, M. Garcez, A. R. M. Dias, Y. A. Volonte, T. Uhlmann, E. Caparros, T. Koyama, A. M. Gontijo, *Nat Commun* **2015**, *6*, 8732.

[82] J. v. Olsen, M. Mann, *Molecular and Cellular Proteomics* **2013**, *12*, 3444–3452.

[83] O. Klykov, B. Steigenberger, S. Pektaş, D. Fasci, A. J. R. Heck, R. A. Scheltema, *Nat Protoc* **2018**, *13*, 2964–2990.

[84] A. R. B. Thomsen, B. Plouffe, T. J. Cahill, A. K. Shukla, J. T. Tarrasch, A. M. Dosey, A. W. Kahsai, R. T. Strachan, B. Pani, J. P. Mahoney, L. Huang, B. Breton, F. M. Heydenreich, R. K. Sunahara, G. Skiniotis, M. Bouvier, R. J. Lefkowitz, *Cell* **2016**, *166*, 907–919.

Chapter 3

Development of subtype-selective covalent ligands for the adenosine A_{2B} receptor by tuning the reactive group

Bert L. H. Beerkens, Xuesong Wang, Maria Avgeropoulou, Lisa N. Adistia, Jacobus P.D. van Veldhoven, Willem Jespers, Rongfang Liu, Laura H. Heitman, Adriaan P. IJzerman and Daan van der Es

Abstract
Signaling through the adenosine receptors (ARs), in particular through the adenosine A_{2B} receptor (A_{2B}AR), has shown to play a role in a variety of pathological conditions, ranging from immune disorders to cancer. Covalent ligands for the A_{2B}AR have the potential to irreversibly block the receptor, as well as inhibit all A_{2B}AR-induced signaling pathways. This will allow a thorough investigation of the pathophysiological role of the receptor. In this study, we synthesized and evaluated a set of potential covalent ligands for the A_{2B}AR. The ligands all contain a core scaffold consisting of a substituted xanthine, varying in type and orientation of electrophilic group (warhead). Here, we find that the right combination of these variables is necessary for a high affinity, irreversible mode of binding and selectivity towards the A_{2B}AR. Altogether, this is the case for sulfonyl fluoride **24** (LUF7982), a covalent ligand that allows for novel ways to interrogate the A_{2B}AR.

RSC Med Chem **2022**, *13*, 850–856.

Introduction

The endogenous molecule adenosine acts as a signaling molecule on the G Protein-Coupled Receptor (GPCR) subfamily of adenosine receptors (ARs): the A_1, A_{2A}, A_{2B} and A_3 adenosine receptors (A_1AR, A_{2A}AR, A_{2B}AR and A_3AR).[1] Elevated concentrations of adenosine have been observed in various pathological conditions, e.g. cancer, inflammation and hypoxia, implying an important role for AR signaling.[2,3] Antagonizing ARs and blocking the adenosine-induced signaling pathways is therefore an interesting strategy to tackle a broad spectrum of pathological conditions.[4]

A_{2B}AR receptor activation has been linked to hallmarks of cancer, i.e. cancer cell proliferation, tumor growth, tumor metastasis and the suppression of surrounding immune cells, among others.[5–7] In fact, multiple clinical trials are currently investigating the inhibition of the A_{2B}AR in cancers, e.g. in combination with an A_{2A}AR antagonist or immune stimulants.[5] Nevertheless, persistent high levels of extracellular adenosine in the tumor microenvironment might hinder the proper inhibition of A_{2B}AR-induced signaling pathways.

Covalent A_{2B}AR ligands on the other hand, cause an 'infinite' blockade of the A_{2B}AR which constitutes a new strategy that may be deployed in targeting cancer progression as well as studying the inhibition of A_{2B}AR signaling in cancerous cell lines and tissues.[8] After binding reversibly, covalent ligands react with an electrophilic substituent ('warhead') to a nearby amino acid residue, allowing the formation of an irreversible bond with the target protein.[9] This in turn leads to an 'infinite' occupancy of the ligand binding pocket, which in case of the A_{2B}AR would prevent even high levels of adenosine from binding to and activating the receptor.

Besides their medicinal potential, covalent ligands have proven especially useful as tools to study GPCR functioning, as they 'lock' the highly dynamic GPCRs into one conformation.[10] This facilitates purification, isolation and crystallization of the receptor and allows for a more thorough pharmacological characterization on a molecular level.[9,11]

Over the past decades, various high affinity xanthine derivatives have been developed as antagonists for the adenosine receptors.[12] In case of the A_{2B}AR these are mostly N^1, N^3-dipropylxanthines, developed by the lab of Jacobson,[13,14] and N^1-propylxanthines, developed by the lab of Müller.[15–17] While both classes exhibit high affinity, the latter type of compounds generally show higher selectivity towards the A_{2B}AR over the other adenosine receptors. This prompted us to design covalent xanthine derivatives, based on the N^1, N^3-dipropyl and N^1-propyl series. Looking at the A_{2A}AR, structurally the most similar to the A_{2B}AR, multiple covalent ligands have been developed.[18–20] A lysine residue on the second extracellular loop (EL2) of the A_{2A}AR is the target of at least one these ligands.[20] We therefore decided to substitute the herein synthesized xanthines with various electrophilic groups known to react with lysine residues. To increase the chances of covalent binding, we also varied the location of the warhead: either *meta*- or *para*-substituted at the C^8-phenyl ring.

Altogether, we have developed a set of twelve potential xanthine-based covalent ligands. Here, we show the synthesis, affinity, selectivity and covalent mode of action of these ligands.

Results and Discussion

Design of covalent A_{2B}AR ligands

Analyzing the binding mode of xanthines into the A_{2A}AR binding pocket,[21,22] as well as the amino acid sequences of the A_{2A}AR and A_{2B}AR, we found three interesting potential anchors for covalent binding: lysines $K265^{EL3}$, $K267^{EL3}$ and $K269^{7.32}$.[23] In this respect, sulfonyl fluoride, fluorosulfonate and isothiocyanate groups were chosen to target either one of these lysine residues. Sulfonyl fluoride groups (-SO_2F) have recently emerged as warheads that have a weak intrinsic reactivity, are often stable under physiological conditions and, under the same conditions, can be directed to react selectively with lysine or tyrosine moieties on drug targets.[24–26] These beneficial properties have helped to coin the term 'SuFEx' (Sulfonyl Fluoride Exchange) as a type of 'click' chemistry.[27] However, even before the use of sulfonyl fluorides in click chemistry applications, they were incorporated in ligands for the A_1, A_{2A} and A_3 adenosine receptors.[20,28–31] Besides sulfonyl fluorides, we also decided to synthesize ligands containing fluorosulfonate groups (-OSO_2F). Fluorosulfonate groups have shown to bear a much lower intrinsic reactivity, as compared to sulfonyl fluoride groups,[25,32] which might reduce off-target binding events. Lastly, we chose the isothiocyanate group (-NCS) as warhead to be incorporated in the series of ligands. Although known for its reactivity towards cysteine residues, the isothiocyanate group has shown to form a more stable product upon reacting with lysine residues.[33,34] Moreover, the isothiocyanate group has been used to develop potent agonists and antagonists that irreversibly bind to the A_1AR.[35–37] In recent work from our lab, the isothiocyanate group was incorporated in a putative covalent ligand for the A_{2B}AR.[38] This inspired us to further investigate this electrophilic substituent as a warhead to target the A_{2B}AR.

Synthesis of covalent A_{2B}AR ligands

Twelve potential covalent ligands were targeted for synthesis, each containing one of the abovementioned electrophilic warheads at the *meta* or *para* position on the C8-substituted phenyl ring of the xanthines. The synthesis started with 1,3-dipropyl 5,6-diamino uracil (**1**) (commercially obtained), or 1-propyl 5,6-diamino uracil (**16**), synthesized according to procedures reported by Müller *et al.*[39–42] These building blocks were subjected to an EDC-mediated peptide coupling, using 3- or 4-fluorosulfonyl benzoic acid (**2**, **3**, **17** and **18**), 3- or 4-fluorosulfonate benzoic acid (**4**, **5**, **19** and **20**), or benzoic acid containing a protected amine group at the 3- or 4-position (**6**, **7**, **21** and **22**) (Scheme 1). Purification of Boc-protected anilines turned out to be cumbersome in case of the N^1-propyl series, therefore an Fmoc-protection was chosen instead. Next, the substituted uracil derivatives were subjected to a ring closure using trimethylsilyl polyphosphate (PPSE).[43,44] Gratifyingly, the electrophilic sulfonyl fluoride and fluorosulfonate groups stayed intact upon heating at 170 °C and in the presence of PSSE for several hours. In case of the Boc-protected anilines, basic conditions (reflux in 2 M NaOH) were chosen to achieve ring closure.[41] The anilines were then deprotected and subsequently subjected to thiophosgene to yield the corresponding isothiocyanates. Altogether this yielded sulfonyl fluoride-containing ligands **8**, **9**, **23** and **24**, fluorosulfonate-containing ligands **10**, **11**, **25** and **26**, and isothiocyanate-containing ligands **13**, **15**, **28** and **30.**

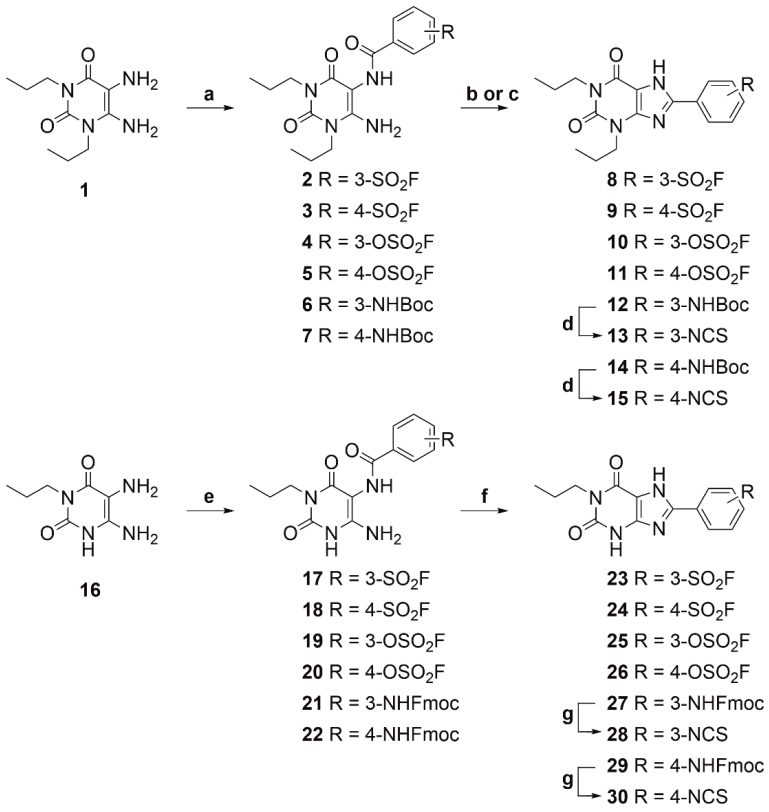

Scheme 1. Synthesis of potential covalent ligands for the A_{2B}AR. Reagents and conditions: (a) EDC·HCl, DIPEA, respective benzoic acid, dry DMF, rt, 2-20 h, 41-68%; (b) PPSE, 170 °C, 1-4 h, 10-53%; (c) 2 M NaOH, dioxane, 120 °C, 2-3 h, 60-84%; (d) (i) TFA, DCM, rt, 1 h; (ii) thiophosgene, 3 M HCl, rt, 2 h, 68-77%; (e) EDC·HCl, respective benzoic acid, dry DMF, rt, 1 h – 2 days, 13-54%; (f) PPSE, 150-170 °C, 2-7 h, 55-88%; (g) (i) piperidine, DMF, rt, 5 min; (ii) thiophosgene, 3 M HCl, rt, 2-4 h, 71-75%.

Assessment of time-dependent affinity towards the A_{2B}AR

To investigate the affinity of the twelve ligands and their potential to bind irreversibly to the A_{2B}AR, radioligand displacement assays were carried out using CHO-spap membranes stably overexpressing the A_{2B}AR. Two different conditions were chosen: no pre-incubation of receptor with ligand (pre 0 h) or a 4 h pre-incubation of receptor with ligand (pre 4 h), prior to the addition of radioligand. The pre-incubation step should allow any covalently binding ligand to irreversibly block the available receptor binding sites, thus increasing its apparent affinity for the receptor.[20,30,31] The reference A_{2B}AR antagonist PSB-1115 was taken along as a non-covalent control.

Interestingly, substitution of the chosen warheads onto the xanthines mostly increased the apparent affinity towards the A_{2B}AR (Table 1; pre 0 h), as compared to the affinity of PSB-1115 in our hands.[15] Various patterns were deducted. First of all, the *para*-substituted xanthines all show a higher apparent affinity than their *meta*-substituted counterparts at 0 h of pre-incubation. Secondly, at 0 h of pre-incubation, the N^1-propyl xanthines show a higher apparent affinity than the N^1, N^3-dipropyl xanthines. The best performing compounds are thus N^1-propyl

xanthines containing a *para*-substituted group. This is in line with the compounds presented in literature.[14–17] Looking at 4 h of pre-incubation (Table 1; pre 4 h), the SO_2F-substituted xanthines and NCS-substituted xanthines all show decent shifts in K_i (>3), regardless of the positioning of the warhead (*meta* or *para*) (Examples depicted in Figures 1A and 1C). On the other hand, the shifts observed for the OSO_2F-substituted xanthines are rather small, close to the values found for PSB-1115 (example in Figure 1B). This suggests a reversible binding mode. The SO_2F-containing xanthines have a higher affinity and K_i shift when substituted at the 4-position, while the NCS-containing xanthines show a higher shift when substituted at the 3-position. The biggest shifts are observed for the 3-NCS-substituted xanthines **13** and **28** (K_i shift of 19 and 74). This is probably the result of a low apparent affinity at 0 h of pre-incubation, in combination with the relatively high reactivity of the NCS group. This K_i shift data hints towards a covalent mode of action among the majority of the xanthine-based ligands.

Table 1. Time-dependent characterization of the synthesized adenosine A_{2B} receptor ligands.

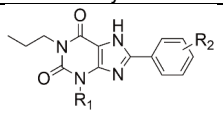

Compound	R_1	R_2	*p*Ki (pre 0 h)[a]	*p*Ki (pre 4 h)[b]	Ki shift[c]
8	Propyl	3-SO_2F	6.02 ± 0.10	6.80 ± 0.16*	7.1
9	Propyl	4-SO_2F	7.22 ± 0.28	8.62 ± 0.18*	27.3
10	Propyl	3-OSO_2F	6.25 ± 0.14	6.28 ± 0.09	1.2
11	Propyl	4-OSO_2F	7.31 ± 0.04	7.29 ± 0.04	1.0
13	Propyl	3-NCS	6.21 ± 0.21	7.31 ± 0.15*	19.3
15	Propyl	4-NCS	7.62 ± 0.11	8.49 ± 0.18*	7.7
23	H	3-SO_2F	6.88 ± 0.08	7.88 ± 0.14**	10.2
24 (LUF7982)	H	4-SO_2F	8.10 ± 0.06	9.17 ± 0.12**	12.1
25	H	3-OSO_2F	6.85 ± 0.44	7.15 ± 0.32	1.6
26 (LUF7993)	H	4-OSO_2F	7.93 ± 0.22	8.26 ± 0.20	2.2
28	H	3-NCS	6.96 ± 0.27	8.55 ± 0.08**	74.3
30 (LUF8002)	H	4-NCS	8.67 ± 0.14	9.18 ± 0.01*	3.4
PSB-1115	H	4-SO_2OH	6.71 ± 0.09	6.72 ± 0.18	1.1

[a] Apparent affinity determined from displacement of specific [^{3}H]PSB-603 binding on CHO-spap cell membranes stably expressing hA_{2B}AR at 25 °C after 0.5 h co-incubation; [b] Apparent affinity determined from displacement of specific [^{3}H]PSB-603 binding on CHO-spap cell membranes stably expressing hA_{2B}AR at 25 °C with compounds pre-incubated for 4 h, followed by a 0.5 h co-incubation with [^{3}H]PSB-603. [c] K_i shift determined by ratio K_i(0 h)/K_i(4 h). Data represent the mean ± SEM of three individual experiments performed in duplicate. * $p < 0.05$, ** $p < 0.01$ compared to the *p*K_i values obtained from the displacement assay with 0 h pre-incubation of [^{3}H]PSB-603, determined by a two-tailed unpaired Student's t-test.

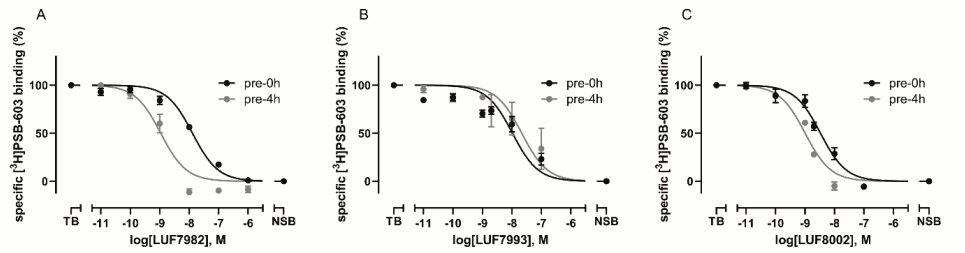

Figure 1. Displacement of [^{3}H]PSB-603 from the A_{2B}AR by (A) SO_2F-substituted LUF7982; (B) OSO_2F-substituted LUF7993 and (C) NCS-substituted LUF8002. Displacement measured after 0 or 4 h of pre-incubation of the respective ligand with CHO-spap membranes stably overexpressing the A_{2B}AR. Data represent the mean ± SEM of three individual experiments performed in duplicate.

Evaluation of binding towards the other adenosine receptors

As mentioned in the introduction, xanthine-based ligands are prone to promiscuous AR binding. To investigate the selectivity of the synthesized ligands towards the A_{2B}AR specifically, radioligand displacement experiments were carried out using 1 µM of ligand on CHO (A_1AR and A_3AR) or HEK (A_{2A}AR) membranes stably overexpressing the respective other adenosine receptor (Table 2). Similar to the experiments for the A_{2B}AR, the compounds were tested either with or without 4 hours of pre-incubation prior to radioligand addition. In our experiments, hardly any ligand showed a strong displacement of radioligand from the structurally similar A_{2A}AR. Only compound **11** seems to bind decently, showing a displacement that exceeds 50%. In case of the A_1AR, all of the N^1,N^3-dipropyl xanthines (**8**-**13** and **15**) show a strong displacement (>50%) of radioligand from the receptor. This is in line with earlier reports on such substituted N^1,N^3-dipropyl xanthines as generally excellent A_1AR antagonists.[28,45,46]

Considering the isothiocyanates (**13**, **15**, **28** and **30**), a moderate to high displacement of radioligand from A_1 and A_3 receptors was observed. Interestingly, the 3-NCS substituted xanthines (**13** and **28**) seem to perform especially well at the A_3AR. A notable loss of displacement at the other adenosine receptors is observed upon removal of the N^3-propyl group. Also the introduction of a sulfonyl group has a beneficial effect on selectivity towards the A_{2B}AR over the other ARs. This group might be stabilized by interactions with K269$^{7.32}$, not present in any of the other ARs.[17] This is especially seen for the OSO_2F-containing **26** (LUF7993), showing the highest selectivity for the A_{2B}AR. Among the compounds with the highest apparent pK_i values, **24** (LUF7982) shows a good selectivity towards the A_{2B}AR and about 50% displacement of radioligand at the A_{2A}AR. The latter suggests **24** (LUF7982) displays a 100-fold selectivity for the A_{2B}AR without pre-incubation (and >1000-fold after 4 h of pre-incubation). Besides, the displacement at the A_{2A}AR is not time-dependent and therefore it is expected that **24** (LUF7982) does not bind covalently to the A_{2A}AR. The high affinity compound **30** (LUF8002) on the other hand, also binds to the A_1AR and A_3AR.

Table 2. Radioligand displacement of the synthesized adenosine A_{2B} receptor ligands on other adenosine receptors.

	(%) displacement at 1 µM					
	hA$_1$AR[a]		hA$_{2A}$AR[b]		hA$_3$AR[c]	
Compound	**0 h**	**4 h**	**0 h**	**4 h**	**0 h**	**4 h**
8	52	61	19	23	30	43
9	61	69	54	55	12	5
10	76	77	13	12	64	58
11	79	85	63	69	47	49
13	73	96	47	34	89	100
15	77	92	40	39	48	96
23	6	36	20	6	14	10
24 (LUF7982)	29	41	52	43	7	9
25	6	1	2	0	14	5
26 (LUF7993)	17	12	35	24	8	8
28	7	16	0	6	58	95
30 (LUF8002)	51	97	25	27	15	66

[a] % displacement at 1 µM concentration of specific [^{3}H]DPCPX binding on CHO cell membranes stably expressing hA$_1$AR pre-incubated with the compounds for 4 or 0 hours at 25 °C, followed by a co-incubation with [^{3}H]DPCPX for 0.5h at 25 °C. [b] % displacement at 1 µM concentration of specific [^{3}H]ZM241385 binding on HEK293 cell membranes stably expressing hA$_{2A}$AR pre-incubated with the compounds for 4 or 0 hours at 25 °C, followed by a co-incubation with [^{3}H]ZM241385 for 0.5h at 25 °C. [c] % displacement at 1 µM concentration of specific [^{3}H]PSB-11 binding on CHO cell membranes stably expressing hA$_3$AR pre-incubated with the compounds for 4 or 0 hours at 25 °C, followed by a co-incubation with [^{3}H]PSB-11 for 0.5h at 25 °C. Data represent the mean of two individual experiments performed in duplicate.

Evaluation of the covalent mode of action of selected compounds

As final validation of the putative covalent mode of binding, wash-out experiments were performed using the compounds highest in affinity and selectivity: **24** (LUF7982), **26** (LUF7993) and **30** (LUF8002). PSB-1115 was taken along as reversible control compound. CHO-spap membranes stably overexpressing the A_{2B}AR were incubated with ligand, followed by either a four-cycle wash treatment or no washing (control), before being exposed to radioligand (Figure 2). Both PSB-1115 and **26** (LUF7993) show an almost full recovery of radioligand binding after washing, indicating that all receptor-bound ligand has been washed away. These results correspond to the previously observed K_i shifts (Table 1), in which no great shifts were observed for PSB-1115 and the OSO_2F-containing xanthines. Of note: it is possible that LUF7993 forms an adduct with the receptor, which is then hydrolyzed to produce a sulfonylated lysine and a reversibly bound phenol.[32] **24** (LUF7982) and **30** (LUF8002) on the other hand, show a persistent mode of binding, with no recovery of radioligand binding after four wash treatments (Figure 2). **24** (LUF7982) and **30** (LUF8002) thus form a stable adduct with the A_{2B}AR, resistant to multiple washing steps and are therefore most likely covalent ligands for the A_{2B}AR. **24** (LUF7982) is the most interesting of these two irreversible compounds due to its high selectivity towards the A_{2B}AR. This compound was therefore further examined in docking experiments.

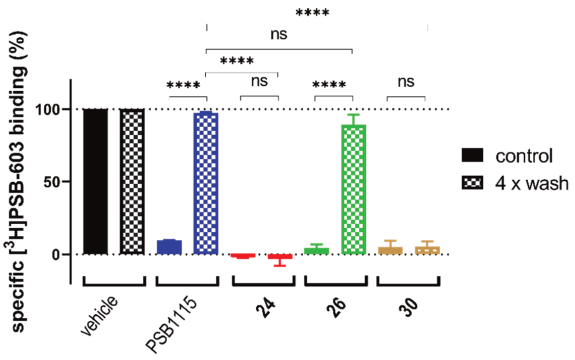

Figure 2. Wash-out assays on the adenosine A_{2B} receptor using the *N*^{1}-propyl xanthines with *para*-substituted warheads. CHO-spap cell membranes stably expressing the adenosine A_{2B} receptor were pre-incubated with buffer (vehicle) or 1 µM of ligand (10 µM in case of PSB-1115), followed by a four-cycle washing treatment (4 x wash) or no washing at all (control) before being exposed to [^{3}H]PSB-603. Data represent the mean ± SEM of three individual experiments performed in duplicate. Statistics were determined using unpaired student's *t* tests. ns: no significant difference; ****P < 0.0001.

Docking of LUF7982 into the A_{2B}AR binding pocket

To predict the binding mode of LUF7982, we generated a model of the A_{2B}AR-LUF7982 binding site based on homology modelling and docking. The first step was to identify the orientation of the xanthine core. The orientation of this chemotype in the AR family binding site is well studied and typically involves hydrogen bonding with N254$^{6.55}$ and π-π stacking with F173^{EL2}.[47] This pattern was also observed for the predicted A_{2B}AR-LUF7982 binding complex (Figure 3A). This leaves the warhead of LUF7982 oriented towards the extracellular vestibule, pointing towards the region of the third extracellular loop (EL3). As mentioned in the introduction, three lysine residues (K265^{EL3}, K267^{EL3} and K269$^{7.32}$) in and near EL3 were identified as potential attachment point for covalent binding of the compounds herein reported. In our model, two out of three lysine residues were in close vicinity to the warhead, namely K267^{EL3} and K269$^{7.32}$ (5.7 and 3.9 Å, respectively) (Figure 3B). K267^{EL3} is predicted to form a salt bridge with E174^{EL2}, similar to the salt bridge observed between a histidine and glutamic acid in the A_{2A}AR.[47]

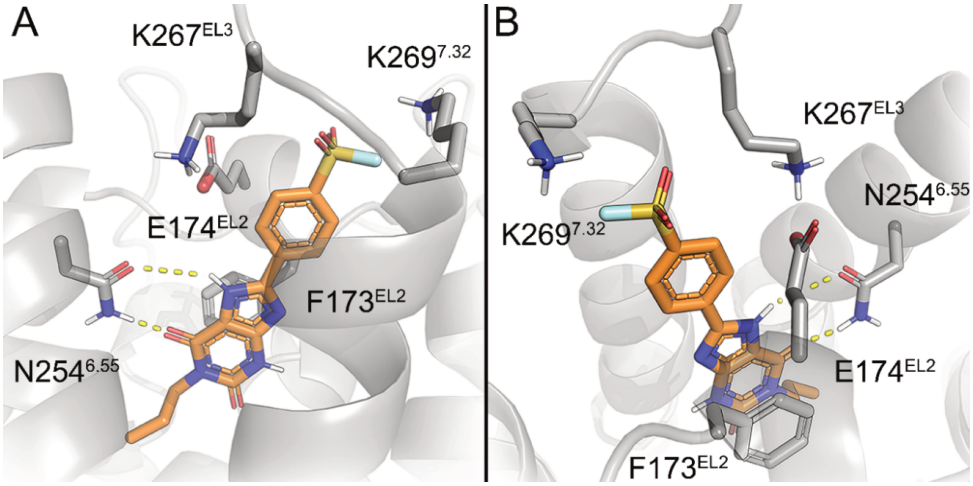

Figure 3. Predicted binding mode of LUF7982. Panel A: overview of the key interactions of LUF7982 in the binding site, which include two hydrogen bonds (yellow dashed lines) with N254$^{6.55}$ and π-π stacking with F173^{EL2}, both are conserved interactions in adenosine receptor ligand recognition. The sulfonyl fluoride warhead points towards the extracellular vestibule. Panel B: top view of the A_{2B}AR-LUF7982 binding pocket, showing potential lysine residues involved in covalent binding (K267^{EL3} and K269$^{7.32}$).

K265^{EL3} on the other hand was too far away from the warhead in our model (10.6 Å) to form a plausible target for covalent attachment. Whilst K267^{EL3} thus is within range, it would be energetically more unfavorable to disrupt the formed salt-bridge, and we therefore expect that K269$^{7.32}$ is the most likely target for covalent attachment. Lysine residues K265^{EL3} and K269$^{7.32}$ are not present on the other three adenosine receptors, while K267^{EL3} is also present on the A_1AR. A covalent mode of binding involving K269$^{7.32}$ might therefore further explain the selectivity of **24** (LUF7982) towards the A_{2B}AR. Further studies using single point mutations in the receptor would need to be carried out to prove this.

Conclusion

Herein we present the development of a set of twelve novel xanthine ligands for the A_{2B}AR, all containing electrophilic groups to covalently target lysine residue(s) on the receptor. The xanthine moiety is a well-known and promiscuous scaffold for all four of the adenosine receptors. Nevertheless, among the synthesized ligands, sulfonyl fluoride- and fluorosulfonate-substituted xanthines appear to be highly selective towards the A_{2B}AR over the other adenosine receptors. This selectivity might be explained by the covalent (SO_2F) and/or non-covalent (OSO_2F) interactions with lysine residue K269$^{7.32}$. Isothiocyanate (NCS)-containing ligands on the other hand, showed to be less selective towards the A_{2B}AR. This is most likely due to a higher intrinsic reactivity of the NCS group. Furthermore, sulfonyl fluoride **24** (LUF7982) showed persistent binding to the A_{2B}AR in radioligand displacement and wash-out assays. This points towards a covalent mode of action of the respective compound.

The A_{2B}AR is an emerging drug target that has been found to play a role in a broad spectrum of pathologies, such as cancers and immune disorders. Antagonizing adenosine signaling through inhibition of the A_{2B}AR is therefore an interesting strategy to tackle a broad spectrum of conditions. Having covalent ligands for the A_{2B}AR will pave the way for studies towards irreversible blockade of the receptor, e.g. in biochemical assays. LUF7982 might thus be used to study the behavior of the A_{2B}AR in pathological conditions, to obtain insight in the structure of the A_{2B}AR and to pharmacologically characterize the receptor.

Experimental

Chemistry

General

All commercially available reagents and solvents were obtained from Sigma Aldrich, Fisher Scientific, VWR chemicals, Biosolve and J&K Scientific. All reactions were carried out under an N_2 atmosphere, unless noted otherwise. Thin layer chromatography was performed on TLC Silica gel 60 F254 (Merck) and visualized using UV irradiation at a wavelength of 254 or 366 nM. ^{1}H NMR, ^{13}C NMR and ^{19}F NMR spectra were recorded on a Bruker AV-400 (400 MHz), Bruker AV-500 spectrometer (500 MHz) or Bruker AV-600 spectrometer (600 MHz). Chemical shift values are reported in ppm (δ) using tetramethylsilane or solvent resonance as the internal standard. Coupling constants (J) are reported in Hz. Multiplicities are indicated by s (singlet), d (doublet), t (triplet), h (hexuplet) or m (multiplet) followed by the number of represented hydrogen atoms. Compound purity was determined by LC-MS, using a LCMS-2020 system (Shimadzu) coupled to a Gemini® 3 µm C18 110Å column (50 x 3 mm). In brief, compounds were dissolved in H2O:MeCN:t-BuOH 1:1:1, injected onto the column and eluted with a linear gradient of H2O:MeCN 90:10 + 0.1% formic acid to H2O:MeCN 10:90 + 0.1% formic acid over the course of 15 minutes.

Synthetic Procedures

Dipropyl-substituted xanthines

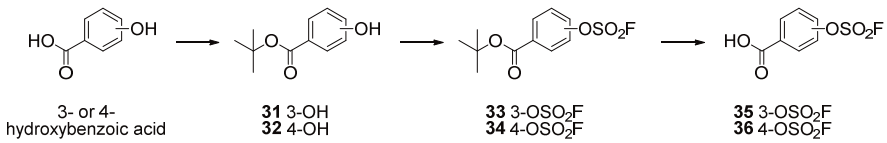

Scheme 1 Synthesis of 3- and 4-fluorosulfonate benzoic acid.

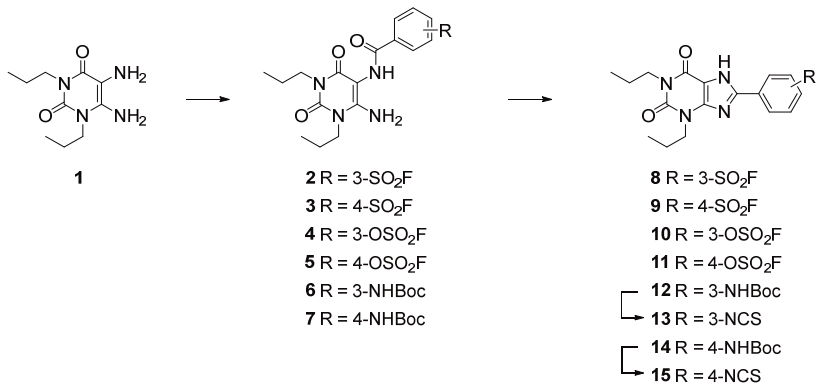

Scheme 2 Synthesis of the *N*[1], *N*[3]-dipropyl-substituted xanthines.

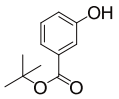

***tert*-Butyl 3-hydroxybenzoate (31)**[48]

3-Hydroxybenzoic acid (849 mg, 6.15 mmol, 1.0 eq) was suspended in dry benzene (100 mL) and refluxed. N,N-Dimethylformamide di-*tert*-butyl acetal (5.0 g, 24.59 mmol, 4.0 eq) was added dropwise over 20 minutes and the mixture was refluxed an additional 30 minutes. The mixture was then cooled, washed with water (50 mL), a saturated $NaHCO_3$ solution (2 x 50 mL) and brine (50 mL). The organic layer was dried over $MgSO_4$, filtered and concentrated under reduced pressure. The residue was purified by column chromatography (Pentane:EtOAc 5:1) to yield **31** as a colorless oil (440 mg, 2.27 mmol, 37%). **TLC** (Pentane:EtOAc 5:1) R_f = 0.43. **^{1}H NMR** (400 MHz, $CDCl_3$) δ [ppm] = 7.64 (dd, *J* = 2.7, 1.6 Hz, 1H), 7.54 (dt, *J* = 7.7, 1.3 Hz, 1H), 7.48 (s, 1H), 7.27 (t, *J* = 7.9 Hz, 1H), 7.08 (ddd, *J* = 8.1, 2.6, 1.0 Hz, 1H), 1.58 (s, 9H). **HPLC** 99%, RT 9.686 min. **LC-MS** [ESI - H]$^+$: 193.00.

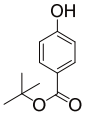

***tert*-Butyl 4-hydroxybenzoate (32)**[49]

tert-Butanol (49.5 mL, 521 mmol, 36.0 eq) was added to a solution of 4-hydroxybenzoic acid (2.0 g, 14.48 mmol, 1.0 eq) and DMAP (88 mg, 0.72 mmol, 0.05 eq) in dry THF (50 mL). A solution of DCC (3.0 g, 14.48 mmol, 1.0 eq) in dry THF (50 mL) was added dropwise over 30 minutes. The mixture was stirred overnight at rt. The formed side-product was removed by filtration and the filtrate was concentrated, dissolved in DCM. A saturated $NaHCO_3$ solution was added and the aqueous layer was extracted with DCM (3 x), dried over $MgSO_4$, filtered and concentrated under reduced pressure. The residue was purified by column chromatography (Pentane:EtOAc 5:1) to yield **32** as a white solid (1.4 g, 7.41 mmol, 51%). **TLC** (Pentane:EtOAc 5:1) R_f = 0.50. **^{1}H NMR** (400 MHz, $CDCl_3$) δ [ppm] = 7.89 (d, *J* = 8.8 Hz, 2H), 6.86 (d, *J* = 8.8 Hz, 2H), 1.59 (s, 9H).

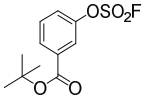

***tert*-Butyl 3-((fluorosulfonyl)oxy)benzoate (33)**[50]

[4-(Acetylamino)phenyl]imidosulfuryl difluoride (AISF) (854 mg, 2.72 mmol, 1.2 eq) was added to a solution of **31** (440 mg, 2.27 mmol, 1.0 eq) in dry THF (10 mL). DBU (751 µL, 4.98 mmol, 2.2 eq) was added and the mixture was stirred at rt for 1 h. EtOAc (50 mL) and 0.5 M HCl (50 mL) were added and the mixture was extracted with EtOAc (3 x 50 mL). The organic layers were combined, washed with brine, dried over $MgSO_4$, filtered and concentrated under reduced pressure. The residue was purified by column chromatography (Pentane:EtOAc 9:1) to yield **33** as a colorless oil (571 mg, 2.07 mmol, 91%). **TLC** (Pentane:EtOAc 9:1) R_f = 0.90. **^{1}H NMR** (400 MHz, $CDCl_3$) δ [ppm] = 8.05 (dt, *J* = 7.4, 1.5 Hz, 1H), 7.96 – 7.92 (m, 1H), 7.58 – 7.53 (m, 1H), 7.53 – 7.48 (m, 1H), 1.61 (s, 9H). **^{13}C NMR** (101 MHz, $CDCl_3$) δ [ppm] = 163.7, 150.0, 134.9, 130.4, 129.7, 124.9, 122.1, 82.5, 28.2.

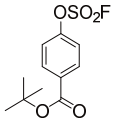

***tert*-Butyl 4-((fluorosulfonyl)oxy)benzoate** (**34**)
AISF (777 mg, 2.47 mmol, 1.2 eq) was added to a solution of **32** (400 mg, 2.06 mmol, 1.0 eq) in dry THF (10 mL). DBU (683 µL, 4.53 mmol, 2.2 eq) was added and the mixture was stirred at rt for 1 h. EtOAc (50 mL) and 0.5 M HCl (50 mL) were added and the aqueous layer was extracted with EtOAc (3 x 50 mL). The organic layers were combined, washed with brine, dried over $MgSO_4$, filtered and concentrated under reduced pressure. The residue was purified by column chromatography (Pentane:EtOAc 9:1) to yield **34** as a colorless oil (494 mg, 1.79 mmol, 87%). **TLC** (DCM:MeOH 98:2) R_f = 0.83. **^{1}H NMR** (400 MHz, $CDCl_3$) δ [ppm] = 8.12 (d, *J* = 8.9 Hz, 2H), 7.39 (dd, *J* = 9.0, 0.9 Hz, 2H), 1.60 (s, 9H).

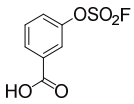

3-((Fluorosulfonyl)oxy)benzoic acid (**35**)
TFA (8.27 mL, 107 mmol, 60.0 eq) was added to a solution of **33** (571 mg, 2.07 mmol, 1.0 eq) in DCM (8 mL). The mixture was stirred for 3 h at rt, after which the reaction showed full completion. The solvents were evaporated under reduced pressure to yield **35** as a white solid (455 mg, 2.07 mmol, quant). **^{1}H NMR** (400 MHz, $CDCl_3$) δ [ppm] = 11.83 (s, 1H), 8.23 – 8.17 (m, 1H), 8.10 (s, 1H), 7.68 – 7.60 (m, 2H).

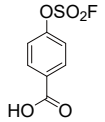

4-((Fluorosulfonyl)oxy)benzoic acid (**36**)
TFA (8.27 mL, 107 mmol, 60.0 eq) was added to a solution of **34** (494 mg, 1.79 mmol, 1.0 eq) in DCM (8 mL). The mixture was stirred for 3 h at rt, after which the reaction showed full completion. The solvents were evaporated under reduced pressure to yield **36** as a white solid (394 mg, 1.79 mmol, quant). **^{1}H NMR** (400 MHz, $CDCl_3$) δ [ppm] = 8.26 (d, *J* = 9.0 Hz, 2H), 7.48 (d, *J* = 8.5 Hz, 2H).

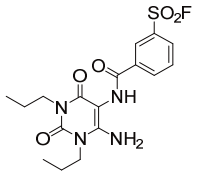

3-((6-Amino-2,4-dioxo-1,3-dipropyl-1,2,3,4-tetrahydropyrimidin-5-yl)carbamoyl)benzenesulfonyl fluoride (**2**)
EDC·HCl (933 mg, 4.86 mmol, 1.1 eq) and DIPEA (770 µL, 4.42 mmol, 1.0 eq) were added to a solution of 5,6-diamino-1,3-dipropyluracil (**1**) hydrochloride (1511 mg, 5.75 mmol, 1.3 eq) and 3-(fluorosulfonyl)benzoic acid (903 mg, 4.42 mmol, 1.0 eq) in dry DMF (21 mL). The mixture was stirred overnight at rt. EtOAc (15 mL) was added and the organic layer was washed with water (400 mL) and brine (100 mL), dried over $MgSO_4$ and concentrated under reduced pressure. The residue was purified by column chromatography (DCM:MeOH 99:1 →

97:3) to yield **2** as yellow solid (1085 mg, 2.63 mmol, 60%). **TLC** (DCM:MeOH 98:2) R_f = 0.27. **^{1}H NMR** (400 MHz, CD_3OD) δ [ppm] = 8,75 (s, *J* = 1.8 Hz, 1H), 8.51 (d, *J* = 7.9, 1.4 Hz, 1H), 8.28 (d, *J* = 8.1, 1.3Hz, 1H), 7,89 (t, *J* = 7.9 Hz, 1H), 3.98 – 3.92 (t, 2H), 3.92 – 3.86 (t, 2H), 1.79 – 1.70 (d, 2H), 1.70 – 1.61 (d, 2H), 1.02 (t, *J* = 7.4 Hz, 3H), 0.96 (t, *J* = 7.5 Hz, 3H).

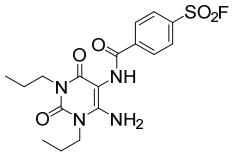

4-((6-Amino-2,4-dioxo-1,3-dipropyl-1,2,3,4-tetrahydropyrimidin-5-yl)carbamoyl)benzenesulfonyl fluoride (**3**)

EDC·HCl (932 mg, 4.86 mmol, 1.1 eq) and DIPEA (752 µL, 4.32 mmol, 1.0 eq) were added to a solution of 5,6-diamino-1,3-dipropyluracil (**1**) hydrochloride (1161 mg, 4.42 mmol, 1.0 eq) and 4-(fluorosulfonyl)benzoic acid (902 mg, 4.42 mmol, 1.0 eq) in dry DMF (20 mL). The mixture was stirred for 2.5 h at rt. EtOAc (150 mL) was then added and the organic layer was washed with water (150 mL). The aqueous layer was extracted with EtOAc (2 x 50 mL). The organic layers were combined, washed with water (3 x 100 mL), brine (100 mL), combined, dried over $MgSO_4$ and concentrated under reduced pressure to yield **3** as an off-white solid (749 mg, 1.82 mmol, 41%). **TLC** (Pentane:EtOAc 1:1) R_f = 0.49. **^{1}H NMR** (400 MHz, $(CD_3)_2CO$) δ [ppm] = 8.34 (d, *J* = 8.3 Hz, 2H), 8.19 (d, *J* = 8.5 Hz, 2H), 6.46 (s, 1H), 3.97 (t, *J* = 7.8 Hz, 2H), 3.82 (t, *J* = 7.3 Hz, 2H), 1.72 (h, *J* = 7.4 Hz, 2H), 1.58 (h, *J* = 7.5 Hz, 2H), 0.94 (t, *J* = 7.4 Hz, 3H), 0.87 (t, *J* = 7.5 Hz, 3H).

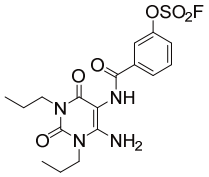

3-((6-Amino-2,4-dioxo-1,3-dipropyl-1,2,3,4-tetrahydropyrimidin-5-yl)carbamoyl)phenyl sulfurofluoridate (**4**)

EDC·HCl (420 mg, 2.19 mmol, 1.1 eq) was added to a solution of **35** (439 mg, 1.99 mmol, 1.0 eq) in dry DMF (10 mL). 5,6-Diamino 1,3-dipropyl uracil (**1**) hydrochloride (524 mg, 1.99 mmol, 1.0 eq) was added and the mixture became a pink solution. DIPEA (693 µL, 3.98 mmol, 2.0 eq) was added and to form a clear orange solution. The mixture was then stirred for 4 h, upon which no starting material was detected anymore by LCMS. EtOAc (50 mL) was added and the organic mixture was washed with brine (3 x 50 mL). The aqueous layers were combined and back-extracted with EtOAc (3 x 50 mL). The organic layers were combined, dried over $MgSO_4$, filtered and concentrated under reduced pressure. The residue was purified by silica column chromatography to yield **4** as yellow substance (329 mg, 0.77 mmol, 39%). **TLC** (DCM:MeOH 96:4): Rf = 0.41. **^{1}H NMR** (500 MHz, $(CD_3)_2SO$) δ [ppm] = 9.17 (s, 1H), 8.16 – 8.10 (m, 2H), 7.80 (dd, *J* = 8.3, 1.4 Hz, 1H), 7.72 (t, *J* = 8.0 Hz, 1H), 6.84 (s, 2H), 3.85 (t, *J* = 8.1, 7.2 Hz, 2H), 3.73 (t, *J* = 7.2 Hz, 2H), 1.60 – 1.54 (m, 2H), 1.53 – 1.47 (m, 2H), 0.89 (t, *J* = 7.4 Hz, 3H), 0.83 (t, *J* = 7.4 Hz, 3H). **^{13}C NMR** (126 MHz, $(CD_3)_2SO$) δ [ppm] = 164.6, 159.0, 151.7, 150.4, 149.4, 137.3, 130.7, 128.7, 123.8, 120.5, 86.8, 43.7, 41.9, 20.9, 20.8, 11.2, 10.7. **^{19}F NMR** (471 MHz, $(CD_3)_2SO$) δ 39.0.

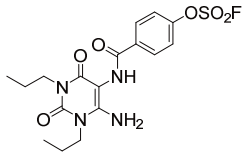

4-((6-Amino-2,4-dioxo-1,3-dipropyl-1,2,3,4-tetrahydropyrimidin-5-yl)carbamoyl)phenyl sulfurofluoridate (**5**)

EDC·HCl (312 mg, 1.63 mmol, 0.9 eq) was added to a solution of **36** (376 mg, 1.71 mmol, 0.9 eq) in dry DMF (7.5 mL). The mixture was stirred for 30 min and then 5,6-diamino 1,3-dipropyl uracil (**5**) hydrochloride (476 mg, 1.81 mmol, 1.0 eq) and DIPEA (257 µL, 1.48 mmol, 1.0 eq) were added. The mixture was stirred for 5 h, upon which DIPEA (257 µL, 1.48 mmol, 1.0 eq) was added. The mixture was then stirred overnight. EtOAc (25 mL) was added and the organic layer was washed with water (2 x 25 mL), dried over $MgSO_4$, filtered and concentrated under reduced pressure. The residue was purified by column chromatography (PE:EtOAc 7:3 → 0:1) to yield **5** as an orange solid (387 mg, 0.90 mmol, 50%). **TLC** (DCM:MeOH 98:2) R_f = 0.53. **^{1}H NMR** (500 MHz, $(CD_3)_2CO$) δ [ppm] = 9.13 (s, 1H), 8.18 (d, *J* = 8.9 Hz, 2H), 7.44 (d, *J* = 8.7 Hz, 2H), 6.63 (s, 2H), 3.88 (t, *J* = 7.8 Hz, 2H), 3.77 (t, *J* = 7.2 Hz, 2H), 1.65 (h, *J* = 7.2 Hz, 2H), 1.52 (h, *J* = 7.5 Hz, 2H), 0.91 (t, *J* = 7.4 Hz, 3H), 0.82 (t, *J* = 7.5 Hz, 3H). **^{13}C NMR** (126 MHz, $(CD_3)_2CO$) δ [ppm] = 165.1, 160.5, 152.1, 151.6, 150.2, 134.6, 130.4, 120.5, 88.0, 44.2, 42.3, 21.0, 21.0, 10.6, 10.2. **^{19}F NMR** (471 MHz, $(CD_3)_2CO$) δ [ppm] = 38.2.

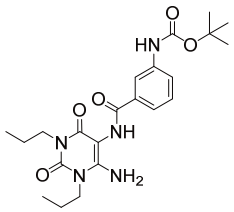

***tert*-Butyl (3-((6-amino-2,4-dioxo-1,3-dipropyl-1,2,3,4-tetrahydropyrimidin-5-yl)carbamoyl)phenyl)carbamate** (**6**)

3-(Boc-amino)benzoic acid (474 mg, 2.00 mmol, 1.0 eq), EDC·HCl (422 mg, 2.20 mmol, 1.1 eq) and DIPEA (350 µL, 2.00 mmol, 1.0 eq) were added to a solution of 5,6-diamino 1,3-dipropyl uracil (**1**) hydrochloride (525 mg, 2.00 mmol, 1.0 eq) in dry DMF (10 mL). The mixture was stirred for 3 h, after which another 2.0 equivalents of DIPEA were added (350 µL, 2.00 mmol, 1.0 eq). The mixture was stirred for another hour and then diluted with EtOAc (80 mL). The organic layer was washed with water (3 x 80 mL), brine (80 mL), dried over $MgSO_4$, filtered and concentrated under reduced pressure. The residue was purified by column chromatography (DCM:MeOH 90:10 → 95:5) to yield **6** as an off-white solid (446 mg, 1.00 mmol, 50%). **TLC** (DCM:MeOH 97:3) R_f = 0.42. **^{1}H NMR** (400 MHz, $(CD_3)_2CO$) δ [ppm] = 8.05 (t, *J* = 2.0 Hz, 1H), 7.70 (dd, *J* = 8.0, 1.5 Hz, 1H), 7.62 (ddd, *J* = 7.8, 1.8, 1.1 Hz, 1H), 7.36 (t, *J* = 7.9 Hz, 1H), 3.94 (t, *J* = 7.8 Hz, 2H), 3.80 (t, *J* = 7.3 Hz, 2H), 1.72 (h, *J* = 7.1 Hz, 2H), 1.65 – 1.51 (m, 2H), 1.49 (s, 9H), 0.94 (t, *J* = 7.4 Hz, 3H), 0.87 (t, *J* = 7.5 Hz, 3H).

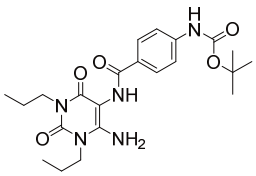

***tert*-Butyl (4-((6-amino-2,4-dioxo-1,3-dipropyl-1,2,3,4-tetrahydropyrimidin-5-yl)carbamoyl)phenyl)carbamate** (**7**)
4-(Boc-amino)benzoic acid (237 mg, 1.00 mmol, 1.0 eq), EDC·HCl (211 mg, 1.10 mmol, 1.1 eq) and DIPEA (174 µL, 1.00 mmol, 1.0 eq) were added to a solution of 5,6-diamino 1,3-dipropyl uracil (**1**) hydrochloride (263 mg, 1.00 mmol, 1.0 eq) in dry DMF (5 mL). The mixture was stirred for 4 h, after which LCMS indicated full consumption of starting material. EtOAc (50 mL) was added and the organic layer was washed with water (2 x 50 mL) and brine (50 mL). The aqueous layers were combined and back-extracted with EtOAc (2 x 50 mL). The organic layers were combined, dried over $MgSO_4$, filtered and concentrated under reduced pressure. The residue was purified by column chromatography (DCM:MeOH 99:1 → 90:10) to yield **7** as an off-white solid (302 mg, 0.68 mmol, 68%). **TLC** (DCM:MeOH 95:5) R_f = 0.27. **^{1}H NMR** (400 MHz, CD_3OD) δ [ppm] = 7.93 (d, *J* = 8.8 Hz, 2H), 7.49 (d, *J* = 8.8 Hz, 2H), 3.88 – 3.81 (m, 2H), 3.81 – 3.75 (m, 2H), 1.68 – 1.56 (m, 4H), 1.54 (s, 9H), 0.96 (t, *J* = 7.4 Hz, 3H), 0.90 (t, *J* = 7.4 Hz, 3H). **^{13}C NMR** (101 MHz, MeOD) δ [ppm] = 170.3, 162.1, 154.7, 154.2, 152.2, 144.4, 130.0, 128.4, 118.4, 89.0, 81.2, 45.7, 44.0, 28.7, 22.2, 22.0, 11.6, 11.2.

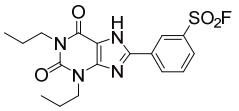

3-(2,6-Dioxo-1,3-dipropyl-2,3,6,7-tetrahydro-1H-purin-8-yl)benzenesulfonyl fluoride (**8**)
PPSE (approximately 5 mL) was added to **2** (1085 mg, 2.63 mmol, 1.0 eq). The mixture was refluxed for 4 h at 170 °C and afterwards cooled down to rt overnight. MeOH (50 mL) was added and the formed residue was collected by filtration and subsequently purified by silica column chromatography (DCM:MeOH 99.5:0.5 → 85:15) to yield **8** as an off-white solid (281 mg, 0.71 mmol, 27%). **TLC** (DCM:MeOH 99.5:0.5) R_f = 0.60. **^{1}H NMR** (400 MHz, $(CD_3)_2SO$) δ [ppm] = 14.32 (s, 1H), 8.83 (t, *J* = 1.7 Hz, 1H), 8.61 (d, *J* = 8.0 Hz, 1H), 8.22 (d, *J* = 8.9 Hz, 1H), 7.93 (t, *J* = 8.0 Hz, 1H), 4.02 (t, *J* = 7.4 Hz, 3H), 3.86 (t, *J* = 7.4 Hz, 2H), 1.74 (hept, *J* = 7.4 Hz, 2H), 1.58 (hept, *J* = 7.5 Hz, 2H), 0.91 (d, *J* = 7.4 Hz, 3H), 0.87 (t, *J* = 7.4 Hz, 3H). **^{13}C NMR** (101 MHz, $(CD_3)_2SO$) δ [ppm] = 155.1, 151.5, 149.0, 147.9, 134.8, 133.6 (d, *J* = 24.1 Hz), 132.4, 131.7. 130.3, 126.4, 109.6, 45.5, 43.2, 21.8, 21.8, 12.1, 12.0. **^{19}F NMR** (471 MHz, $(CD_3)_2SO$) δ [ppm] = 66.5. **HPLC** 100%, RT 11.292 min. **LC-MS** $[ESI + H]^+$: 395.05.

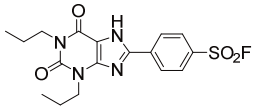

4-(2,6-Dioxo-1,3-dipropyl-2,3,6,7-tetrahydro-1H-purin-8-yl)benzenesulfonyl fluoride (**9**)
PPSE (approximately 2 mL) was added to **3** (500 mg, 1.21 mmol, 1.0 eq), refluxed for 1 h at 170 °C and afterwards cooled down to rt. MeOH was added and the product was allowed to crystallize overnight. The residue was collected and purified by silica column chromatography (DCM:MeOH 99.5:0.5 → 98.5:1.5) to yield **9** as an off-white solid (46 mg, 0.12 mmol, 10%). **TLC** (DCM:MeOH 98:2) R_f = 0.40. **^{1}H NMR** (500 MHz, $(CD_3)_2SO$) δ [ppm] = 14.41 (s, 1H), 8.47 (d, *J* = 8.6 Hz, 2H), 8.29 (d, *J* = 8.7 Hz, 2H), 4.03 (t, *J* = 7.2 Hz, 2H), 3.88 (t, *J* = 7.3 Hz, 2H), 1.75 (h, *J* = 7.4 Hz, 2H), 1.59 (h, *J* = 7.5 Hz, 2H), 0.91 (t, *J* = 7.5 Hz, 3H), 0.88 (t, *J* = 7.4 Hz,

3H). **^{19}F NMR** (471 MHz, $(CD_3)_2SO$) δ [ppm] = 66.8. **HPLC:** 97%, RT 11.395 min. LC-MS [ESI + H]+: 395.05.

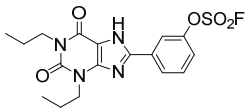

3-(2,6-Dioxo-1,3-dipropyl-2,3,6,7-tetrahydro-1H-purin-8-yl)phenyl sulfurofluoridate (**10**)
PPSE (2 mL) was added to **4** (329 mg, 0.77 mmol, 1.0 eq) and refluxed at 170 °C. The mixture was stirred for 4 h and afterwards cooled down to rt. Water (50 mL) was added and the aqueous mixture was extracted with DCM (3 x 50 mL). The organic layers were combined, washed with brine (50 mL), dried over $MgSO_4$, filtered and concentrated under reduced pressure. The residue was purified by column chromatography (DCM:MeOH 99.5:0.5 → 98:2) to yield **10** as a white solid (186 mg, 0.45 mmol, 59%). **TLC** (DCM:MeOH 99.5:0.5): Rf = 0.44. **^{1}H NMR** (500 MHz, $(CD_3)_2SO$) δ 14.11 (s, 1H), 8.28 – 8.20 (m, 2H), 7.77 – 7.68 (m, 2H), 4.01 (t, *J* = 7.2 Hz, 2H), 3.86 (t, *J* = 7.4 Hz, 2H), 1.74 (h, *J* = 7.4 Hz, 2H), 1.58 (h, *J* = 7.4 Hz, 2H), 0.89 (dt, *J* = 12.1, 7.4 Hz, 6H). **^{13}C NMR** (126 MHz, $(CD_3)_2SO$) δ 154.2, 150.6, 150.0, 148.1, 147.5, 131.7, 131.4, 127.0, 122.5, 118.5, 108.4, 44.5, 42.2, 20.8, 11.2, 11.0. **^{19}F NMR** (471 MHz, $(CD_3)_2SO$) δ 39.6.

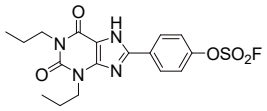

4-(2,6-Dioxo-1,3-dipropyl-2,3,6,7-tetrahydro-1H-purin-8-yl)phenyl sulfurofluoridate (**11**)
PPSE (2 mL) was added to **5** (387 mg, 0.90 mmol, 1.0 eq) and refluxed at 170 °C. The mixture was stirred for 4 h and afterwards cooled down to rt. Water (50 mL) was added and the aqueous layer was extracted with DCM (3 x 25 mL). The organic layers were combined, washed with brine (50 mL) and concentrated under reduced pressure. The residue was purified by column chromatography (DCM:MeOH 99.75:0.25 → 99.5:0.5) to yield **11** as a white solid (198 mg, 0.48 mmol, 53%). **TLC** (DCM:MeOH 98:2) R_f = 0.68. **^{1}H NMR** (500 MHz, $(CD_3)_2SO$) δ [ppm] = 14.06 (s, 1H), 8.32 – 8.26 (m, 2H), 7.76 (d, *J* = 8.9 Hz, 2H), 4.01 (t, *J* = 6.9 Hz, 2H), 3.90 – 3.83 (m, 2H), 1.74 (h, *J* = 7.4 Hz, 2H), 1.58 (h, *J* = 7.5 Hz, 2H), 0.90 (t, *J* = 7.4 Hz, 3H), 0.87 (t, *J* = 7.5 Hz, 3H). **^{13}C NMR** (126 MHz, $(CD_3)_2SO$) δ [ppm] = 154.2, 150.6, 150.3, 148.2, 148.0, 129.6, 128.8, 121.9, 108.4, 44.5, 42.2, 20.8, 20.8, 11.2, 11.0. **^{19}F NMR** (471 MHz, $(CD_3)_2SO$) δ [ppm] = 39.0. **HPLC** 98%, RT 11.524 min. **LC-MS** $[ESI + H]^+$: 411.10.

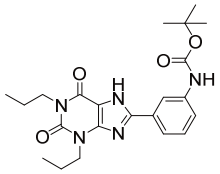

***tert*-Butyl (3-(2,6-dioxo-1,3-dipropyl-2,3,6,7-tetrahydro-1H-purin-8-yl)phenyl)carbamate** (**12**)
2 M NaOH (5 mL) was added to a solution of **6** (446 mg, 1.00 mmol, 1.0 eq) in dioxane (5 mL). The mixture was refluxed for 3 h at 120 °C. The reaction was then cooled down to rt and water (65 mL) was added. The aqueous layer was washed with EtOAc (4 x 80 mL). The organic layers were combined, dried over $MgSO_4$, filtered and concentrated under reduced pressure. The residue was purified by column chromatography (DCM:MeOH 99:1 → 97:3) to yield **12** (170 mg, 0.40 mmol, 40%) and Boc-deprotected **12** (65 mg, 0.20 mmol, 20%), both as an off-

white powder. The products were combined and used directly in the next reaction (0.60 mmol, 60%). **TLC** (DCM:MeOH 98:2) R_f = 0.42. **^{1}H NMR** (400 MHz, $(CD_3)_2SO$) δ [ppm] = 13.88 (s, 1H), 9.57 (s, 1H), 8.27 (s, 1H), 7.75 (d, *J* = 7.7 Hz, 1H), 7.55 (d, *J* = 8.0 Hz, 1H), 7.41 (t, *J* = 7.9 Hz, 1H), 4.06 (t, *J* = 6.9 Hz, 2H), 3.90 (t, *J* = 7.5 Hz, 2H), 1.85 – 1.72 (m, 2H), 1.71 – 1.55 (m, 2H), 1.53 (s, 9H), 0.95 (t, *J* = 6.2 Hz, 3H), 0.91 (t, *J* = 6.4 Hz, 3H).

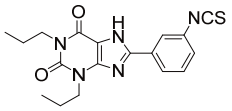

8-(3-Isothiocyanatophenyl)-1,3-dipropyl-3,7-dihydro-1H-purine-2,6-dione (**13**)
TFA (3 mL) was added to a suspension of **12** (0.60 mmol, 1.0 eq) in DCM (7 mL) and the mixture was stirred for 1 h at rt. TLC indicated full consumption of starting material and therefore 2 M NaOH (65 mL) was added to neutralize the reaction. The aqueous layer was extracted with EtOAc (4 x 60 mL). The organic layers were combined, dried over $MgSO_4$, filtered and concentrated to yield the respective amine. 3 M HCl (32 mL) was added to the crude amine to form a suspension. Thiophosgene (450 µL, 5.87 mmol, 9.8 eq) was added and the mixture was stirred for 2 h at rt. The mixture was then diluted with water (75 mL) and the aqueous layer was extracted with EtOAc (4 x 100 mL). The organic layers were combined, dried over $MgSO_4$, filtered and concentrated under reduced pressure. The residue was purified by column chromatography (DCM:MeOH 98:2 → 90:10) to yield **13** as an off-white powder (173 mg, 0.46 mmol, 77% over two steps). **TLC** (DCM:MeOH 9:1) R_f = 0.26. **^{1}H NMR** (400 MHz, $(CD_3)_2SO$) δ [ppm] = 13.99 (s, 1H), 8.13 (s, 1H), 8.09 (d, *J* = 7.9 Hz, 1H), 7.58 (t, *J* = 7.9 Hz, 1H), 7.51 (d, *J* = 9.0 Hz, 1H), 4.01 (t, *J* = 6.8 Hz, 2H), 3.86 (t, *J* = 7.3 Hz, 2H), 1.74 (h, *J* = 7.4 Hz, 2H), 1.58 (h, *J* = 7.5 Hz, 2H), 0.91 (t, *J* = 7.4 Hz, 3H), 0.87 (t, *J* = 3.6 Hz, 3H). **^{13}C NMR** (101 MHz, $(CD_3)_2SO$): δ [ppm] = 154.1 , 150.6 , 148.1 , 148.0, 134.9, 131.0, 130.7, 130.4, 127.1, 125.6, 123.7, 108.2, 44.5, 42.2, 20.9, 20.9, 11.2, 11.1. **HPLC** 97%, RT 12.229 min. **LC-MS** $[ESI + H]^+$: 370.10.

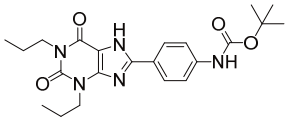

***tert*-Butyl (4-(2,6-dioxo-1,3-dipropyl-2,3,6,7-tetrahydro-1H-purin-8-yl)phenyl)carbamate** (**14**)
2 M NaOH (10 mL) was added to a solution of **7** (302 mg, 0,68 mmol, 1.0 eq) in dioxane (10 ml). The mixture was refluxed at 120 °C for 2 h and afterwards allowed to cool down to rt. Water (50 mL) was then added and the aqueous layer was extracted with EtOAc (3 x 50 mL). The organic layers were combined, dried with $MgSO_4$, filtered and concentrated under reduced pressure to yield **14** as an off-white solid (242 mg, 0,566 mmol, 84 % yield). **TLC** (DCM:MeOH 98:2): Rf = 0.42. **^{1}H NMR** (400 MHz, $CDCl_3$) δ [ppm] = 13.11 (s, 1H), 8.22 (d, *J* = 8.3 Hz, 2H), 7.51 (d, *J* = 8.3 Hz, 2H), 4.16 (t, *J* = 7.4 Hz, 2H), 4.06 (t, *J* = 7.6 Hz, 2H), 1.93 – 1.81 (m, 2H), 1.78 – 1.69 (m, 2H), 1.54 (s, 9H), 1.02 – 0.93 (m, 6H). **^{13}C NMR** (101 MHz, $CDCl_3$) δ [ppm] = 155.8, 152.7, 151.8, 151.2, 149.9, 140.8, 128.1, 123.5, 118.3, 107.9, 67.2, 45.4, 43.4, 28.5, 21.5, 21.5, 11.6, 11.3.

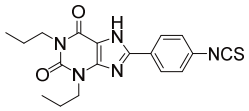

8-(4-Isothiocyanatophenyl)-1,3-dipropyl-3,7-dihydro-1H-purine-2,6-dione (**15**)
TFA (6 mL) was added to a suspension of **14** (242 mg, 0.57 mmol, 1.0 eq) in DCM (12 mL). The mixture immediately became a clear solution. The mixture was stirred for 1 h, upon which TLC showed full consumption of starting material. 2 M NaOH (50 mL) was added and the aqueous phase was extracted with EtOAc (3 x 50 mL). The organic layers were combined, dried over $MgSO_4$, filtered and concentrated. 3 M HCl (30 mL) was added to the crude amine to form a suspension. Thiophosgene (437 µL, 5.70 mmol, 10.0 eq) was added and the mixture was stirred for 2 h at rt. Water (70 mL) was then added and the aqueous layer was extracted with EtOAc (4 x 100 mL). The organic layers were combined, dried over $MgSO_4$, filtered and concentrated under reduced pressure. The residue was purified by column chromatography (DCM:MeOH 99.75:0.25 → 99:1) to yield **15** as a white powder (144 mg, 0.39 mmol, 68% over two steps). **TLC** (DCM:MeOH 9:1) R_f = 0.30. **^{1}H NMR** (500 MHz, $(CD_3)_2SO$) δ [ppm] = 13.95 (s, 1H), 8.16 (d, *J* = 8.7 Hz, 2H), 7.56 (d, *J* = 8.7 Hz, 2H), 4.01 (t, *J* = 7.5, 7.0 Hz, 2H), 3.86 (t, *J* = 7.3 Hz, 2H), 1.74 (h, *J* = 7.3 Hz, 2H), 1.58 (h, *J* = 7.4 Hz, 2H), 0.93 – 0.85 (m, 6H). **^{13}C NMR** (126 MHz, $(CD_3)_2SO$) δ [ppm] = 154.1, 150.6, 148.5, 148.3, 134.7, 131.3, 127.9, 127.7, 126.6, 108.2, 44.4, 42.2, 20.8 (2C), 11.2, 11.0. **HPLC** 98%, RT 12.194 min. **LC-MS** $[ESI + H]^+$: 370.10.

Monopropyl-substituted xanthines

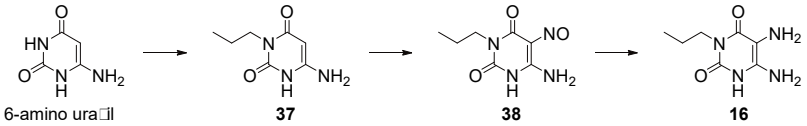

Scheme 3 Synthesis of 1-propyl 5-6-diamino uracil.

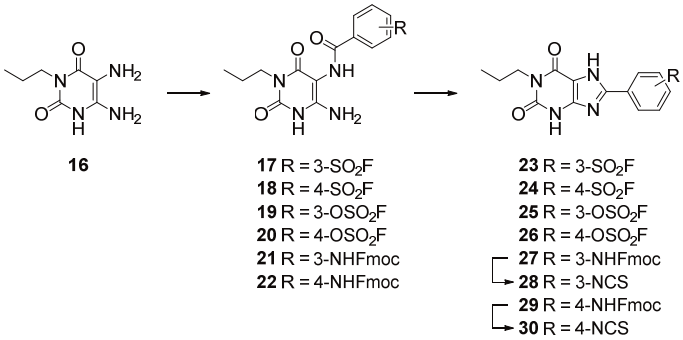

Scheme 4 Synthesis of the *N*^{1}-propyl-substituted xanthines.

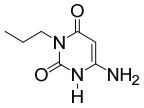

6-Amino-3-propylpyrimidine-2,4(1H,3H)-dione (**37**)[42]

6-aminouracil (20.00 g, 157 mmol, 1.0 eq) and ammonium sulfate (500 mg, 3.78 mmol) were added to a three-neck flask. HMDS (99 ml, 472 mmol, 3.0 eq) was added and the suspension was refluxed at 200 °C. After 2 h the suspension became a clear solution. The solution was cooled down to 80 °C and the HMDS was distilled off by boiling at 200 °C for 8 h. The solution was then cooled to 70 °C and iodine (150 mg, 0.591 mmol, cat) and 1-bromopropane (29 mL, 314 mmol, 2.0 eq) were added. The mixture was refluxed at 70 °C overnight. Extra 1-bromopropane (14.5 mL, 157 mmol, 1.0 eq) was added and the mixture was refluxed at 120 °C for 8 h, following by stirring at 70 °C overnight. Full conversion of starting material was observed and the mixture was put on ice. A saturated bicarb solution (400 mL) was gradually added. The dirty pink suspension was filtered over a glass filter and subsequently washed with water (100 mL), toluene (100 mL) and diethyl ether (100 mL). This yielded pure **37** as an orange/brown solid (21.439 g, 127 mmol, 81 % yield). **TLC** (DCM:MeOH 9:1): R_f = 0.46. **^{1}H NMR** (500 MHz, $(CD_3)_2SO$) δ [ppm] = 10.31 (s, 1H), 6.16 (s, 2H), 4.53 (d, *J* = 1.9 Hz, 1H), 3.71 – 3.50 (m, 2H), 1.46 (h, *J* = 7.5 Hz, 2H), 0.81 (t, *J* = 7.5 Hz, 3H). **^{13}C NMR** (126 MHz, $(CD_3)_2SO$) δ [ppm] = 162.9, 153.5, 151.0, 74.1, 40.2, 21.0, 11.2.

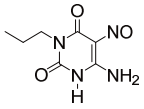

6-Amino-5-nitroso-3-propylpyrimidine-2,4(1H,3H)-dione (**38**)[42]

37 (21.439 g, 127 mmol, 1.0 eq) was dissolved in 300 mL H_2O:AcOH 1:1 at 65 °C. Sodium nitrite (10.97 g, 159 mmol, 1.3 eq) was added in parts to the stirring solution. An immediate color change was observed from brown to purple and back to brown. After approximately 30 minutes brown vapors started to form (NO_x). At this point the reaction was cooled on ice, filtered over a glass filter and washed thoroughly with water. This yielded **38** as a brown solid (18.429 g, 93 mmol, 73 % yield). **TLC** (DCM:MeOH 9:1): R_f = 0.29. **^{1}H NMR** (400 MHz, $(CH_3)_2SO$) δ [ppm] = 11.40 (s, 1H), 8.03 (s, 1H), 3.79 (t, *J* = 7.4 Hz, 2H), 1.59 (h, *J* = 7.5 Hz, 2H), 0.89 (t, *J* = 7.5 Hz, 3H). **^{13}C NMR** (101 MHz, $(CH_3)_2SO$) δ [ppm] = 161.2, 149.2, 144.5, 139.7, 41.4, 20.8, 11.2.

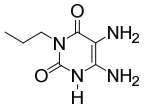

5,6-Diamino-3-propylpyrimidine-2,4(1H,3H)-dione (**16**)[51]

38 (1000 mg, 5.05 mmol, 1.0 eq) was dissolved in MeOH (40 ml) and brought under an N_2 atmosphere. platinum(IV) oxide (20 mg, cat) was added and the mixture was flushed two times with H_2 (g). The mixture was stirred for 1 h under H_2(g), after which a white/grey precipitate had formed. DCM (180 mL) was added and the mixture was filtered over Celite. The Celite was washed with 10% MeOH in DCM (100 mL) and the filtrate was concentrated under reduced pressure. This yielded **16** as an orange/brown solid (806 mg, 4.38 mmol, 87 % yield). This was used in the next steps without further purification. **^{1}H NMR** (400 MHz, $(CD_3)_2SO$) δ [ppm] = 5.56 (s, 2H), 3.70 – 3.59 (m, 2H), 1.48 (m, 2H), 0.81 (t, *J* = 7.5 Hz, 3H).

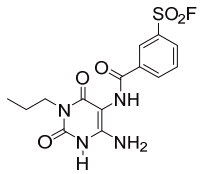

3-((6-Amino-2,4-dioxo-3-propyl-1,2,3,4-tetrahydropyrimidin-5-yl)carbamoyl)benzenesulfonyl fluoride (**17**)

EDC·HCl (688 mg, 3.59 mmol, 1.20 eq) was added to a solution of crude **16** (551 mg, 2.99 mmol, 1.0 eq) and 3-(fluorosulfonyl)benzoic acid (641 mg, 3.14 mmol, 1.05 eq) in dry DMF (10 mL). The mixture was stirred overnight at rt. Water (80 mL) was then added and the aqueous layer was extracted with EtOAc (13x). The organic layers were combined, washed with brine (10 mL), dried over $MgSO_4$ and concentrated under reduced pressure. The residue was purified by column chromatography (DCM:MeOH 96:4 → 90:10) to yield **17** as a white solid (598 mg, 2.99 mmol, 54%). **TLC** (DCM:MeOH 9:1): R_f = 0.48. **^{1}H NMR** (500 MHz, $(CD_3)_2SO$) δ [ppm] = 10.55 (s, 1H), 9.37 (s, 1H), 8.66 (t, *J* = 1.8 Hz, 1H), 8.45 (dt, *J* = 7.9, 1.4 Hz, 1H), 8.31 (ddd, *J* = 8.0, 2.0, 1.1 Hz, 1H), 7.92 (t, *J* = 7.9 Hz, 1H), 6.28 (s, 2H), 3.66 (t, *J* = 7.2 Hz, 2H), 1.51 (h, *J* = 7.5 Hz, 2H), 0.84 (t, *J* = 7.5 Hz, 3H). **^{13}C NMR** (126 MHz, $(CD_3)_2SO$) δ [ppm] = 164.3, 160.6, 150.6, 149.9, 136.6, 135.8, 131.6 (d, *J* = 23.6 Hz), 130.7, 130.6, 127.6, 86.3, 40.9, 21.0, 11.2. **^{19}F NMR** (471 MHz, $(CD_3)_2SO$) δ [ppm] = 66.1. **HPLC** RT 7.393 min. **LC-MS** $[ESI + H]^+$: 371.00.

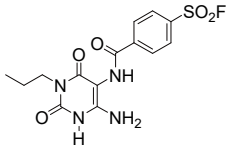

4-((6-Amino-2,4-dioxo-3-propyl-1,2,3,4-tetrahydropyrimidin-5-yl)carbamoyl)benzenesulfonyl fluoride (**18**)

EDC·HCl (513 mg, 2.67 mmol, 1.3 eq) was added to a solution of crude **16** (379 mg, 2.06 mmol, 1.0 eq) and 4-(fluorosulfonyl)benzoic acid (462 mg, 2.26 mmol, 1.1 eq) in dry DMF (8 mL). The mixture was stirred at rt overnight. Water (80 mL) was then added and the aqueous layers was extracted with EtOAc (7x). The organic layers were combined, washed with brine (10 mL), dried over $MgSO_4$ and concentrated under reduced pressure. The residue was purified by column chromatography (DCM:MeOH 95:5 → 90:10) to yield **18** as a yellow solid (100 mg, 0.27 mmol, 13%). **TLC** (DCM:MeOH 9:1): R_f = 0.48. **^{1}H NMR** (500 MHz, $(CD_3)_2SO$) δ [ppm] = 10.55 (s, 1H), 9.30 (s, 1H), 8.27 (s, 4H), 6.26 (s, 2H), 3.66 (t, *J* = 7.4 Hz, 2H), 1.55 – 1.46 (m, 2H), 0.84 (t, *J* = 7.5 Hz, 3H). **^{13}C NMR** (126 MHz, $(CD_3)_2SO$) δ [ppm] = 164.8, 160.5, 150.5, 149.9, 141.8, 133.4 (d, *J* = 23.7 Hz), 129.7, 128.3, 86.3, 40.9, 21.0, 11.2. **^{19}F NMR** (471 MHz, $(CD_3)_2SO$) δ [ppm] = 66.0. **HPLC** RT 7.370 min. **LC-MS** $[ESI + H]^+$: 371.00.

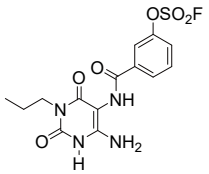

3-((6-amino-2,4-dioxo-3-propyl-1,2,3,4-tetrahydropyrimidin-5-yl)carbamoyl)phenyl sulfurofluoridate (**19**)

EDC·HCl (428 mg, 2.24 mmol, 1.2 eq) was added to a solution of crude **16** (343 mg, 1.86 mmol, 1.0 eq) and **35** (430 mg, 1.96 mmol, 1.05 eq) in dry DMF (10 mL). The mixture was stirred overnight at rt. TLC and LCMS showed full conversion of starting material and therefore water (80 mL) was added. The formed precipitate was collected and the filtrate was extracted with 5% MeOH in hot $CHCl_3$. The organic layer was concentrated and both residues were purified by column chromatography ($CHCl_3$:MeOH 98:2 → 92.5:7.5), combined and re-crystallized in MeOH to yield **19** as a white solid (237 mg, 0.61 mmol, 33%). **TLC** ($CHCl_3$:MeOH 95:5) R_f = 0.32. **^{1}H NMR** (500 MHz, $(CD_3)_2SO$) δ [ppm] = 10.54 (s, 1H), 9.17 (s, 1H), 8.11 (d, *J* = 7.6 Hz, 2H), 7.86 – 7.76 (m, 1H), 7.72 (t, *J* = 8.0 Hz, 1H), 6.24 (s, 2H), 3.66 (t, *J* = 7.3 Hz, 2H), 1.50 (h, *J* = 7.5 Hz, 2H), 0.83 (t, *J* = 7.4 Hz, 3H). **^{13}C NMR** (126 MHz, $(CD_3)_2SO$) δ [ppm] = 164.5, 160.6, 150.6, 150.0, 149.4, 137.3, 130.8, 128.6, 123.8, 120.5, 86.4, 41.0, 21.0, 11.2. **^{19}F NMR** (471 MHz, $(CD_3)_2SO$) δ [ppm] = 38.9. **HPLC** 100%, RT 7.817 min. **LC-MS** [ESI + H]$^+$: 386.95.

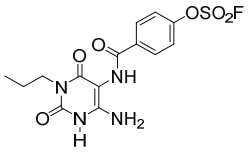

4-((6-Amino-2,4-dioxo-3-propyl-1,2,3,4-tetrahydropyrimidin-5-yl)carbamoyl)phenyl sulfurofluoridate (**20**)

EDC·HCl (446 mg, 2.33 mmol, 1.3 eq) was added to a solution of crude **16** (330 mg, 1.79 mmol, 1.0 eq) and **36** (394 mg, 1.79 mmol, 1.0 eq) in dry DMF (10 mL). The mixture was stirred overnight at rt. TLC and LCMS showed full conversion of starting material and therefore water (80 mL) was added. The aqueous layer was extracted with EtOAc (4 x). The organic layers were combined, washed with brine (10 mL), dried over $MgSO_4$, filtered and concentrated under reduced pressure. The residue was purified by column chromatography (DCM:MeOH 94:6 → 90:10) and re-crystallized in MeOH to yield **20** as a white solid (104 mg, 0.27 mmol, 15%). **TLC** ($CHCl_3$:MeOH 94:6) R_f = 0.32. **^{1}H NMR** (500 MHz, $(CD_3)_2SO$) δ [ppm] = 10.51 (s, 1H), 9.09 (s, 1H), 8.14 (d, *J* = 8.5 Hz, 2H), 7.72 (d, *J* = 8.4 Hz, 2H), 6.19 (s, 2H), 3.66 (t, *J* = 7.2 Hz, 2H), 1.50 (h, *J* = 7.4 Hz, 2H), 0.84 (t, *J* = 7.4 Hz, 3H). **^{13}C NMR** (126 MHz, $(CD_3)_2SO$) δ [ppm] = 164.0, 159.6, 150.2, 149.6, 149.0, 134.4, 129.6, 119.9, 85.5, 39.9, 20.0, 10.2. **^{19}F NMR** (471 MHz, $(CD_3)_2SO$) δ [ppm] = 38.9. **HPLC** 100%, RT 7.875 min. **LC-MS** [ESI + H]$^+$: 386.95.

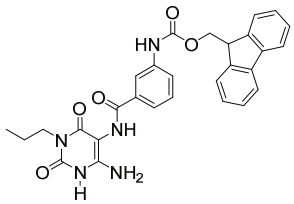

(9H-Fluoren-9-yl)methyl (3-((6-amino-2,4-dioxo-3-propyl-1,2,3,4-tetrahydropyrimidin-5-yl)carbamoyl)phenyl)carbamate (**21**)

3-(Fmoc-amino)benzoic acid (1.34 g, 3.74 mmol, 1.05 eq) and EDC·HCl (819 mg, 4.27 mmol, 1.2 eq) were added to a solution of crude **16** (656 mg, 3.56 mmol, 1.0 eq) in dry DMF (20 mL). The mixture was stirred for 2 days, after which LCMS and TLC showed full conversion of starting material. The DMF was removed by heating under reduced pressure and water (100 mL) was added. The mixture was extracted with EtOAc (4 x 100 mL), washed with brine (100 mL), dried over $MgSO_4$, filtered and concentrated under reduced pressure. The residue was collected, washed several times with MeOH and acetone and further purified by column chromatography ($CHCl_3$:MeOH 95:5) to yield **21** as an off-white solid (397 mg, 0.76 mmol, 21%). **TLC** ($CHCl_3$:MeOH 95:5) R_f = 0.20. **^{1}H NMR** (400 MHz, $(CD_3)_2SO$) δ [ppm] = 10.47 (s, 1H), 9.89 (s, 1H), 8.84 (s, 1H), 7.99 (s, 1H), 7.91 (d, *J* = 7.5 Hz, 2H), 7.77 (d, *J* = 7.4 Hz, 2H), 7.65 (d, *J* = 8.1 Hz, 2H), 7.43 (t, *J* = 7.4 Hz, 2H), 7.35 (td, *J* = 7.4, 1.3 Hz, 3H), 6.07 (s, 2H), 4.47 (d, *J* = 6.8 Hz, 2H), 4.32 (t, *J* = 6.8 Hz, 1H), 3.66 (t, *J* = 7.6, 7.1 Hz, 2H), 1.50 (h, *J* = 7.5 Hz, 2H), 0.84 (t, *J* = 7.5 Hz, 3H).

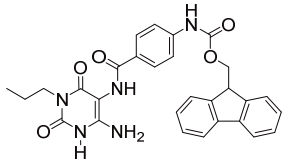

(9H-fluoren-9-yl)methyl (4-((6-amino-2,4-dioxo-3-propyl-1,2,3,4-tetrahydropyrimidin-5-yl)carbamoyl)phenyl)carbamate (**22**)

4-(Fmoc-amino)benzoic acid (1.89 g, 5.25 mmol, 1.2 eq) and EDC·HCl (1.09 g, 5.70 mmol, 1.3 eq) were added to a solution of **16** (806 mg, 4.38 mmol, 1.0 eq) in dry DMF (16 mL). The mixture was stirred for 1 h, after which LCMS showed completion of the reaction. EtOAc (250 mL) was added and the organic layer was washed with brine (3 x 100 mL). Upon addition of brine, a precipitate formed in the organic layer. The precipitate was collected and recrystallized in MeOH to yield **22** as yellow/green solid (1.17 g, 2.22 mmol, 51%). **TLC** (DCM:MeOH 98:2): Rf = 0.44. **^{1}H NMR** (400 MHz, $(CD_3)_2SO$) δ [ppm] = 10.62 (s, 1H), 10.01 (s, 1H), 8.76 (s, 1H), 7.92 (dd, *J* = 13.8, 7.9 Hz, 4H), 7.78 (d, *J* = 7.5 Hz, 2H), 7.54 (s, 2H), 7.45 (t, *J* = 7.4 Hz, 2H), 7.37 (t, *J* = 6.8 Hz, 2H), 6.20 (s, 2H), 4.53 (d, *J* = 6.7 Hz, 2H), 4.34 (t, *J* = 6.6 Hz, 1H), 3.66 (t, *J* = 7.5 Hz, 2H), 1.51 (h, *J* = 7.1 Hz, 2H), 0.84 (t, *J* = 7.4 Hz, 3H). **^{13}C NMR** (101 MHz, $(CD_3)_2SO$) δ [ppm] = 165.8, 160.7, 153.3, 150.6, 149.9, 143.7, 141.7, 140.8, 128.8, 128.3, 127.7, 127.2, 125.2, 120.2, 117.1, 87.0, 65.8, 46.6, 40.9, 21.0, 11.2.

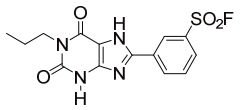

3-(2,6-Dioxo-1-propyl-2,3,6,7-tetrahydro-1H-purin-8-yl)benzenesulfonyl fluoride (**23**)
Trimethylsilyl polyphosphate (PPSE) (2.50 g, 13.72 mmol, 9.0 eq) was added to **17** (568 mg, 1.53 mmol, 1.0 eq). The mixture was refluxed at 150 °C for 3.5 h under an N_2 atmosphere. LCMS measurements indicated full conversion of the reaction. The mixture was cooled on ice and MeOH (25 mL) was added. The mixture was stirred for 15 minutes and filtrated. The filtrate was stirred in MeOH (15 mL) and filtrated again. The residues were combined, washed with cold MeOH and dried *in vacuo* to yield **23** as a white powder (467 mg, 1.33 mmol, 86%). **TLC** (DCM:MeOH 98:2) R_f = 0.44. **^{1}H NMR** (500 MHz, $(CD_3)_2SO$) δ [ppm] = 14.11 (s, 1H), 11.95 (s, 1H), 8.78 (s, 1H), 8.55 (d, *J* = 8.0 Hz, 1H), 8.17 (d, *J* = 8.0 Hz, 1H), 7.89 (t, *J* = 7.9 Hz, 1H), 3.80 (t, *J* = 7.4 Hz, 2H), 1.56 (h, *J* = 7.5 Hz, 2H), 0.87 (t, *J* = 7.4 Hz, 3H). **^{13}C NMR** (126 MHz, $(CD_3)_2SO$) δ [ppm] = 154.9, 150.9, 147.4, 147.0, 133.5, 132.6 (d, *J* = 24.0 Hz), 131.4, 130.8, 129.1, 125.5, 108.5, 41.5, 20.9, 11.2. **^{19}F NMR** (471 MHz, $(CD_3)_2SO$) δ [ppm] = 66.0. **HPLC:** 100%, RT 9.095 min **LC-MS** [ESI + H]$^+$: 353.00.

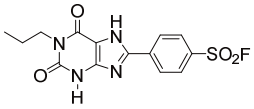

4-(2,6-Dioxo-1-propyl-2,3,6,7-tetrahydro-1H-purin-8-yl)benzenesulfonyl fluoride (**24**) **(LUF7982)**
PPSE (430 mg, 2.36 mmol, 9.0 eq) was added to **18** (97 mg, 0.26 mmol, 1.0 eq) and refluxed at 150 °C for 7 h under an N_2 atmosphere. More PPSE (430 mg, 2.36 mmol, 9.0 eq) was added and the mixture was refluxed for another 4 h, upon which LCMS measurements indicated full conversion of starting material. The mixture was cooled on ice, MeOH (25 mL) was added and the formed crystals were filtrated. The filtrate was stirred in MeOH (15 mL) for 15 minutes and filtrated again. The residues were combined, washed with cold MeOH and dried *in vacuo* to yield **24** (LUF7982) as a white powder (68 mg, 0.19 mmol, 74%). **TLC** (DCM:MeOH 98:2) R_f = 0.44. **^{1}H NMR** (300 MHz, $(CD_3)_2SO$) δ [ppm] = 14.24 (s, 1H), 12.05 (s, 1H), 8.43 (d, *J* = 8.3 Hz, 2H), 8.28 (d, *J* = 8.3 Hz, 2H), 3.83 (t, *J* = 7.5 Hz, 2H), 1.69 – 1.47 (m, 2H), 0.88 (t, *J* = 7.4 Hz, 3H). **^{13}C NMR** (126 MHz, $(CD_3)_2SO$) δ [ppm] = 154.98, 150.92, 147.68, 146.98, 135.92, 131.67 (d, *J* = 23.9 Hz), 129.23, 128.02, 109.08, 41.54, 20.85, 11.19. **^{19}F NMR** (471 MHz, $(CD_3)_2SO$) δ [ppm] = 66.8. **HPLC** 99%, RT 9.124 min. **LC-MS** [ESI + H]$^+$: 353.00.

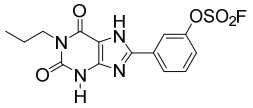

3-(2,6-Dioxo-1-propyl-2,3,6,7-tetrahydro-1H-purin-8-yl)phenyl sulfurofluoridate (**25**)
PPSE (2.2 g, 12.07 mmol, 22.2 eq) was added to **19** (210 mg, 0.54 mmol, 1.0 eq) and refluxed at 150 °C. LCMS showed full conversion of starting material after 3h. Therefore the mixture was cooled on ice and MeOH (50 mL) was added. The formed residue was collected and washed with cold MeOH. Recrystallization in $CHCl_3$/MeOH yielded **25** as a white solid (161 mg, 0.44 mmol, 80%). **TLC** (DCM:MeOH 95:5) R_f = 0.63. **^{1}H NMR** (400 MHz, $(CD_3)_2SO$) δ [ppm] = 14.00 (s, 1H), 11.98 (s, 1H), 8.22 (dd, *J* = 6.3, 2.0 Hz, 2H), 7.79 – 7.67 (m, 2H), 3.82 (t, *J* = 7.5 Hz, 2H), 1.57 (h, *J* = 7.5 Hz, 2H), 0.88 (t, *J* = 7.4 Hz, 3H). **^{13}C NMR** (126 MHz, $(CD_3)_2SO$) δ [ppm] = 154.9, 150.9, 150.0, 147.6, 147.5, 131.7, 131.5, 126.7, 122.9, 118.4,

108.3, 41.5, 20.9, 11.2. **^{19}F NMR** (471 MHz, $(CD_3)_2SO$) δ [ppm] = 38.9. **HPLC** 97%, RT 9.332 min. **LC-MS** $[ESI + H]^+$: 368.95.

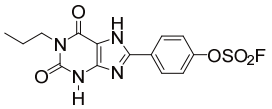

4-(2,6-Dioxo-1-propyl-2,3,6,7-tetrahydro-1H-purin-8-yl)phenyl sulfurofluoridate (**26**) **(LUF7993)**

PPSE (1.2 g, 6.59 mmol, 25.7 eq) was added to **20** and refluxed at 150 °C. The mixture was refluxed for 2 h, after which LCMS indicated full conversion of starting material. The mixture was cooled on ice and MeOH (25 mL) was added. The formed precipitate was collected, washed with cold MeOH and recrystallized in MeOH (15 mL). This yielded **26** (LUF7993) as a white powder (83 mg, 0.23 mmol, 88%). **TLC** (DCM:MeOH 95:5) R_f = 0.55. **^{1}H NMR** (500 MHz, $(CD_3)_2SO$) δ [ppm] = 13.90 (s, 1H), 11.94 (s, 1H), 8.26 (d, *J* = 8.9 Hz, 2H), 7.74 (d, *J* = 8.4 Hz, 2H), 3.81 (t, *J* = 7.4 Hz, 2H), 1.57 (h, *J* = 7.4 Hz, 2H), 0.87 (t, *J* = 7.4 Hz, 3H). **^{13}C NMR** (126 MHz, $(CD_3)_2SO$) δ [ppm] = 154.9, 151.0, 150.3, 148.1, 147.6, 129.8, 128.7, 121.9, 108.2, 41.5, 20.9, 11.2. **^{19}F NMR** (471 MHz, $(CD_3)_2SO$) δ [ppm] = 38.94. **HPLC** 99%, RT 9.327 min. **LC-MS** $[ESI + H]^+$: 369.00.

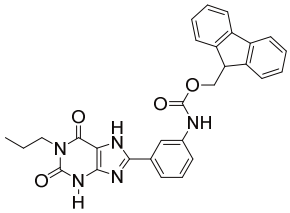

(9H-Fluoren-9-yl)methyl (3-(2,6-dioxo-1-propyl-2,3,6,7-tetrahydro-1H-purin-8-yl)phenyl)carbamate (**27**)

PPSE (3.44 g, 18.88 mmol, 25.0 eq) was added to **21** (397 mg, 0.76 mmol, 1.0 eq) and the mixture was refluxed at 150 °C. After 3 h of stirring, TLC showed full conversion of the reaction. The mixture was cooled down to rt and water (40 mL) and brine (10 mL) were added. The aqueous layer was extracted by EtOAc (6 x 80 mL). The organic layers were combined, dried over $MgSO_4$, filtered and concentrated under reduced pressure. This yielded **27** (269 mg, 0.53 mmol, 70%) as an off-white solid. **TLC** ($CHCl_3$:MeOH 95:5) R_f = 0.55. **^{1}H NMR** (400 MHz, $(CD_3)_2SO$) δ [ppm] = 13.71 (s, 1H), 11.92 (s, 1H), 9.94 (s, 1H), 8.33 (s, 1H), 7.92 (d, *J* = 7.5 Hz, 2H), 7.76 (t, *J* = 7.1 Hz, 3H), 7.43 (t, *J* = 7.5 Hz, 3H), 7.40 – 7.32 (m, 3H), 4.49 (d, *J* = 6.8 Hz, 2H), 4.33 (t, *J* = 6.8 Hz, 1H), 3.82 (t, *J* = 7.5 Hz, 2H), 1.57 (h, *J* = 7.1 Hz, 2H), 0.88 (t, *J* = 7.4 Hz, 3H). **HPLC** 95%, RT 11.075 min. **LC-MS** $[ESI + H]^+$: 508.10.

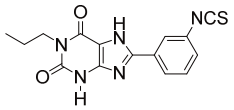

8-(3-Isothiocyanatophenyl)-1-propyl-3,7-dihydro-1H-purine-2,6-dione (**28**)
20% Piperidine in DMF (6 mL) was added to remove the Fmoc group of **27** (265 mg, 0.52 mmol, 1.0 eq). The deprotection was complete after 5 min of stirring at rt. The solvents were then removed under reduced pressure and the residue was washed with MeOH to remove the remaining N-Fmoc-piperidine. 3 M HCl (25 mL) was added to the crude amine to form a suspension. Thiophosgene (333 µL, 4.35 mmol, 8.4 eq) was added and the mixture was stirred for 4 h at rt. The aqueous suspension was filtered and the precipitate was washed thoroughly with EtOAc to yield **28** as a white solid (129 mg, 0.39 mmol, 75% over two steps). **TLC** (DCM:MeOH 95:5) R_f = 0.62. **^{1}H NMR** (500 MHz, $(CD_3)_2SO$) δ [ppm] = 14.01 – 13.74 (s, 1H), 11.94 (s, 1H), 8.12 (t, *J* = 1.9 Hz, 1H), 8.06 (dt, *J* = 7.9, 1.3 Hz, 1H), 7.57 (t, *J* = 7.9 Hz, 1H), 7.48 (dd, *J* = 8.0, 1.0 Hz, 1H), 3.80 (t, *J* = 7.3 Hz, 2H), 1.56 (h, *J* = 7.3 Hz, 2H), 0.87 (t, *J* = 7.4 Hz, 3H). **^{13}C NMR** (126 MHz, $(CD_3)_2SO$) δ [ppm] = 154.8, 150.9, 148.1, 147.4, 135.3, 131.0, 130.7, 130.5, 126.8, 125.5, 123.6, 108.1, 41.4, 20.8, 11.2. **HPLC** 99%, RT 9.825 min. **LC-MS** [ESI - H]$^-$: 326.95.

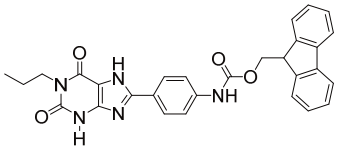

(9H-Fluoren-9-yl)methyl (4-(2,6-dioxo-1-propyl-2,3,6,7-tetrahydro-1H-purin-8-yl)phenyl)carbamate (**29**)
PPSE (22 mL) was added to **22** (1.17 g, 2.22 mmol, 1.0 eq) and refluxed at 170 °C. After 5 h of stirring, the mixture was cooled down to rt and water (250 mL) was added. The formed precipitate was collected and purified by column chromatography (DCM:MeOH 99.5:0.5 → 95:5) to yield **29** as an off-white solid (618 mg, 1.22 mmol, 55%). **TLC** (DCM:MeOH 98:2) R_f = 0.38. **^{1}H NMR** (400 MHz, $(CD_3)_2SO$) δ [ppm] 13.50 (s, 1H), 11.87 (s, 1H), 9.98 (s, 1H), 8.01 (dd, *J* = 16.6, 8.5 Hz, 2H), 7.92 (d, *J* = 7.4 Hz, 2H), 7.76 (d, *J* = 7.4 Hz, 2H), 7.63 – 7.51 (m, 2H), 7.43 (t, *J* = 7.4 Hz, 2H), 7.36 (t, *J* = 7.3 Hz, 2H), 4.54 (d, *J* = 6.6 Hz, 2H), 4.33 (t, *J* = 6.5 Hz, 1H), 3.81 (t, *J* = 7.5 Hz, 2H), 1.57 (m, 2H), 0.87 (t, *J* = 7.4 Hz, 3H).

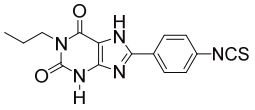

8-(4-Isothiocyanatophenyl)-1-propyl-3,7-dihydro-1H-purine-2,6-dione (**30**) **(LUF8002)**
20% Piperidine in DMF (6 mL) was added to remove the Fmoc group of **29** (85 mg, 0.17 mmol, 1.0 eq). The deprotection was complete after 5 min of stirring at rt. The solvents were then removed under reduced pressure and the residue was washed with MeOH to remove the remaining N-Fmoc-piperidine. 3 M HCl (3 mL) was then added to the crude amine to form a suspension. Thiophosgene (150 µL, 1.96 mmol, 11.9 eq) was added and the mixture was stirred for 2 h at rt. LCMS indicated full conversion of starting material, therefore water (50 mL) was added. The formed precipitate was collected and washed with DCM (50 mL) and EtOAc (50 mL). The residue was dried under reduced pressure to yield **30** (LUF8002) as an off-white powder (40 mg, 0.12 mmol, 71% over two steps). **TLC** (DCM:MeOH 95:5) R_f = 0.55. **^{1}H NMR** (500 MHz, $(CD_3)_2SO$) δ [ppm] = 13.81 (s, 1H), 11.94 (s, 1H), 8.13 (d, *J* = 8.7 Hz, 2H), 7.56 (d, *J* = 8.7 Hz, 2H), 3.82 (t, *J* = 7.5 Hz, 2H), 1.57 (h, *J* = 7.3 Hz, 2H), 0.88 (t, *J* = 7.4 Hz, 3H). **^{13}C**

NMR (151 MHz, $(CD_3)_2SO$) δ [ppm] = 154.9, 151.0, 148.6, 147.6, 134.7, 131.3, 128.1, 127.7, 126.7, 108.1, 41.5, 20.9, 11.2. **HPLC** 95%, RT 9.834 min. **LC-MS** $[ESI + H]^+$: 327.95.

Biology

Cell lines

CHO-spap cells stably expressing the human A_{2B} receptor (CHO-spap-hA_{2B}AR) were kindly provided by S.J. Dowell (Glaxo Smith Kline, UK). Chinese hamster ovary (CHO) cells stably expressing the human adenosine A_1 receptor (CHOhA_1AR) were kindly provided by Prof. S.J. Hill (University of Nottingham, UK). Human embryonic kidney 293 cells stably expressing the human adenosine A_{2A} receptor (HEK293hA_{2A}AR) were kindly provided by Dr. J. Wang (Biogen/IDEC, Cambridge, MA). CHO cells stably expressing the human adenosine A_3 receptor (CHOhA_3AR) were a kindly provided by Dr. K.N. Klotz (University of Würzburg, Germany).

Radioligands

$[^3H]$8-(4-(4-(4-Chlorophenyl)piperazide-1-sulfonyl)phenyl)-1-propylxanthine ($[^3H]$PSB-603, specific activity 79 Ci/mmol) was purchased from Quotient Bioresearch. $[^3H]$1,3-dipropyl-8-cyclopentyl-xanthine ($[^3H]$DPCPX, specific activity 137 Ci/mmol) was purchased from ARC, Inc. $[^3H]$4-(-2-[7-amino-2-(furan-2-yl)-[1,2,4]triazolo[1,5-a][1,3,5]triazin-5-ylamino)ethyl) phenol ($[^3H]$-ZM241385, specific activity 50 Ci/mmol) was purchased from ARC, Inc. $[^3H]$8-Ethyl-4-methyl-2-phenyl-(8R)-4,5,7,8-tetrahydro-1H-imidazo[2,1-i]-purin-5-one ($[^3H]$PSB-11, specific activity 56 Ci/mmol) was a gift from Prof. C.E. Müller (University of Bonn, Germany).

Chemicals

5'-N-ethylcarboxamidoadenosine (NECA), N^6-Cyclopentyladenosine (CPA) and adenosine deaminase (ADA) were purchased from Sigma Aldrich. ZM241385 was kindly donated by Dr. S.M. Poucher (Astra Zeneca, Manchester, UK). CGS21680 was purchased from Ascent Scientific. PSB 1115 potassium salt was purchased from Tocris Bioscience. All other chemicals were of analytical grade and obtained from standard commercial sources.

Cell culture and membrane preparation

CHO-spap-hA_{2B}R cells, CHOhA_1AR cells, HEK293hA_{2A}AR cells and CHOhA_3AR were cultured and membranes were prepared as previously reported.[52]

Radioligand displacement assays

Single point radioligand displacement assays on CHOhA_1AR cells, HEK293hA_{2A}AR cells and CHOhA_3AR cells were performed as previously reported.[52] Full curve radioligand displacement assays were performed using ChO-spap-hA_{2B}AR membranes and a concentration rage of competing ligand. 30 µg of protein in a total volume of 100 µL assay buffer (0.1% CHAPS in 50 mM Tris-HCl pH 7.4) was taken and pre-incubated for either 0 or 4 h with the competing ligand. ~1.5 nM $[^3H]$PSB-603 was then added and the membranes were co-incubated for 30 min at 25 °C. Nonspecific binding was determined in the presence of 10 µM ZM241385. Incubations were terminated by vacuum filtration to separate the bound and free radioligand through prewetted 96-well GF/C filter plates using a Filtermate-harvester (PerkinElmer). Filters were subsequently washed 5 times with ice-cold wash buffer (0.1% BSA in 50 mM Tris-HCl pH 7.4). The plates were dried at 55 °C after which 25 µL of MicroscintTM-20 cocktail (PerkinElmer) was added to each well. After 3 h the filter-bound radioactivity was determined by scintillation spectrometry using a 2450 MicroBeta^2 Microplate Counter (PerkinElmer).

Wash-out assays

100 µL of assay buffer (0.1% CHAPS in 50 mM Tris-HCl pH 7.4) containing 1 µM of competing ligand (10 µM in case of PSB 1115) and 200 µL of assay buffer were added to 100 µL of ChO-spap-hA_{2B}AR membrane suspension (80 µg of protein) in a 2 mL Eppendorf tube. The tubes were incubated 2 h at 25 °C while shaking. The 'washed' group of samples was centrifuged (5 min, 13 200 rpm, 4 °C), the supernatant was removed, the pellet was resuspended in 1 mL of assay buffer and incubated for 10 min at 25 °C while shaking at 900 rpm. The washing steps were repeated three times. After the last washing step, the membrane pellets were resuspended in 300 µL of assay buffer to determine radioligand displacement. Both washed and unwashed samples were transferred to test tubes and incubated together with 100 µL of 1.5 nM [^{3}H]PSB-603 for 2 h at 25 °C. Nonspecific binding was determined in the presence of 10 µM ZM241385. The incubation was terminated by vacuum filtration through prewetted 96-well GF/C filter plates using a Brandol M24 Scintillation harvester. Filters were subsequently washed 3 times with ice-cold wash buffer (0.1% BSA in 50 mM Tris-HCl pH 7.4). The filter-bound radioactivity was determined using a Tri-Carb 2900TR Liquid Scintillation Analyzer (PerkinElmer).

Data Analysis

All data from radioligand displacement and wash-out assays were analyzed using GraphPad Prism 9.0 (GraphPad Software Inc., San Diego, CA). IC_{50} values were converted to K_i values using the Cheng-Prusoff equation.[53] The K_D values of [^{3}H]PSB603 at CHO-spap-hA_{2B}AR membranes (1.7 nM) was taken from in-house determinations.

Computational Procedures

Docking of LUF7982 in the adenosine A_{2B} receptor

The A_{2B}AR homology model was retrieved from the GPCRdb.[54] Several orientations of the extracellular loop 3 (EL3) loop region (between residue numbers 258 and 270) were generated using MODELLER,[55] to obtain viable orientations of the Lysine residues in the binding site. 3D coordinates of LUF7982 were generated using rdkit.[56] Thereafter, LUF7982 was manually docked in the receptor model using PyMOL,[57] and subsequently minimized using the all-atom minimization tool in ICM Pro.[58] Residue numbers are presented with their Ballosteros-Weinstein numbering scheme.[23] Distances given in Å are the distances calculated between the N-atom of the lysine residue and the S-atom of the sulfonyl fluoride warhead.

Author Contributions

B.L.H.B., M.A. and J.P.D.V. synthesized compounds. X.W., L.N.A. and R.L. performed radioligand displacement experiments. B.L.H.B., M.A. and W.J. performed molecular docking experiments. L.H.H., A.P.IJ. and D.v.d.E. supervised the project.

References

[1] B. B. Fredholm, A. P. IJzerman, K. A. Jacobson, K.-N. Klotz, J. Linden, *Pharmacol Rev* **2001**, *53*, 527–552.

[2] B. B. Fredholm, A. P. IJzerman, K. A. Jacobson, J. Linden, C. E. Müller, *Pharmacol Rev* **2011**, *63*, 1–34.

[3] B. Allard, D. Allard, L. Buisseret, J. Stagg, *Nat Rev Clin Oncol* **2020**, *17*, 611–629.

[4] J.-F. Chen, H. K. Eltzschig, B. B. Fredholm, *Nat Rev Drug Discov* **2013**, *12*, 265–286.

[5] Z. Gao, K. A. Jacobson, *Int J Mol Sci* **2019**, *20*, 5139.

[6] C. Cekic, J. Linden, *Nat Rev Immunol* **2016**, *16*, 177–192.

[7] P. A. Borea, S. Gessi, S. Merighi, F. Vincenzi, K. Varani, *Physiol Rev* **2018**, *98*, 1591–1625.

[8] T. Zhang, J. M. Hatcher, M. Teng, N. S. Gray, M. Kostic, *Cell Chem Biol* **2019**, *26*, 1486–1500.

[9] D. Weichert, P. Gmeiner, *ACS Chem Biol* **2015**, *10*, 1376–1386.

[10] A. Glukhova, D. M. Thal, A. T. Nguyen, E. A. Vecchio, M. Jörg, P. J. Scammells, L. T. May, P. M. Sexton, A. Christopoulos, *Cell* **2017**, *168*, 867–877.

[11] X. Yang, L. H. Heitman, A. P. IJzerman, D. van der Es, *Purinergic Signal* **2021**, *17*, 85–108.

[12] C. E. Müller, K. A. Jacobson, *Biochim Biophys Acta* **2011**, *1808*, 1290–1308.

[13] K. A. Jacobson, A. P. IJzerman, J. Linden, *Drug Dev Res* **1999**, *47*, 45–53.

[14] Y.-C. Kim, X. Ji, N. Melman, J. Linden, K. A. Jacobson, *J Med Chem* **2000**, *43*, 1165–1172.

[15] A. M. Hayallah, J. Sandoval-Ramírez, U. Reith, U. Schobert, B. Preiss, B. Schumacher, J. W. Daly, C. E. Müller, *J Med Chem* **2002**, *45*, 1500–1510.

[16] T. Borrmann, S. Hinz, D. C. G. Bertarelli, W. Li, N. C. Florin, A. B. Scheiff, C. E. Müller, *J Med Chem* **2009**, *52*, 3994–4006.

[17] J. Jiang, C. J. Seel, A. Temirak, V. Namasivayam, A. Arridu, J. Schabikowski, Y. Baqi, S. Hinz, J. Hockemeyer, C. E. Müller, *J Med Chem* **2019**, *62*, 4032–4055.

[18] X.-D. Ji, C. Gallo-Rodriguez, K. A. Jacobson, *Drug Dev Res* **1993**, *29*, 292–298.

[19] J. C. Shryock, S. Snowdy, P. G. Baraldi, B. Cacciari, G. Spalluto, A. Monopoli, E. Ongini, S. P. Baker, L. Belardinelli, *Circulation* **1998**, *98*, 711–718.

[20] X. Yang, G. Dong, T. J. M. Michiels, E. B. Lenselink, L. H. Heitman, J. Louvel, A. P. IJzerman, *Purinergic Signal* **2017**, *13*, 191–201.

[21] A. S. Doré, N. Robertson, J. C. Errey, I. Ng, K. Hollenstein, B. Tehan, E. Hurrell, K. Bennett, M. Congreve, F. Magnani, C. G. Tate, M. Weir, F. H. Marshall, *Structure* **2011**, *19*, 1283–1293.

[22] R. K. Y. Cheng, E. Segala, N. Robertson, F. Deflorian, A. S. Doré, J. C. Errey, C. Fiez-Vandal, F. H. Marshall, R. M. Cooke, *Structure* **2017**, *25*, 1275–1285.

[23] J. A. Ballesteros, H. Weinstein, in *Methods in Neurosciences* (Ed.: S.C. Sealfon), Academic Press, **1995**, pp. 366–428.

[24] A. Narayanan, L. H. Jones, *Chem Sci* **2015**, *6*, 2650–2659.

[25] H. Mukherjee, J. Debreczeni, J. Breed, S. Tentarelli, B. Aquila, J. E. Dowling, A. Whitty, N. P. Grimster, *Org Biomol Chem* **2017**, *15*, 9685–9695.

[26] D. E. Mortenson, G. J. Brighty, L. Plate, G. Bare, W. Chen, S. Li, H. Wang, B. F. Cravatt, S. Forli, E. T. Powers, K. B. Sharpless, I. A. Wilson, J. W. Kelly, *J Am Chem Soc* **2018**, *140*, 200–210.

[27] J. Dong, L. Krasnova, M. G. Finn, K. B. Sharpless, *Angewandte Chemie - International Edition* **2014**, *53*, 9430–9448.

[28] A. R. Beauglehole, S. P. Baker, P. J. Scammells, *J Med Chem* **2000**, *43*, 4973–4980.

[29] M. Jörg, A. Glukhova, A. Abdul-Ridha, E. A. Vecchio, A. T. N. Nguyen, P. M. Sexton, P. J. White, L. T. May, A. Christopoulos, P. J. Scammells, *J Med Chem* **2016**, *59*, 11182–11194.

[30] X. Yang, J. P. D. van Veldhoven, J. Offringa, B. J. Kuiper, E. B. Lenselink, L. H. Heitman, D. van Der Es, A. P. IJzerman, *J Med Chem* **2019**, *62*, 3539–3552.

[31] X. Yang, M. A. Dilweg, D. Osemwengie, L. Burggraaff, D. van der Es, L. H. Heitman, A. P. IJzerman, *Biochem Pharmacol* **2020**, *180*, DOI 10.1016/j.bcp.2020.114144.

[32] A. Baranczak, Y. Liu, S. Connelly, W.-G. H. Du, E. R. Greiner, J. C. Genereux, R. L. Wiseman, Y. S. Eisele, N. C. Bradbury, J. Dong, L. Noodleman, K. B. Sharpless, I. A. Wilson, S. E. Encalada, J. W. Kelly, *J Am Chem Soc* **2015**, *137*, 7404–7414.

[33] M. Gehringer, S. A. Laufer, *J Med Chem* **2019**, *62*, 5673–5724.

[34] T. Nakamura, Y. Kawai, N. Kitamoto, T. Osawa, Y. Kato, *Chem Res Toxicol* **2009**, *22*, 536–542.

[35] G. L. Stiles, K. A. Jacobson, *Mol Pharmacol* **1988**, *34*, 724–728.

[36] K. A. Jacobson, S. Barone, U. Kammula, G. L. Stiles, *J Med Chem* **1989**, *32*, 1043–1051.

[37] J. Zhang, L. Belardinelli, K. A. Jacobson, D. H. Otero, S. P. Baker, *Mol Pharmacol* **1997**, *52*, 491–498.

[38] A. Vlachodimou, H. de Vries, M. Pasoli, M. Goudswaard, S.-A. Kim, Y.-C. Kim, M. Scortichini, M. Marshall, J. Linden, L. H. Heitman, K. A. Jacobson, A. P. IJzerman, *Biochem Pharmacol* **2022**, *200*, 115027.

[39] C. E. Müller, *Tetrahedron Lett* **1991**, *32*, 6539–6540.

[40] C. E. Müller, *Synthesis (Stuttg)* **1993**, *1*, 125–128.

[41] C. E. Müller, J. Sandoval-Ramirez, *Synthesis (Stuttg)* **1995**, *10*, 1295–1299.

[42] J. Hockemeyer, J. C. Burbiel, C. E. Müller, *Journal of Organic Chemistry* **2004**, *69*, 3308–3318.

[43] Y. Imai, A. Mochizuki, M. Kakimoto, *Synthesis (Stuttg)* **1983**, 851.

[44] C. E. Müller, D. Shi, M. Manning, J. W. Daly, *J Med Chem* **1993**, *36*, 3341–3349.

[45] J. R. Pfister, L. Belardinelli, G. Lee, R. T. Lum, P. Milner, W. C. Stanley, J. Linden, S. P. Baker, G. Schreiner, *J Med Chem* **1997**, 1773–1778.

[46] S. Weyler, F. Fülle, M. Diekmann, B. Schumacher, S. Hinz, K.-N. Klotz, C. E. Müller, *ChemMedChem* **2006**, *1*, 891–902.

[47] W. Jespers, A. C. Schiedel, L. H. Heitman, R. M. Cooke, L. Kleene, G. J. P. van Westen, D. E. Gloriam, C. E. Müller, E. Sotelo, H. Gutiérrez-de-Terán, *Trends Pharmacol Sci* **2018**, *39*, 75–89.

[48] M. G. Moloney, D. R. Paul, R. M. Thompson, E. Wright, *Tetrahedron Asymmetry* **1996**, *7*, 2551–2562.

[49] M. Söftje, S. Acker, R. Plarre, J. C. Namyslo, D. E. Kaufmann, *RSC Adv* **2020**, *10*, 15726–15733.

[50] H. Zhou, P. Mukherjee, R. Liu, E. Evrard, D. Wang, J. M. Humphrey, T. W. Butler, L. R. Hoth, J. B. Sperry, S. K. Sakata, C. J. Helal, C. W. Am Ende, *Org Lett* **2018**, *20*, 812–815.

[51] C. E. Müller, J. Sandoval-Ramirez, *Synthesis (Stuttg)* **1995**, *19995*, 1295–1299.

[52] T. Amelia, J. P. D. Van Veldhoven, M. Falsini, R. Liu, L. H. Heitman, G. J. P. Van Westen, E. Segala, G. Verdon, R. K. Y. Cheng, R. M. Cooke, D. Van Der Es, A. P. IJzerman, *J Med Chem* **2021**, *64*, 3827–3842.

[53] Y.-C. Cheng, W. H. Prusoff, *Biochem Pharmacol* **1973**, *22*, 3099–3108.

[54] A. J. Kooistra, S. Mordalski, G. Pándy-Szekeres, M. Esguerra, A. Mamyrbekov, C. Munk, G. M. Keserű, D. E. Gloriam, *Nucleic Acids Res* **2021**, *49*, D335–D343.

[55] B. Webb, A. Sali, *Curr Protoc Bioinformatics* **2016**, *54*, 5.6.1-5.6.37.

[56] "RDKit: Open-source cheminformatics," can be found under http://www.rdkit.org

[57] Schrödinger LLC, *The PyMOL Molecular Graphics System, Version 2.6.0a0*

[58] M. Totrov & R. Abagyan, in *Drug-Receptor Thermodynamics: Introduction and Applications*, Wiley & Sons, **2001**, pp. 603–624.

Chapter 4

A Chemical Biological Approach to Study G Protein-Coupled Receptors: Labeling the Adenosine A_1 Receptor using an Electrophilic Covalent Probe

Bert L. H. Beerkens, Çağla Koç, Rongfang Liu, Bogdan I. Florea, Sylvia E. Le Dévédec, Laura H. Heitman, Adriaan P. IJzerman, and Daan van der Es

Abstract
G Protein-Coupled Receptors (GPCRs) have been known for decades as attractive drug targets. This has led to the development and approval of many ligands targeting GPCRs. Although ligand binding effects have been studied thoroughly for many GPCRs, there are multiple aspects of GPCR signaling that remain poorly understood. The reasons for this are the difficulties that are encountered upon studying GPCRs, e.g. a poor solubility and low expression levels. In this work, we have managed to overcome some of these issues by developing an affinity-based probe for a prototypic GPCR, the Adenosine A_1 Receptor (A_1AR). Here we show the design, synthesis and biological evaluation of this probe in various biochemical assays, such as SDS-PAGE, confocal microscopy and chemical proteomics.

ACS Chem Biol **2022**, *17*, 3131–3139.

Introduction

The adenosine receptors (A_1, A_{2A}, A_{2B} and A_3) are class A G Protein-coupled receptors (GPCRs) that respond to extracellular levels of adenosine.[1,2] These receptors play a role in a wide variety of physiological and pathological processes, ranging from the suppression of immune responses to the regulation of nociception.[3,4] This versatile role has prompted decades of research towards the effects of modulating adenosine receptors and led to the development of multiple clinical candidates. However only few chemical entities have thus far reached the markets.[5,6]

One reason for the lack of success might be the multitasking role of the adenosine receptors throughout the human body, e.g. the adenosine A_1 receptor (A_1AR) influences lipolysis in adipocytes, reduces ischemic injury in cardiomyocytes and shows analgesic activity in the spinal cord.[4,7,8] Other reasons might be receptor oligomerization, biased downstream signaling and the presence/absence of post-translational modifications (PTMs).[9,10]

The latter observations are not limited to the adenosine receptors, but have been found to play a role in the signaling of GPCRs in general.[11,12] Altogether, there is a plethora of possible mechanisms that could affect targeting of GPCRs in a specific disease state. As GPCRs are the target of roughly one third of the FDA approved drugs (~34% in 2017)[13], it is important to get a better picture of all possible aspects that have an influence on receptor signaling.

Parallel to the development of novel assays and more accurate read-outs in existing assay setups, the development of tool compounds is a valid approach to obtain a better understanding of GPCRs.[14,15] To this end, our group recently developed LUF7746: a partial agonist for the A_1AR equipped with an electrophilic fluorosulfonyl group, which facilitated covalent binding to the A_1AR (Figure 1A).[16] Covalent ligands for GPCRs have especially proven useful in structural studies, 'locking' multiple individual receptors into the same conformation.[17,18]

Aside from covalent ligands, multiple functional ligands have been developed over the years to expand the scope of GPCR profiling.[15] Among these tool molecules are ligands that are conjugated to e.g. fluorophores, bio-orthogonal click handles and photo-activatable groups.[19–22] In other protein families such as hydrolases and proteases, many so-called activity-based probes have already been developed to broadly characterize the respective protein family.[23,24] Having such an extensive arsenal of probes for GPCRs would allow for a more thorough investigation of these important drug targets in biological systems.

Activity-based probes consist of three parts: a selective targeting moiety, a reactive electrophilic group (warhead), and a reporter tag to detect the probe-bound proteins.[25] Classical activity-based probes target the active site of an enzyme, using warheads that make use of the enzyme's intrinsic mechanism to react.[23,24] GPCRs on the other hand, do not have such an active site pocket. Therefore, in case of GPCRs, affinity-based probes (AfBPs) have been developed that either use photoactivatable or highly electrophilic groups as warhead.[26–31] AfBPs thus rely on high affinity and selectivity towards a protein target for selective labeling. Besides that, there are various challenges associated with the biochemical profiling of GPCRs. First, most receptors have low expression levels, even when stably overexpressed in model cell lines.[32–34] Second, as mentioned before, oligomerization and PTMs greatly influence the behavior and appearance of GPCRs.[35,36] Third, GPCRs are membrane proteins, which are poorly soluble in aqueous media and thus prone to solubility issues.[37–39]

Recently, a handful of AfBPs has been developed to target and label the adenosine receptors. Among these are a clickable antagonist for the A_{2A}AR and a clickable antagonist with high

affinity for both the A_1AR and A_3AR.[29,31] The application of these probes however, has been limited to gel-based experiments. Presumably the aforementioned issues, such as expression levels and presence of PTMs, have impeded the detection of adenosine receptors in a biochemical setup. Therefore, further exploration on the design, synthesis and applicability of such probes is warranted.

In this study, we explored another avenue to study the adenosine receptors with AfBPs, enabling the profiling of the A_1AR in a multitude of biochemical assays. To achieve this, we developed the first agonistic AfBP for the A_1AR, starting from the aforementioned covalent partial agonist LUF7746. LUF7746 already contains two elements of an AfBP, the only element lacking is the reporter tag for detection.[16] An alkyne group was chosen as ligation handle to be conjugated to a reporter tag in the Copper(I)-catalyzed Azide-Alkyne Cycloaddition (CuAAC).[40,41] The choice of the alkyne moiety has two advantages compared to a direct conjugation with a reporter group (one-step-probe). First, the alkyne group is a small moiety and thus accounts for minimal steric clashes in the binding pocket of the A_1AR. Secondly, having such a ligation handle provides the flexibility to 'click' various types of reporter tags onto the probe-bound protein.

In an exemplary GPCR profiling assay, live cells or membrane fractions are first incubated with the probe to selectively label the desired receptor in the presence of other proteins (Figure 1B). In the subsequent incubation step, the desired reporter group is 'clicked' onto the probe, effectively labeling the receptor. Lastly, the reporter-bound receptor is further processed, depending on the type of detection method. In our case, three different techniques were used to detect the A_1AR: SDS-PAGE, chemical proteomics and confocal microscopy. Here, we show our synthesized probe, LUF7909, was successfully used in all three of these profiling setups. Taken together, this allows us to gain more insight into various receptor properties, such as expression, glycosylation and the effects of ligand binding.

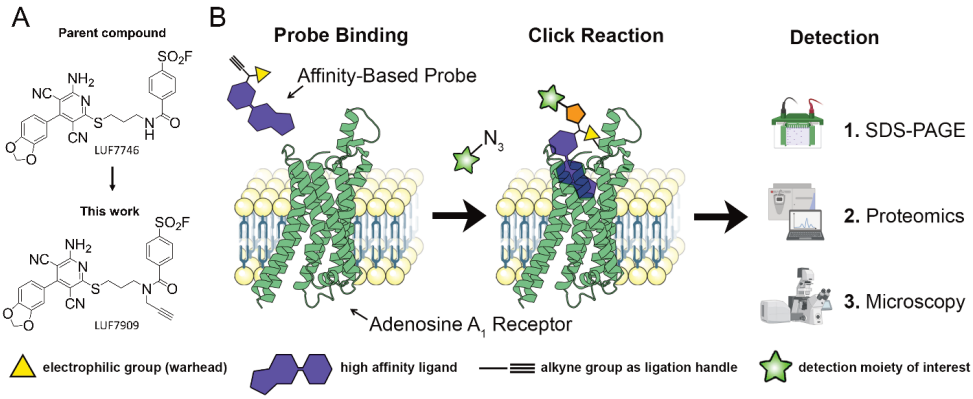

Figure 1. (A) A_1AR-targeting 3,5-dicyanopyridines: covalent partial agonist LUF7746 and AfBP LUF7909. (B) Typical affinity-based protein profiling workflow used in this study. First, membrane fractions or live cells are incubated with alkyne-containing AfBP. Second, the alkyne moiety of the probe is conjugated to an azide-containing reporter group through the Copper(I)-catalyzed Azide-Alkyne Cycloaddition (CuAAC). Third, the probe-bound proteins are being processed for further detection methods. These include SDS-PAGE experiments, chemical proteomics and confocal microscopy. Figure partly created with BioRender.com.

Results and Discussion

Design and Synthesis of A_1AR-targeting AfBPs

As mentioned before, our AfBP-design includes an alkyne moiety. In order to explore the effects that introducing an alkyne has on the binding of LUF7746 to the receptor, multiple ligands were synthesized (i.e. **1**, **2**, **3** and **4**) each having the alkyne group substituted at a different position of the scaffold (Scheme 1). In all four cases, the synthesis started from the respective benzaldehydes (**6a-c**) which were converted to the corresponding 3,5-dicyanopyridines (**7a-c**) through a multiple component reaction using malononitrile and thiophenol.[42] 3,5-Dicyanopyridine **7c** was subjected to a Sandmeyer reaction (to furnish chloride **8**), followed by a substitution by propargyl amine (to give alkyne **9**).[8] The four 3,5-dicyanopyridines (**7a-c** and **9**) were deprotected using thioacetate, (**10**, **11a-c**) and subsequently used in a nucleophilic substitution reaction with compound **20** to yield the AfBPs **1**, **2**, and **3**.

In case of probe **4**, the alkyne group was introduced onto the warhead-containing linker moiety prior to nucleophilic attack of the thiol. In brief, 3-bromopropanol was protected with a TBDMS group (**13**) and converted to compound **14** by a dropwise addition of propargyl amine. 4-Fluorsulfonyl benzoic acid (**19**) was coupled to the same amine in a peptide coupling (**15**), followed by a TBDMS-deprotection (**16**) and a tosylation (**17**) of the compound. The tosylate **20** was then used in the substitution reaction, yielding AfBP LUF7909 (**4**) as a mixture of two rotamers, as determined by NMR and LCMS measurements.

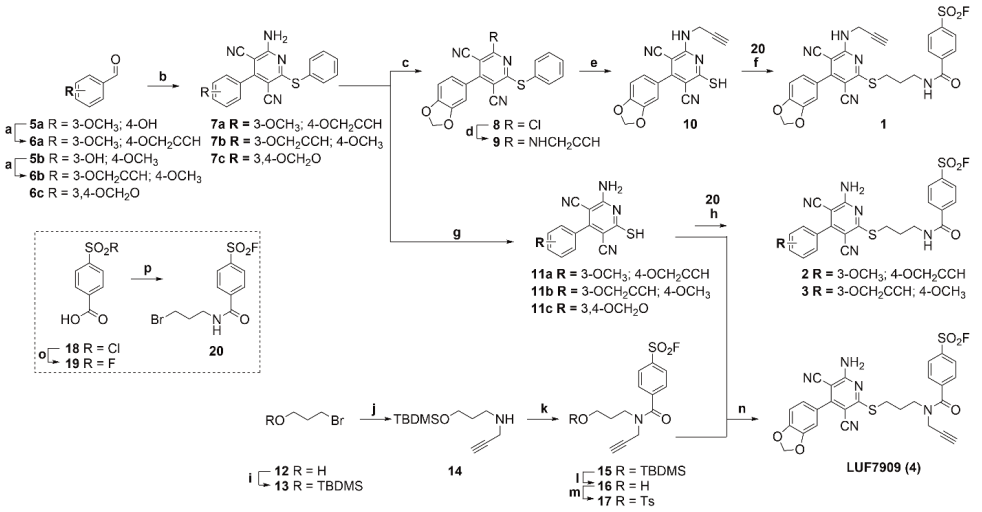

Scheme 1. Synthesis of A_1AR-targeting AfBPs. Reagents and conditions: (a) Propargyl bromide (80% in toluene), K_2CO_3, acetone, reflux, overnight, 80-100%; (b) Malononitrile, thiophenol, Et_3N, EtOH, 50-75 °C, 4-10 h, 30-47%; (c) Isopentyl nitrite, $CuCl_2$, MeCN, 60 °C, 20 h, 72%; (d) Propargyl amine, dry THF, RT, overnight, 92%; (e) Potassium thioacetate, dry DMF, RT, 8 h, 99%; (f) **20**, $NaHCO_3$, dry DMF, 20-50 °C, 4 days, 40%; (g) (i) Potassium thioacetate, dry DMF, RT, 1-5 days; (ii) 2 M NaOH, RT, 1-3 days, 62-78%; (h) **20**, $NaHCO_3$, dry DMF, RT, 1-2 days, 29-53%; (i) TBDMS-Cl (50% in toluene), 1H-imidazole, dry DMF, RT, 5 h, quant.; (j) Propargylamine, DIPEA, MeCN , RT, 5 h, 52%; (k) **19**, EDC·HCl, DIPEA, dry DMF, RT, 3 days, 58%; (l) $Et_3N{\cdot}_3HF$, dry THF, RT, overnight, 92%; (m) TsCl, Et_3N, dry DMF, RT, 2 days, 55%; (n) $NaHCO_3$, dry DMF, RT, overnight, 31%; (o) Potassium bifluoride, H_2O, dioxane, 3 h, 95%; (p) 3-Bromopropylamine·HBr, Pybrop, DIPEA, dry DMF, RT, 12 days, 41%.

Evaluation of the AfBPs in radioligand binding assays and docking studies

With the molecules in hand, our attention was shifted towards the assessment of the potential probes' binding affinity towards the A_1AR, as well as the selectivity towards other adenosine receptors. The dicyanopyridine scaffold in particular is known to bind other adenosine receptor subtypes dependent on its substitutions.[42,43] In a single point radioligand displacement assay using 1 μM of probe at all four of the adenosine receptors, no considerable displacement of radioligand from the A_{2A}AR, A_{2B}AR and A_3AR was observed (Figure 2A). Probes **2** and **3** did not show considerable displacement of radioligand from the A_1AR, while **1** showed moderate (~70%) displacement and LUF7909 full (~100%) displacement. This indicates high affinity of LUF7909 towards the A_1AR and selectivity over the other adenosine receptors.

These differences can be rationalized by covalently docking the four ligands into the A_1AR binding pocket. Using the crystal structure of adenosine-bound A_1AR (PDB: 6D9H) and the binding pose of LUF7909 most similar (lowest RMSD) to the recently obtained crystal structure of structurally similar LUF5833 in the A_{2A}AR, a representative image was generated (Figure 3).[44] From this pose, it was deduced that the methylenedioxy group of LUF7909 is located deep inside the binding pocket of the A_1AR. Substitutions at this position might therefore result in a loss in binding affinity, as observed for compounds **2** and **3**. Furthermore, the alkyne group of LUF7909 does not seem to hinder the important interactions that take place in the binding pocket (with residues F171, E172 and N254), thus explaining the high affinity.

Next, LUF7909 was submitted to a full curve radioligand displacement assay. To study the potential covalent binding mode of the probe, the assay was executed at two different time points, i.e. incorporating 0 or 4 hours of pre-incubation of probe with the receptor (Figure 2B). Without pre-incubation (0 h), LUF7909 showed an apparent pK_i of 7.8, while this increased to an apparent pK_i of 9.5 upon 4 hours of pre-incubation (Table S1). Such an increase in apparent pK_i (K_i shift of 44.0) is a strong indicator of a covalent mode of action. A wash-out experiment confirmed the persistent mode of binding of LUF7909 to the receptor, even after multiple washing steps (Figure S1). Besides that, LUF7909 acted as a partial agonist in a functional [^{35}S]GTPγS assay (Figure S2), having a similar potency as the full agonist N^6-cyclopentyladenosine (CPA) (pEC_{50} of 8.7), but a significantly lower E_{max} (74%). Hence, LUF7909 behaves as a partial agonist that binds covalently, with high affinity and selectivity towards the A_1AR.

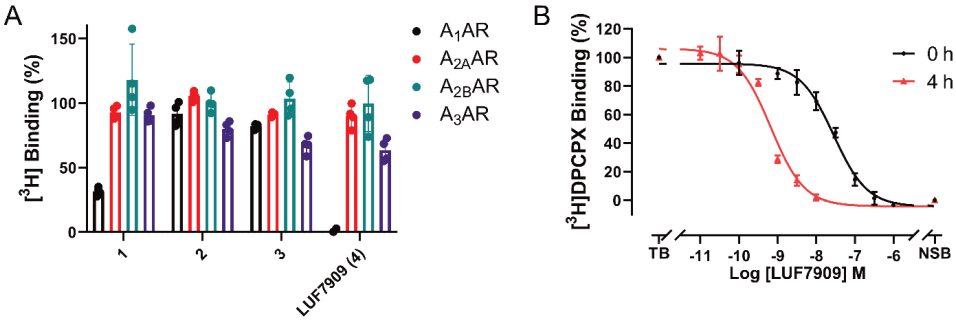

Figure 2. Affinities of LUF7909 and analogs for the four adenosine receptor subtypes. (A) Displacement of [^{3}H]DPCPX (A_1AR), [^{3}H]ZM241385 (A_{2A}AR), [^{3}H]PSB-603 (A_{2B}AR) and [^{3}H]PSB-11 binding (A_3AR) by 1 μM of the respective AfBP. Data represent the values of two individual experiments performed in duplicate and are normalized to the vehicle control (100%). (B) Displacement of [^{3}H]DPCPX from the A_1AR by LUF7909 measured after 0 or 4 hours of pre-incubation of LUF7909 with CHO membranes stably overexpressing the A_1AR. TB = total radioligand binding; NSB = non-specific radioligand binding. Data represent the mean ± SEM of three individual experiments performed in duplicate.

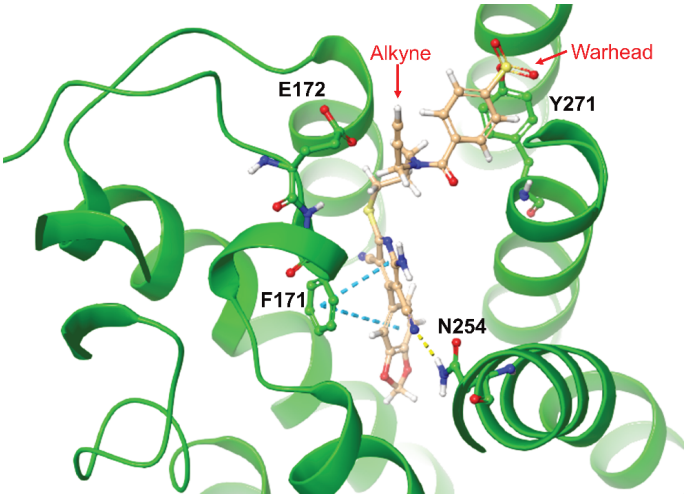

Figure 3. Top-down view of docked LUF7909 into the ligand binding pocket of the A_1AR. Crystal structure taken from the adenosine-bound A_1AR (PDB: 6D9H). The final ligand pose was selected based on the crystal structure of LUF5833 in the A_{2A}AR (PDB: 7ARO). Shown are the main amino acids that interact with LUF7909. The SO_2F-containing warhead is located close to tyrosine 271 (Y271), while the alkyne moiety is pointing outwards from the receptor.

Labeling of the A_1AR in SDS-PAGE experiments

As a first assessment of the labeling potential of our probe, SDS-PAGE experiments were carried out on CHO membranes that overexpress the A_1AR. Membranes were incubated with LUF7909 and subjected to click conjugation of probe to the fluorophore AF647-N_3. Samples were denatured, loaded on gel and the gel was visualized by in-gel fluorescence scanning. First, various concentrations of LUF7909 were investigated (Figure 4A). At roughly the apparent K_i of LUF7909 (16 nM at 0 h pre-incubation) a band at ~45 kDa appeared on the gel. Increasing the concentration of LUF7909 revealed additional labeling of a protein at ~30 kDa, where a probe concentration of 1 µM shows multiple extra proteins being labeled. This apparent non-specific binding at high concentrations is presumably due to the electrophilic nature of the fluorosulfonyl warhead.

The optimal balance between selective labeling and intensity of the observed bands seemed to occur at a concentration of 100 nM of LUF7909 (Table S2), which was therefore used in further SDS-PAGE experiments. Of note, no labeling was observed in the absence of copper(I) or probe during the click reaction (Figure 4B). Furthermore, the band at ~45 kDa disappeared upon pre-incubation with 1 µM of various A_1AR-selective ligands, such as the full agonist CPA (CP), partial agonist Capadenoson (CA), parent compound LUF7746 (LUF), reference antagonist DPCPX (D) and covalent antagonist FSCPX (F; structures in Figure S3). Western Blot experiments (Figure S4) further confirmed that the band at ~45 kDa, though slightly higher than the expected mass of the A_1AR (~36 kDa), is indeed the A_1AR.

The slightly higher mass can be explained by N-glycosylation of the A_1AR, as has been seen in early purification studies of endogenous A_1AR.[45,46] Indeed, upon incubation with PNGase, a strong reduction is seen in molecular weight of the corresponding band (Figure 4C). Pre-incubation with the reversible antagonist DPCPX resulted in full disappearance of both bands, thereby confirming that this pattern represents the A_1AR.

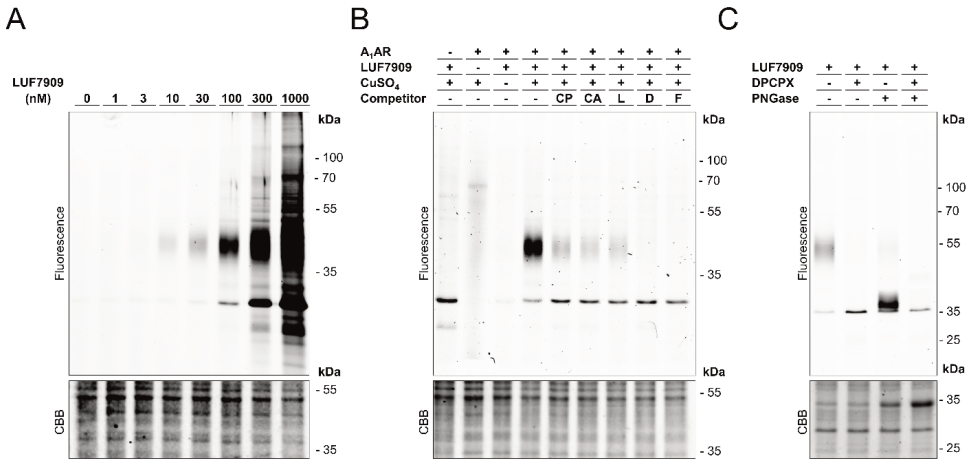

Figure 4. Specific labeling of the A_1AR using LUF7909 in CHO membranes overexpressing the A_1AR. Membranes were pre-incubated with or without competitor, incubated with LUF7909, subsequently 'clicked' to AF647-N_3, denatured, subjected to SDS-PAGE and analyzed using in-gel fluorescence scanning. (A) Concentration-dependent labeling of the A_1AR. (B) Labeling of the A_1AR is dependent on the presence of copper(I) and probe during the click reaction, as well as the presence of known A_1AR ligands: agonist CPA (CP), partial agonist Capadenoson (CA), covalent partial agonist LUF7746 (L), antagonist DPCPX (D) and covalent antagonist FSCPX (F; structures in Figure S3). (C) Labeling of the A_1AR shows a strong reduction in molecular weight upon incubation with PNGase. Pre-incubation with 1 μM of DPCPX shows full disappearance of both bands. CBB = Coomassie Brilliant Blue. The band that appears upon Coomassie staining (lane 3 and 4) corresponds to the molecular weight of PNGase.

Enrichment and detection of the A_1AR in chemical proteomics experiments

To further explore binding of LUF7909 to the A_1AR, as well as possible off-targets, chemical proteomics experiments were carried out. In brief, CHO cell membranes overexpressing the A_1AR were incubated with LUF7909. A concentration of 1 μM was chosen to obtain a full proteomic profile of all the LUF7909-labeled proteins. Probe-bound proteins were 'clicked' to biotin-azide, denatured, precipitated, reduced, alkylated and pulled-down using streptavidin beads. The bound proteins were first washed and then digested. The obtained peptides were measured by LC-MS/MS. Initial attempts using Trypsin as digestion enzyme did not lead to detection of A_1AR-specific peptides. Therefore Chymotrypsin was chosen as digestion enzyme. Experiments without LUF7909 lead to detection of only one peptide of the A_1AR. However, upon affinity purification with LUF7909, an average sequence coverage of 40% of the receptor was detected by LC-MS/MS (Figure 5A; Table S2).

In the past years, considerable efforts have been done regarding the detection of GPCRs in chemical proteomics experiments.[28,47–51] This includes mostly work using photoactivatable groups, such as diazirines and 2,5-disubstituted tetrazoles.[28,47,50,52] To our knowledge, only one example of the use of an electrophilic ligand has been reported.[51] Besides that, most of these experiments yielded a low sequence coverage when a non-purified receptor was measured. Only in case of the metabotropic glutamate receptors in brain slices, a higher sequence coverage was found.[50] It is therefore remarkable that our experiment yielded an average sequence coverage of 40%. The detected peptides mostly include the non-membrane domains: C-terminus, N-terminus, intra- and extracellular loops.

Compared to DMSO-treated samples, a strong enrichment of the A_1AR (>200-fold) was observed (Figure 5B). This fold change was greatly reduced upon pre-incubation of the samples with 10 µM of covalent ligand LUF7746 (Figure S5). Other proteins that showed a significant but substantially lower enrichment as compared to DMSO-treated samples were the G Protein subunit beta-1, malate dehydrogenase and ATPase subunit alpha. These off-targets might be the result of using a high concentration (1 µM) of electrophilic probe in membrane fractions.

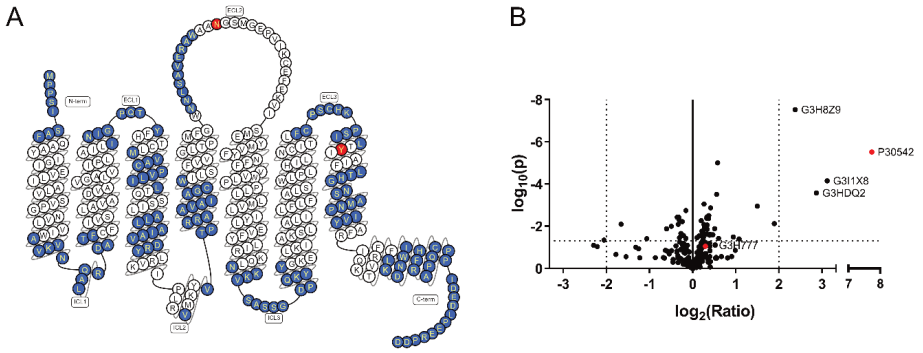

Figure 5. Proteomic detection of the A_1AR. (A) Snake plot of the adenosine A_1 receptor. Highlighted in blue are the peptides that were detected upon affinity purification using 1 µM of LUF7909 in CHOhA_1AR membranes. Amino acids highlighted in red are the glycosylation site (N159) and predicted probe binding site (Y271). Snake plot derived from gpcrdb.org.[53] (B) Volcano plot of affinity purification experiments comparing samples treated with 1 µM LUF7909 to samples containing DMSO as control. Plotted are the enrichment ratio (log_2(Ratio)) and the probability (-log_{10}(p)) as determined in a multiple *t* test. All data originate from six technical replicates. The Uniprot codes are given for proteins that meet a threshold value of ratio>2 and p-value<0.05 (dotted lines). These are the G protein subunit beta-1 (G3I1X8), malate dehydrogenase (G3HDQ2), sodium/potassium-transporting ATPase subunit alpha (G3H8Z9) and the adenosine A_1 receptor (P30542) (highlighted in red). Also shown in red is the Adenine Nucleotide Translocator (G3H777).

Investigation of the potential off-targets of LUF7909 in CHOhA_1AR membrane fractions

In Figure 4 it is visible that a potential off-target of LUF7909 (concentrations up to 300 nM) has an approximate molecular mass of 30 kDa. This molecular weight does not correspond to any of the proteins that were significantly 'pulled-down' by LUF7909 during the chemical proteomics experiments. To further investigate this probable off-target, we performed similar chemical proteomics experiments, this time using CHO membrane fractions that do not overexpress the A_1AR. Contrary to the CHOhA_1AR membranes, only small -fold changes were observed for the detected proteins (vs DMSO control) (Figure S6A). There are however two proteins that show a significant enrichment (>4): Elongation factor 1-alpha 1 and an isoform of the Adenine Nucleotide Translocator (ANT), the latter being an interesting target due to its binding of adenine-containing substrates. We therefore pre-incubated both CHO and CHOhA_1AR membranes with various concentrations of bongkrekic acid, a known inhibitor of ANT,[54] prior to the sequential addition of LUF7909, clicking to AF647-N_3 subjecting to SDS-PAGE and scanning using in-gel fluorescence (Figure S6B).

Pre-incubation with bongkrekic acid resulted in a concentration-dependent inhibition of the band observed for the 'empty' CHO membranes, as well as the lower band observed for the CHOhA_1AR membranes. This suggests that the extra band seen on gel corresponds to ANT. Also the pull-down experiments with LUF7909 in CHOhA_1AR membranes show the presence

of ANT (Figure 5B), although not significantly enriched compared to the DMSO control samples (fold change of 1.2). The reason for this may be the high expression level of ANT in mitochondria,[55] causing an enrichment of ANT in our membrane fractions. We assume that binding of LUF7909 to ANT occurs because of a high concentration of ANT in combination with the electrophilic nature of the probe.

Labeling of the A_1AR on live cells

Moving a step closer to a more endogenous system, we tested the labeling properties of LUF7909 in live CHO cells. First, CHO cells with or without overexpression of the A_1AR were incubated with 100 nM of probe, prior to membrane collection and click reaction with AF647-N_3. The samples were denatured, loaded on SDS-PAGE and analyzed using in-gel fluorescence (Figure 6A and S7). A 'smear' was observed at the height of the A_1AR, which was not present upon pre-incubation with DPCPX (1 µM). This smear is presumably due to different glycosylation states of the A_1AR. No other strong bands were detected, both in the CHO cells with and without overexpression of the A_1AR. Secondly, affinity-based pull-down experiments were performed using live CHOhA_1AR cells. Again, a high enrichment of the A_1AR was found (Figure 6B), however less labeling of other proteins compared to the experiments with membrane fractions. It thus seems that labeling of the A_1AR by LUF7909 is more specific in live CHOhA_1AR cells, as compared to labeling in membrane fractions derived from these CHOhA_1AR cells (Figure 4 and 5).

To confirm these observations, labeling of the receptor in live CHO cells was studied using confocal microscopy. Live CHO cells with or without overexpression of the A_1AR were incubated with LUF7909 and subsequently fixed. The probe-bound proteins were stained with TAMRA-N_3 (via a click reaction) and the cellular nuclei were stained with DAPI. As compared to the DMSO control, LUF7909 showed clear labeling of cell-cell contacts and cellular membranes by TAMRA-N_3 (Figure 6C). The degree of labeling was diminished by pre-incubation with 1 µM of covalent ligand FSCPX, and absent upon using CHO cells that do not overexpress the A_1AR. These controls confirm that the observed labelling, in gel, LC-MS/MS and under the microscope, is indeed due to selective labeling of the A_1AR and not an off-target protein. Furthermore, signs of A_1AR labeling inside the cells were observed in Figure 6C. The reason for this might be internalization, an effect that has been reported to take place upon incubating the A_1AR with an agonist.[56] Having a clickable (partial) agonist thus allows further studies towards receptor internalization.

Labeling of LUF7909 in cells endogenously expressing the A_1AR

Having established labeling of the A_1AR in CHOhA_1AR membranes and live cells, we attempted to label the receptor in membrane fractions that endogenously contain the A_1AR as a next step. For this, we used membranes derived from adipocytes: a cell type that is known to express the A_1AR.[7,58] Adipocyte membranes were collected from gonadal fat pads from female mice and subsequently incubated with 100 nM LUF7909, deglycosylated with PNGase, clicked to AF647-N_3, denatured, resolved by SDS-PAGE and analyzed using in-gel fluorescence scanning. This resulted in multiple bands (Lane 1, Figure 7) at molecular weights of roughly 90, 65 and 60 kDa, and a smear of presumably two bands at 30 kDa. The intensity of the bands at 30 kDa (indicated with an arrow) is strongly diminished upon pre-incubation with 1 µM of the selective covalent A_1AR antagonist FSCPX. Full reduction of this band was observed when using a high concentration of FSCPX (Figure S9A), which gives a strong indication that this band is in fact the A_1AR. The band at ~30 kDa (lane 1) shows a great difference in mass compared to observed A_1AR in CHO cells. The presumable reason for this is a difference in glycosylation pattern of the receptors, an effect that has also been observed when comparing the A_1AR from brain to the A_1AR from testis.[45]

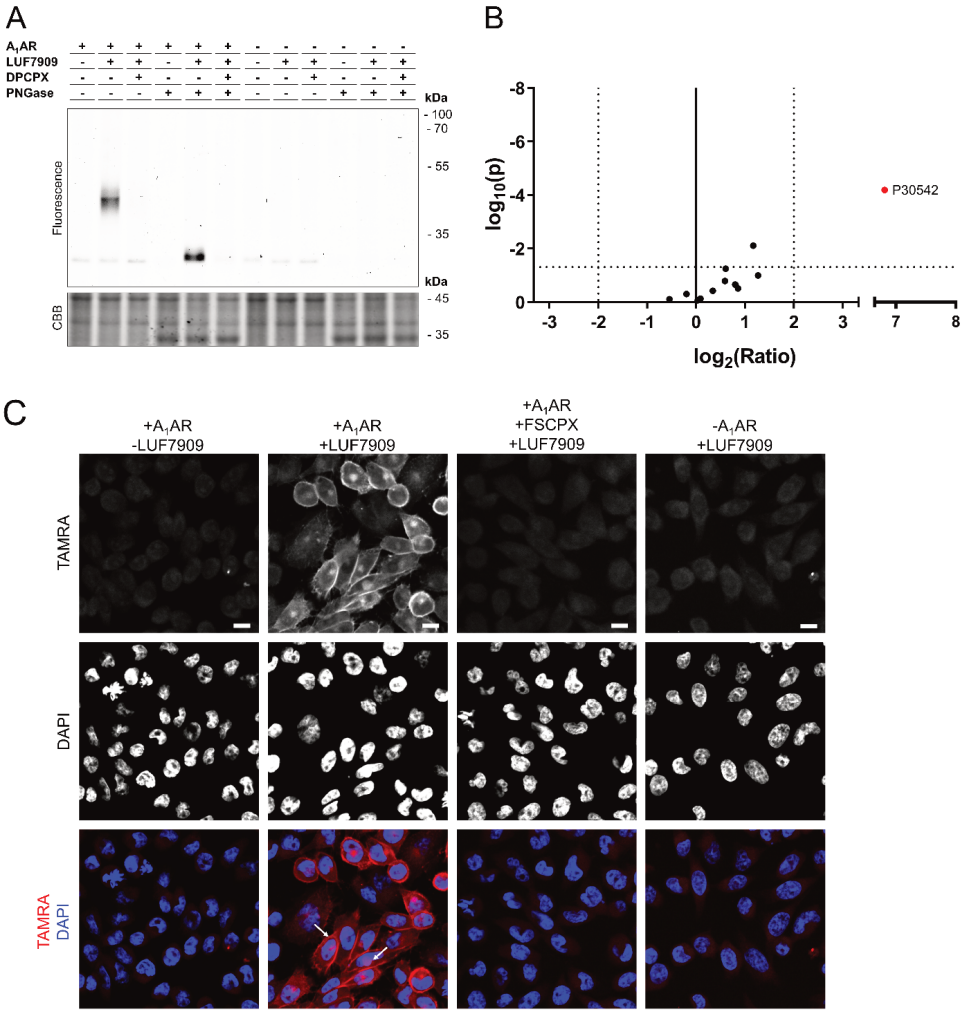

Figure 6. Selective labeling of the A_1AR in live CHO cells. (A) CHO cells with or without overexpression of the A_1AR were pre-treated for 1 h with DPCPX (1 µM) or 1% DMSO and incubated for 1 h with LUF7909 (100 nM) or 1% DMSO (control). Membranes were collected, treated with PNGase and incubated with click mix containing AF647-N_3. The samples were then subjected to SDS-PAGE and analyzed by in-gel fluorescence scanning. CBB = Coomassie Brilliant Blue. (B) Volcano plot of affinity purification experiments comparing live CHOhA_1AR cells treated with 1 µM LUF7909 to cells treated with 1% DMSO (control). All data originate from six technical replicates. Shown is the uniprot code for the A_1AR (P30542) (highlighted in red). (C) Confocal microscopy images. CHO cells with or without overexpression of the A_1AR were pre-treated for 1 h with FSCPX (1 µM) or 1% DMSO and incubated for 1 h with of LUF7909 (100 nM) or 1% DMSO (control). The cells were then fixed and stained with TAMRA-N_3 (first row) and DAPI (second row). The third row shows an overlay of both stains. TAMRA = red, DAPI = blue. Arrows indicate examples of labeled membranes and labeling inside cells. Images were selected manually as representatives of blinded measurements from two separate experiments (see Figure S8). Scale bar = 10 µm. Figure was created using OMERO.[57]

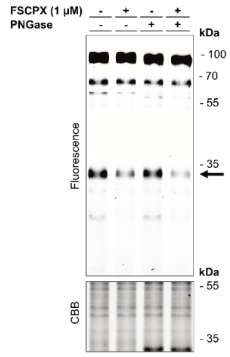

Figure 7. Labeling of the A_1AR in adipocyte membranes derived from mouse gonadal fat pads. The membranes were pre-treated with the covalent antagonist FSCPX (1 µM) or 1% DMSO prior to incubation with LUF7909 (100 nM) and subsequent incubation with click mix containing AF647-N_3. The samples were then denatured, subjected to SDS-PAGE and analyzed using in-gel fluorescence scanning. CBB = Coomassie Brilliant Blue. The band that appears upon Coomassie staining (lane 3 and 4) corresponds to the molecular weight of PNGase.

Besides the A_1AR, LUF7909 also labeled multiple off-target proteins in these experiments, e.g. the bands at ~90 and ~65 kDa. Preliminary experiments showed a clear reduction in intensity for the band at ~90 kDa upon pre-incubation with a protease inhibitor cocktail (Figure S9B). This would indicate off-target binding to a presumable protease. We did not further examine this finding. The labeling and visualization of low-abundant GPCRs in SDS-PAGE experiments thus seems to be challenging when high levels of potential off-targets are present. For future studies using AfBPs we therefore suggest to perform affinity-based pull-down proteomics, confocal microscopy or flow cytometry experiments to investigate GPCRs on native cells and tissues.

Conclusion

In this study we have described the design and synthesis of LUF7909, a versatile probe molecule acting as a partial agonist that was used to characterize the A_1AR in a broad spectrum of assays. LUF7909 showed labeling of the A_1AR at about its apparent K_i, as well as labeling of other proteins in SDS-PAGE experiments. The observed off-targets on gel were not significantly enriched in proteomic studies, nor found in live cell experiments, both carried out in A_1AR overexpressing cells. In the latter two types of experiments, LUF7909 proved to be highly specific towards the A_1AR.

Altogether, this work shows various methods to implement AfBPs within the broad field of GPCR research. This paves the way towards an investigation of more physiologically relevant processes, e.g. the presence/absence of PTMs on GPCRs (through LC-MS/MS investigations) and receptor internalization (through confocal microscopy). This will ultimately help to get a better understanding of GPCRs in both physiological and pathological conditions, opening up new avenues for drug discovery in general.

Acknowledgements

We thank P.C.N. Rensen and M. Schönke (LUMC, Leiden, The Netherlands) for their kind donation of female mouse gonadal fat pads. We also thank I. Boom (LACDR, Leiden, The Netherlands) for performing high-resolution mass spectrometry measurements. The authors gratefully acknowledge the imaging core facility, the Leiden University Cell Observatory, for their support and assistance in this work.

Supporting Tables

Table S1. Time-dependent characterization of the affinity of LUF7909.

Compound	pKi (0 h)[a]	pKi (4 h)[b]	Ki shift[c]
LUF7909	7.8 ± 0.04	9.5 ± 0.01	44.0 ± 5.1

Values represent apparent pKi ± SEM (n = 3) of individual experiments each performed in duplicate. [a] Affinity determined from displacement of specific [^{3}H]DPCPX binding on CHO cell membranes stably expressing hA_1AR at 25 °C after 0.5 h co-incubation; [b] Affinity determined from displacement of specific [^{3}H]DPCPX binding on CHO cell membranes stably expressing hA_1AR at 25 °C with compounds pre-incubated for 4 h, followed up by a 0.5 h co-incubation with [^{3}H]DPCPX. [c] Ki shift determined by ratio Ki(0 h)/Ki(4 h).

Table S2. Concentration-dependent labeling by LUF7909 in SDS-PAGE experiments. A concentration of 100 nM LUF7909 shows both a high intensity (70% intensity compared to the band at 1000 nM) and a low degree of off-target labeling (11%).

Concentration LUF7909 (nM)	Relative band intensity (%)[a]	A_1AR labeling vs. off-target labeling (%)[b]
1	1 ± 0	31 ± 10
3	5 ± 1	84 ± 6
10	16 + 6	86 ± 5
30	44 ± 12	95 ± 1
100	70 ± 9	89 ± 4
300	90 ± 14	74 ± 8
1000	100	51 ± 13

Values represent the mean percentage ± SEM (n = 3). Band intensities were determined with ImageLab software, using the gel images from Figure S3A. [a] The adjusted volumes of the bands were taken and corrected for the amount of protein after Coomassie staining. The highest band intensity (1000 nM probe) was set to 100%; [b] The bands at approx. 45 kDa (A_1AR) and approx. 30 kDa were selected in each lane and band percentages were calculated by ImageLab. The value in the table shows the percentage of the upper band (band 45 kDa (%) + band 30 kDa (%) = 100 (%)).

Table S3. Detected A_1AR peptides upon affinity purification using LUF7909 in CHO membranes that overexpress the A_1AR.

Sequence	Length	m/z	Charges	Start position	End position	Peptide score[a]
MPPSISAF	8	848.4102	1	1	8	150.82
PPSISAF	7	717.3697	1	2	8	131.42
AVKVNQALRDATF	13	1431.783	3	33	45	58.781
INIGPQTY	8	904.4654	1	69	76	176.41
MVACPVLIL	9	1014.561	2	82	90	97.306
ALLAIAVDRY	10	1103.634	2	97	106	78.334
LAIAVDRY	8	919.5127	2	99	106	104.45
AIAVDRY	7	806.4287	2	100	106	103.29
VVTPRRAAVAIAGCW	15	1625.882	2;3	118	132	58.676
NNLSAVERAW	10	1158.578	2	147	156	131.44
NKKVSASSGDPQKY	14	1507.763	2;3	212	225	197.3
NKKVSASSGDPQKYY	15	1670.826	2;3	212	226	156.51
FCPSCHKPSIL	11	1344.632	3	259	269	47.559
CPSCHKPSIL	10	1197.563	2;3	260	269	128.6
LTHGNSAMNPIVY	13	1415.687	2	276	288	156.83
THGNSAMNPIVY	12	1302.603	2	277	288	157.96
LKIWNDHF	8	1071.55	2;3	300	307	120.65
KIWNDHF	7	958.4661	2	301	307	158.38
RCQPAPPIDEDLPEERPDD	19	2248.007	2;3	308	326	218.16

[a]As determined by MaxQuant.

Supporting Figures

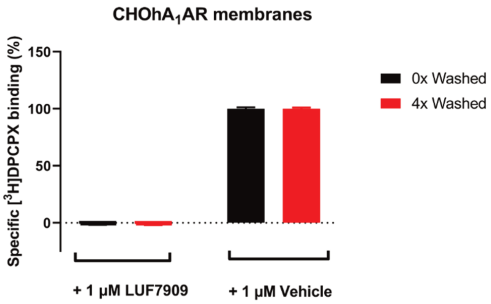

Figure S1 Wash-out assay reveals persistent binding of LUF7909 to the A_1AR. Membranes derived from CHO cells transiently transfected with the A_1AR were pre-incubated with buffer (vehicle) or 1 µM LUF7909, followed by a four cycle washing treatment or no washing at all before being exposed to [^{3}H]DPCPX in a standard radioligand binding assay. Data is expressed as the percentage of the vehicle group (100%) and represents the mean ± SEM of three individual experiments performed in duplicate.

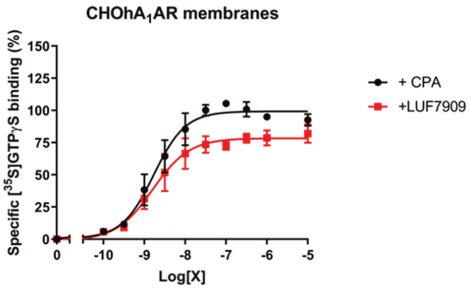

Figure S2 Functional characterization of LUF7909 in a [^{35}S]GTPγS binding assay. Concentration-dependent functional-effect curve of CPA and LUF7909 using membranes derived from CHO cells that were stably transfected with the hA_1AR. Data is expressed as a percentage of the maximal response induced by 100 nM CPA and the mean ± SEM of three individual experiments performed in duplicate. **p < 0.01 as compared to the E_{max} value of CPA, determined by a two-tailed unpaired Student's *t*-test.

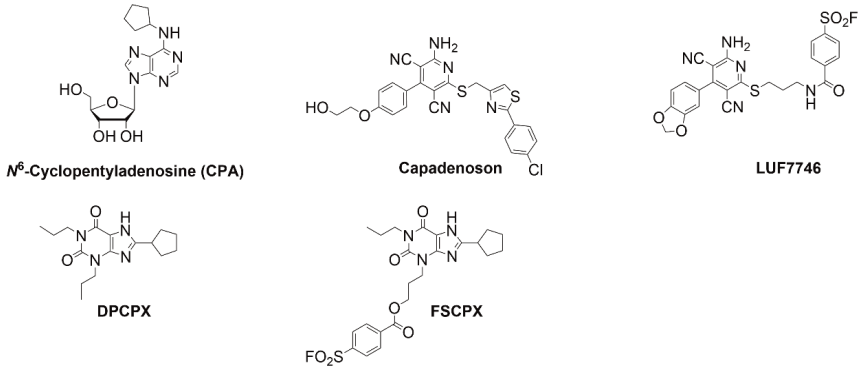

Figure S3. Molecular structures of the selective A_1AR ligands used in this study: full agonist *N*^{6}-cyclopentyladenosine (CPA), partial agonist Capadenoson, covalent partial agonist LUF7746, antagonist DPCPX and covalent antagonist FSCPX.

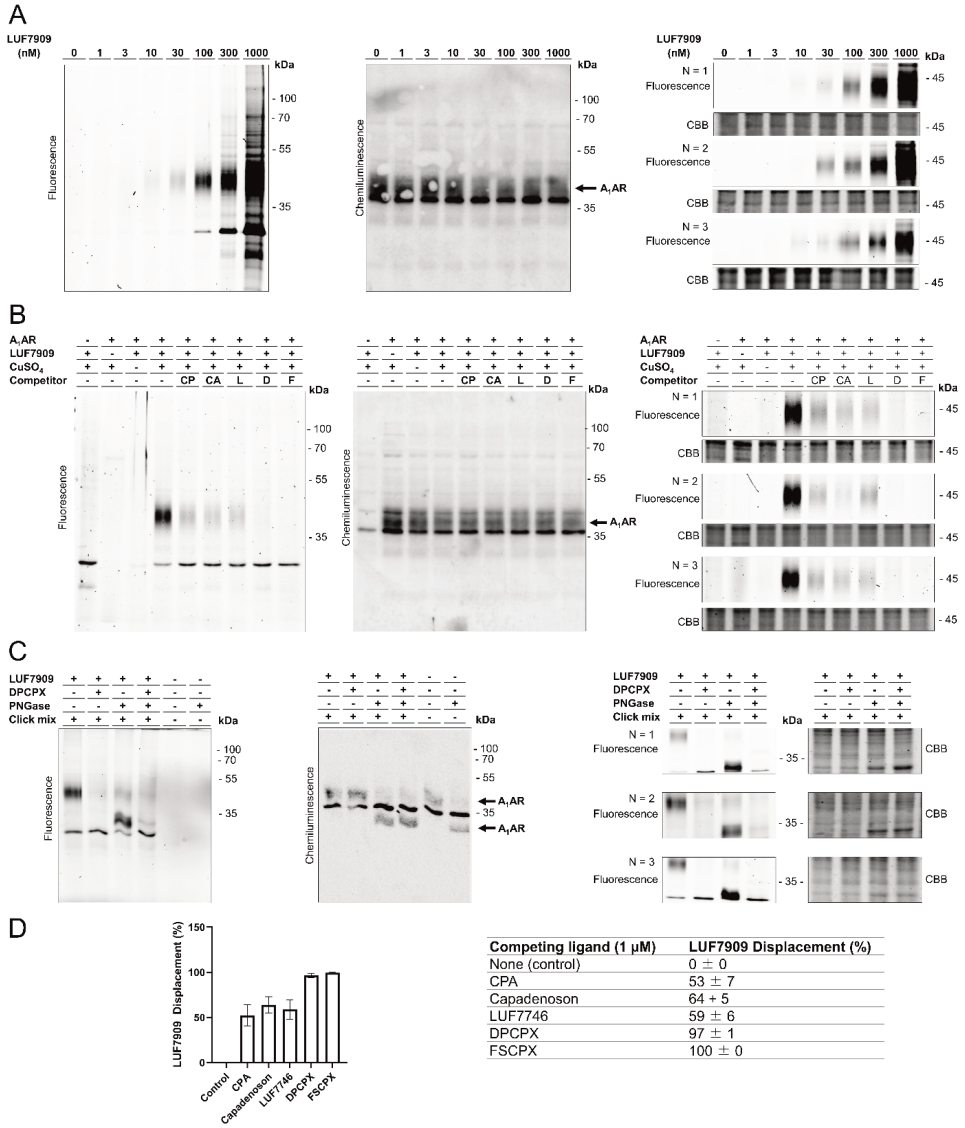

Competing ligand (1 µM)	LUF7909 Displacement (%)
None (control)	0 ± 0
CPA	53 ± 7
Capadenoson	64 + 5
LUF7746	59 ± 6
DPCPX	97 ± 1
FSCPX	100 ± 0

Figure S4. Verification of A_1AR labeling by **LUF7909**. Figures show SDS-PAGE and Western Blot experiments (left side), as well as N=3 data (right side). Conditions for A-D were the same as in Figure 4. The gel was transferred to a 0.2 µm PVDF blot using a Trans-Blot Turbo Transfer System (Bio-Rad)(2.5 A, 7 min) or stained with Coomassie Brilliant Blue (CBB). Blots were blocked with 5% BSA in TBST (1 h, rt), incubated with primary antibody (rabbitαratA_1AR 1:5000 in 1% BSA in TBST)(4 °C, overnight), washed (3 x TBST), incubated with secondary antibody (goatαrabbit-HRP 1:2000 in 1% BSA in TBST)(1h , rt), washed (2 x TBST, 1 x TBS), activated with luminol enhancer and peroxide (3 min, rt, dark) and subsequently scanned on fluorescence and chemiluminescence. (D) Quantification of the amount of **LUF7909** displaced by 1 µM of the respective covalent ligand. Values represent the mean percentage ± SEM (n = 3). Band intensities were determined with ImageLab software using the gel images from Figure S4B. The adjusted volumes of the bands were taken and corrected for the amount of protein after Coomassie staining. The band intensity of lane 4 (no competitor) was set to 0%.

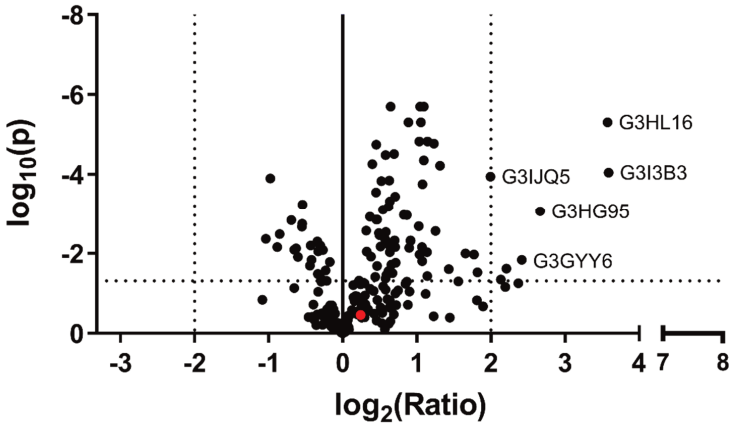

Figure S5. The adenosine A_1 receptor does not show a strong enrichment upon pre-incubation of the samples with **LUF7746**. Volcano plot of affinity purification experiments comparing samples treated with 1 μM **LUF7909** to samples that were pre-treated with 10 μM of **LUF7746**. Plotted are the enrichment ratio (log_2(Ratio)) and the probability (log_{10}(p)) as determined in a multiple *t* test. All data originate from six technical replicates. The Uniprot codes are given for proteins that meet a threshold value of ratio>2 and p-value<0.05 (dotted lines). These are the Splicing factor 3B subunit 1 (G3HL16), Nuclear pore complex protein Nup96 (G3I3B3), Lamin-A/C (G3HG95), Catalase (G3GYY6) and Protein RCC2 (G3IJB6). The adenosine A_1 receptor (P30542) is highlighted in red.

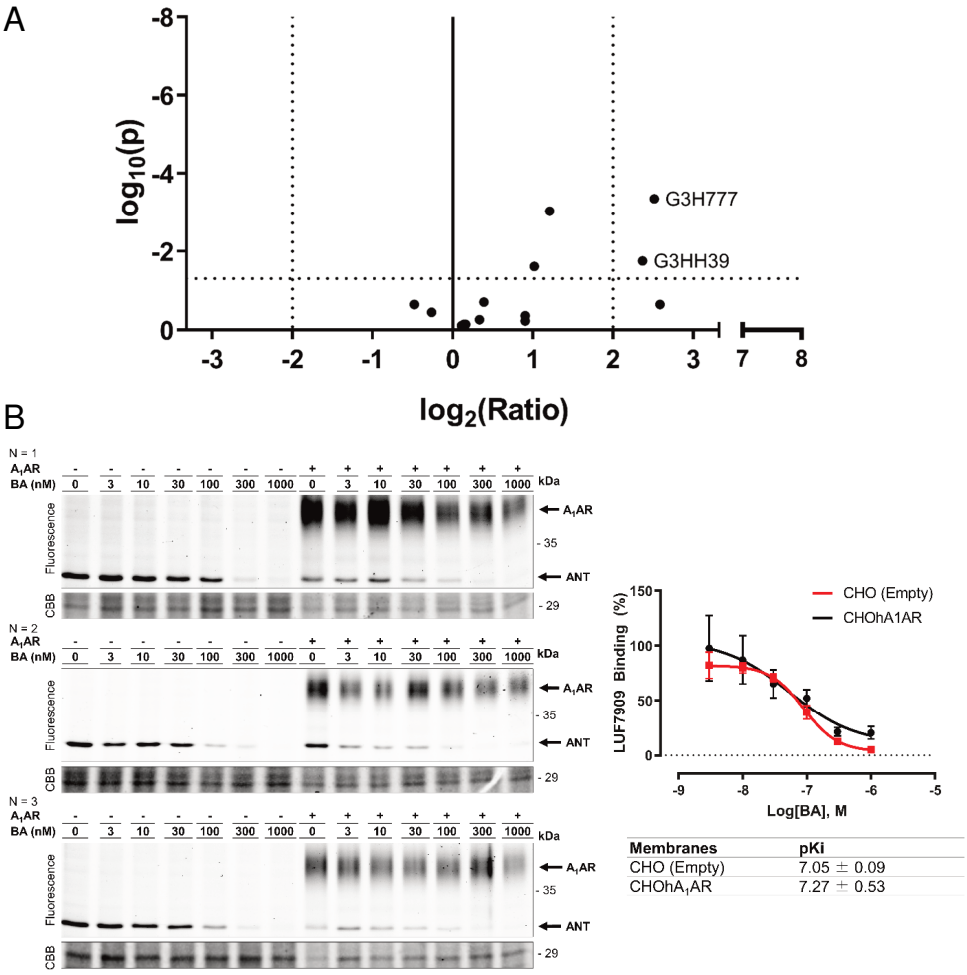

Membranes	pKi
CHO (Empty)	7.05 ± 0.09
CHOhA$_1$AR	7.27 ± 0.53

Figure S6. Off-target investigation of the proteins labeled by **LUF7909**. (A) Volcano plot of affinity purification experiments comparing samples of CHO membrane fractions (not overexpressing the A_1AR) treated with 1 µM **LUF7909** to samples treated with 1% DMSO. Plotted are the enrichment ratio (log_2(Ratio)) and the probability (log_{10}(p)) as determined in a multiple *t* test. All data originate from six technical replicates. The Uniprot codes are given for proteins that meet a threshold value of ratio>2 and p-value<0.05 (dotted lines). These are the Adenine Nucleotide Translocator (ANT)(G3H777) and Elongation factor 1-alpha 1 (G3HH39). (B) SDS-PAGE experiments show a concentration-dependent inhibition of the lower band by the ANT-inhibitor bongkrekic acid (**BA**) (N=3). CHO membrane fractions with and without overexpression of the A_1AR were pre-incubated with various concentrations of **BA**, prior to incubation with 100 nM of **LUF7909**. The samples were then clicked to AF647-N_3, denatured, resolved by SDS-PAGE and scanned using in-gel fluorescence. Coomassie Brilliant Blue (CBB) was used as protein loading control. (C) Quantification of **LUF7909** displacement by **BA**. Values represent the mean percentage ± SEM (graph) or apparent affinity ± SEM (table) (n = 3). Band intensities were determined with ImageLab software using the gel images from Figure S6B. The adjusted volumes of the bands were taken and corrected for the amount of protein after Coomassie staining. The band intensity of lane 1 (no **BA**) was set to 100%.

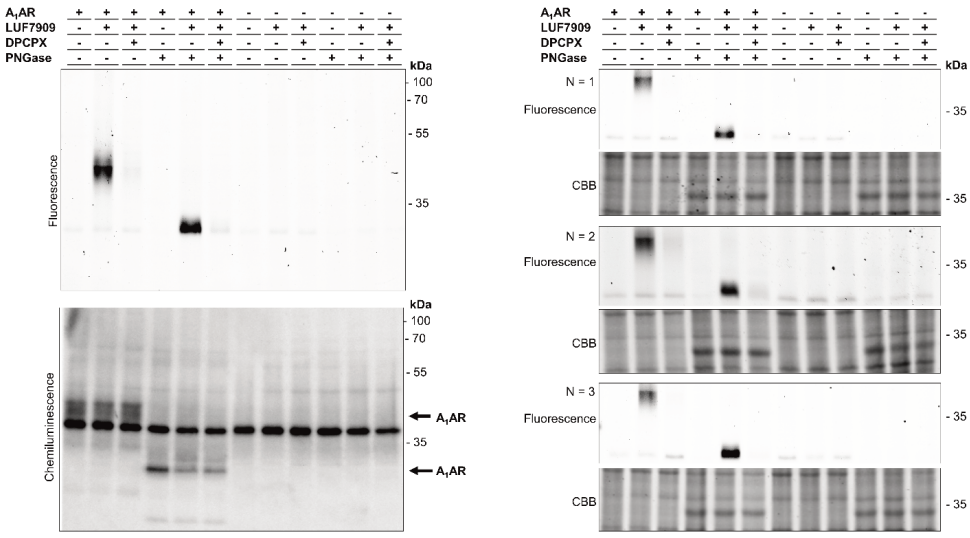

Figure S7 Additional SDS-PAGE experiments supporting Figure 6. Figure shows SDS-PAGE and Western Blot experiments (left side), as well as N=3 data (right side). Live CHOhA_1AR and non-transfected CHO cells were pre-treated with DPCPX (1 µM) or 1% DMSO and incubated with **LUF7909** (100 nM) or 1% DMSO (control). Membranes were collected and incubated with click mix containing AF647-N_3. The samples were then subjected to SDS-PAGE and analyzed by in-gel fluorescence scanning. The gel was transferred to a 0.2 µm PVDF blot using a Trans-Blot Turbo Transfer System (Bio-Rad)(2.5 A, 7 min) or stained with Coomassie Brilliant Blue (CBB). The blot was blocked with 5% BSA in TBST (1 h, rt), incubated with primary antibody (rabbitαratA_1AR 1:5000 in 1% BSA in TBST)(4 °C, overnight), washed (3 x TBST), incubated with secondary antibody (goatαrabbit-HRP 1:2000 in 1% BSA in TBST)(1h , rt), washed (2 x TBST, 1 x TBS), activated with luminol enhancer and peroxide (3 min, rt, dark) and subsequently scanned on fluorescence and chemiluminescence.

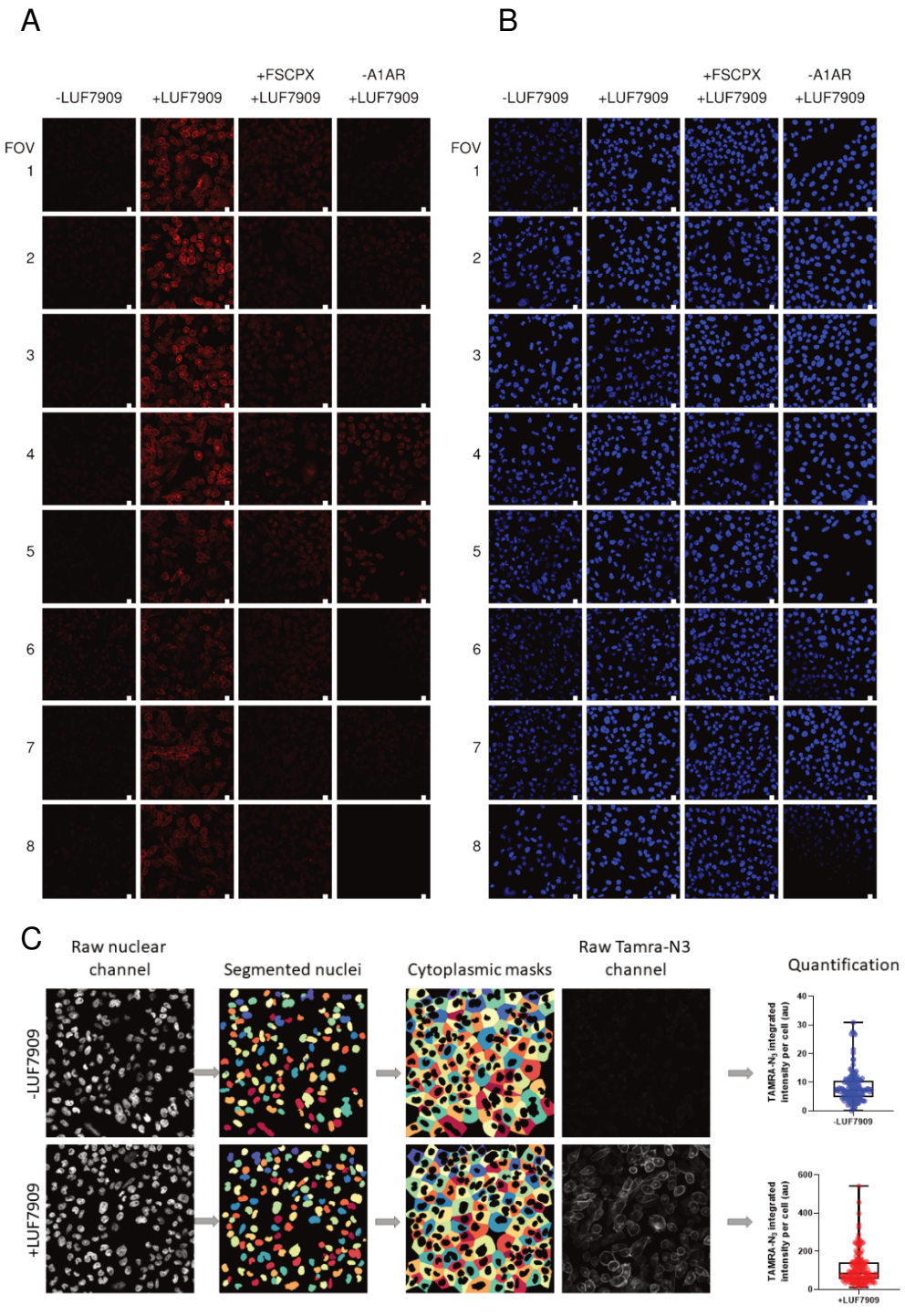
A
B
C
-LUF7909
+LUF7909
+FSCPX +LUF7909
-A1AR +LUF7909
FOV
1
2
3
4
5
6
7
8
Raw nuclear channel
Segmented nuclei
Cytoplasmic masks
Raw Tamra-N3 channel
Quantification
TAMRA-N3 integrated intensity per cell (au)

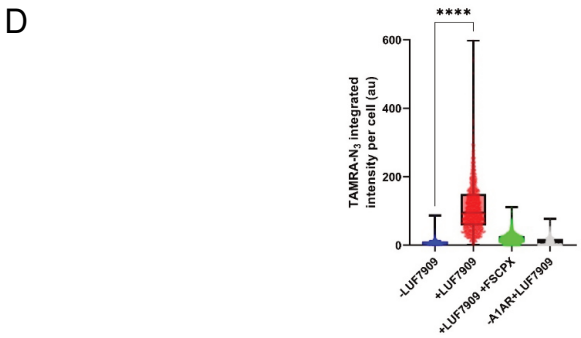

Figure S8. Additional confocal microscopy images supporting Figure 6C. CHO cells with or without overexpression of the A_1AR were pre-treated for 1 h with irreversible antagonist FSCPX (1 µM) or 1% DMSO and incubated for 1 h with LUF7909 (100 nM) or 1% DMSO (control). The cells were then fixed and stained with TAMRA-N_3 (panel A; shown in the red channel) and DAPI (panel B; shown in the blue channel). FOV = Field of view. Images were acquired automatically from two biological experiments performed in duplicate. Shown are four of the FOVs from each of the imaged plates, selected based on a similar amount of cells present in the FOV (FOV 1-4: experiment 1; FOV 5-8: experiment 2). Scale bar = 10 µm. Panel was created using OMERO. (C) Example of automated image analysis of the total intensity of the Tamra-N_3 signal per single cell with and without treatment with LUF7909. Total fluorescence intensity in the cytoplasm of single cells was quantified using CellProfiler. (D) Comparison of the fluorescence intensities between treatment conditions in experiment 2. One single dot represent one single cell. A significant increase in intensity is observed for the cells containing the A_1AR, treated with LUF7909, without competing ligand versus those cells not treated with LUF7909.

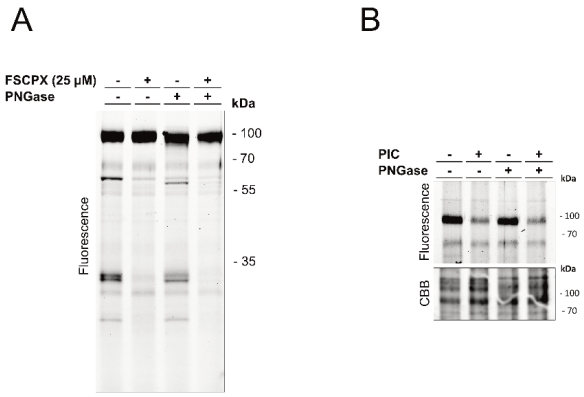

Figure S9 Labeling of LUF7909 in membranes derived from rat adipocytes. The membranes were pre-incubated with competing ligand (25 µM FSCPX or 1 µL protease inhibitor cocktail (PIC), prior to incubation with 100 nM LUF7909. The samples were then incubated with PNGase, clicked to AF647-N_3, denatured and resolved by SDS-PAGE. The gels were scanned using in-gel fluorescence. (A) Competition with 25 µM of covalent antagonist FSCPX; (B) Intensity of the band at 90 kDa is reduced upon pre-incubation with 1 µL of PIC (Sigma Aldrich, cat # p8340).

Experimental

Chemistry

General

All commercially available reagents and solvents were obtained from Sigma Aldrich, Fisher Scientific, VWR chemicals, and Biosolve. All reactions were carried out under a N_2 atmosphere in oven-dried glassware. Thin layer chromatography was performed on TLC Silica gel 60 F254 (Merck) and visualized using UV irradiation. Silica gel flash chromatography was performed using 60-200 µm 60 Å silica gel (VWR Chemicals). ^{1}H-NMR spectra were recorded on a Bruker AV-300 (300 MHz), Bruker AV-400 (400 MHz) or a Bruker AV-500 spectrometer (500 MHz). ^{13}C-NMR spectra were recorded on a Bruker AV-400 (101 MHz) or a Bruker AV-500 (126 MHz) spectrometer. ^{19}F-NMR spectra were recorded a Bruker AV-500 spectrometer (471 MHz). Chemical shift values are reported in ppm (δ) using tetramethylsilane or solvent resonance as the internal standard. Coupling constants (J) are reported in Hz. Multiplicities are indicated by s (singlet), d (doublet), t (triplet), q (quartet), p (pentuplet) or m (multiplet) followed by the number of represented hydrogen atoms. Compound purity was determined by LC-MS, using the LCMS-2020 system of Shimadzu coupled to a Gemini® 3 µm C18 110Å column (50 x 3 mm). In brief, compounds were dissolved in H_2O:MeCN:*t*-BuOH 1:1:1, injected onto the column and eluted with a linear gradient of H_2O:MeCN 90:10 + 0.1% formic acid → H_2O:MeCN 10:90 + 0.1% formic acid over the course of 15 minutes. High-resolution mass spectrometry (HRMS) was performed on a X500R QTOF mass spectrometer (SCIEX). Reaction schemes were created with ChemDraw Professional version 16.0.0.82 (PerkinElmer).

Synthetic Procedures

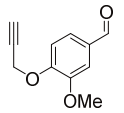

3-Methoxy-4-(prop-2-yn-1-yloxy)benzaldehyde (6a)

3-methoxy-4-hydroxy benzaldehyde (3.80 g, 25.0 mmol, 1.0 eq), propargyl bromide (80% in toluene) (8.30 ml, 74.5 mmol, 3.0 eq) and K2CO3 (5.18 g, 37.5 mmol, 1.5 eq) were dissolved acetone (250 mL). The mixture was refluxed overnight, after which a precipitate had formed. The precipitate was filtrated, dried under reduced pressure and purified by flash column chromatography (PE/EtOAc 95:5 → 70:30) to yield **6a** (3.80 g, 20.0 mmol, 80%) as a white solid. **TLC** (PE/EtOAc 7:3): R_f = 0.57. **^{1}H NMR** (400 MHz, $CDCl_3$): δ [ppm] = 9.87 (s, 1H), 7.46 (dd, *J* = 8.2, 1.9 Hz, 1H), 7.43 (d, *J* = 1.9 Hz, 1H), 7.14 (d, *J* = 8.2 Hz, 1H), 4.86 (d, *J* = 2.4 Hz, 2H), 3.94 (s, 3H), 2.56 (t, *J* = 2.4 Hz, 1H).

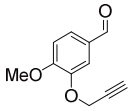

4-Methoxy-3-(prop-2-yn-1-yloxy)benzaldehyde (6b)

3-hydroxy-4-methoxybenzaldehyde (608 mg, 4.00 mmol, 1.0 eq) and K_2CO_3 (830 mg, 6.01 mmol) were dissolved in acetone (20 mL). Propargylbromide (80% in toluene) (1.33 mL, 12.0 mmol, 3.0 eq) was added and the solution was refluxed for 1 h at 80 °C and allowed cooled down to rt overnight. Water (40 mL) was added and the mixture was extracted with EtOAc (3 x 40 mL). The organic layers were combined and washed with brine (1 x 50 mL), dried over

$MgSO_4$ and evaporated to yield **6b** (759 mg, 3.99 mmol, 100 %) as an off-white oil. **TLC** (PE/EtOAc 3:2): R_f = 0.67. **^{1}H NMR** (400 MHz, $CDCl_3$): δ [ppm] = 9.66 (s, 1H), 7.42 – 7.27 (m, 2H), 6.83 (d, *J* = 8.1 Hz, 1H), 4.64 (d, *J* = 2.5 Hz, 2H), 3.76 (s, 3H), 2.50 (t, *J* = 2.4 Hz, 1H). **^{13}C NMR** (101 MHz, $CDCl_3$): δ [ppm] = δ 190.3, 154.5, 146.9, 129.5, 126.9, 111.5, 110.7, 77.6, 76.4, 56.2, 55.8.

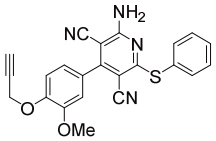

2-Amino-4-(3-methoxy-4-(prop-2-yn-1-yloxy)phenyl)-6-(phenylthio)pyridine-3,5-dicarbonitrile (7a)

Et_3N (140 µL. 1.00 mmol, 0.05 eq) was added dropwise to a suspension of **6a** (3.80 g, 20.0 mmol, 1.0 eq) and malononitrile (2.73 g, 41.3 mmol, 2.1 eq) in EtOH (30 mL). The mixture was brought to 50°C. upon which thiophenol (2.18 ml, 21.3 mmol, 1.1 eq) was added. The mixture was then stirred at 50°C for 4 h, after which TLC revealed full consumption of the aldehyde. The mixture was cooled down to rt and the formed precipitate was collected by filtration to yield **7a** (3.87 g, 9.38 mmol, 47%) as an off-white solid. **TLC** (PE/EtOAc 7:3): R_f = 0.27. **^{1}H NMR** (400 MHz, $(CD_3)_2SO$): δ [ppm] = 7.78 (s, 2H), 7.63 – 7.58 (m, 2H), 7.55 – 7.46 (m, 3H), 7.28 – 7.23 (m, 1H), 7.21 – 7.11 (m, 2H), 4.90 (d, *J* = 1.8 Hz, 2H), 3.81 (s, 3H), 3.64 (t, *J* = 2.1 Hz, 1H).

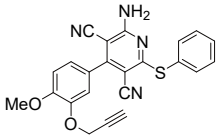

2-Amino-4-(4-methoxy-3-(prop-2-yn-1-yloxy)phenyl)-6-(phenylthio)pyridine-3,5-dicarbonitrile (7b)

Malononitrile (264 mg, 3.99 mmol, 1.0 eq) and piperidine (catalytic amount) were added to a solution of **6b** (759 mg, 3.99 mmol, 1.0 eq) in EtOH (5 mL) at 50 °C. The mixture immediately became a yellow suspension. The mixture was refluxed at 50 °C for 5 h and afterwards cooled down to rt. The formed precipitate was filtrated and dried under reduced pressure to yield 611 mg (2.56 mmol) of the malononitrile-substituted intermediate. This crude intermediate was then re-dissolved in EtOH (10 mL) by heating the mixture to 65 °C. Malononitrile (190 mg, 2.88 mmol, 1.4 eq) and triethylamine (catalytic amount) were added and the solution was refluxed for 45 min at 65 °C. Thiophenol (288 µL, 2.82 mmol, 0.7 eq) was added and the solution was refluxed for 3 h at 65 °C, upon which TLC showed full consumption of the starting material. The mixture was cooled down to rt and allowed to crystallize overnight. The formed precipitate was collected by filtration and dried under reduced pressure to yield **7b** (500 mg, 1.21 mmol, 30% yield). **TLC** (PE/EtOAc 7:3): R_f = 0.22. **^{1}H NMR** (300 MHz, $CDCl_3$): δ [ppm] = 7.59 – 7.52 (m, 2H), 7.50 – 7.44 (m, 3H), 7.25 – 7.20 (m, 2H), 7.04 (d, *J* = 9.0 Hz, 1H), 5.43 (s, 2H), 4.83 (d, *J* = 2.4 Hz, 2H), 3.95 (s, 3H), 2.59 (t, *J* = 2.4 Hz, 1H). **LCMS** (ESI, m/z): $[M+H]^+$: 413.15. **HPLC:** 100%, RT 10.893 min.

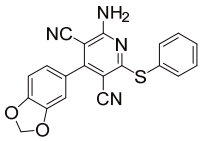

2-Amino-4-(benzo[d][1,3]dioxol-5-yl)-6-(phenylthio)pyridine-3,5-dicarbonitrile (7c)
Piperonal (3.00 g, 20.0 mmol, 1 eq) was added to a solution of malononitrile (1.32 g, 20.0 mmol, 1.0 eq) in EtOH (20 ml). Piperidine (catalytic amount) was added and the solution was refluxed at 75 °C for 3 h, before slowly cooling down to RT. The formed yellow precipitate was collected by filtration, washed with EtOH and water and dried under reduced pressure to yield the malononitrile-substituted intermediate (3.72 g, 18.80 mmol). 1 gram of the crude intermediate was taken for the further steps (1.00 g, 5.05 mmol, 1.0 eq) and dissolved in EtOH (10 ml). Malononitrile (364mg, 5.51 mmol, 1.1 eq), thiophenol (567 µL, 5.56 mmol, 1.1 eq) and triethylamine (catalytic amount) were added and the mixture was refluxed at 75 °C for 10 h before slowly cooling down to rt. The formed yellow precipitate was collected by filtration and the residue was purified by automated flash column chromatography (DCM/MeOH 99:1 → 95:5). The precipitate and the purified filtrate were combined to yield **7c** (885 mg, 2.38 mmol, 44% over two steps) as a yellow solid. **TLC** (PE/EtOAc 7:3): R_f = 0.27. **^{1}H NMR** (300 MHz, $CDCl_3$): δ [ppm] = 7.58 – 7.52 (m, 2H), 7.50 – 7.43 (m, 3H), 7.04 (dd, *J* = 8.0, 1.8 Hz, 1H), 6.99 (d, *J* = 1.7 Hz, 1H), 6.96 (d, *J* = 8.0 Hz, 1H), 6.08 (s, 2H), 5.43 (s, 2H). **LCMS** (ESI, m/z): $[M+H]^+$: 373.10. **HPLC:** 100%, RT 10.924 min.

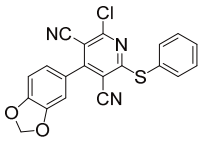

4-(Benzo[d][1,3]dioxol-5-yl)-2-chloro-6-(phenylthio)pyridine-3,5-dicarbonitrile (8)
Isopentyl nitrite (403 µl, 3.00 mmol, 1.4 eq) and copper(II)chloride (402 mg, 2.99 mmol, 1.4 eq) were added to a solution of **7c** (797 mg, 2.14 mmol, 1.0 eq) in acetonitrile (10 ml) The mixture was refluxed at 60 °C for 20 h and afterwards slowly cooled down to rt. 1 M HCl (30 mL) was added and the resulting green aqueous layer was extracted with DCM (4 x 30 mL). The organic layers were combined, dried over $MgSO_4$ and concentrated under reduced pressure. The residue was purified by flash column chromatography (PE/EtOAc 9:1 → 7:3) to yield **8** (606 mg, 1,547 mmol, 72 % yield). **TLC** (PE/EtOAc 7:3): R_f = 0.63. **^{1}H NMR** (400 MHz, $CDCl_3$): δ [ppm] = 7.64 – 7.44 (m, 5H), 7.06 (dd, *J* = 8.0, 1.9 Hz, 1H), 7.01 – 6.98 (m, 2H), 6.10 (s, 2H). **^{13}C NMR** (101 MHz, $CDCl_3$) δ 169.3, 158.5, 156.1, 150.8, 148.6, 135.7, 130.8, 129.8, 125.8, 125.2, 123.9, 113.7, 113.4, 109.3, 109.0, 106.3, 105.0, 102.3. **LCMS** (ESI, m/z): $[M+H]^+$: 392.00. **HPLC:** 100%, RT 11.892 min.

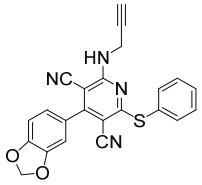

4-(Benzo[d][1,3]dioxol-5-yl)-2-(phenylthio)-6-(prop-2-yn-1-ylamino)pyridine-3,5-dicarbonitrile (9)
Propargyl amine (90 µL, 1.41 mmol, 2 eq) was added to a solution of **8** (274 mg, 0,699 mmol) in dry THF (3.5 ml) and the mixture was stirred at rt overnight. Water (25 mL) was then added and the aqueous layer was extracted with DCM (2 x 25 mL). The organic layers were combined

and washed with 1 M HCl (2 x 25 mL) and brine (25 mL), dried over $MgSO_4$, filtered and concentrated under reduced pressure to yield **9** (265 mg, 0.65 mmol, 92%) as a yellow solid. **TLC** (Pentane/EtOAc 8:2): R_f = 0.31. **^{1}H NMR** (500 MHz, $CDCl_3$): δ [ppm] = 7.59 (dd, *J* = 7.9, 1.7 Hz, 2H), 7.53 – 7.41 (m, 3H), 7.01 (dd, *J* = 8.0, 1.9 Hz, 1H), 6.97 (d, *J* = 1.8 Hz, 1H), 6.94 (d, *J* = 8.0 Hz, 1H), 6.05 (s, 2H), 5.83 (t, *J* = 5.5 Hz, 1H), 3.74 (dd, *J* = 5.5, 2.5 Hz, 2H), 2.18 (t, *J* = 2.5 Hz, 1H). **^{13}C NMR** (126 MHz, $CDCl_3$): δ [ppm] = 169.3, 157.7, 156.9, 150.0, 148.2, 136.2, 130.1, 129.3, 127.2, 126.7, 123.3, 115.3, 115.1, 109.0, 108.9, 102.0, 95.1, 88.1, 78.9, 71.9, 30.9.

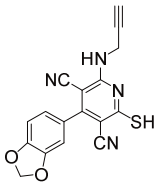

4-(Benzo[d][1,3]dioxol-5-yl)-2-mercapto-6-(prop-2-yn-1-ylamino)pyridine-3,5-dicarbonitrile (10)

Potassium thioacetate (178 mg, 1.56 mmol, 2.0 eq) was added to a solution of **9** (321 mg, 0.78 mmol, 1.0 eq) in dry DMF (4 mL). After 6 h of stirring, 2.0 equivalent of potassium thioacetate (178 mg, 1.56 mmol) was added and the mixture was stirred for another 2 h, upon which the TLC indicated full consumption of starting material. EtOAc (50 mL) was added and the organic layer was washed with brine (3 x 50 mL), dried over $MgSO_4$, filtered and concentrated under reduced pressure to yield **10** as a yellow/brown solid (258 mg, 0.77 mmol, 99%), which was used in the next steps without further purification. **TLC** (DCM:MeOH 95:5): R_f = 0.18. **^{1}H NMR** (500 MHz, $(CD_3)_2SO$) δ [ppm] = 8.71 (t, *J* = 5.6 Hz, 1H), 7.22 (d, *J* = 1.8 Hz, 1H), 7.18 – 7.09 (m, 2H), 6.21 – 6.11 (m, 3H), 4.08 (dd, *J* = 5.7, 2.5 Hz, 2H), 2.81 (t, *J* = 2.4 Hz, 1H). **^{13}C NMR** (126 MHz, $(CD_3)_2SO$) δ [ppm] = 162.4, 158.1, 157.0, 149.3, 147.5, 126.7, 123.4, 114.9, 114.6, 109.0, 108.7, 101.9, 93.8, 89.8, 89.1, 72.0, 30.6. **LCMS** (ESI, m/z): $[M+H]^+$: 334.95.

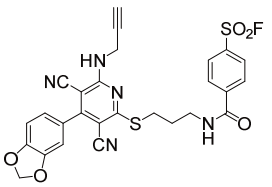

4-((3-((4-(Benzo[d][1,3]dioxol-5-yl)-3,5-dicyano-6-(prop-2-yn-1-ylamino)pyridin-2-yl)thio)propyl)carbamoyl)benzenesulfonyl fluoride (1)

19 (350 mg, 1.08 mmol, 1.4 eq) and $NaHCO_3$ (97 mg, 1.16 mmol, 1.5 eq) were added to a solution of **10** (258 mg, 0.77 mmol, 1.0 eq) in dry DMF (3.4 mL). The mixture was stirred for 2 days, after which another 1.5 eq of $NaHCO_3$ (97 mg, 1.16 mmol) was added. The mixture was then stirred at 50 °C for two days. DCM (50 mL) was added and the organic layer was washed with brine (3 x 50 mL), dried over $MgSO_4$, filtered and concentrated under reduced pressure. The residue was purified by silica column chromatography (DCM:MeOH 99.5:0.5 → 99:1) and recrystallization in DCM to yield **1** as a yellow solid (177 mg, 0.31 mmol, 40%). **TLC** (DCM:MeOH 99:1): R_f = 0.38. **^{1}H NMR** (500 MHz, $(CD_3)_2SO$) δ [ppm] = 8.95 (t, *J* = 5.6 Hz, 1H), 8.56 (t, *J* = 5.6 Hz, 1H), 8.26 (d, *J* = 8.6 Hz, 2H), 8.19 (d, *J* = 8.5 Hz, 2H), 7.18 (d, *J* = 1.8 Hz, 1H), 7.10 (d, *J* = 8.0 Hz, 1H), 7.05 (dd, *J* = 8.1, 1.8 Hz, 1H), 6.15 (s, 2H), 4.21 (dd, *J* = 5.6, 2.4 Hz, 2H), 3.46 (q, *J* = 6.4 Hz, 2H), 3.38 (t, *J* = 6.9 Hz, 2H), 3.09 (t, *J* = 2.4 Hz, 1H), 2.04 (p, *J* = 6.9 Hz, 2H). **^{13}C NMR** (126 MHz, $(CD_3)_2SO$) δ [ppm] = 167.2, 164.5, 157.6, 157.0, 149.0, 147.4, 141.5, 133.4 (d, *J* = 23.8 Hz), 129.1, 128.6, 127.2, 123.1, 115.4, 115.0, 109.0, 108.6, 101.8, 94.4, 87.4, 80.8, 72.8, 38.6, 30.9, 29.1, 27.7. **^{19}F NMR** (471 MHz, $(CD_3)_2SO$) δ [ppm] = 65.94.

HRMS (ESI, m/z): $[M+H]^+$, calculated: 578.0963, found: 578.0970. **HPLC:** 99%, RT 11.262 min.

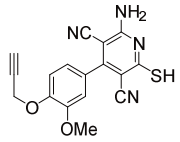

2-Amino-6-mercapto-4-(3-methoxy-4-(prop-2-yn-1-yloxy)phenyl)pyridine-3,5-dicarbonitrile (11a)

Potassium thioacetate (65 mg, 0.57 mmol, 2.4 eq) was added to a solution of **7a** (99 mg, 0.24 mmol, 1.0 eq) in dry DMF (2 mL). The mixture was stirred for 6 h, after which extra potassium thioacetate (65 mg, 0.57 mmol, 2.4 eq) was added. The mixture was stirred overnight and another 2.4 equivalent of potassium thioacetate (65 mg, 0.57 mmol) was added. The mixture was stirred for 4 h, after which full consumption of starting materials was observed by LCMS. 2 M NaOH (5 mL) was added and the mixture was stirred at rt over the weekend. Water (10 mL) and 1 M HCl (10 mL) were then added. Immediately a yellow precipitate formed, which was collected by extraction with EtOAc (3 x 20 mL). The organic layers were combined, dried over $MgSO_4$, filtered and concentrated under reduced pressure to yield **11a** (60 mg, 0.18 mmol, 74%) a yellow solid, which was used in the next steps without further purification. **TLC** (DCM:MeOH 95:5): R_f = 0.15. **^{1}H NMR** (500 MHz, $(CD_3)_2SO$) δ [ppm] = 12.98 (s, 1H), 7.95 (s, 2H), 7.20 – 7.17 (m, 1H), 7.16 (s, 1H), 7.09 (dd, *J* = 8.4, 2.1 Hz, 1H), 4.89 (d, *J* = 2.4 Hz, 2H), 3.80 (s, 4H), 3.62 (t, *J* = 2.4 Hz, 1H). **^{13}C NMR** (126 MHz, $(CD_3)_2SO$) δ [ppm] = 179.3, 158.4, 154.5, 148.5, 148.2, 127.0, 120.9, 116.8, 114.8, 113.0, 112.3, 102.4, 81.6, 79.0, 78.7, 55.9, 55.8. **LCMS** (ESI, m/z): $[M+H]^+$: 337.00.

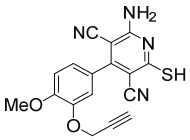

2-Amino-6-mercapto-4-(4-methoxy-3-(prop-2-yn-1-yloxy)phenyl)pyridine-3,5-dicarbonitrile (11b)

Potassium thioacetate (276 mg, 2.42 mmol, 2.0 eq) was added to a solution of **7b** (500 mg, 1,21 mmol, 1.0 eq) in dry DMF (6 mL). The mixture was stirred at rt overnight and the next day another equivalent of potassium thioacetate (138 mg, 1.21 mmol, 1 eq) was added. The mixture was stirred over 3 days, upon which no starting material was visible anymore on TLC. 2 M NaOH (6 mL) was added to hydrolyze the formed thioacetate. After stirring for 8 h at rt, another 6 mL of 2 M NaOH was added and the mixture was stirred overnight. Water (62 mL) and 1 M HCl (24 mL) were added to acidify the mixture. The product was allowed to crystallize overnight. The formed precipitate was collected by filtration, dried under reduced pressure and recrystallized in a mixture of EtOH and MeOH to yield **11b** (253 mg, 0.75 mmol, 62%) as a yellow solid. **TLC** (DCM/MeOH 95:5): R_f = 0.17. **^{1}H NMR** (400 MHz, CD_3OD): δ [ppm] = 7.30 – 7.09 (m, 3H), 4.79 (d, *J* = 2.5 Hz, 2H), 3.92 (s, 3H), 2.97 (t, *J* = 2.4 Hz, 1H).

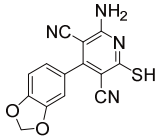

2-Amino-4-(benzo[d][1,3]dioxol-5-yl)-6-mercaptopyridine-3,5-dicarbonitrile (11c)
Potassium thioacetate (863 mg, 7.56, mmol, 2.0 eq) was added to **7c** (1409 mg, 3.78 mmol, 1.0 eq) in dry DMF (19 mL). The solution was stirred at rt overnight, after which no starting material was observed anymore by TLC. Therefore 2 M NaOH (20 mL) was added to hydrolyze the formed thioacetate and the mixture was stirred for 7 h. Water (20 mL) was added to quench the and 1 M HCl (40 mL) was slowly added to bring the solution to a pH of 5. Upon addition, a yellow precipitate started to form. Another 80 mL of water was then added and the product was crystallized over 3 days. Afterwards the crystals were collected by filtration and re-crystallized in EtOH and MeOH to yield **11c** (877 mg, 2.96 mmol, 78%) as a yellow solid. **TLC** (DCM/MeOH 95:5): R_f = 0.23. **^{1}H NMR** (400 MHz, CD_3OD): δ [ppm] = 7.12 – 6.89 (m, 3H), 6.07 (s, 2H). **LCMS** (ESI, m/z): $[M+H]^+$: 296.95. **HPLC:** 84%, RT 8.200 min.

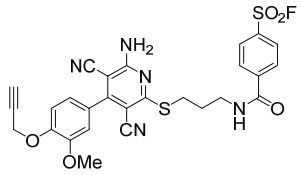

4-((3-((6-Amino-3,5-dicyano-4-(3-methoxy-4-(prop-2-yn-1-yloxy)phenyl)pyridin-2-yl)thio)propyl)carbamoyl)benzenesulfonyl fluoride (2)
19 (50 mg, 0.15 mmol, 1.4 eq) and $NaHCO_3$ (19 mg, 0.23 mmol, 1.5 eq) were added to a solution of **11a** in dry DMF (2 mL) and the mixture was stirred overnight. DCM was added and the organic layer was washed with brine (3 x 30 mL), dried over $MgSO_4$, filtered and concentrated. The residue was purified by silica column chromatography (DCM:MeOH 99.5:0.5 → 95:5) and recrystallization in DCM to yield **2** as a white solid (46 mg, 0.08 mmol, 53% yield). **TLC** (DCM:MeOH 99:1): R_f = 0.30. **^{1}H NMR** (500 MHz, $(CD_3)_2SO$) δ [ppm] = 8.93 (t, *J* = 5.6 Hz, 1H), 8.26 (d, *J* = 8.6 Hz, 2H), 8.18 (d, *J* = 8.5 Hz, 2H), 7.97 (s, 2H), 7.22 (d, *J* = 2.1 Hz, 1H), 7.18 (d, *J* = 8.4 Hz, 1H), 7.10 (dd, *J* = 8.3, 2.1 Hz, 1H), 4.89 (d, *J* = 2.4 Hz, 2H), 3.81 (s, 3H), 3.62 (t, *J* = 2.4 Hz, 1H), 3.45 (q, *J* = 6.5 Hz, 2H), 3.30 (t, *J* = 7.0 Hz, 2H), 1.97 (p, *J* = 6.9 Hz, 2H). **^{13}C NMR** (126 MHz, $(CD_3)_2SO$) δ [ppm] = 167.0, 164.6, 159.8, 157.9, 148.6, 148.1, 141.5, 133.4 (d, *J* = 23.7 Hz), 129.1, 128.6, 126.8, 121.2, 115.7, 115.5, 113.2, 112.6, 93.7, 85.7, 79.0, 78.7, 55.9, 55.8, 38.5, 28.6, 27.3. **^{19}F NMR** (471 MHz, $(CD_3)_2SO$) δ [ppm] = 65.94. **HRMS** (ESI, m/z): $[M+H]^+$, calculated: 580.1117, found: 580.1119. **HPLC**: 95%, RT 10.910 min.

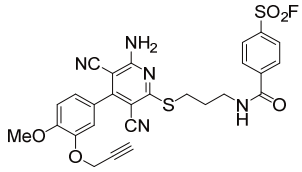

4-((3-((6-Amino-3,5-dicyano-4-(4-methoxy-3-(prop-2-yn-1-yloxy)phenyl)pyridin-2-yl)thio)propyl)carbamoyl)benzenesulfonyl fluoride (3)
$NaHCO_3$ (43 mg, 0.51 mmol, 1.5 eq) and **19** (150 mg, 0.46 mmol, 1.4 eq) in dry DMF (3 ml) were added to **11b** (115 mg, 0.34 mmol, 1.0 eq) and the mixture was stirred for two days at RT. DCM (20 mL) was then added and the mixture was washed with water (20 mL), dried over

$MgSO_4$, filtered and concentrated under reduced pressure. The residue was purified by flash column chromatography (Pentane/EtOAc 1:1 → 1:4) to yield **3** (60 mg, 0.10 mmol, 29%) as an off-white solid. **TLC** (Pentane/EtOAc 7:3): R_f = 0.31. **^{1}H NMR** (500 MHz, $CDCl_3$): δ [ppm] = 8.08 – 8.00 (m, 4H), 7.20 – 7.16 (m, 2H), 7.02 (d, *J* = 8.1 Hz, 1H), 6.99 (t, *J* = 6.0 Hz, 1H), 6.04 (s, 2H), 4.80 (d, *J* = 2.4 Hz, 2H), 3.59 (q, *J* = 6.6 Hz, 2H), 3.24 (t, *J* = 7.1 Hz, 2H), 2.59 (t, *J* = 2.4 Hz, 1H), 2.10 (p, *J* = 7.1 Hz, 2H). **^{13}C NMR** (126 MHz, $CDCl_3$): δ [ppm] = 168.6, 165.7, 159.7, 157.6, 152.0, 146.9, 141.0, 135.4 (d, *J* = 25.1 Hz), 128.8, 128.5, 125.3, 123.3, 115.7, 115.6, 114.7, 111.8, 96.1, 86.7, 78.0, 77.0, 57.2, 56.1, 39.6, 28.8, 28.1. **^{19}F NMR** (471 MHz, $CDCl_3$): δ [p5pm] = 65.72. **HRMS** (ESI, m/z): $[M+H]^+$, calculated: 580.1119, found: 580.1113. **HPLC**: 96%, RT 10.861 min.

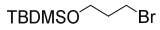

(3-Bromopropoxy)(tert-butyl)dimethylsilane (13)

A solution of TBDMS-Cl (50 wt% in toluene)(7.83 mL, 22.50 mmol, 1.5 eq) was added to a solution of 3-bromopropanol(1.36 ml, 15.00 mmol) in dry DMF (10 mL). 1H-imidazole (2.04 g, 30.00 mmol) was added the mixture was stirred for 5 h. DCM (100 mL) was then added and the mixture was washed with water (3 x 100 mL) and brine (1 x 100 mL), dried over $MgSO_4$ and concentrated under reduced pressure to yield crude **13** (7.60 g, 30.00 mmol, quant). **^{1}H NMR** (300 MHz, $CDCl_3$): δ [ppm] = 3.73 (t, *J* = 5.7 Hz, 2H), 3.51 (t, *J* = 6.4 Hz, 2H), 2.04 (p, *J* = 6.5, 6.1 Hz, 2H), 0.89 (s, 9H), 0.06 (s, 6H). **^{13}C NMR** (75 MHz, $CDCl_3$): δ [ppm] = 60.5, 35.7, 30.8, 26.0, 25.8, -5.2.

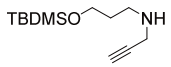

N-(3-((*tert*-Butyldimethylsilyl)oxy)propyl)prop-2-yn-1-amine (14)

A solution of **13** (3.80 g, 15.00 mmol, 1.0 eq) and DIPEA (5.22 mL, 30.00 mmol, 2.0 eq) in acetonitrile (15 mL) was added dropwise to propargylamine (4.80 ml, 75.00 mmol, 3 eq) over a time period of 5 h using a syringe pump. After 5 h, the mixture had turned orange and LCMS analysis revealed mono- and disubstituted product. EtOAc (200 mL) was added and the mixture was washed with brine (3 x 150 mL), dried over $MgSO_4$, filtered and concentrated under reduced pressure. The residue was purified by flash column chromatography (Pentane/EtOAc 6:4 → 4:6) to yield **14** (1.78 g, 7.81 mmol, 52%) as a brown oil. **TLC** (EtOAc): R_f = 0.48. **^{1}H NMR** (400 MHz, $CDCl_3$): δ [ppm] = 3.70 (t, *J* = 6.1 Hz, 2H), 3.42 (d, *J* = 2.4 Hz, 2H), 2.78 (t, *J* = 6.8 Hz, 2H), 2.20 (t, *J* = 2.4 Hz, 1H), 1.71 (p, *J* = 6.4 Hz, 2H), 0.89 (s, 9H), 0.05 (s, 6H). **^{13}C NMR** (101 MHz, $CDCl_3$): δ [ppm] = δ 82.4, 71.3, 61.9, 46.3, 38.4, 32.8, 28.2, 18.4, -3.3. **LCMS** (ESI, m/z): $[M+H]^+$: 228.10.

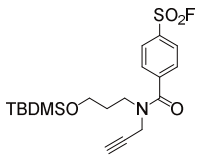

4-((3-((*tert*-Butyldimethylsilyl)oxy)propyl)(prop-2-yn-1-yl)carbamoyl)benzenesulfonyl fluoride (15)

EDC·HCl (1.65 g, 8.59 mmol, 1.1 eq) and **14** (1776 mg, 7,81 mmol, 1.0 eq) in dry DMF (10 mL) were added to a solution of 4-fluorosulfonyl benzoic acid (1.75 g, 8.59 mmol, 1.1 eq) in dry DMF (10 mL) and the mixture was stirred at rt. After stirring for 1 h, DIPEA (2.72 mL, 15.62 mmol, 2.0 eq) was added and the mixture was stirred overnight. The next day additional DIPEA (1.36 mL, 7.81 mmol, 1.0 eq) and **2** (616 mg, 3.02 mmol, 0.4 eq) were added and the mixture was stirred overnight. DIPEA (1.36 mL, 7.81 mmol, 1.0 eq) was added and the mixture was

stirred for another night. As no further progress of the reaction was observed, water (100 mL) was added and the aqueous layer was extracted with DCM (100 mL). The organic layer was washed with water (2 x 100 mL) and the aqueous layers were combined and back-extracted with DCM (100 mL). The organic layers were combined, washed with brine (100 mL), dried over $MgSO_4$, filtered and concentrated under reduced pressure. The residue was purified by flash column chromatography (Pentane/EtOAc 95:5 → 75:25) to yield yellow oil **15** (1.88 mg, 4.53 mmol, 58%) as a mixture of two rotamers, as determined by ^{1}H NMR, ^{13}C NMR, ^{19}F NMR and LCMS measurements. **TLC** (Pentane/EtOAc 8:2): R_f = 0.77. **^{1}H NMR** (500 MHz, $CDCl_3$): δ [ppm] = 8.08 – 7.92 (m, 2H), 7.66 (dd, *J* = 49.1, 8.0 Hz, 2H), 4.11 (d, *J* = 216.9 Hz, 2H), 3.78 – 3.54 (m, 2H), 3.45 (dt, *J* = 37.9, 6.6 Hz, 2H), 2.31 (d, *J* = 43.6 Hz, 1H), 1.83 (d, *J* = 79.6 Hz, 2H), 0.94 – 0.55 (m, 9H), 0.14 – -0.25 (m, 6H). **^{13}C NMR** (126 MHz, $CDCl_3$): δ [ppm] = 168.8, 168.5, 143.2, 143.1, 133.9, 133.7, 128.7, 128.0, 78.1, 73.6, 72.5, 60.5, 59.6, 46.0, 43.3, 39.5, 34.0, 31.2, 30.8, 30.3, 25.9, 25.9, 25.7, 25.6, -5.4, -5.6. **^{19}F NMR** (471 MHz, $CDCl_3$): δ [ppm] = 65.81, 65.71. **LCMS** (ESI, m/z): $[M+H]^+$: 414.05. **HPLC**: 99%, RT 10.437 min.

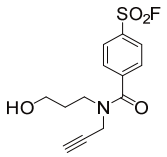

4-((3-Hydroxypropyl)(prop-2-yn-1-yl)carbamoyl)benzenesulfonyl fluoride (16)

$Et_3N{\cdot}3HF$ (1.01 mL, 6.18 mmol, 6 eq) was added to a solution of **15** (426 mg, 1,03 mmol, 1.0 eq) in dry THF (5 mL). The mixture was stirred overnight at room temperature, after which DCM (50 mL) was added. The mixture was then washed with brine (2 x 50 mL). The aqueous layers were combined and back-extracted with DCM (50 mL). The organic layers were combined and concentrated under reduced pressure. The residue was purified by flash column chromatography (DCM/MeOH 99.5:0.5 → 98:2) to yield **16** (283 mg, 0.95 mmol, 92%) as a colorless oil. **TLC** (DCM/MeOH 98:2): R_f = 0.38. **^{1}H NMR** (400 MHz, $CDCl_3$): δ [ppm] = 8.06 (d, *J* = 8.1 Hz, 2H), 7.81 – 7.58 (m, 2H), 3.98 – 3.81 (m, 2H), 3.76 (t, *J* = 6.5 Hz, 2H), 3.65 – 3.47 (m, 2H), 2.51 – 2.27 (m, 1H), 1.87 (p, *J* = 6.1 Hz, 2H). **^{13}C NMR** (101 MHz, $CDCl_3$): δ [ppm] = δ 169.8, 142.3, 134.3 (d, *J* = 25.0 Hz), 128.9, 128.1, 77.9, 74.2, 58.8, 42.6, 39.5, 29.7. **^{19}F NMR** (471 MHz, $CDCl_3$): δ [ppm] = 65.70. **LCMS** (ESI, m/z): $[M+H]^+$: 299.95. **HPLC:** 100%, RT 8.158 min.

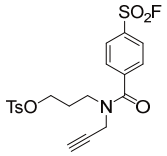

3-(4-(Fluorosulfonyl)-N-(prop-2-yn-1-yl)benzamido)propyl 4-methylbenzenesulfonate (17)

TsCl (906 mg, 4.75 mmol, 5.0 eq) and Et_3N (264 µL, 1.90 mmol, 2.0 eq) were added to a solution of **16** (283 mg, 0.95 mmol, 1.0 eq) in dry DMF (5 mL). The mixture was stirred for two days at rt, after which another 2 equivalents of Et_3N (264 µL, 1.90 mmol, 2.0 eq) were added. The mixture was stirred overnight and 2 equivalents of Et_3N (264 µL, 1.90 mmol, 2.0 eq) were added. The mixture was stirred for another 2 h and afterwards diluted with DCM (25 mL). The organic layer was washed with H_2O (25 mL) and brine (25 mL), dried over $MgSO_4$, filtered and concentrated under reduced pressure. The residue was purified by flash column chromatography (Pentane/Et_2O 7:3 → 3:7) to yield the colorless oil **17** (238 mg, 0.52 mmol, 55%) as a mixture of two rotamers, as determined by ^{1}H NMR, ^{13}C NMR, ^{19}F NMR and LCMS

measurements. **TLC** (Pentane/EtOAc 1:1): R_f = 0.46. **^{1}H NMR** (500 MHz, $CDCl_3$)* δ [ppm] = 8.17 (d, *J* = 8.2 Hz, 2H), 7.96 (d, *J* = 8.5 Hz, 2H), 7.69 (d, *J* = 7.9 Hz, 2H), 7.11 (d, *J* = 7.9 Hz, 2H), 4.40 (t, *J* = 5.9 Hz, 2H), 4.05 – 3.95 (m, 2H), 3.37 – 3.25 (m, 2H), 2.51 (t, *J* = 2.5 Hz, 1H), 2.46 – 2.41 (m, 2H), 2.30 (s, 3H). **^{13}C NMR** (126 MHz, $CDCl_3$)* δ [ppm] = 164.3, 142.6, 141.1, 136.7 (d, *J* = 25.3 Hz), 136.2, 130.9, 129.1, 128.5, 125.9, 78.1, 73.3, 62.6, 43.7, 36.9, 25.3, 21.4. **^{19}F NMR** (471 MHz, $CDCl_3$)* δ [ppm] = 65.44. **LCMS** (ESI, m/z): $[M+H]^+$: 453.95. **HPLC**: 96%, RT 10.945 min. *Only the values of the most abundant rotamer are given.

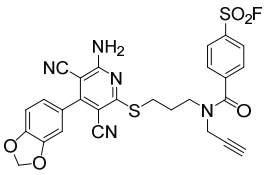

4-((3-((6-Amino-4-(benzo[d][1,3]dioxol-5-yl)-3,5-dicyanopyridin-2-yl)thio)propyl)(prop-2-yn-1-yl)carbamoyl)benzenesulfonyl fluoride (LUF7909) (4)

11 (238 mg, 0.52 mmol, 1.0 eq) in dry DMF (3 mL) was added to **14** (231 mg, 0.80 mmol, 1.5 eq). $NaHCO_3$ (44 mg, 0.52 mmol, 1.0 eq) was added and the mixture was stirred overnight at rt. The mixture was then diluted with DCM (25 mL). The organic layer was washed with brine (4 x 25 mL), dried over $MgSO_4$, filtered and concentrated under reduced pressure. The residue was purified by flash column chromatography (Pentane/Et_2O 4:6 → 1:9) to yield **3** (90 mg, 0.16 mmol, 31%) as an off-white solid. **TLC** (Pentane/EtOAc 1:1): R_f = 0.47. **^{1}H NMR** (500 MHz, $CDCl_3$, *20 °C*): δ [ppm] = 8.09 (d, *J* = 7.8 Hz, 2H), 7.87 – 7.61 (m, 2H), 7.00 (dd, *J* = 8.0, 1.7 Hz, 1H), 6.95 (d, *J* = 1.7 Hz, 1H), 6.93 (d, *J* = 8.0 Hz, 1H), 6.28 – 5.82 (m, 4H), 4.20 (d, *J* = 256.2 Hz, 2H), 3.68 (d, *J* = 99.6 Hz, 2H), 3.12 (d, *J* = 114.7 Hz, 2H), 2.54 – 2.31 (m, 1H), 2.31 – 2.13 (m, 2H). **^{1}H NMR** (500 MHz, $CDCl_3$, *59 °C*): δ [ppm] = 8.08 (d, *J* = 7.9 Hz, 2H), 7.74 (d, *J* = 7.8 Hz, 2H), 7.00 (dd, *J* = 8.0, 1.8 Hz, 1H), 6.96 (d, *J* = 1.8 Hz, 1H), 6.93 (d, *J* = 8.0 Hz, 1H), 6.05 (s, 2H), 5.93 (s, 2H), 4.01 (s, 2H), 3.73 (s, 2H), 3.20 (s, 2H), 2.45 – 2.27 (m, 1H), 2.27 – 1.92 (m, 2H). **^{13}C NMR** (126 MHz, $CDCl_3$): δ [ppm] = 169.1, 168.7, 159.7, 157.8, 150.0, 148.3, 142.5, 134.5 (d, *J* = 25.7 Hz), 129.1, 128.1, 126.8, 123.3, 115.6, 115.2, 109.0, 108.9, 102.0, 96.4, 86.7, 78.0, 74.4, 45.9, 40.1, 28.3, 27.0. **^{19}F NMR** (471 MHz, $CDCl_3$): δ [ppm] = 65.78. **HRMS** (ESI, m/z): $[M+H]^+$, calculated: 578.0963, found: 578.1054. **HPLC**: 96%, RT 11.122 min.

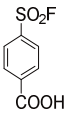

4-(Fluorosulfonyl)benzoic acid (18)

A solution of potassium bifluoride (2.34 g, 30,0 mmol, 3 eq) in water (20 mL) (1.5 M) was added to a solution of 4-(chlorosulfonyl)benzoic acid (2.21 g, 10,0 mmol, 1 eq) in dioxane (25 mL). The mixture was stirred for 3 h, after which TLC and LCMS showed full consumption of starting material. EtOAc (120 mL) was added and the organic layer was washed with water (2 x 150 mL) and brine (1 x 100 mL). The aqueous layers were combined and back-extracted with EtOAc (100 mL). The organic layers were collected, dried over $MgSO_4$, filtered and concentrated under reduced pressure to yield **18** (1.93 g, 9,47 mmol, 95%) as a white solid. **TLC** (PE/EtOAc 3:2 + 1% AcOH): R_f = 0.34. **^{1}H-NMR** (500 MHz, CD_3OD): δ [ppm] = 8.33 (d, *J* = 7.9 Hz, 2H), 8.18 (d, *J* = 8.3 Hz, 2H). **^{19}F NMR** (471 MHz, CD_3OD): δ [ppm] = 63.37.

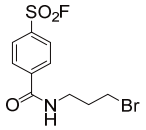

4-((3-Bromopropyl)carbamoyl)benzenesulfonyl fluoride (19)
3-bromopropylamine hydrobromide (2.18 g, 10.0 mmol, 1.3 eq) and PyBrop (4.26 g, 9.1 mmol, 1.2 eq) were added to a solution of **18** (1.55 g, 7.6 mmol, 1 eq) in anhydrous DMF (1 mL) under N_2. DiPEA (2.7 ml, 15.0 mmol, 2 eq) was added dropwise and the mixture was stirred at room temperature. After 3 days of stirring, TLC indicated starting material to be still present. Therefore an additional 0.6 eq of PyBrop (2,13 g, 4.6 mmol) and 1 eq of DiPEA (1.3 mL, 7.6 mmol) were added and the mixture was stirred for another 9 days at rt. The mixture was then diluted with EtOAc (350 mL) and the organic layer was washed brine (350 mL) and water (2 x 350 mL), dried over MgSO4, filtrated and concentrated under reduced pressure. The residue was purified by flash column chromatography (PE/EtOAc 2:1) to yield **19** (1.00 g, 3.1 mmol, 41%) as a white solid. **TLC** (PE/EtOAc 2:1): R_f = 0.57. **^{1}H NMR** (400 MHz, $CDCl_3$): δ [ppm] = 8.10 (d, *J* = 8.5 Hz, 2H), 8.01 (d, *J* = 8.0 Hz, 2H), 6.45 (s, 1H), 3.68 (q, *J* = 6.5 Hz, 2H), 3.51 (t, *J* = 6.3 Hz, 2H), 2.25 (p, *J* = 6.5 Hz, 2H). **^{19}F NMR** (471 MHz, CDCl3): δ [ppm] = 65.75.

Biology

Cell lines
Chinese hamster ovary (CHO) cells stably expressing the human adenosine A_1 receptor ($CHOhA_1AR$) were kindly provided by Prof. S.J. Hill (University of Nottingham, UK). Human embryonic kidney 293 cells stably expressing the human adenosine A_{2A} receptor ($HEK293hA_{2A}AR$) were kindly provided by Dr. J. Wang (Biogen/IDEC, Cambridge, MA). CHO-spap cells stably expressing the wildtype (WT) hA_{2B} receptor ($CHO\text{-}spap\text{-}hA_{2B}AR$) were kindly provided by S.J. Dowell (Glaxo Smith Kline, UK). CHO cells stably expressing the human adenosine A_3 receptor ($CHOhA_3AR$) were a kindly provided by Dr. K.N. Klotz (University of Würzburg, Germany).

Radioligands
[^{3}H]1,3-dipropyl-8-cyclopentyl-xanthine ([^{3}H]DPCPX, specific activity 137 Ci/mmol) and [^{3}H]4-(-2-[7-amino-2-(furan-2-yl)-[1,2,4]triazolo[1,5-a][1,3,5]triazin-5-ylamino)ethyl) phenol ([^{3}H]-ZM241385, specific activity 50 Ci/mmol) were purchased from ARC Inc. (St. Louis, USA). [^{3}H]8-(4-(4-(4-Chlorophenyl)piperazide-1-sulfonyl)phenyl)-1-propylxanthine ([^{3}H]PSB-603, specific activity 79 Ci/mmol) was purchased from Quotient Bioresearch. [^{3}H]8-Ethyl-4-methyl-2-phenyl-(8R)-4,5,7,8-tetrahydro-1H-imidazo[2,1-i]-purin-5-one ([^{3}H]PSB-11, specific activity 56 Ci/mmol) was obtained with the kind help of Prof. C.E. Müller (University of Bonn, Germany). [^{35}S]-guanosine 5'-(γ-thio)triphosphate ([^{35}S]GTPγS, specific activity 1250 Ci/mmol) was purchased from PerkinElmer.

Chemicals
5'-N-ethylcarboxamidoadenosine (NECA), N6-Cyclopentyladenosine (CPA) and adenosine deaminase (ADA) were purchased from Sigma Aldrich. 4-(-2-[7-amino-2-(furan-2-yl)-[1,2,4]triazolo[1,5-a][1,3,5]triazin-5-ylamino)ethyl) phenol (ZM241385) was a gift from Dr. S.M. Poucher (Astra Zeneca, Manchester, UK). 3-[4-[2-[[6-amino-9-[(2R,3R,4S,5S)-5-(ethylcarbamoyl)-3,4-dihydroxy-oxolan-2-yl]purin-2-yl]amino]ethyl]phenyl] propanoic acid (CGS21680) was purchased from Ascent Scientific (Bristol, UK). Bongkrekic acid was obtained from Enzo Life Sciences (cat # BML-CM113). Protease inhibitor cocktail was purchased from Sigma Aldrich (cat # p8340). Bicinchoninic acid (BCA) protein assay reagents were obtained

from Pierce Chemical Company (Rockford, IL, USA).[61] AF647-N_3 was obtained from Jena Bioscience, Azide-Fluor-545 and Biotin-PEG3-Azide were ordered from Sigma Aldrich. Pierce™ Avidin agarose beads (cat # 11846734) and Pierce™ ECL Western Blotting Substrate (cat # 32209) were ordered from Thermo Scientific. All other chemicals were of analytical grade and obtained from standard commercial sources.

Biologicals

Collagenase type I was purchased from Sigma Aldrich (Cat # C0130), PNGase was purchased from Promega (cat # V4831), Chymotrypsin was ordered from Promega (cat # V1062) and Enolase digest was ordered from Waters (cat # 186002325). RabbitαratA$_1$AR antibody was ordered from Sigma Aldrich (cat # A268) and goatαrabbit-HRP antibody was purchased from Jackson ImmunoResearch Laboratories (cat # 115-035-003). Bovine Serum Albumin (BSA) was purchased from Acros Organics (cat # 268131000).

Fat pads

Gonadal fat pads from female mice were kindly donated by prof. Patrick C.M. Rensen and dr. Milena Schönke and obtained from APOE*3-Leiden.CETP mice (C57Bl/6J background). Mice were between 28 and 34 weeks old and 19.9-25.3 g at the time of sacrifice. All mouse experiments were performed in accordance with the Institute for Laboratory Animal Research Guide for the Care and Use of Laboratory Animals after approval from the Central Animal Experiments Committee ("Centrale Commissie Dierproeven").

Cell culture and membrane preparation

CHO cells were grown in Dulbecco's Modified Eagle's Medium (DMEM) and Ham's F12 medium (1:1) supplemented with 10% (v/v) newborn calf serum 50 µg/mL streptomycin, 50 IU/mL penicillin and 5% CO_2. CHO cells were subcultured twice a week at a ratio of 1:15 on 10 cm Ø plates. CHOhA$_1$AR and CHOhA3AR cells were grown in DMEM and Ham's F12 medium (1:1) supplemented with 10% (v/v) newborn calf serum, 50 µg/mL streptomycin, 50 IU/mL penicillin, and 200 µg/mL G418 at 37 °C and 5% CO_2. CHOhA$_1$AR cells were subcultured twice a week at a ratio of 1:20 on 10 cm Ø plates. CHOhA$_3$AR cells were subcultured twice a week at a ratio of 1:8 on 10 cm Ø plates. HEK293hA$_{2A}$AR cells were grown in culture medium consisting of DMEM supplemented with 10% newborn calf serum, 50 µg/mL streptomycin, 50 IU/mL penicillin, and 500 µg/mL G418 at 37 °C and 7% CO_2. Cells were subcultured twice a week at a ratio of 1:8 on 10 cm Ø plates. CHO-spap-hA2BR cells were grown in DMEM and Ham's F12 medium (1:1) supplemented with 10% (v/v) newborn calf serum, 100 µg/mL streptomycin, 100 IU/mL penicillin, 1 mg/mL G418, and 0.4 mg/mL hygromycin at 37 °C and 5% CO_2. Cells were subcultured twice a week at a ratio of 1:20 on 10 cm Ø plates.

All cells were grown to 80-90% confluency and detached from plates by scraping them into 5 mL PBS. Detached cells were collected and centrifuged (5 min, 200 G). The supernatant was removed and the pellets were resuspended in cold Tris-HCl buffer, pH 7.4. A Heidolph Diax 900 homogenizer was used to homogenize the cell suspension. Membranes and the cytosolic fraction were separated by centrifugation in a Beckman Optima LE-80 K ultracentrifuge (Beckman Coulter, Fullerton, CA) (20 min, 100 000 G, 4 °C). The pellet was resuspended in Tris-HCl buffer, and homogenization and centrifugation steps were repeated. Tris-HCl buffer was used to resuspend the pellet, and ADA was added (0.8 U/mL) to break down endogenous adenosine. Membranes were stored in 250 µL and 500 µL aliquots at -80 °C. Total protein concentrations were measured using the BCA method.

Preparation of adipocyte membranes from mouse gonadal fat pads[58,62,63]

Gonadal fat pads of 6 mice were placed into a 10 Ø petri dish containing Krebs-Ringer-HEPES (KRH) buffer (100 mM NaCl, 4.7 mM KCl, 2.5 mM $CaCl_2$, 3.6 mM $NaHCO_3$, 1.19 mM $MgSO_4$, 1.18 mM KH_2PO_4, 5 mM dextrose, 5 mM pyruvic acid, 1 mM ascorbic acid and 5 mM HEPES (pH 7.4) containing 1% fatty acid free BSA (Tebu-Bio). The fat pads were minced with scissors, added to a 50 mL centrifuge tube and KRH buffer was added to a final volume of 46 mL. 50 mg Collagenase type I and 2 µM nicotinic acid in 4 mL KRH buffer were added and the mixture was digested for 1 h at 37 °C.[64] The resulting mixture was poured through a 200 µm cell strainer (pluriSelect Life Science) that was put onto a new 50 mL centrifuge tube. The filtrate was centrifuged (1 min, 400 G) and subsequently left for 5 min, upon which the adipocytes floated on top of the solution. The infranatant was removed and the adipocyte layer (±5 mL) was washed by addition of 45 mL KRH buffer and repetition of the centrifugation and floatation steps. The remaining 5 mL of adipocytes was dissolved in 45 mL of homogenization buffer (0.25 M sucrose, 1 mM EDTA and 10 mM Tris-HCl (pH 7.4)), put on ice and homogenized by 20 up-and-down strokes of a motor-driven pestle (700 rpm). The homogenate was kept cold and centrifuged (30 min, 15 000 G, 4°C). The upper fat layer (45 mL) was transferred to a new 50 mL centrifuge tube, homogenization buffer (5 mL) was added and the homogenization steps were repeated twice, yielding three supernatant fractions in total. The supernatant fractions were combined and centrifuged (30 min, 15 000 G, 4 °C) to pellet the membranes. The supernatant was removed and the pellet was redissolved in assay buffer (50 mM Tris-HCl, pH 7.4). Adipocyte membranes from mice typically contain about 0.5-2 pmol of adenosine A_1 receptor per mg of membrane protein.[58]

Radioligand displacement assays

Single point radioligand displacement experiments were performed using 1 µM of competing ligand, full curve radioligand displacement experiments were performed using a concentration range of competing ligand, ranging from 10^{-11} to 10^{-6} M. Experiments were carried out using 1.6 nM [^{3}H]DPCPX for CHOhA_1AR, 5.5 nM [^{3}H]ZM241385 for HEK293hA_{2A}AR, 1.5 nM [^{3}H]PSB-603 for CHO-spap-h_{A2B}AR, and 10 nM [^{3}H]PSB11 for CHOhA_3AR. Nonspecific binding was determined in the presence of 100 µM CPA for CHOhA_1AR, 100 µM NECA for HEK293hA_{2A}AR and CHOhA_3AR, and 10 µM ZM241385 for CHO-spap-hA_{2B}AR. Competing ligand (50 µL) and radioligand (50 µL) were co-incubated with membrane aliquots containing the respective receptor. Membrane aliquots containing 5 µg (CHOhA_1AR) total protein were incubated in a total volume of 100 µL assay buffer (50 mM Tris-HCl, pH 7.4) at 25 °C for 1 h. Membrane aliquots containing 30 µg (HEK293hA_{2A}AR) total protein were incubated in a total volume of 100 µL assay buffer (50 mM Tris-HCl, pH 7.4) at 25 °C for 1 h. Membrane aliquots containing 30 µg (CHO-spap-hA_{2B}R) total protein were incubated in a total volume of 100 µL assay buffer (0.1% CHAPS in 50 mM Tris-HCl, pH 7.4) at 25 °C for 2 h. Membrane aliquots containing 15 µg (CHOhA_3AR) total protein were incubated in a total volume of 100 µL assay buffer (50 mM Tris-HCl, 10 mM $MgCl_2$, 1mM EDTA, 0.01% (w/v) CHAPS, pH 8.0) at 25 °C for 2 h. During full curve displacement experiments, CHOhA_1AR membranes and competing ligand were pre-incubated for either 0 or 4 h at 25 °C, prior to addition of radioligand and subsequent co-incubation. Incubations were terminated by rapid vacuum filtration to separate the bound and free radioligand through prewetted 96-well GF/B filter plates using a PerkinElmer Filtermate-harvester (PerkinElmer). Filters were subsequently washed 12 times with ice-cold wash buffer: 50 mM Tris-HCl, pH 7.4 for CHOhA_1AR and HEK293hA_{2A}AR; 0.1% BSA in 50 mM Tris-HCl, pH 7.4 for CHO-spap-hA_{2B}AR; and 50 mM Tris-HCl, 10 mM $MgCl_2$, 1mM EDTA, pH 8.0 for CHOhA_3AR. The plates were dried at 55 °C after which MicroscintTM-20 cocktail was added (PerkinElmer). After 3 h the filter-bound radioactivity was determined by scintillation spectrometry using a 2450 MicroBeta Microplate Counter (PerkinElmer).

Wash-out assay

Wash-out assays were performed as previously described, using 100 µg of protein in 100 µL cell membrane suspension.[16]

Functional [^{35}S]GTPγS binding assay

[^{35}S]GTPγS binding assays were performed as previously described, using CHO cells that were stably transfected with the A_1AR.[16]

Data Analysis

All experimental data were analyzed using the non-linear regression curve fitting program GraphPad Prism 7.0 (GraphPad Software Inc., San Diego, CA). IC_{50} values obtained from competition displacement binding data were converted into K_i values using the Cheng-Prusoff equation.[65] The K_D value of [^{3}H]DPCPX (1.6 nM) at CHOhA_1AR membranes was taken from Kourounakis *et al*.[66] The K_D value (1.0 nM) of [^{3}H]ZM241385 at hA_{2A}AR membranes, the K_D value (1.7 nM) of [^{3}H]PSB603 at CHO-spap-hA_{2B}AR membranes, and the K_D value (17.3 nM) of [^{3}H]PSB11 at CHOhA_3AR membranes were taken from in-house determinations.

SDS-PAGE experiments of LUF7909 in membrane fractions

18 µL of membrane fractions (1 mg/mL) were pre-incubated with 1 µL competing ligand (final concentration: 1 µM, unless stated otherwise) or DMSO (1%) for 1 h (rt, 650 rpm). 1 µl of LUF7909 was added (final concentration: 100 nM, unless stated otherwise) and the membranes were incubated for 1 h (rt, 650 rpm). 1 µL PNGase (10u) or MilliQ water was added and the membranes were incubated for 1 h (rt, 650 rpm). Click mix was prepared freshly by mixing 50 µL 100 mM $CuSO_4$, 30 µL 1 M sodium ascorbate (NaAsc), 10 µL 100 mM tris(3-hydroxypropyltriazolylmethyl)amine (THPTA) and 10 µL 100 µM AF647-N_3. 2.3 µL of click mix was added and the membranes were shaken for 1 h (rt, 650 rpm). 7.8 µL of 4 x Laemmli Sample Buffer (Bio-Rad) containing β-mercaptoethanol was added and the membranes were shaken for 2 h (rt, 650 rpm). The samples were then subjected to 12.5% SDS-PAGE (180 V, 100 min). In-gel fluorescence was measured on a Bio-Rad Universal Hood III using Cy3 (605/50 filter) or Cy5 (695/55 filter) settings. Gels were transferred to 0.2 µm PVDF blots using a Trans-Blot Turbo Transfer System (Bio-Rad)(2.5 A, 7 min) or stained with Coomassie Brilliant Blue. Gel images were analyzed with Image Lab software (Bio-Rad).

SDS-PAGE experiments of LUF7909 in live CHOhA_1AR and CHO cells

CHOhA_1AR or CHO medium (as described above) containing 1 µM DPCPX or 1% DMSO (control) was added to a 10 cm Ø plate containing the respective cells (~90% confluence). The cells were incubated for 1 h (37 °C, 5% CO_2). The medium was removed, replaced by medium containing 100 nM LUF7909 or 1% DMSO (control) and the cells were incubated for 1 h (37 °C, 5% CO_2). The cells were washed with PBS and membranes were collected (as described above). Membrane pellets were diluted to 1 mg/mL and 20 µL was taken per sample. Click mix was prepared freshly by mixing 50 µL 100 mM $CuSO_4$, 30 µL 1 M NaAsc, 10 µL 100 mM THPTA and 10 µL 100 µM AF647-N_3. 2.2 µL of click mix was added and the membranes were shaken for 1 h (rt, 650 rpm). 7.4 µL of 4 x Laemmli Sample Buffer containing β-mercaptoethanol was added and the membranes were shaken for 2 h (rt, 650 rpm). The samples were then subjected to 12.5% SDS-PAGE (180 V, 100 min) and in-gel fluorescence was measured on a Bio-Rad Universal Hood III. Gels were transferred to 0.2 µm PVDF blots using a Trans-Blot Turbo Transfer System (Bio-Rad)(2.5 A, 7 min) or stained with Coomassie Brilliant Blue. Gel images were analyzed with Image Lab software (Bio-Rad).

Western Blot experiments

Blots were blocked in 5% BSA in TBST (1 h, rt), prior to incubation with primary antibody: rabbitαratA_1AR (Sigma Aldrich, cat # A268) 1:5000 in 1% BSA in TBST (overnight, 4 °C). The blots were washed (3 x TBST) and incubated with secondary antibody: goatαrabbit-HRP (Jackson ImmunoResearch Laboratories, cat # 111-035-003) 1:2000 in 1% BSA in TBST. The blots were washed (2 x TBST, 1 x TBS), incubated with 1 mL of luminol enhancer solution and 1 mL of peroxide solution (Pierce™, ThermoFisher cat # 32106)(3 min, rt, dark) and scanned using chemiluminescence and fluorescence. Blot images were analyzed with Image Lab software (Bio-Rad).

Affinity-based pull-down proteomics[67]

Probe Incubation

A. CHOhA_1AR and CHO membranes

CHOhA_1AR or CHO membrane fractions were resuspended in assay buffer (50 mM Tris-HCl, pH 7.4) and diluted to a concentration of 2 mg/mL. 25 µL of LUF7746 (final concentration: 10 µM), 10% SDS or 1% DMSO in assay buffer was added to 200 µL of membranes and the membranes were incubated for 1 h (rt, 650 rpm). 25 µL of LUF7909 (final concentration: 1 µM) or 1% DMSO in assay buffer was added and the membranes were incubated for 2 h (rt, 650 rpm).

B. Live CHOhA_1AR cells

CHOhA_1AR medium (as described above) containing 1 µM LUF7909 or 1% DMSO (control) was added to a 10 cm Ø plate containing CHOhA_1AR cells (~90% confluence). The cells were incubated for 2 h (37 °C, 5% CO_2). The medium was removed, the cells were washed with PBS and membranes were collected (as described above). Membrane pellets were diluted to 2 mg/mL, 225 µL was taken per sample and 25 µL of 1% DMSO in assay buffer (50 mM Tris-HCl, pH 7.4) was added.

Click reaction, precipitation, reduction and alkylation

Click mix was prepared freshly by mixing 350 µL 100 mM $CuSO_4$, 210 µL 1 M NaAsc, 70 µL 100 mM THPTA and 70 µL 1 mM Biotin-PEG3-Azide. 27.5 µL of click mix was added per sample (from A or B) and the samples were incubated for 1 h (rt, 650 rpm). 92.5 µL 10% SDS (final SDS concentration: 2.5%) was added and the proteins were denatured for 1 h (rt, 650 rpm). Proteins were precipitated based on the method of Wessel and Flügge.[68] In brief, 800 µL MeOH, 400 µL $CHCl_3$ and 400 µL water were added and the proteins were pelleted by centrifugation (10 min, 1 500 G, rt). The upper (aqueous) layer was removed and 600 µL MeOH was added. The samples were centrifuged a second time (10 min, 1 500 G, rt) and supernatant was removed to yield a more purified protein fraction. The proteins were then resuspended in 500 µL 1% SDS containing 25 mM NH_4HCO_3. Probe sonication (Sonics Vibra-Cell, 3 x 5 s, 30% amplitude) was necessary to fully dissolve the membrane proteins. The proteins were reduced by addition of 10 µL 0.5 M dithiothreitol (DTT) (15 min, 65 °C, 700 rpm), alkylated by addition of 80 µL 0.25 M iodoacetamide (IAA) (30 min, rt, dark) and further reduced by addition of 10 µL 0.5 M DTT (15 min, rt, 700 rpm).

Pull-down

1400 µL of Avidin Agarose beads was divided over two 15 mL centrifuge tubes, washed with PBS (4 mL) and centrifuged (2 min, 2 500 G, rt). The supernatant was removed and the washing steps were repeated twice. The washed beads were resuspended in 2.3 mL PBS. 250 µL of the beads solution was added per protein-containing sample and the mixture was added to a 15 mL centrifuge tube containing 9.1 mL PBS (final SDS concentration: 0.05%). The tubes were incubated overnight while rotating at 4 °C. The next day, beads were pelleted (200 G, 2 min, rt), supernatant was removed and the beads were transferred to a 2 mL Eppendorf tube. The beads were washed subsequently with 1 mL 0.1% SDS in PBS, 1 mL PBS (3 x) and 1 mL on-bead digestion buffer (100 mM Tris-HCl pH 8.0, 100 mM NaCl, 10 mM $CaCl_2$ and 2% (v/v) acetonitrile),[67] samples were centrifuged (2 min, 2 500 G, rt) after each step and supernatant fractions were removed.

Digestion and desalting

The remaining beads were dissolved in 250 µL on-bead digestion buffer. 2 µL chymotrypsin (0.5 µg/µL in 1 mM HCl) (cat # V1062, Promega) was added and the proteins were digested overnight (1000 rpm, 37 °C). The samples were quenched by addition of 12.5 µL of formic acid and beads were removed by centrifugation with Bio-spin columns (Bio-Rad) (2 min, 600 G, rt). Samples were purified using StageTips, as reported by Rappsilber *et al*. and van Rooden *et al*.[67,69] Briefly, StageTips were pre-conditioned with 50 µL MeOH, 50 µL of 0.5% (v/v) formic acid in H_2O:MeCN 2:8 and 50 µL of 0.5% (v/v) formic acid in H_2O. Peptide samples were then loaded on the StageTips and washed by addition of 100 µL of 0.5% (v/v) formic acid in H_2O and centrifugation (2 min, 600 G, rt). Peptides were eluted in low-binding Eppendorf tubes by addition of 0.5% (v/v) H_2O:MeCN 8:2 to the StageTips and subsequent centrifugation (2 min, 600 G, rt). The solvents were evaporated in an Eppendorf Concentrator Plus (60 °C).

Nano-LC-MS Settings

Desalted peptide samples were reconstituted in 50 µl 97:3:0.1 solution (H2O, MeCN, FA) containing 10 fmol/µl yeast enolase digest. The desalted peptides solution was separated on an UltiMate 3000 RSLCnano system set in a trap-elute configuration with a nanoEase M/Z Symmetry C18 100Å, 5µm, 180µm x 20 mm (Waters) trap column for peptide loading/retention and nanoEase M/Z HSS C18 T3 100Å, 1.8µm, 75 µm x 250 mm (Waters) analytical column for peptide separation. The column was kept at 40°C in a column oven. Samples were injected on the trap column at a flow rate of 15 µl/min for 2 min with 99%A, 1%B eluent. The 85 min LC method, using mobile phase A (0.1% formic acid (FA) in ULC-MS grade water (Biosolve)) and mobile phase B (0.1% FA in ULC-MS grade acetonitrile (MeCN, Biosolve)) controlled by a flow sensor at 0.3µl/min with average pressure of 400-500 bar (5500-7000 psi), was programmed as gradient with linear increment to 1% B from t0 to t2 min, 5%B at t5 min, 22%B at t55, 40%B at t64, 90%B at t65 to t74 and 1%B at t75 to t85 min. The eluent was introduced by electro-spray ionization (ESI) via the nanoESI source (Thermo) using stainless steel Nano-bore emitters (40 mm, OD 1/32", ES542, Thermo Scientific). The QExactive HF was operated in positive mode with data dependent acquisition without the use of lock mass, default charge of 2+ and external calibration with LTQ Velos ESI positive ion calibration solution (88323, Pierce, Thermo) every 5 days to less than 2 ppm. The tune file for the survey scan was set to scan range of 350 – 1400 m/z, 60.000 resolution (m/z 200), 1 microscan, automatic gain control (AGC) of 1e6, max injection time of 50 ms, no sheath, aux or sweep gas, spray voltage ranging from 1.7 to 3.0 kV, capillary temp of 250°C and an S-lens value of 80. For the 10 data dependent MS/MS events the loop count was set to 10 and the general settings were resolution to 15,000, AGC target 1e5, max IT time 100 ms, isolation window of 1.6 m/z, no fixed first mass and normalized collision energy (NCE) of 28 eV. For individual peaks the data dependent

settings were 5.00e4 for the minimum AGC target yielding an intensity threshold of 5.0e5 that needs to be reached prior of triggering an MS/MS event. No apex trigger was used, unassigned, +1 and charges >+8 were excluded with peptide match mode preferred, isotope exclusion on and dynamic exclusion of 20 sec. In between experiments, routine wash and control runs were done by injecting 5 µl 97.3.0.1 solution, 5 µl of 10 fmol/µl BSA or enolase digest and 1 µl of 10 fmol/µl angiotensin III (Fluka, Thermo)/oxytocin (Merck) to check the performance of the platform on each component (nano-LC, the mass spectrometer (mass calibration/quality of ion selection and fragmentation) and the search engine).

LC-MS/MS Data processing

MaxQuant (version 1.6.17.0)[70] was used for peptide identification and quantification using a custom made fasta file consisting of the Chinese Hamster proteome from the Uniprot database (UPID: UP000001075, downloaded January 12, 2021), the BETAS background (BSA P02769, yeast enolase P00924, trypsin pig P00761, avidin P02701 and streptavidin P22629) and the adenosine A_1 receptor plus its isoform (P30542-1 and P30542-2). The following changes and additions were made to the standard settings of MaxQuant: The digestion enzyme was set to Chymotrypsin+ with 2 max. missed cleavages. Label-free quantification was chosen with an LFQ min. ratio count of 2. “Match between runs” was enabled. The minimum amount of peptides for protein identification was set to 3. The peptide length was set to be between 7 and 25 with a max. peptide mass of 4600 Da. Oxidation (M) was set as possible peptide modifications and Carbamidomethyl (C) was set as fixed peptide modification. Contaminants were included. An FDR of 0.01 was used for PSM FDR, Protein FDR and Site decoy FDR. Six technical replicates of four different conditions were analyzed in the same MaxQuant analysis. The “peptides.txt” and “proteingroups.txt” files were used for further analysis. Proteins labelled as contaminant were removed from the output files. The LFQ intensities of major proteins were further analyzed in GraphPad Prism 8.1.1. for Windows (GraphPad Software Inc., San Diego, CA). Values of six technical replicates were used per condition. The log_2(ratio) and p-values were determined by standard Volcano Plot settings, using multiple t-tests to calculate the p-values. Log_2(ratio) values show the ratio between the probe positive samples (+1 µM LUF7909) and the control samples (DMSO, or pre-incubation with 1%SDS or 10 µM LUF7746).

Click microscopy experiments using LUF7909 in CHOhA$_1$AR and CHO cells[71]

CHOhA$_1$AR and CHO cells were seeded in 96-wells plates and grown overnight in their respective medium (as described above). The next day, medium was replaced by medium containing 1 µM of DPCPX, 1 µM of FSCPX or 1% DMSO (control) and the cells were incubated for 1 h (37 °C, 5% CO_2). The medium was then replaced by medium containing 100 nM LUF7909 or 1% DMSO (control) and the cells were incubated for 1 h (37 °C, 5% CO_2). Excess probe was washed away with PBS and the cells were fixed by incubation with a solution of 4% PFA in 10% formalin for 10 min. The remaining fixative was washed away with PBS and 20 mM glycine in PBS and subsequently the cells were permeabilized by a 10 min incubation with 0.1% saponin in PBS. Remaining saponin was washed away with PBS and the fixed cells were stored at 4 °C until further steps were taken. Click mix was prepared freshly by mixing 100 µL 100 mM $CuSO_4$, 100 µL 1 M NaAsc, 100 µL 100 mM THPTA, 9.66 mL HEPES buffer (pH = 7.4) and 40 µL 1 mM Azide-Fluor-545. 100 µL of click mix was added per well and the fixed cells were incubated for 1 h (rt, dark). Remaining click mix was washed away with PBS and by incubation for 30 min with 1% BSA in PBS. The fixed cells were stored in PBS containing 300 nM DAPI until imaging by confocal microscopy.

Image acquisition

Microscopy was performed on a Nikon Eclipse Ti2 C2+confocal microscope (Nikon, Amsterdam, The Netherlands) and this system included an automated xy-stage, an integrated Perfect Focus System (PFS) and 408 and 561 lasers. The system was controlled by Nikon's NIS software. All images were acquired using a 20x objective with 0.7 NA, at a resolution of 1024×1024 pixels for the main figure and 512x512 pixels for the SI figure. The acquisition of 9 fields of view per well was done automatically using the NIS Jobs functionality. Representative images are shown in the figure and created by using OMERO.[57]

Quantification of the Tamra-N_3 signal at single cell level

CellProfiler (version 2.2.0) was used to create a binary image of the Dapi channel and to propagate the cytoplasmic area based on the Dapi binary. An overlay of the binary cytoplasm/Tamra-N_3 channel was generated to quantify per segmented pixel the Tamra-N_3 intensity. The sum of these intensities in the cytoplasm mask is referred to as the integrated Tamra-N_3 intensity in the cytoplasm. Segmentation results were further processed using Excel while GraphPadPrism 9 was used for data visualization and statistics.

Computational Procedures

Covalent Docking of LUF7909 in the adenosine A_1 receptor

All calculations were performed in the Schrödinger Suite (release 2019-1) using the standard settings in Maestro (version 11.9).[59] The crystal structure of adenosine-bound human A_1AR (PDB: 6D9H) was used for docking LUF7909. The protein and ligand were prepared for docking using the protein preparation tool and LigPrep tool, respectively. Adenosine was removed and induced fit docking was performed to dock LUF7909. Docking poses were compared to the binding pose of LUF5833 in the human A_{2A}AR (PDB: 7ARO) using the superposition tool. The pose with the lowest scoring RMSD was further used in covalent docking calculations.[60] A custom reaction type was made to allow nucleophilic substitution of the phenolic OH onto the fluorosulfonyl group. This contained the following lines of code:

```
RECEPTOR_SMARTS_PATTERN 2,[c;r6]-[S,O;H1,-1]
RECEPTOR_SMARTS_PATTERN 2,[C]-[N;H2,H3]
LIGAND_SMARTS_PATTERN 1,[*][F,Cl,Br,I]
CUSTOM_CHEMISTRY ("<1>",("charge",0,(1)))
CUSTOM_CHEMISTRY ("<1>|<2>",("bond",1,(1,2)))
CUSTOM_CHEMISTRY ("<2>[F,Cl,Br,I]",("delete",2))
```

The covalent binding poses of LUF7909 were compared to the binding pose of LUF5833 in the human A_{2A}AR using the superposition tool, as well as evaluated by visual inspection.

Author Contributions

B.L.H.B. and C.K. synthesized compounds. R.L. performed radioligand displacement experiments. B.L.H.B. performed SDS-PAGE experiments. B.L.H.B. performed molecular docking experiments. B.L.H.B. and B.I.F. performed MS-based pull-down experiments and carried out MS data analysis. B.L.H.B. and S.L.D. performed confocal microscopy experiments. S.L.D. carried out confocal microscopy data analysis. L.H.H., A.P.IJ. and D.v.d.E. supervised the project.

References

[1] B. B. Fredholm, A. P. IJzerman, K. A. Jacobson, J. Linden, C. E. Müller, Pharmacol Rev 2011, 63, 1–34.

[2] A. P. IJzerman, K. A. Jacobson, C. E. Müller, B. N. Cronstein, R. A. Cunha, Pharmacol Rev 2022, 74, 340–372.

[3] B. Allard, D. Allard, L. Buisseret, J. Stagg, Nat Rev Clin Oncol 2020, 17, 611–629.

[4] C. J. Draper-Joyce, R. Bhola, J. Wang, A. Bhattarai, A. T. N. Nguyen, I. Cowie-Kent, K. O'Sullivan, L. Y. Chia, H. Venugopal, C. Valant, D. M. Thal, D. Wootten, N. Panel, J. Carlsson, M. J. Christie, P. J. White, P. Scammells, L. T. May, P. M. Sexton, R. Danev, Y. Miao, A. Glukhova, W. L. Imlach, A. Christopoulos, Nature 2021, 597, 571–576.

[5] C. E. Müller, K. A. Jacobson, Biochim Biophys Acta 2011, 1808, 1290–1308.

[6] J. F. Chen, H. K. Eltzschig, B. B. Fredholm, Nat Rev Drug Discov 2013, 12, 265–286.

[7] Y. Yun, J. Chen, R. Liu, W. Chen, C. Liu, R. Wang, Z. Hou, Z. Yu, Y. Sun, A. P. IJzerman, L. H. Heitman, X. Yin, D. Guo, Biochem Pharmacol 2019, 164, 45–52.

[8] D. Meibom, B. Albrecht-Küpper, N. Diedrichs, W. Hübsch, R. Kast, T. Krämer, U. Krenz, H. G. Lerchen, J. Mittendorf, P. G. Nell, F. Süssmeier, A. Vakalopoulos, K. Zimmermann, ChemMedChem 2017, 12, 728–737.

[9] E. A. Vecchio, J. A. Baltos, A. T. N. Nguyen, A. Christopoulos, P. J. White, L. T. May, Br J Pharmacol 2018, 175, 4036–4046.

[10] C. K. Goth, U. E. Petäjä-Repo, M. M. Rosenkilde, ACS Pharmacol Transl Sci 2020, 3, 237–245.

[11] D. Wootten, A. Christopoulos, P. M. Sexton, Nat Rev Drug Discov 2013, 12, 630–644.

[12] K. A. Jacobson, Biochem Pharmacol 2015, 98, 541–555.

[13] A. S. Hauser, M. M. Attwood, M. Rask-Andersen, H. B. Schiöth, D. E. Gloriam, Nat Rev Drug Discov 2017, 16, 829–842.

[14] D. Weichert, P. Gmeiner, ACS Chem Biol 2015, 10, 1376–1386.

[15] X. Yang, L. H. Heitman, A. P. IJzerman, D. van der Es, Purinergic Signal 2021, 17, 85–108.

[16] X. Yang, M. A. Dilweg, D. Osemwengie, L. Burggraaff, D. van der Es, L. H. Heitman, A. P. IJzerman, Biochem Pharmacol 2020, 180, 114144.

[17] M. Jörg, P. J. Scammells, ChemMedChem 2016, 11, 1488–1498.

[18] A. Glukhova, D. M. Thal, A. T. Nguyen, E. A. Vecchio, M. Jörg, P. J. Scammells, L. T. May, P. M. Sexton, A. Christopoulos, Cell 2017, 168, 867-877.e13.

[19] E. Kozma, P. S. Jayasekara, L. Squarcialupi, S. Paoletta, S. Moro, S. Federico, G. Spalluto, K. A. Jacobson, Bioorg Med Chem Lett 2013, 23, 26–36.

[20] P. S. Jayasekara, K. Phan, D. K. Tosh, T. S. Kumar, S. M. Moss, G. Zhang, J. J. Barchi, Z. G. Gao, K. A. Jacobson, Purinergic Signal 2013, 9, 183–198.

[21] M. I. Bahamonde, J. Taura, S. Paoletta, A. A. Gakh, S. Chakraborty, J. Hernando, V. Fernández-Dueñas, K. A. Jacobson, P. Gorostiza, F. Ciruela, Bioconjug Chem 2014, 25, 1847–1854.

[22] J. Taura, E. G. Nolen, G. Cabré, J. Hernando, L. Squarcialupi, M. López-Cano, K. A. Jacobson, V. Fernández-Dueñas, F. Ciruela, Journal of Controlled Release 2018, 283, 135–142.

[23] D. Greenbaum, K. F. Medzihradszky, A. Burlingame, M. Bogyo, Chem Biol 2000, 7, 569–581.

[24] Y. Liu, M. P. Patricelli, B. F. Cravatt, Proceedings of the National Academy of Sciences 1999, 96, 14694–14699.

[25] H. S. Overkleeft, B. I. Florea, Activity-Based Proteomics: Methods and Protocols, 2017.

[26] K. J. Gregory, R. Velagaleti, D. M. Thal, R. M. Brady, A. Christopoulos, P. J. Conn, D. J. Lapinsky, ACS Chem Biol 2016, 11, 1870–1879.

[27] V. Garcia, A. Gilani, B. Shkolnik, V. Pandey, F. F. Zhang, R. Dakarapu, S. K. Gandham, N. R. Reddy, J. P. Graves, A. Gruzdev, D. C. Zeldin, J. H. Capdevila, J. R. Falck, M. L. Schwartzman, Circ Res 2017, 120, 1776–1788.

[28] M. Soethoudt, S. C. Stolze, M. V. Westphal, L. Van Stralen, A. Martella, E. J. Van Rooden, W. Guba, Z. V. Varga, H. Deng, S. I. Van Kasteren, U. Grether, A. P. IJzerman, P. Pacher, E. M. Carreira, H. S. Overkleeft, A. Ioan-Facsinay, L. H. Heitman, M. van der Stelt, J Am Chem Soc 2018, 140, 6067–6075.

[29] X. Yang, T. J. M. Michiels, C. de Jong, M. Soethoudt, N. Dekker, E. Gordon, M. van der Stelt, L. H. Heitman, D. van der Es, A. P. IJzerman, J Med Chem 2018, 61, 7892–7901.

[30] S. D. Hellyer, S. Aggarwal, A. N. Y. Chen, K. Leach, D. J. Lapinsky, K. J. Gregory, ACS Chem Neurosci 2020, 11, 1597–1609.

[31] P. N. H. Trinh, D. J. W. Chong, K. Leach, S. J. Hill, J. D. A. Tyndall, L. T. May, A. J. Vernall, K. J. Gregory, J Med Chem 2021, 64, 8161–8178.

[32] A. O. Helbig, A. J. R. Heck, M. Slijper, J Proteomics 2010, 73, 868–878.

[33] D. M. Rosenbaum, S. G. F. Rasmussen, B. K. Kobilka, Nature 2009, 459, 356–363.

[34] B. B. Fredholm, A. P. IJzerman, K. A. Jacobson, J. Linden, C. E. Müller, Pharmacol Rev 2011, 63, 1–34.

[35] E. A. Vecchio, J. A. Baltos, A. T. N. Nguyen, A. Christopoulos, P. J. White, L. T. May, Br J Pharmacol 2018, 175, 4036–4046.

[36] C. K. Goth, U. E. Petäjä-Repo, M. M. Rosenkilde, ACS Pharmacol Transl Sci 2020, 3, 237–245.

[37] O. Vit, J. Petrak, J Proteomics 2017, 153, 8–20.

[38] A. O. Helbig, A. J. R. Heck, M. Slijper, J Proteomics 2010, 73, 868–878.

[39] D. M. Rosenbaum, S. G. F. Rasmussen, B. K. Kobilka, Nature 2009, 459, 356–363.

[40] K. B. Rostovtsev, V. V., Green, L. G., Fokin, V. V. and Sharpless, Angew. Chem. Int. Ed. 2002, 41, 2596–2599.

[41] E. M. Sletten, C. R. Bertozzi, Acc Chem Res 2011, 44, 666–676.

[42] M. W. Beukers, L. C. W. Chang, J. K. von Frijtag Drabbe Künzel, T. Mulder-Krieger, R. F. Spanjersberg, J. Brussee, A. P. IJzerman, J Med Chem 2004, 47, 3707–3709.

[43] D. Guo, T. Mulder-Krieger, A. P. IJzerman, L. H. Heitman, Br J Pharmacol 2012, 166, 1846–1859.

[44] T. Amelia, J. P. D. van Veldhoven, M. Falsini, R. Liu, L. H. Heitman, G. J. P. van Westen, E. Segala, G. Verdon, R. K. Y. Cheng, R. M. Cooke, D. van der Es, A. P. IJzerman, J Med Chem 2021, 64, 3827–3842.

[45] H. Nakata, Journal of Biological Chemistry 1990, 265, 671–677.

[46] Z. Gao, A. S. Robeva, J. Linden, Biochemical Journal 1999, 338, 729–736.
[47] C. Blex, S. Michaelis, A. K. Schrey, J. Furkert, J. Eichhorst, K. Bartho, F. Gyapon Quast, A. Marais, M. Hakelberg, U. Gruber, S. Niquet, O. Popp, F. Kroll, M. Sefkow, R. Schülein, M. Dreger, H. Köster, ChemBioChem 2017, 18, 1639–1649.
[48] N. Sobotzki, M. A. Schafroth, A. Rudnicka, A. Koetemann, F. Marty, S. Goetze, Y. Yamauchi, E. M. Carreira, B. Wollscheid, Nat Commun 2018, 9, 1519.
[49] F. M. Müskens, R. J. Ward, D. Herkt, H. van de Langemheen, A. B. Tobin, R. M. J. Liskamp, G. Milligan, Mol Pharmacol 2019, 95, 196–209.
[50] R. Miyajima, K. Sakai, Y. Otani, T. Wadatsu, Y. Sakata, Y. Nishikawa, M. Tanaka, Y. Yamashita, M. Hayashi, K. Kondo, T. Hayashi, ACS Chem Biol 2020, 15, 2364–2373.
[51] M. Ma, S. Guo, X. Lin, S. Li, Y. Wu, Y. Zeng, Y. Hu, S. Zhao, F. Xu, X. Xie, W. Shui, ACS Chem Biol 2020, 15, 3275–3284.
[52] H. Muranaka, T. Momose, C. Handa, T. Ozawa, ACS Med Chem Lett 2017, 8, 660–665.
[53] A. J. Kooistra, S. Mordalski, G. Pándy-Szekeres, M. Esguerra, A. Mamyrbekov, C. Munk, G. M. Keserű, D. E. Gloriam, Nucleic Acids Res 2021, 49, D335–D343.
[54] P. J. F. Henderson, H. A. Lardy, Journal of Biological Chemistry 1970, 245, 1319–1326.
[55] M. Klingenberg, Biochim Biophys Acta Biomembr 2008, 1778, 1978–2021.
[56] E. C. Klaasse, A. P. IJzerman, W. J. de Grip, M. W. Beukers, Purinergic Signal 2008, 4, 21–37.
[57] C. Allan, J. M. Burel, J. Moore, C. Blackburn, M. Linkert, S. Loynton, D. MacDonald, W. J. Moore, C. Neves, A. Patterson, M. Porter, A. Tarkowska, B. Loranger, J. Avondo, I. Lagerstedt, L. Lianas, S. Leo, K. Hands, R. T. Hay, A. Patwardhan, C. Best, G. J. Kleywegt, G. Zanetti, J. R. Swedlow, Nat Methods 2012, 9, 245–253.
[58] H.-X. Liang, L. Belardinelli, M. J. Ozeck, J. C. Shryock, Br J Pharmacol 2002, 135, 1457–1466.
[59] Schrödinger LLC, Schrödinger Release 2019-1: Maestro, New York, 2019.
[60] K. Zhu, K. W. Borrelli, J. R. Greenwood, T. Day, R. Abel, R. S. Farid, E. Harder, Journal of Chemical Information and Modeling 2014, 54, 1932–1940.
[61] P. K. Smith, R. I. Krohn, G. T. Hermanson, A. K. Mallia, F. H. Gartner, M. D. Provenzano, E. K. Fujimoto, N. M. Goeke, B. J. Olson, D. C. Klenk, Analytical Biochemistry 1985, 150, 76–85.
[62] M. Rodbell, J Biol Chem 1964, 239, 375–380.
[63] D. W. McKeel, L. Jarett, Journal of Cell Biology 1970, 44, 417–432.
[64] A. Green, G. Milligan, S. B. Dobias, Journal of Biological Chemistry 1992, 267, 3223–3229.
[65] Y.-C. Cheng, W. H. Prusoff, Biochemical Pharmacology 1973, 22, 3099–3108.
[66] A. Kourounakis, C. Visser, M. de Groote, A. P. IJzerman, Biochemical Pharmacology 2001, 61, 137–144.
[67] E. J. van Rooden, B. I. Florea, H. Deng, M. P. Baggelaar, A. C. M. van Esbroeck, J. Zhou, H. S. Overkleeft, M. van der Stelt, Nature Protocols 2018, 13, 752–767.
[68] D. Wessel, U. I. Flügge, Analytical Biochemistry 1984, 138, 141–143.
[69] J. Rappsilber, M. Mann, Y. Ishihama, Nature Protocols 2007, 2, 1896–1906.
[70] J. Cox, M. Mann, Nature Biotechnology 2008, 26, 1367–1372.
[71] F. J. van Dalen, T. Bakkum, T. van Leeuwen, M. Groenewold, E. Deu, A. J. Koster, S. I. van Kasteren, M. Verdoes, Frontiers in Chemistry 2021, 8, 1–13.

Chapter 5

Development of an Affinity-Based Probe to Profile Endogenous Human Adenosine A_3 Receptor Expression

Bert L. H. Beerkens, Inge M. Snijders, Joep Snoeck, Rongfang Liu, Anton T. J. Tool, Sylvia E. Le Dévédec, Willem Jespers, Taco W. Kuijpers, Gerard J.P. van Westen, Laura H. Heitman, Adriaan P. IJzerman, and Daan van der Es

Abstract

The adenosine A_3 receptor (A_3AR) is a G protein-coupled receptor (GPCR) that exerts immunomodulatory effects in pathophysiological conditions such as inflammation and cancer. Thus far, studies towards the downstream effects of A_3AR activation have yielded contradictory results, thereby motivating the need for further investigations. Various chemical and biological tools have been developed for this purpose, ranging from fluorescent ligands to antibodies. Nevertheless, these probes are limited by their reversible mode of binding, relatively large size and often low specificity. Therefore, in this work, we have developed a clickable and covalent affinity-based probe (AfBP) to target the human A_3AR. Herein, we show validation of the synthesized AfBP in radioligand displacement, SDS-PAGE and confocal microscopy experiments, as well as utilization of the AfBP for the detection of endogenous A_3AR expression in flow cytometry experiments. Ultimately, this AfBP will aid future studies towards the expression and function of the A_3AR in pathologies.

J Med Chem **2023**, 66, 11399-11413.

Introduction

Adenosine is a signaling molecule that is the endogenous agonist to four adenosine receptors (ARs): the A_1, A_{2A}, A_{2B} and A_3 adenosine receptors (A_1AR, A_{2A}AR, A_{2B}AR and A_3AR) that are members of the larger G protein-coupled receptor (GPCR) family.[1–3] Activation of the ARs via binding of adenosine induces a cascade of intracellular signaling pathways, that in turn modulate the cellular response to physiological and pathophysiological conditions, examples being inflammation, autoimmune disorders and cancers.[4–6] The ARs are expressed on diverse cell and tissue types, in which the receptors all exert their own functions.[1] In case of the human A_3AR (hA_3AR), the receptor has been found expressed on granulocytes: eosinophils, neutrophils and mast cells, among other cell types.[7–10] Here, activation of the hA_3AR leads to various immunomodulatory effects, ranging from degranulation to influencing chemotaxis.[7–13] However, multiple contradictory observations have been reported regarding the activation of hA_3ARs. For example, both inhibition and promotion of chemotaxis have been observed upon addition of a selective hA_3AR agonist to neutrophils.[11,13,14] Next to that, expression of the hA_3AR is species-dependent, and large differences in hA_3AR activity have been found between humans and rodents.[15,16] Thus, many questions regarding activity and functioning of the hA_3AR, whether on granulocytes or on other cell types and tissues, remain unanswered.

Most of the aforementioned studies have been carried out using selective ligands, e.g. agonists or antagonists to induce a cellular response as read-out. This has yielded valuable information on a biological level but ignores multiple factors that influence receptor signaling on a molecular level, such as receptor localization, protein-protein interactions (PPIs) and post-translational modifications (PTMs).[17] Traditionally, these aspects would be studied using antibodies. However, antibodies for GPCRs are hindered in their selectivity due to the low expression levels of GPCRs and the high conformational variability of extracellular epitopes on GPCRs.[18] This is especially true for the ARs that are lacking an extended extracellular N-terminus.

In the past decade, multiple small molecules have been developed as tool compounds to study the hA_3AR on a molecular level. Most prominently developed are the fluorescent ligands: agonists or antagonists conjugated to a fluorophore.[19–28] Noteworthy, one of these fluorescent ligands has been used to study internalization, localization and certain PPIs of the hA_3AR on hA_3AR-overexpressing Chinese hamster ovary (CHO) cells, as well as activated neutrophils.[12,24] Yet, the current use of fluorescent ligands is limited to the type of fluorophore conjugated, a fluorescent read-out in specific assay types and reversible binding to the receptor. Therefore, in this study, we aimed to develop a clickable affinity-based probe (AfBP) to broaden the current possibilities to measure and detect the receptor.

AfBPs are tool compounds that consist of three parts. Firstly, an electrophilic group ('warhead') is incorporated, that ensures covalent binding of the AfBP to the receptor (Figure 1).[29,30] This allows usage of the probe in biochemical assays that rely on denaturation of proteins (e.g. SDS-PAGE and chemical proteomics). The warhead is coupled to a high affinity scaffold (the second part) that induces selectivity to the protein target of interest and thirdly, a detection moiety is introduced. Our lab has recently reported the development of electrophilic antagonist LUF7602 as an irreversible ligand of the hA_3AR (Figure S1).[31] This compound contains two out of three functionalities of an AfBP, the only part missing being the detection moiety. Here, we introduced an alkyne group as ligation handle, that can be 'clicked' to a detection moiety through the Copper-catalyzed Alkyne-Azide Cycloaddition (CuAAC).[32,33] Together this approach results in a 'modular' probe that can be clicked *in situ* to any detection moiety of interest. The new probe allows specific detection of overexpressed hA_3AR in various assay types, such as SDS-PAGE and confocal microscopy, as well as detection of endogenous hA_3AR in flow cytometry experiments on granulocytes.

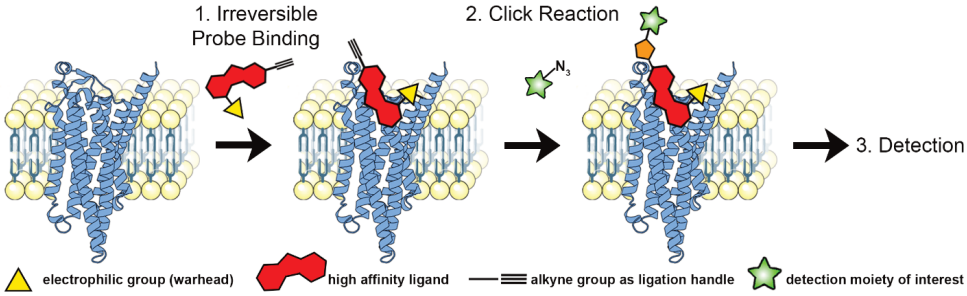

Figure 1. Strategy to label the hA_3AR with an AfBP. First, the AfBP is added to cells or membrane fractions to allow irreversible bond formation between receptor and probe. Click reagents are then added to install a detection moiety onto the probe-bound receptor. Lastly, cells are further processed for detection, dependent on the detection method of interest. The image of the hA_3AR was generated using Protein Imager,[34] using the structure of the hA_3AR (AF-P0DMS8-F1) as predicted by Alphafold.[35,36]

Results and Discussion

DESIGN AND SYNTHESIS

As mentioned in the introduction, a functional AfBP consists of three parts: warhead, pharmacological scaffold, and detection moiety. We decided on an alkyne moiety, to enable click-based incorporation of a detection moiety of choice onto the AfBP. Similar click strategies have already been used in the synthesis of fluorescent ligands for the hA_3AR.[20,21,26,27,37] These ligands are however all lacking the electrophilic warhead. Additionally, contrary to those studies, we mainly performed the click reaction after binding of the AfBP to the receptor, preventing a loss of affinity due to bulky substituents. Such an approach has recently successfully been applied for the detection of other adenosine receptors, namely the A_1AR and $A_{2A}AR$.[38–40] Also a non-selective AfBP for the hA_3AR has been reported, albeit without successful detection experiments.[38] In previous studies we observed that the position of the alkyne moiety on the scaffold can greatly influence the affinity of the AfBP towards the receptor, thereby affecting the functionality of the AfBP.[39] To increase the chances of obtaining a successful AfBP, we therefore introduced the alkyne group on three divergent locations onto the scaffold of LUF7602 (Scheme 1).

All three synthetic routes started with compound **1**, a high affinity selective antagonist for the hA_3AR reported over two decades ago.[41] First, **1** was alkylated with bromopropane yielding tricyclic compound **2**. The benzylic moiety was then removed using palladium over carbon and an excess of NH_4HCO_2.[31] The secondary amine of **3** was alkylated with alkyne-containing fluorosulfonyl moiety **4**, synthesized as recently described,[39] to yield compound **5** (LUF7930) as the first out of three AfBPs. For the second AfBP, the secondary amine of **3** was alkylated by a protected propylamine, followed by deprotection of the Boc-group to yield compound **7**. The methoxy group of **7** was removed using BBr_3, yielding a zwitterionic intermediate that, after removal of remaining BBr_3, was used immediately in a peptide coupling to synthesize fluorosulfonyl derivative **8**. The alkyne moiety was then substituted onto the phenolic OH to yield compound **9** (LUF7960) as the second out of three AfBPs. For the last AfBP, the benzyl group of compound **1** was removed in the first step. However, synthesis and purification of **10** turned out to be cumbersome. Therefore a crude mixture of **10** was used in the following alkylation step, resulting in a poor but sufficient yield of compound **11**. The alkyne moiety was then substituted onto compound **11** using propargyl bromide, followed by deprotection of the Boc-group to yield compound **12**. Lastly, fluorosulfonyl benzoic acid was introduced using peptide coupling conditions, yielding compound **13** (LUF7934) as the final out of three AfBPs.

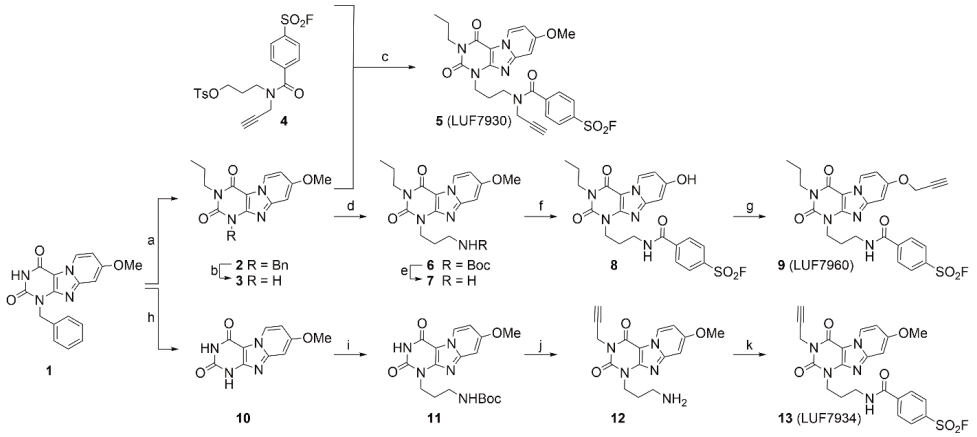

Scheme 1 Synthesis of hA$_3$AR-targeting affinity-based probes. Reagents and conditions: a) diazabicycloundecene (DBU), 1-bromopropane, MeCN, 70 °C, 1 h, quant.; b) Pd(OH)$_2$/C, NH$_4$HCO$_2$, EtOH, 80 °C, 7 days, 53%; c) K$_2$CO$_3$, DMF, rt, overnight, 29%; d) *tert*-butyl (3-bromopropyl)carbamate, K$_2$CO$_3$, DMF, 100 °C, 2 h, 97%; e) TFA, CHCl$_3$, 60 °C, overnight, 90%; f) (i) BBr$_3$ 1 M in DCM, CHCl$_3$, 50 °C, 6 days; (ii) 4-fluorosulfonyl benzoic acid, EDC·HCl, DIPEA, DMF, rt, two days, 13% over two steps; g) propargyl bromide (80% in toluene), K$_2$CO$_3$, DMF, rt, overnight, 30%; h) Pd(OH)$_2$/C, NH$_4$HCO$_2$, EtOH, 80 °C, 7 days; i) *tert*-butyl (3-bromopropyl)carbamate, K$_2$CO$_3$, DMF, 0-40 °C, 6 days, 25%; j) (i) propargyl bromide (80% in toluene), DBU, MeCN, rt, overnight; (ii) TFA, DCM, rt, 2 h, 67%; k) 4-fluorosulfonyl benzoic acid, EDC·HCl, DIPEA, DMF, rt, 3 h, 13%.

AFFINITY AND SELECTIVITY TOWARDS THE hA$_3$AR

The affinity of the synthesized AfBPs was determined in radioligand binding experiments. First, single concentration displacement assays were carried out on all four human adenosine receptors, using a final probe concentration of 1 µM (Table 1). Over 90% displacement was observed on the hA$_3$AR, while all probes showed minimal displacement (≤25%) of radioligand on the other ARs. This indicates good selectivity towards the hA$_3$AR over the other human ARs, a trend that was also observed in case of the parent compound.[31] Next, the 'apparent' affinities (depicted as pK_i values) towards the hA$_3$AR were determined using full curve displacement assays. To study the presumable covalent mode of action, the apparent affinity was determined with (pre-4h) and without (pre-0h) four hours of pre-incubation of AfBP with hA$_3$AR, prior to addition of radioligand. The three synthesized AfBPs show very similar affinities at pre-0h with apparent pK_i values in the double digit nanomolar range (Table 2). In all three cases, the apparent pK_i shows a strong increase upon 4 h of pre-incubation, towards values in the single digit nanomolar range. This difference in affinity is reflected in a shift in apparent pK_i. Hence, substitution of an alkyne moiety at all three of the divergent positions is well tolerated in case of binding affinity. To investigate the binding mode of the probes within the orthosteric binding pocket, covalent docking experiments were performed using the previously determined nucleophile Y265 as anchor (Figure 2).[31] All three compounds show a hydrogen bond interaction with the conserved N250 and π-π stacking with Phe168, two well-known interactions in ligand recognition in adenosine receptors.[42] Thus, the alkyne substitution seems to be well tolerated for all three of the probes, thereby supporting the outcome of the radioligand displacement experiments. To further confirm the covalent mode of action, wash-out experiments were performed. Compounds **5**, **9** and **13** all showed to bind persistently to the hA$_3$AR, while full recovery of radioligand binding was observed in case of the reversible control compound LUF7714 (Figure 3, Figure S1).[31] Altogether, this indicates that the three synthesized AfBPs bind covalently to the hA$_3$AR.

Table 1. Radioligand displacement (%) of the synthesized hA_3AR probes on the four adenosine receptors.

Compound	hA_1AR[a]	$hA_{2A}AR$[b]	$hA_{2B}AR$[c]	hA_3AR[d]
5 (LUF7930)	2 (3, 0)	0 (0, 0)	10 (22, -2)	95 (96, 94)
9 (LUF7960)	21 (24, 18)	7 (11, 2)	1 (0, 2)	95 (94, 96)
13 (LUF7934)	25 (24, 26)	8 (9, 7)	5 (4, 5)	92 (90, 93)

[a] % specific [^{3}H]DPCPX displacement by 1 μM of respective probe on CHO cell membranes stably expressing the human A_1AR (hA_1AR); [b] % specific [^{3}H]ZM241385 displacement by 1 μM of respective probe on HEK293 cell membranes stably expressing the human $A_{2A}AR$ ($hA_{2A}AR$); [c] % specific [^{3}H]PSB-603 displacement by 1 μM of respective probe on CHO-spap cell membranes stably expressing the human $A_{2B}AR$ ($hA_{2B}AR$); [d] % specific [^{3}H]PSB-11 displacement at 1 μM of respective probe on CHO cell membranes stably expressing hA_3AR. Probes were co-incubated with radioligand for 30 min at 25 °C. Data represent the mean of two individual experiments performed in duplicate.

Table 2. Time-dependent apparent affinity values of the synthesized hA_3AR probes.

Compound	pK_i (pre-0h)[a]	pK_i (pre-4h)[b]	Fold change [c]
5 (LUF7930)	7.55 ± 0.01	8.52 ± 0.05****	9.5 ± 1.0
9 (LUF7960)	7.27 ± 0.07	8.40 ± 0.03****	13.5 ± 1.2
13 (LUF7934)	7.17 ± 0.04	8.38 ± 0.05****	16.6 ± 3.5

[a] Apparent affinity determined from displacement of specific [^{3}H]PSB-11 binding on CHO cell membranes stably expressing the hA_3AR at 25 °C after 0.5 h of co-incubating probe and radioligand. [b] Apparent affinity determined from displacement of specific [^{3}H]PSB-11 binding on CHO cell membranes stably expressing the hA_3AR at 25 °C after 4 h of pre-incubation with the respective probe, followed by an additional 0.5 h of co-incubation with radioligand. [c] Fold change determined by ratio K_i(0 h)/K_i(4 h). Data represent the mean ± SEM of three individual experiments performed in duplicate. **** $p < 0.0001$ compared to the pKi values obtained from the displacement assay with 0 h pre-incubation of probe, determined by a one-way ANOVA test using multiple comparisons.

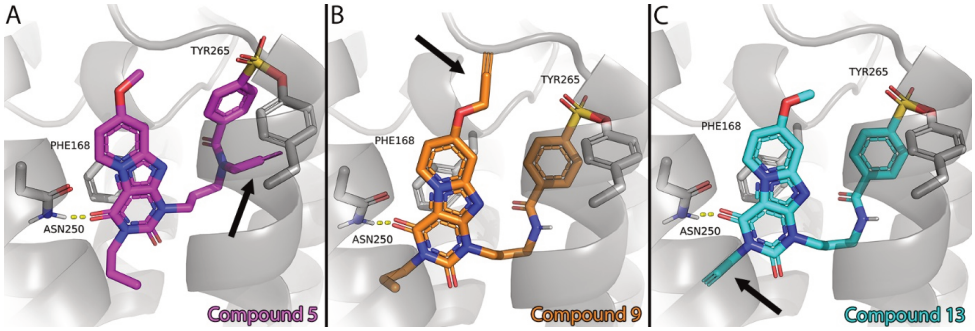

Figure 2. Putative binding modes of compounds 5 (panel A), 9 (panel B) and 13 (panel C). All three compounds show a hydrogen bond interaction with the conserved N250 and π-π stacking with Phe168, two well-known interactions in ligand recognition in adenosine receptors.[42] The alkyne group, indicated with an arrow in each panel, fits into the binding pocket on each exit vector, and the binding orientation of the core compound, as published previously by our group, is maintained.[31]

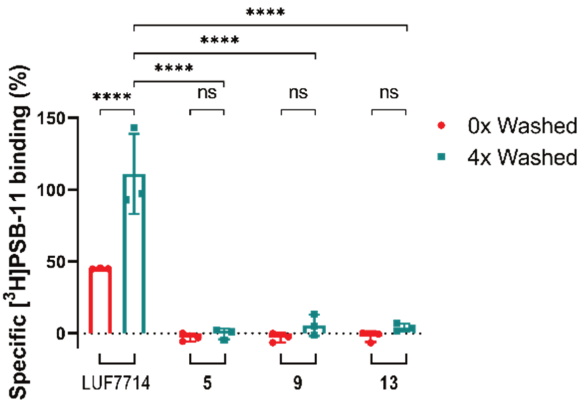

Figure 3. Wash-out assay reveals covalent binding of all three probes to the hA_3AR. CHO cells membranes stably transfected with the hA_3AR were pre-incubated with 1% DMSO (vehicle), 1 µM of non-covalent control compound (LUF7714) or 1 µM of compounds **5** (LUF7930), **9** (LUF7960) or **13** (LUF7934). The samples were washed for either 0 or 4 times, before being exposed to [^{3}H]PSB-11 in a radioligand displacement assay. Data is expressed as the percentage of the vehicle group (100%) and represents the mean ± SEM of three individual experiments performed in duplicate. **** $p < 0.0001$ determined by a two-way ANOVA test using multiple comparisons.

LABELING OF THE hA_3AR IN SDS-PAGE EXPERIMENTS

Next, the potential AfBPs were investigated on their ability to label the hA_3AR in SDS-PAGE experiments. Membrane fractions with stable expression of the hA_3AR were incubated for 1 h with 50 nM (roughly the apparent K_i) of AfBPs **5**, **9** or **13**, subjected to click ligation with a Cy5-fluorophore, denatured and resolved by SDS-PAGE. Pre-incubation with the hA_3AR-selective antagonist PSB-11 was used as negative control,[43] and an extra incubation step with PNGase was introduced to remove N-glycans.[39] Detection of labeled hA_3AR turned out to be difficult if not deglycosylated: the receptor appeared as a smear at about 70 kDa (Figure 4A and 5A). Yet, this mass corresponds to the band of rat A_3AR as has been shown in SDS-PAGE experiments on overexpressing CHO cells.[44,45] N-deglycosylation of the mixture of membrane proteins revealed a protein band at ±30 kDa in case of all three AfBPs. This protein was not labeled after pre-incubation with reversible antagonist PSB-11 and is therefore most likely the hA_3AR. To select one of these AfBPs for further labeling studies, the intensities of the bands at ±30 kDa were compared between the probes (Figure 4B), but no significant differences were found. Correspondingly, the alkyne groups do not inflict any strong unfavorable interactions upon covalent docking of the compounds in the hA_3AR model (Figure 2). Examination of the amount of off-target labeling instead indicated there are fewer other proteins labeled by **9** (LUF7960) than by the other two probes **5** and **13** (Figure 4A). Therefore we decided to continue our subsequent experiments with AfBP **9** (LUF7960). Further control experiments were performed: labeling in CHO membrane fractions without expression of the hA_3AR, no addition of probe and clicking without copper or Cy5-N_3 (Figure 4C). The band at ±30 kDa was not observed in any of the control lanes, confirming that this band is the hA_3AR. Notably, we did not observe any hA_3AR-specific labeling by a commercially available hA_3AR antibody in Western Blot experiments (Figure S2). Presumably the selectivity and affinity of antibodies is compromised by the relatively short N-terminus and extracellular loops of the hA_3AR.

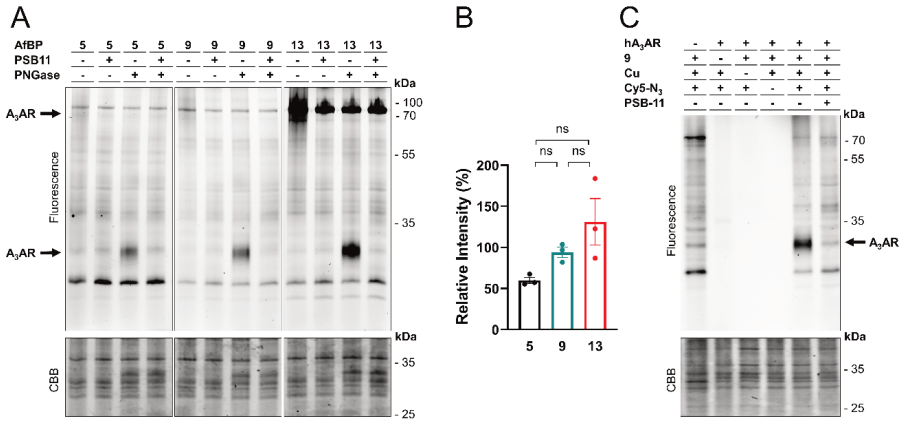

Figure 4. Labeling of the hA_3AR by the synthesized affinity-based probes. (A) Labeling of proteins by **5** (LUF7930), **9** (LUF7960) and **13** (LUF7934). Membrane fractions from CHO cells stably overexpressing the hA_3AR were pre-incubated for 30 min with antagonist (PSB-11, 1 µM final concentration) or 1% DMSO (control), prior to incubation for 1 h with the respective probe (50 nM final concentration). The proteins were subjected to PNGase or MilliQ (control) for 1 h to remove N-glycans. Samples were then clicked to Cy5-N_3 (1 µM final concentration), denatured using Laemmli buffer (4x) and resolved by SDS-PAGE. Gels were imaged using in-gel fluorescence and stained with Coomassie Brilliant Blue (CBB) as protein loading control. (B) Quantification of the lower hA_3AR band (± 30 kDa). The band intensities were taken and corrected for the observed amount of protein per lane upon CBB staining. The band at 55 kDa of the PageRuler Plus ladder (not shown) was set to 100% for each gel and band intensities were calculated relative to this band. The mean values ± SEM of three individual experiments are shown. Significance was calculated using a one-way ANOVA test using multiple comparisons (ns = not significant). (C) Control experiments with probe **9** (LUF7960). Membrane fractions from CHO cells with or without (first lane) stable expression of the hA_3AR were pre-incubated for 30 min with antagonist (PSB-11, 1 µM final concentration) or 1% DMSO (control), prior to incubation for 1 h with **9** (LUF7960) (50 nM final concentration) or 1% DMSO (control). Proteins were deglycosylated with PNGase for 1 h. Click mix was then added, containing $CuSO_4$ or MilliQ (control) and Cy5-N_3 (1 µM final concentration) or DMSO (control). The samples were then denatured with Laemmli buffer (4x) and resolved by SDS-PAGE. Gels were imaged using in-gel fluorescence and afterwards stained with CBB. The image shown is a representative of three individual experiments.

LABELING OF hA_3AR ON LIVE CHO CELLS

Having confirmed binding and labeling of the hA_3AR in CHO membrane fractions, we moved towards labeling experiments on live CHO cells stably expressing the hA_3AR. Live cells were incubated with 50 nM of AfBP **9** (LUF7960), prior to processing for either SDS-PAGE or microscopy experiments. In case of SDS-PAGE experiments, membranes were collected, the probe-bound proteins clicked to a Cy5-fluorophore, denatured and resolved by SDS-PAGE. This yielded 'cleaner' gels as compared to labeling in membrane fractions: no strong off-target bands were observed (Figure 5). The smear of glycosylated hA_3AR at ±70 kDa is now better visible (Figure 5A) and absent in the control lanes (no hA_3AR, no AfBP or pre-incubation with PSB-11). Similar to the experiments on cell membranes, a strong reduction in size of the band is observed upon pre-incubation with PNGase (Figure 5B). Both signals were significantly reduced by pre-incubation with PSB-11 (Figure 5C-D). Thus, AfBP **9** (LUF7960) also binds and labels the hA_3AR on live cells. We speculate that the increased amount of off-target labeling in membrane fractions is due to the high enrichment of subcellular membrane proteins. Together with the electrophilic nature of the AfBP, this can result in an increased amount of protein labeling, as we have observed in our experiments using an electrophilic A_1AR probe (chapter 4).[39]

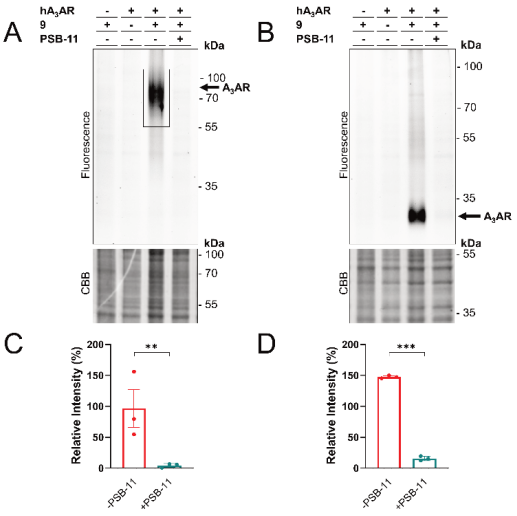

Figure 5. Labeling of the hA$_3$AR on live CHO cells. CHO cells with or without (first lane) stable expression of the hA$_3$AR were pre-incubated for 1 h with antagonist (PSB-11, 1 µM final concentration) at 37 °C, prior to incubation with **9** (LUF7960) (50 nM final concentration) for 1 h at 37 °C. After the incubation, unbound probe was washed away with PBS. Membranes were prepared, brought to a concentration of 1 µg/µL and subjected to the click reaction with Cy5-N$_3$ (1 µM final concentration). Samples were then denatured with Laemmli buffer (4x), resolved by SDS-PAGE and imaged using in-gel fluorescence. Gels were stained by Coomassie Brilliant Blue (CBB) as loading control. (A) Labeling of glycosylated hA$_3$AR. (B) Labeling of deglycosylated hA$_3$AR. PNGase was added prior to the addition of click reagents. (C-D) Quantification of the observed signals with and without addition of antagonist (PSB-11). The band intensities were calculated using ImageLab and corrected for the amount of protein measured after CBB staining. The band at 55 kDa of the PageRuler Plus ladder (not shown) was set to 100% for each gel and band intensities were calculated relative to this band. The mean values ± SEM of three individual experiments are shown. Significance was calculated by a two-way ANOVA test using multiple comparisons (*** $p < 0.001$; ** $p < 0.01$).

In case of the microscopy experiments, cells were fixed after probe incubation, followed by a click reaction with TAMRA-N$_3$, multiple washing steps and staining of the cellular nuclei with DAPI prior to confocal imaging. A strong increase in TAMRA intensity was observed at the cell membranes upon addition of probe to the wells (Figure 6A), visible by the increase in signal at cell-cell contacts. This signal was reduced by pre-incubation with PSB-11 and was absent for CHO cells not expressing the hA$_3$AR (Figure 6B-C). We therefore conclude that labeling of overexpressed hA$_3$AR by **9** (LUF7960) on living CHO cells can be studied by both SDS-PAGE and confocal microscopy experiments. Multiple fluorescent ligands have already been verified in similar fluorescence microscopy assays.[19,21–24,28] Together these fluorescent ligands comprise a molecular 'toolbox' that allows extensive characterization of the hA$_3$AR in microscopy assays, as well as localization and internalization (with fluorescent agonists) of the receptor.[12,24] The introduction of an electrophilic warhead and clickable handle on probe **9** (LUF7960) extends the possibilities to study the hA$_3$AR in microscopy assays, e.g. by allowing workflows that are dependent on thorough washing steps and/or denaturation of proteins.

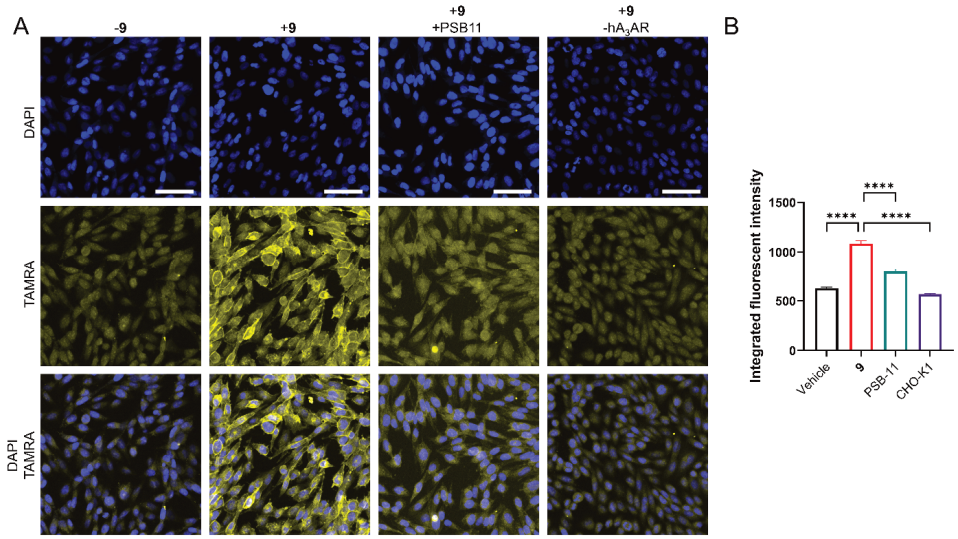

Figure 6. Labeling of the hA_3AR observed by confocal microscopy. CHO cells with (CHO-hA_3AR) or without (CHO-K1) stable expression of the hA_3AR were pre-incubated for 30 min with PSB-11 (1 µM final concentration) or 1% DMSO (control) and incubated for 60 min with **9** (LUF7960) or 1% DMSO (vehicle control). Cells were fixed, permeabilized and clicked to TAMRA-N_3 as fluorophore (1 µM final concentration). The cells were then washed and kept in PBS containing 300 nM DAPI during confocal imaging. (A) Shown are DAPI staining (blue, first row), TAMRA staining (yellow, second row) and an overlay of both stains (third row). Images were acquired automatically at multiple positions in the well of interest and are representatives from two biological experiments. Scale bar = 50 µM. Figure was created using OMERO.[46] (B) Comparison of the integrated fluorescence intensity between treatment conditions. Data was obtained from 2x9 fields of view, from the same experiment performed in duplicate. Each data point represents the integrated fluorescent intensity of the TAMRA signal per individual cell. Shown in the bar graph is the average integrated fluorescence intensity of all individual cells ± SEM. Significance was calculated using a one-way ANOVA test using multiple comparisons. A significant increase in intensity is observed for the cells containing the hA_3AR and treated with **9** (LUF7960), versus the other conditions.

LABELING OF ENDOGENOUS hA_3AR IN FLOW CYTOMETRY EXPERIMENTS

Having established the potential of **9** (LUF7960) in overexpressing cell systems, we turned to native hA_3AR expression in flow cytometry experiments in order to cope with expected low levels of observable fluorescence after receptor labeling caused by the notoriously low expression levels of GPCRs. Similar usage of fluorescent probes in flow cytometry experiments have thus far led to kinetic studies of ligand binding,[20,27] and detection of the hA_3AR on the HL-60 model cell line.[21] In order to establish an assay setup for primary cells we first used CHO cells as a model system. To avoid the use of excess copper on live cells, AfBP **9** (LUF7960) was first clicked to a Cy5-fluorophore and desalted, before being incubated for 1 h with living CHO cells with or without stable expression of the hA_3AR. Unbound probe was removed by washing steps and cells were analyzed by flow cytometry. The two types of CHO cells (+/- hA_3AR) showed a difference in Cy5 mean fluorescence intensity (MFI), i.e.: hA_3AR-expressing CHO cells showed a significant increase in Cy5 MFI upon probe labeling, which was absent for CHO cells without hA_3AR (Figure 7A-B). Next to that, pre-incubation with PSB-11 significantly reduced the observed signal in case of the hA_3AR-expressing CHO cells (Figure 7A-B), indicating that the observed signal is hA_3AR-specific. Noteworthy, no significant labeling was observed with a commercially available fluorophore-conjugated hA_3AR antibody.

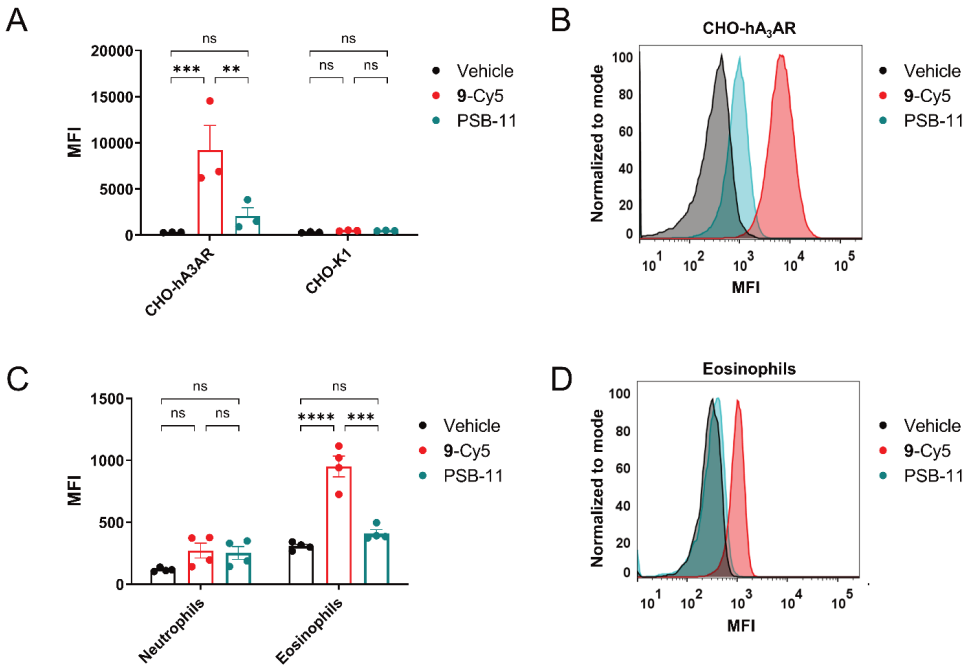

Figure 7. Labeling of the hA_3AR in flow cytometry experiments. Samples were pre-incubated for 30 min with the antagonist PSB-11 and incubated for 60 min with **9** (LUF7960) pre-clicked to a Cy5 fluorophore (**9**-Cy5). Samples were then washed and analyzed on Cy5 fluorescence by flow cytometry. (A) Cy5 mean fluorescence intensity (MFI) in CHO cells with (CHO-hA_3AR) and without (CHO-K1) stable expression of the hA_3AR. Values represent the mean ± SEM of three individual experiments performed in duplicate. Significance was calculated by a one-way ANOVA test using multiple comparisons (*** $p < 0.001$; ** $p < 0.01$; ns = not significant). (B) Representative graph showing the observed shift in MFI related to hA_3AR labeling in CHO-hA_3AR cells. (C) MFI of **9**-Cy5 in neutrophils and eosinophils purified from human blood samples. Values represent the mean ± SEM (n=4) of four donors from two individual experiments. Significance was calculated by a one-way ANOVA test using multiple comparisons (**** $p < 0.0001$; *** $p < 0.001$; ns = not significant). (D) Representative graph showing the observed shift in MFI related to hA_3AR labeling in human eosinophils.

Next we used the optimized procedure for further investigation of hA_3AR expression on human granulocytes. Eosinophils and neutrophils were purified from human blood samples obtained from four donors, subjected to Cy5-clicked AfBP **9** (LUF7960) and analyzed by flow cytometry. Within these experiments, purified neutrophils did not show a significant increase in Cy5 MFI upon incubation with probe (Figure 7C). The purified eosinophils however, showed a significant increase in MFI that was reduced upon pre-incubation with the antagonist PSB-11 (Figure 7C-D). Thus, with the aid of AfBP **9** (LUF7960) we were able to selectively detect hA_3AR expression on human eosinophils, but not on human neutrophils. In the past hA_3AR expression has been observed on both human eosinophils and neutrophils,[7–9,12–14] though the basal hA_3AR expression levels on human neutrophils were low in comparison to the expression on stimulated neutrophils.[12,13] Correspondingly, the herein investigated neutrophils showed little to no hA_3AR expressed on the cell surface.

Future studies that make use of AfBP **9** (LUF7960) might therefore yield new information on hA_3AR expression levels on stimulated neutrophils, among other leukocytes. Furthermore, the role of the hA_3AR in inflammatory conditions, such as asthma, ischemic injury and sepsis,[47–49] might be elucidated using AfBP **9** (LUF7960) as tool to detect receptor expression.

Conclusion

In this work, we have synthesized and evaluated three affinity-based probes **5**, **9** and **13**, that are all shown to bind covalently and with similar apparent affinities to the hA_3AR. Although all three probes were able to label the hA_3AR in SDS-PAGE experiments, we decided to continue with **9** (LUF7960) due to the low number of off-target protein bands detected on gel. We show that AfBP **9** (LUF7960) is a versatile AfBP that can be used together with different fluorophores, examples in this study being Cy5 and TAMRA. The combination of **9** (LUF7960) with click chemistry allowed us to label the hA_3AR in various assay types, such as SDS-PAGE, confocal microscopy and flow cytometry experiments, on both model cell lines and cells derived from human blood samples. In our hands, **9** (LUF7960) showed to be successful in the selective labeling of the hA_3AR, while commercial antibodies were not. We therefore believe that probe **9** (LUF7960) will be of great use in the detection and characterization of the hA_3AR in different types of granulocytes, among other cell types.

Acknowledgements

We thank I. Boom (LACDR, Leiden, The Netherlands) for performing high-resolution mass spectrometry measurements and B. Slütter (LACDR, Leiden, The Netherlands) for flow cytometry. We also thank the Leiden University Cell Observatory for access to the confocal microscope and support and assistance in this work.

Supplementary Figures

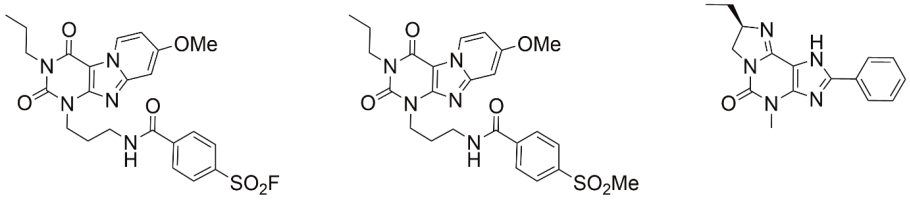

Figure S1. A_3AR ligands used in this study: covalent antagonist LUF7602, reversible control LUF7714 and antagonist PSB-11.[31,43]

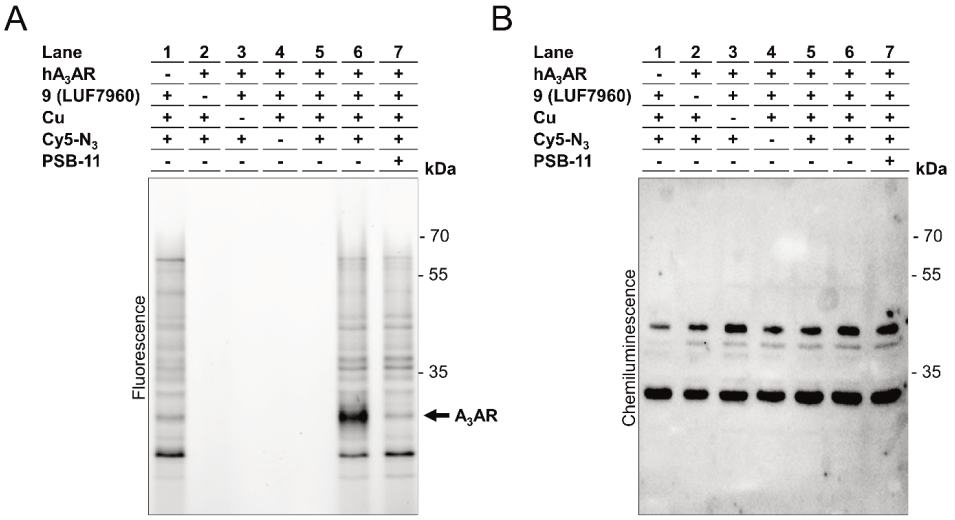

Figure S2. Labelling of the hA_3AR is evident in SDS-PAGE, but not in western blot experiments. (A) A specific hA_3AR band (lane 6) is observed upon measuring in-gel fluorescence after protein labelling by AfBP **9** (LUF7960); (B) No specific hA_3AR band is observed upon measuring chemiluminescence after protein labelling by the commercially available antibody, i.e.: the labelled proteins appear in both membrane fractions with and without (lane 1) expression of the hA_3AR. (A-B) Membrane fractions from CHO cells with and without (first lane) overexpression over the hA_3AR were pre-incubated for 30 min with the selective antagonist PSB-11 or 1% DMSO (vehicle control), prior to incubation for 1 h with AfBP **9** (LUF7960). *N*-Glycans were removed using PNGase, probe-bound proteins clicked to Cy5-N_3, denatured using Laemmli buffer and subjected to SDS-PAGE. The gel was imaged using in-gel fluorescence (Figure A) and subsequently transferred to 0.2 µM PVDF blots (Bio-Rad) using a Bio-Rad Trans-Blot Turbo system (2.5 A, 7 min). The blot was blocked in 5% BSA in TBST (1 h, rt) and subjected to primary antibody (rabbitαhA_3AR) 1: 10.000 in 1% BSA in TBST (overnight, 4 ºC). The blot was washed (3 x TBST), subjected to secondary antibody (goatαrabbit-HRP) 1:2.000 in 1% BSA in TBST (1 h, rt), washed again (2 x TBST, 1 x TBS), activated with luminol enhancer and peroxide (3 min, rt, dark) and subsequently scanned on fluorescence (Figure A) and chemiluminescence (Figure B). Images are representatives of three individual experiments.

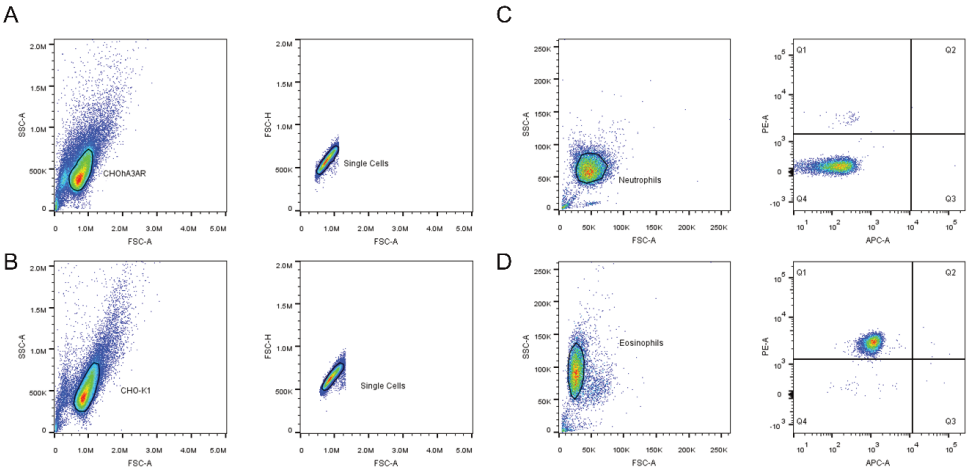

Figure S3. Gating strategy during analysis of the flow cytometry data. CHOhA_3AR (A) and CHO-K1 (B) cells were selected based on population density using SSC-A vs FSC-A gating and possible doublets were removed using FSC-H vs FSC-A gating. Neutrophils (C) and eosinophils (D) were selected based on population density using SSC-A vs FSC-A gating and PE signal of the PE-conjugated Siglec-8 antibody (selective marker for eosinophils) using PE-A vs APC-A gating. Q4 (neutrophils) and Q1 (eosinophils) were further analyzed on Cy5 intensity (APC channel).

Experimental

Chemistry

All reactions were carried out using commercially available reagents, unless noted otherwise. Reagents and solvents were purchased from Sigma-Aldrich (Merck), Fisher Scientific or VWR chemicals. All reactions were carried out under an N_2 atmosphere in oven-dried glassware. Reactions were monitored by thin layer chromatography (TLC) using TLC Silica gel 60 F254 plates (Merck) and UV irradiation (254 or 366 nM) as detection method. ^{1}H, ^{13}C and ^{19}F NMR spectra were recorded on a Bruker AV-300 (300 MHz), Bruker AV-400 (400 MHz) or Bruker AV-500 (500 MHz) spectrometer. Chemical shift values are reported in ppm (δ) using tetramethylsilane (TMS) or solvent resonance as internal standard. Coupling constants (*J*) are reported in Hz and multiplicities are indicated by s (singlet), d (doublet), dd (double doublet), t (triplet), q (quartet), p (pentuplet), h (hexuplet) or m (multiplet). Compound purity was determined by LC-MS, using the LCMS-2020 system (Shimadzu) coupled to a Gemini® 3 µm C18 110Å column (50 x 3 mm). In short, compounds were dissolved in H_2O:Acetonitrile (MeCN):*t*-BuOH 1:1:1, injected onto the column and eluted with a linear gradient of H_2O:MeCN 90:10 + 0.1% formic acid → H_2O:MeCN 10:90 + 0.1% formic acid over the course of 15 minutes. High-resolution mass spectrometry (HRMS) was performed on a X500R QTOF mass spectrometer (SCIEX).

Synthesis of 5 (LUF7930)

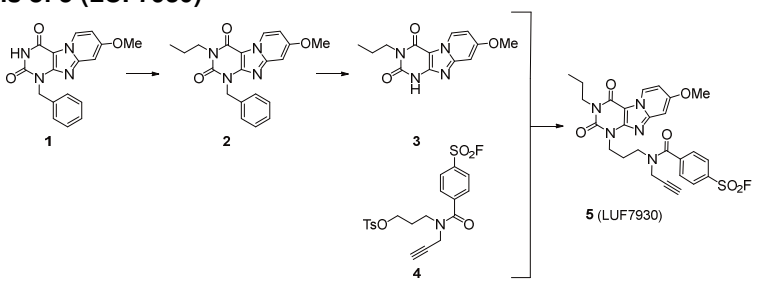

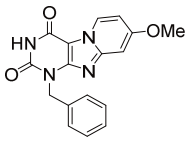

1-Benzyl-8-methoxypyrido[2,1-f]purine-2,4(1H,3H)-dione (1)

Compound **1** was synthesized in our lab as previously reported.[31]

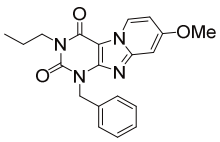

1-Benzyl-8-methoxy-3-propylpyrido[2,1-f]purine-2,4(1H,3H)-dione (2)

1 (7.37 g, 22.9 mmol, 1.0 eq) was dissolved in acetonitrile (145 mL) and diazabicycloundecene (DBU) (9.58 mL, 64.1 mmol, 2.8 eq) and 1-bromopropane (6.30 mL, 68.6 mmol, 3.0 eq) were added. The mixture was stirred for 1 h at 70 °C and cooled with ice overnight. The solvent was then removed under vacuum. The residue was filtered and washed with H_2O, EtOH and Et_2O and further dried under vacuum. This yielded **2** (quant., 8.33 g, 22.9 mmol) as a white solid.

TLC (DCM:MeOH 98:2): R_f = 0.88. **^{1}H NMR** (400 MHz, $(CD3)_2SO$): δ [ppm] = 8.81 (d, *J* = 7.4 Hz, 1H), 7.43 – 7.38 (m, 2H), 7.35 (t, *J* = 7.3 Hz, 2H), 7.33 – 7.26 (m, 2H), 6.98 (dd, *J* = 7.4, 2.6 Hz, 1H), 5.29 (s, 2H), 3.94 (s, 3H), 3.91 (t, *J* = 7.4 Hz, 2H), 1.63 (h, *J* = 7.5 Hz, 2H), 0.91 (t, *J* = 7.5 Hz, 3H). **^{13}C NMR** (101 MHz, $(CD3)_2SO$): δ [ppm] = 162.2, 154.6, 151.8, 150.5, 137.7, 129.4, 128.7, 128.4, 128.3, 108.8, 101.0, 96.7, 57.2, 46.9, 42.9, 21.9, 12.1.

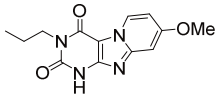

8-Methoxy-3-propylpyrido[2,1-f]purine-2,4(1H,3H)-dione (3)

2 (4.04 g, 11.1 mmol, 1.0 eq), $Pd(OH)_2/C$ (4.05 g, 28.8 mmol, 2.6 eq) and ammonium formate (0.72 g, 11.4 mmol, 1.0 eq) were suspended in EtOH (500 mL) and stirred at 80 °C under reflux conditions. Over the course of one week, 3 extra portions of ammonium formate (0.72 g, 11.4 mmol, 1.0 eq) were gradually added. The mixture was then cooled to rt and filtered over Celite. The residue was extracted with hot DMF and the filtrate was concentrated. The residue was purified by column chromatography (DCM:MeOH 98:2 → 90:10) to yield **3** (1.60 g, 5.82 mmol, 53 % yield) as a white solid. **TLC** (DCM:MeOH 95:5): R_f = 0.38. **^{1}H NMR** (400 MHz, $(CD_3)_2SO$): δ [ppm] = 12.05 (s, 1H), 8.74 (d, *J* = 7.4 Hz, 1H), 7.12 (d, *J* = 2.5 Hz, 1H), 6.90 (dd, *J* = 7.4, 2.5 Hz, 1H), 3.91 (s, 3H), 3.82 (t, *J* = 7.6 Hz, 2H), 1.63 – 1.52 (m, 2H), 0.88 (t, *J* = 7.3 Hz, 3H). **^{13}C NMR** (101 MHz, $(CD_3)_2SO$): δ [ppm] = 161.1, 154.5, 151.1, 150.5, 149.8, 127.5, 107.3, 95.4, 56.2, 41.0, 21.0, 11.2.

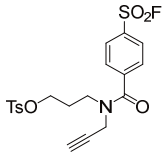

3-(4-(Fluorosulfonyl)-N-(prop-2-yn-1-yl)benzamido)propyl 4-methylbenzenesulfonate (4)

Compound **4** was synthesized in our lab as described in chapter 4.

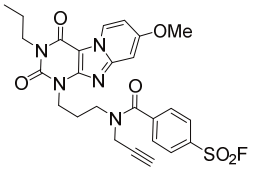

4-((3-(8-Methoxy-2,4-dioxo-3-propyl-3,4-dihydropyrido[2,1-f]purin-1(2H)-yl)propyl)(prop-2-yn-1-yl)carbamoyl)benzenesulfonyl fluoride (5) (LUF7930)

To a solution of **3** (37 mg, 0.14 mmol, 1.0 eq), **4** (63 mg, 0.14 mmol, 1.0 eq) in dry DMF (1.5 mL) and K_2CO_3 (29 mg, 0.20 mmol, 1.5 eq) were added. The reaction stirred over two nights at rt. The mixture was diluted with EtOAc (5 mL) and washed with water (2 x 5 mL). The water layers were combined and extracted with EtOAc (2 x 10 mL). The organic layers were combined, dried with $MgSO_4$ and concentrated under reduced pressure. The crude product was purified with column chromatography (DCM:MeOH 98:2 → 95:5) to yield **5** (22 mg, 0.04 mmol, 29%) as a white solid. NMR measurements revealed the presence of two rotamers at 20 °C, but not at 100 °C. **TLC** (DCM:MeOH 98:2 + 1% Et_3N): R_f= 0.63. **^{1}H NMR** (500 MHz, $(CD_3)_2SO$, *20 °C*): δ [ppm] = 8.74 (dd, *J* = 23.1, 7.2 Hz, 1H), 8.25 (d, *J* = 8.3 Hz, 1H), 7.93 (d, *J* = 8.3 Hz, 1H), 7.81 (d, *J* = 8.6 Hz, 1H), 7.63 (d, *J* = 8.1 Hz, 1H), 7.23 (d, *J* = 15.1 Hz, 1H), 6.95 (t, *J* = 7.9 Hz, 1H), 4.35 (s, 1H), 4.16 (t, *J* = 6.2 Hz, 1H), 4.03 (s, 1H), 3.91 (d, *J* = 10.1

Hz, 5H), 3.78 (t, *J* = 6.8 Hz, 1H), 3.60 (t, *J* = 6.4 Hz, 1H), 3.40 (s, 1H), 3.32 – 3.24 (m, 1H), 2.19 – 2.12 (m, 1H), 2.11 – 2.03 (m, 1H), 1.64 – 1.56 (m, 1H), 1.56 – 1.47 (m, 1H), 0.86 (dt, *J* = 23.2, 7.4 Hz, 3H). **^{1}H NMR** (500 MHz, $(CD_3)_2SO$, *100 °C*): δ [ppm] = 8.79 (d, *J* = 7.3 Hz, 1H), 8.09 (d, *J* = 7.8 Hz, 2H), 7.74 (d, *J* = 8.1 Hz, 2H), 7.15 (d, *J* = 2.7 Hz, 1H), 6.94 (dd, *J* = 7.4, 2.6 Hz, 1H), 4.20 (s, 2H), 4.10 (d, *J* = 5.3 Hz, 2H), 3.95 (s, 3H), 3.90 (t, *J* = 7.3 Hz, 2H), 3.52 (s, 2H), 3.11 (s, 1H), 2.16 (p, *J* = 6.6 Hz, 2H), 1.63 (h, *J* = 7.5 Hz, 2H), 0.90 (t, *J* = 7.5 Hz, 3H). **^{13}C NMR** (126 MHz, $(CD_3)_2SO$, *20 °C*): δ [ppm] = 168.2, 167.9, 161.2, 153.7, 153.3, 150.9, 150.8, 150.5, 149.5, 149.4, 143.4, 132.4, 132.2, 132.0, 131.8, 128.9, 128.6, 128.3, 127.9, 127.7, 107.7, 100.1, 99.8, 95.6, 95.5, 79.3, 79.2, 75.9, 74.6, 56.2, 46.2, 42.8, 41.7, 40.7, 40.2, 38.8, 33.7, 26.9, 25.5, 20.9, 11.2. **^{13}C NMR** (126 MHz, $(CD_3)_2SO$, *100 °C*) δ [ppm] = 167.7, 160.9, 153.2, 151.6, 150.5, 149.1, 143.0, 132.2 (d, *J* = 23.7 Hz), 127.9, 127.7, 127.2, 107.0, 99.6, 95.4, 78.6, 74.3, 55.7, 41.4, 40.1, 25.8, 20.3, 10.4. **^{19}F NMR** (471 MHz, $(CD_3)_2SO$, *20 °C*): δ [ppm] = 67.08, 66.35. **^{19}F NMR** (471 MHz, $(CD_3)_2SO$, *100 °C*): δ [ppm] = 65.99. **HRMS** (ESI, m/z): $[M+H]^+$, calculated: 556.1661, found: 556.1628. **HPLC** 97%, RT 10.830 min.

Synthesis of 9 (LUF7960)

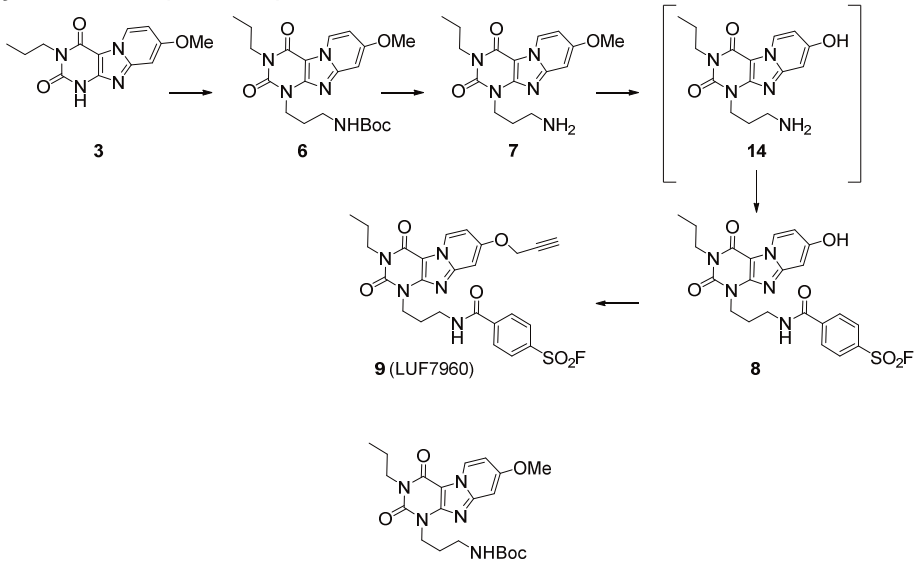

***Tert*-butyl (3-(8-methoxy-2,4-dioxo-3-propyl-3,4-dihydropyrido[2,1-f]purin-1(2H)-yl)propyl)carbamate (6)**

3 (1.18 g, 4.3 mmol, 1.0 eq), *tert*-butyl (3-bromopropyl)carbamate (1.54 g, 6.5 mmol, 1.5 eq) and K_2CO_3 (890 mg, 6.5 mmol, 1.5 eq) were dissolved in DMF (60 mL) and refluxed at 100°C for 2 h. Afterwards the mixture was allowed to cool down to rt overnight. The next day, the solvents were removed by evaporation under reduced pressure. The residue was dissolved in chloroform (100 mL), washed with H_2O (3 x 100 mL), dried over $MgSO_4$ and concentrated under reduced pressure to yield **6** (1.80 g, 4.2 mmol, 97%) as a white solid. **TLC** (DCM:MeOH 99:1): R_f = 0.76. **^{1}H NMR** (300 MHz, $CDCl_3$): δ [ppm] = 8.82 (d, *J* = 7.3 Hz, 1H), 6.94 (d, *J* = 2.5 Hz, 1H), 6.75 (dd, *J* = 7.4, 2.5 Hz, 1H), 5.62 (s, 1H), 4.26 (t, *J* = 6.2 Hz, 2H), 4.01 (d, *J* = 7.5 Hz, 2H), 3.92 (s, 3H), 3.17 – 3.06 (m, 2H), 2.03 – 1.92 (m, 2H), 1.80 – 1.61 (m, 2H), 1.45 (s, 9H), 0.98 (t, *J* = 7.4 Hz, 3H). **^{13}C NMR** (75 MHz, $CDCl_3$): δ [ppm] = 161.8, 156.2, 154.7, 151.9, 150.1, 128.1, 107.9, 95.3, 79.1, 56.0, 42.9, 40.9, 37.2, 28.6, 21.6, 11.5.

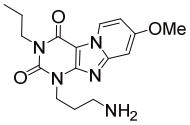

1-(3-Aminopropyl)-8-methoxy-3-propylpyrido[2,1-f]purine-2,4(1H,3H)-dione (7)
TFA (12.8 mL, 166.6 mmol, 40.0 eq) was added to a solution of **6** (1.80 g, 4.2 mmol, 1.0 eq) in chloroform (40 mL) and the mixture was stirred at 60°C overnight. Afterwards, the pH was increased with 2M NaOH (50 mL) to a value of approx. 10. The aqueous layer was extracted with EtOAc (2 x 50 mL) dried over $MgSO_4$, filtered and concentrated under reduced pressure to yield **7** (1.25 g, 3.8 mmol, 90%) as a white solid. **TLC** (DCM:MeOH 90:10 + 1% NEt_3): R_f = 0.44. **^{1}H NMR** (400 MHz, $CDCl_3$): δ [ppm] = 8.83 (dd, *J* = 7.3, 0.7 Hz, 1H), 6.95 (d, *J* = 1.9 Hz, 1H), 6.74 (dd, *J* = 7.4, 2.5 Hz, 1H), 4.29 (t, *J* = 6.7 Hz, 2H), 4.02 (t, *J* = 7.6 Hz, 2H), 3.92 (s, 3H), 2.74 (t, *J* = 6.5 Hz, 2H), 1.97 (p, *J* = 6.6 Hz, 2H), 1.71 (h, *J* = 7.4 Hz, 2H), 1.24 (t, *J* = 7.0 Hz, 2H), 0.98 (t, *J* = 7.4 Hz, 3H). **^{13}C NMR** (101 MHz, $CDCl_3$): δ [ppm] = 161.6, 154.5, 151.5, 151.3, 149.9, 127.8, 107.6, 100.9, 95.1, 55.9, 42.6, 40.7, 38.8, 31.9, 21.4, 11.3.

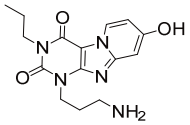

1-(3-Aminopropyl)-8-hydroxy-3-propylpyrido[2,1-f]purine-2,4(1H,3H)-dione (14)
BBr_3 (1M solution in DCM) (30.2 mL, 30.2 mmol, 10 eq) was added to a solution of **7** (1.00 g, 3.0 mmol, 1.0 eq) in $CHCl_3$ (40 mL). The mixture was refluxed at 50 °C overnight. As the reaction was not complete (as determined by LC-MS) additional BBr_3 (1M solution in DCM) (30.2 mL, 30.2 mmol, 10 eq) was added and the mixture was refluxed for 5 days. The reaction was then cooled to rt, upon which H_2O (100 mL) was added dropwise to quench the reaction. The mixture was stirred for 1 h and afterwards the organic layer was removed. The aqueous layer was concentrated to yield crude **14**. This was used in subsequent reaction steps without further purification.

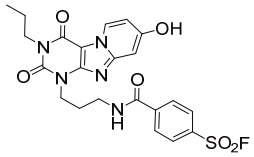

4-((3-(8-Hydroxy-2,4-dioxo-3-propyl-3,4-dihydropyrido[2,1-f]purin-1(2H)-yl)propyl)carbamoyl)benzenesulfonyl fluoride (8)
4-Fluorosulfonyl benzoic acid (678 mg, 3.3 mmol, 1.1 eq) and EDC·HCl (868 mg, 4.5 mmol, 1.5 eq) were dissolved in dry DMF (10 mL) and stirred at rt. After one hour, the mixture was added to a solution of crude **14** (958 mg, 3.0 mmol, 1.0 eq) in dry DMF (20 mL). DIPEA (1.8 mL, 10.6 mmol, 3.5 eq) was added and the mixture was stirred overnight. The reaction was not completed by then (as indicated by LC-MS) and therefore additional 4-fluorosulfonyl benzoic acid (678 mg, 3.3 mmol, 1.1 eq) and EDC·HCl (868 mg, 4.5 mmol, 1.5 eq) were added. The mixture was stirred overnight and the next day DCM (150 mL) was added. The organic layer was washed with 1M HCl (2 x 200 mL), dried over $MgSO_4$, filtrated and concentrated under reduced pressure. The residue was purified by column chromatography (DCM:MeOH 98:2 → 80:20) to yield **8** (194 mg, 0.4 mmol, 13% over two steps) as a white solid. **TLC** (DCM:MeOH 95:5): R_f = 0.45. **^{1}H NMR** (500 MHz, $CDCl_3$): δ [ppm] = 8.77 (d, *J* = 7.1 Hz, 1H), 8.69 (t, *J* = 6.2 Hz, 1H), 8.18 (d, *J* = 8.1 Hz, 2H), 8.06 (d, *J* = 8.1 Hz, 2H), 7.96 (m, 1H), 6.96 (s, 1H), 6.80 (d, *J* = 7.0 Hz, 1H), 4.27 (t, *J* = 5.9 Hz, 2H), 3.99 (t, *J* = 7.4 Hz, 2H), 3.44 (m, 2H),

2.10 (m, 2H), 1.68 (h, *J* = 6.9 Hz, 2H), 0.93 (t, *J* = 7.4 Hz, 3H). **^{13}C NMR** (126 MHz, $CDCl_3$): δ [ppm] = 165.5, 161.0, 154.3, 151.9, 151.3, 150.2, 141.0, 135.3 (d, J = 25.1 Hz), 128.8, 128.6, 108.3, 100.9, 98.1, 43.0, 40.9, 36.4, 27.4, 21.5, 11.4. **^{19}F NMR** (471 MHz, $CDCl_3$): δ [ppm] = 65.58.

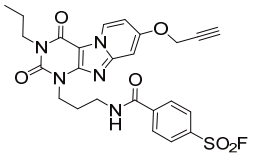

4-((3-(2,4-Dioxo-8-(prop-2-yn-1-yloxy)-3-propyl-3,4-dihydropyrido[2,1-f]purin-1(2H)-yl)propyl)carbamoyl)benzenesulfonyl fluoride (9) (LUF7960)

A 80% v/v solution of propargyl bromide in toluene (0.42 mL, 0.4 mmol, 1.0 eq) was further diluted in dry DMF (4.2 mL) and added to a solution of **8** (194 mg, 0.4 mmol, 1.0 eq) in dry DMF (20 mL). K_2CO_3 (53 mg, 0.4 mmol, 1.0 eq) was added to the mixture, which was stirred overnight. The mixture was then diluted with EtOAc (80 mL) and the organic layer was washed with H_2O (2 x 100 mL) and brine (100 mL), dried over $MgSO_4$ and concentrated under reduced pressure. The residue was purified by column chromatography (Pentane:EtOAc 3:7) to yield **9** (63 mg, 0.1 mmol, 30%) as a white solid. **TLC** (EtOAc): R_f = 0.54. **^{1}H NMR** (500 MHz, $CDCl_3$): δ [ppm] = 8.91 (d, *J* = 7.4 Hz, 1H), 8.47 (t, *J* = 6.3 Hz, 1H), 8.27 (d, *J* = 8.0 Hz, 2H), 8.18 (d, *J* = 8.5 Hz, 2H), 7.03 (d, *J* = 2.5 Hz, 1H), 6.85 (dd, *J* = 7.4, 2.5 Hz, 1H), 4.82 (d, *J* = 2.4 Hz, 2H), 4.35 (t, *J* = 5.8 Hz, 2H), 4.09 – 4.02 (m, 2H), 3.46 (q, *J* = 6.1 Hz, 2H), 2.64 (t, *J* = 2.4 Hz, 1H), 2.16 (p, *J* = 5.9 Hz, 2H), 1.74 (h, *J* = 7.5 Hz, 2H), 1.00 (t, *J* = 7.4 Hz, 3H). **^{13}C NMR** (126 MHz, $CDCl_3$): δ [ppm] = 164.8, 159.8, 154.5, 152.1, 151.4, 149.5, 141.6, 135.4 (d, *J* = 29.1 Hz), 128.9, 128.6, 128.4, 108.3, 101.3, 96.6, 77.7, 76.6, 56.6, 43.0, 40.8, 35.8, 27.6, 21.6, 11.5. **^{19}F NMR** (471 MHz, $CDCl_3$): δ [ppm] = 65.76. **HRMS** (ESI, m/z): $[M+H]^+$, calculated: 542.1504, found: 542.1478. **HPLC** 98%, RT 10.875 min.

Synthesis of 13 (LUF7934)

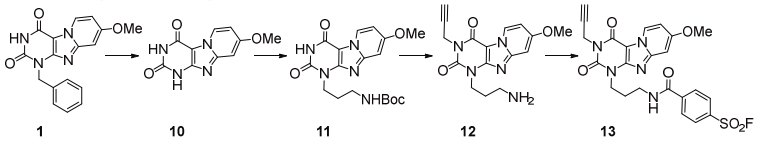

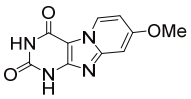

8-Methoxypyrido[2,1-f]purine-2,4(1H,3H)-dione (10)

1 (5.0 g, 15.51 mmol, 1.0 eq) was suspended in EtOH (250 mL) . $Pd(OH)_2/C$ (2.2 g, 15.5 mmol, 1.0 eq) was added and the reaction was brought under a nitrogen atmosphere. Ammonium formate (6.6 g, 105 mmol, 4.6 eq) was added and the mixture was refluxed at 80 °C. Over a period of one week, ten portions of ammonium formate (6.6 g, 105 mmol, 4.6 eq) were gradually added, as well as one portion of extra $Pd(OH)_2/C$ (2.20 g, 15.5 mmol, 1.0 eq). Afterwards, the mixture was cooled to rt and filtered over Celite. The residue was extracted five times with hot DMF (100 mL). The filtrates were combined and concentrated. The residue was purified by column chromatography (DCM:MeOH 90:10 → 80:2) to yield 3.0 g of crude mixture **10**. This compound was used in subsequent reaction steps without further purifications. LC-MS [ESI+H]+: 233.00.

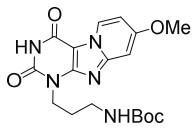

***Tert*-butyl (3-(8-methoxy-2,4-dioxo-3,4-dihydropyrido[2,1-f]purin-1(2H)-yl)propyl)carbamate (11)**

Crude **10** (1.57 g, 6.8 mmol, 1.0 eq) was dissolved in dry DMF (70 mL) and *tert*-butyl (3-bromopropyl)carbamate (1.61 g, 6.8 mmol, 1.0 eq) was added. The mixture was cooled to 0 °C and K_2CO_3 was added (1.40 g, 10.1 mmol, 1.5 eq). The mixture was allowed to warm up to rt overnight and was stirred for another 3 days. Due to the slow progress of the reaction, the mixture was heated at 40 °C and stirred for another 2 days. Extra *tert*-butyl (3-bromopropyl)carbamate was then added (0.32 g, 1.4 mmol, 0.2 eq), which resulted in the slow formation of double substituted **3** (as determined by LC-MS). The reaction was therefore stopped. EtOAc (180 mL) was added and the organic layer was washed with H_2O (3 x 180 mL) and brine (90 mL), dried over $MgSO_4$, filtered and concentrated under reduced pressure. The residue was purified by column chromatography (DCM:MeOH 98:2 → 95:5) to yield **11** (486 mg, 1.68 mmol, 25%). LC-MS [ESI+H]+: 390.15.

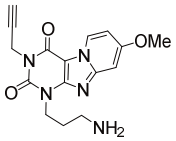

***1-(3-Aminopropyl)-8-methobxy-3-(prop-2-yn-1-yl)pyrido[2,1-f]purine-2,4(1H,3H)-dione* (12)**

(i) Propargylbromide (80% in toluene) (446 µL, 4.14 mmol, 3.0 eq) and DBU (0.619 mL, 4.14 mmol, 3.0 eq) were added to a mixture of **11** (536 mg, 1.38 mmol, 1.0 eq) in acetonitrile (7 mL), upon which the suspension became a clear solution. The mixture was stirred overnight and the next day H_2O (25 mL) was added. The aqueous layer was extracted with DCM (2 x 35 mL). The organic layers were combined, dried over $MgSO_4$, filtered and concentrated under reduced pressure. (ii) The resulting residue was dissolved in DCM (10 mL) and TFA (5 mL) was added. The mixture was stirred for 2 h and afterwards quenched by the addition of 2M NaOH (50 mL). The aqueous layer was extracted with EtOAc (2 x 50 mL). The organic layers were combined, dried with $MgSO_4$, filtered and concentrated under reduced pressure. The residue was purified by column chromatography (DCM:MeOH 95:5 → 85:15) to yield **12** (300 mg, 0.92 mmol, 67%) as an off-white solid. **TLC** (DCM:MeOH 85:15 + 1% Et_3N): R_f = 0.67. **^{1}H NMR** (500 MHz, CD_3OD): δ [ppm] = 8.69 (d, *J* = 7.3 Hz, 1H), 6.99 (d, *J* = 2.5 Hz, 1H), 6.83 (dd, *J* = 7.4, 2.5 Hz, 1H), 4.70 (d, *J* = 2.4 Hz, 2H), 4.23 (t, *J* = 6.4 Hz, 2H), 3.90 (s, 3H), 2.99 (t, *J* = 7.2 Hz, 2H), 2.48 (t, *J* = 2.4 Hz, 1H), 2.15 (p, *J* = 6.8 Hz, 2H).

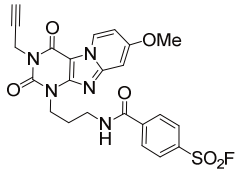

4-((3-(8-Methoxy-2,4-dioxo-3-(prop-2-yn-1-yl)-3,4-dihydropyrido[2,1-f]purin-1(2H)-yl)propyl)carbamoyl)benzenesulfonyl fluoride (13) (LUF7934)

EDC·HCl (347 mg, 1.81 mmol, 2.0 eq), 4-(fluorosulfonyl)benzoic acid (347 mg, 1.70 mmol, 1.9 eq) and DIPEA (387 µl, 2,26 mmol) were added to a solution of **12** (300 mg, 0.92 mmol, 1.0

eq) in dry DMF (6 mL). The mixture was stirred for 3 h, after which all starting material was consumed (as determined by TLC). DCM (50 mL) was added and the organic layer was washed with water (50 mL) and brine (50 mL), dried over $MgSO_4$, filtered and concentrated under reduced pressure. The residue was purified by column chromatography (DCM:MeOH 99:1 → 98:2) and (Pentane:EtOAc 1:1 → 0:1) to yield **13** (60 mg, 0.12 mmol, 13%) as a white solid. **TLC** (DCM:MeOH 99:1): R_f = 0.35. **^{1}H NMR** (500 MHz, $CDCl_3$): δ [ppm] = 8.85 (d, *J* = 7.3 Hz, 1H), 8.27 (t, *J* = 6.2 Hz, 1H), 8.24 (d, *J* = 8.3 Hz, 2H), 8.14 (d, *J* = 8.5 Hz, 2H), 6.86 (d, *J* = 2.5 Hz, 1H), 6.82 (dd, *J* = 7.3, 2.5 Hz, 1H), 4.86 (d, *J* = 2.4 Hz, 2H), 4.37 (t, *J* = 6.0 Hz, 2H), 3.92 (s, 3H), 3.48 (q, *J* = 6.0 Hz, 2H), 2.21 (t, *J* = 2.4 Hz, 1H), 2.20 – 2.14 (m, 2H). **^{13}C NMR** (126 MHz, $CDCl_3$): δ [ppm] = 165.0, 162.5, 153.3, 151.5, 151.2, 149.9, 141.6, 135.4 (d, *J* = 25.4 Hz), 128.8, 128.7, 128.4, 108.6, 101.0, 95.1, 78.5, 71.0, 56.2, 41.2, 36.0, 30.6, 27.5. **^{19}F NMR** (471 MHz, $CDCl_3$): δ [ppm] = 65.71. **HRMS** (ESI, m/z): $[M+H]^+$, calculated: 514.1191, found: 514.1149. **HPLC** 100%, RT 10.077 min.

Biology

Ethics approval

The parts of the study involving human participants were reviewed and approved by Sanquin Institutional Ethical Committee (project number NVT0606.01). All blood samples were obtained after informed consent and according to the Declaration of Helsinki 1964. The patients and participants provided informed consent to participate in this study.

Cell lines

Chinese hamster ovary (CHO) cells stably expressing the human adenosine A_3 receptor ($CHOhA_3AR$) were kindly provided by Prof. K.N. Klotz (University of Würzburg). CHO cells stably expressing the human adenosine A_1 receptor ($CHOhA_1AR$) were kindly provided by Prof. S.J. Hill (University of Nottingham), human embryonic kidney 293 (HEK293) cells stably expressing the human adenosine A_{2A} receptor ($HEKhA_{2A}AR$) were kindly provided by Dr. J. Wang (Biogen) and CHO cells stably expressing the human A_{2B} receptor (CHO-spap-$hA_{2B}AR$) were kindly provided by S.J. Dowell (GlaxoSmithKline).

Radioligands

[^{3}H]PSB-11, specific activity 56 Ci/mmol, was a kind gift from Prof. C.E. Müller (University of Bonn). [^{3}H]DPCPX, specific activity 137 Ci/mmol, and [^{3}H]ZM241385, specific activity 50 Ci/mmol, were purchased from ARC Inc. and [^{3}H]PSB-603, specific activity 79 Ci/mmol, was purchased from Quotient Bioresearch.

Chemicals

5'-(N-Ethylcarboxamido)adenosine (NECA), N^6-Cyclopentyladenosine (CPA) and adenosine deaminase (ADA) were purchased from Sigma-Aldrich. ZM241385 was kindly provided by Dr. S.M. Poucher (AstraZeneca), CGS21680 was purchased from Ascent Scientific, PSB 1115 potassium salt was purchased from Tocris Bioscience and PSB-11 hydrochloride was purchased from Abcam Biochemicals. Bicinchoninic acid (BCA) protein assay reagents were purchased from Thermo Scientific. All click reagents ($CuSO_4$, sodium ascorbate (NaAsc), Tris(3-hydroxypropyltriazolylmethyl)amine (THPTA), Cy5-N_3 and Azide-Fluor-545 (TAMRA-N_3)) were purchased from Sigma-Aldrich. Pierce™ ECL Western Blotting Substrate was ordered from Thermo Scientific. 4x Laemmli Sample Buffer was ordered from Bio-Rad. All other chemicals were of analytical grade and obtained from standard commercial sources.

Biologicals

PNGase (cat# V4831) was purchased from Promega (Leiden, The Netherlands). RabbitαhA$_3$AR antibody (cat# bs-1225R) was ordered from Thermo Scientific (Landsmeer, The Netherlands), rabbitαhA$_3$AR PE conjugate (cat# orb495084) was ordered from Biorbyt (Huissen, The Netherlands), goatαrabbit-HRP antibody (cat# 115-035-003) was purchased from Brunschwig Chemie (Amsterdam, The Netherlands) and PE anti-human Siglec-8 Antibody (mouse IgG1 clone 7C9) (cat# 347104) was purchased from Biolegend (San Diego, CA, USA). Bovine Serum Albumin (BSA)(cat# 268131000) was purchased from Acros Organics (Geel, Belgium).

Cell culture and membrane preparation

CHOhA$_3$AR, CHOhA$_1$AR, CHOhA$_{2A}$AR, CHO-spap-hA$_{2B}$AR and CHO-K1 cells were cultured as previously reported.[50] Membranes were prepared in the following manner: cells were detached from plates by scraping in PBS (5 mL). The cells were collected and centrifuged (5 min, 1000 rpm). Supernatant was removed and cells were resuspended in ice-cold Tris-HCl buffer (pH 7.4). The cells were homogenized (Heidolph Diax 900 homogenizer) and the membranes were separated from the cytosolic fraction by centrifugation (20 min, 31000 rpm, 4°C) using a Beckman Optima LE-80 K ultracentrifuge. The pellet was resuspended in Tris-HCl buffer and the homogenization and centrifugation steps were repeated. The resulting pellet was resuspended in Tris-HCl buffer and ADA was added (0.8 U/mL) to break down endogenous adenosine. Total protein concentrations were determined using the BCA method.[51]

Radioligand displacement assays

Single point assay on all four adenosine receptors

Membrane aliquots containing 15 µg (CHOhA$_3$AR), 5 µg (CHOhA$_1$AR) or 30 µg (HEK293hA$_{2A}$AR and CHO-spap-A$_{2B}$AR) of protein were resuspended in assay buffer (A$_3$AR: 50 mM Tris-HCl, pH 8.0, 10 mM $MgCl_2$, 1mM EDTA, 0.01% CHAPS; A$_1$AR and A$_{2A}$AR: 50 mM Tris-HCl, pH 7.4; A$_{2B}$AR: 50 mM Tris-HCl, pH 7.4, 0.1% CHAPS). Competing ligand (1 µM) and radioligand (A$_3$AR: 10 nM [^{3}H]PSB-11; A$_1$AR: 1.6 nM [^{3}H]DPCPX; A$_{2A}$AR: 1.7 nM [^{3}H]ZM241385; A$_{2B}$AR: 1.5 nM [^{3}H]PSB-603) were added and the samples were incubated in a total volume of 100 µL of the respective assay buffer for 30 min at 25 °C. Nonspecific binding was determined in the presence of 100 µM NECA (A$_3$AR), 100 µM CPA (A$_1$AR), 100 µM NECA (A$_{2A}$AR) and 10 µM ZM241385 (A$_{2B}$AR). Incubations were terminated by rapid vacuum filtration to separate the bound and free radioligand through prewetted 96-well GF/C filter plates using a PerkinElmer Filtermate-harvester. Filters were subsequently washed 12 times with ice-cold wash buffer (A$_3$AR: 50 mM Tris-HCl, pH 8.0, 10 mM $MgCl_2$, 1mM EDTA; A$_1$AR and A$_{2A}$AR: 50 mM Tris-HCl, pH 7.4; A$_{2B}$AR: 50 mM Tris-HCl, pH 7.4, 0.1% BSA). The plates were dried at 55 °C and MicroscintTM-20 cocktail (PerkinElmer) was added subsequently. After 3 h the filter-bound radioactivity was determined by scintillation spectrometry using a 2450 MicroBeta Microplate Counter (PerkinElmer).

Full curve assay on the adenosine A_3 receptor

Membrane aliquots containing 15 µg of protein (CHOhA$_3$AR) were resuspended in assay buffer (50 mM Tris-HCl, pH 8.0, 10 mM $MgCl_2$, 1mM EDTA, 0.01% CHAPS). Competing ligand (concentrations ranging from 0.1 to 1000 nM) was added and pre-incubated with the membrane fractions for either 0 or 4 hours. Radioligand (10 nM [^{3}H]PSB-11) was then added and incubated with the samples in a total volume of 100 µL of assay buffer for 30 min at 25 °C. Nonspecific binding was determined in the presence of 100 µM NECA. Incubations were

terminated by rapid vacuum filtration through prewetted 96-well GF/C filter plates using a PerkinElmer Filtermate-harvester. Filters were subsequently washed 12 times with ice-cold wash buffer (50 mM Tris-HCl, pH 8.0, 10 mM $MgCl_2$, 1mM EDTA). The plates were dried at 55 °C and MicroscintTM-20 cocktail (PerkinElmer) was added subsequently. After 3 h the filter-bound radioactivity was determined using a Tri-Carb 2810TR Liquid Scintillation Analyzer (PerkinElmer).

Wash-out assay

200 µL assay buffer (50 mM Tris-HCl, pH 8.0, 10 mM $MgCl_2$, 1 mM EDTA and 0.01% CHAPS), 100 µL assay buffer containing competing ligand (final concentration: 1 µM) and 100 µL of $CHOhA_3AR$ membrane fractions (100 µg protein) were combined and pre-incubated for 2 h at 25 °C while shaking. The '4x washed' samples were centrifuged (5 min, 13000 rpm, 4 °C) and the supernatant removed. The resulting pellet was dissolved in 1 mL assay buffer and incubated for 10 min at 25 °C while shaking. The '4x washed' samples were then again centrifuged (2 min, 13000 rpm, 4 °C), the supernatant removed and the resulting pellet dissolved in 1 mL assay buffer. The latter washing steps were repeated two times (four times washing total) and the final pellet was dissolved in 300 µL assay buffer. Radioligand (10 nM [^{3}H]PSB-11) in 100 µL assay buffer was added to all samples and the samples were incubated at 25 °C for 1 h. Nonspecific binding was determined in the presence of 100 µM NECA. Incubations were terminated by addition of 1 mL ice-cold washing buffer (50 mM Tris-HCl, pH 8.0, 10 mM $MgCl_2$, 1mM EDTA) and rapid vacuum filtration through prewetted 96-well GF/B filter plates using a Brandel harvester. Filters were subsequently washed 5 times with ice-cold wash buffer. The plates were dried under vacuum and MicroscintTM-20 cocktail (PerkinElmer) was added subsequently. After 3 h the filter-bound radioactivity was determined using a 2450 MicroBeta Microplate Counter (PerkinElmer).

Data analysis and statistics

Data analysis was performed using GraphPad Prism version 9.0.0 (San Diego, California USA). pIC_{50} values were obtained by non-linear regression curve fitting and converted to pK_i values using the Cheng-Prusoff equation.[52] As such, the K_D values of 1.6 nM of [^{3}H]DPCPX at $CHOhA_1AR$ membranes and 1.7 nM of [^{3}H]PSB603 at CHO-spap-$hA_{2B}AR$ membranes were taken from previous experiments,[53,54] while the K_D values of 1.0 nM of [^{3}H]ZM241385 at HEK293$hA_{2A}AR$ membranes and 17.3 nM of [^{3}H]PSB-11 at $CHOhA_3AR$ membranes were taken from in-house determinations. Single point displacement values shown are mean percentages of two individual experiments performed in duplicate. All pK_i values shown are mean values ± SEM of three individual experiments performed in duplicate. Statistical analysis was performed using a one-way ANOVA test with multiple comparisons (**** $p < 0.0001$).

SDS-PAGE experiments

SDS-PAGE experiments using membranes

Membrane fractions were prepared as mentioned above and diluted to a concentration of 1 µg/µL. 18 µL of membrane fractions from either $CHOhA_3AR$ or CHO-K1 cells were taken. 1 µL of competing ligand (PSB-11, unless noted otherwise) was added (final concentration: 1 µM in 0.05% DMSO in assay buffer) and the samples were shaken for 30 min at rt. 1 µL of affinity-based probe was then added (final concentration: 50 nM in 0.05% DMSO in assay buffer, unless noted otherwise) and the samples were shaken for 1 h at rt. Deglycosylation was initiated by addition of 0.5 µL PNGaseF (5U), 0.5 µL MilliQ water for the control samples, and the samples were shaken for 1 h at rt. Click mix was freshly prepared by adding together: 5 parts 100 mM $CuSO_4$ in MilliQ, 3 parts 1 M NaAsc in MilliQ, 1 part 100 mM THPTA in MilliQ and 1 part 100 µM Cy5-N_3 in DMSO. 2.28 µL of click mix was added to the samples (final

concentration Cy5-N_3: 1 µM in 1% DMSO in MilliQ) and the samples were shaken for 1 h at rt. Lastly 7.59 µL of 4x Laemmli buffer was added and the samples were shaken for at least 1 h at rt. The samples were then loaded on gel (12.5% acrylamide) and run (180 V, 100 min). In-gel fluorescence was measured on a Bio-Rad Universal Hood III using Cy3 (605/50 filter) or Cy5 (695/55 filter) settings. Pageruler prestained protein ladder was used as molecular weight marker. After scanning, gels were either transferred to 0.2 µM PVDF blots (Bio-Rad) using a Bio-Rad Trans-Blot Turbo system (2.5 A, 7 min) or stained with Coomassie Brilliant Blue.

SDS-PAGE experiments using live CHO cells

CHOhA_3AR and CHO-K1 cells were cultured as mentioned above. Cells were grown to ~90% confluency in 10 cm φ plates. 10 plates were used per condition per experiment. Medium was removed and competing ligand (PSB-11, unless noted otherwise) in medium (final concentration: 1 µM) was added. Cells were incubated for 1 h (37 °C, 5% CO_2). Medium was removed and affinity-based probe (final concentration: 50 nM in medium) was added. The cells were incubated for 1 h (37 °C, 5% CO_2) and washed with PBS to get rid of all the non-bound probe. Subsequently the membranes prepared and collected using the procedure as described above. Membrane aliquots were diluted to a concentration of 1 µg/µL and 20 µL was taken per sample. PNGase (0.5 µL, 5U) or MilliQ was added and the samples were incubated 1 h at rt. Next, click mix was freshly prepared by adding together: 5 parts 100 mM $CuSO_4$ in MilliQ, 3 parts 1 M NaAsc in MilliQ, 1 part 100 mM THPTA in MilliQ and 1 part 100 µM Cy5-N_3 in DMSO. 2.28 µL of click mix was added per sample (final concentration Cy5-N_3: 1 µM in 1% DMSO in MilliQ) and the samples were shaken for 1 h at rt. 7.59 µL of 4x Laemmli buffer was added per sample and the samples were shaken for at least 1 h at rt. The samples were then loaded on gel (12.5% acrylamide) and run (180 V, 100 min). In-gel fluorescence was measured on a Bio-Rad Universal Hood III using Cy3 (605/50 filter) or Cy5 (695/55 filter) settings. Pageruler prestained protein ladder was used as molecular weight marker. After scanning, gels were either transferred to 0.2 µM PVDF blots (Bio-Rad) using a Bio-Rad Trans-Blot Turbo system (2.5 A, 7 min) or stained with Coomassie Brilliant Blue.

Western blot experiments

Blots were blocked for 1 h at rt in 5% BSA in TBST. Primary antibody RabbitαhA3AR (bs-1225R) 1:10.000 in 1% BSA in TBST was then added and the blots were incubated overnight at 4 °C. Blots were washed (3 x TBST) and incubated for 1 h at rt with secondary antibody goatαrabbit-HRP (115-035-003) 1:2.000 in 1% BSA in TBST. The blots were washed (2 x TBST and 1 x TBS) and activated by incubating 3 min in the dark using 1 mL of both reagents of Pierce™ ECL Western Blotting Substrate. Blots were scanned on chemiluminescence and fluorescence using the Bio-Rad Universal Hood III.

Data Analysis and statistics

Gel images were analyzed using Image Lab™ software version 6.0.1 (Bio-Rad). Quantification was done in the following manner: the area under the curve (AUC) of the bands was selected using the 'Lane Profile' tab and the adjusted volumes were taken. The adjusted volumes were then corrected for the amount of protein in each lane, using the adjusted total lane volumes of the Coomassie stained gels. The volume of the band at 55 kDa in the molecular weight marker (PageRuler Plus) was set to 100 (%) and the other bands were normalized accordingly. Further data analysis and statistics were carried out using Graphpad Prism. All given percentages are the mean values ± SEM of three individual experiments. Statistical analysis was performed using a one- or two-way ANOVA test with multiple comparisons (*** $p < 0.001$; ** $p < 0.01$; ns = not significant).

Confocal Microscopy Experiments

Probe binding and click reaction

CHOhA_3AR and CHO-K1 cells were cultured in a 96-well plate. Upon reaching a confluency of about 90%, the medium was replaced by medium containing PSB-11 (final concentration: 1 µM) or 1% DMSO (control) and the cells were pre-incubated for 30 min (37 °C and 5% CO_2). The medium was then replaced with medium containing LUF7960 (final concentration: 50 nM) or 1% DMSO (vehicle) and the cells were incubated for 60 min (37 °C and 5% CO_2). The cells were washed with PBS to remove unbound probe and afterwards fixed using a 4% PFA in 10% formalin solution (15 min, rt). The remaining fixative was removed by washing with PBS and subsequently with 20 mM glycine in PBS. The cells were permeabilized by incubation in 0.1% saponin in PBS (10 min, rt). Remaining saponin was removed by a PBS wash and the cells were stored at 4 °C until further usage. At the day of imaging, PBS was removed and the cells were incubated for 1 h in freshly prepared click mix (100 µL 100 mM $CuSO_4$ in MilliQ, 100 µL 1 M NaAsc in MilliQ, 100 µL mM THPTA in MilliQ, 9.66 mL HEPES pH 7.4 and 40 µL 1 mM TAMRA-N_3 in DMSO, added in the respective order). Remaining click mix was removed by washing with PBS, incubating for 30 min with 1% BSA in PBS and again washing with PBS. Cells were stored in 300 nM DAPI in PBS prior to imaging.

Image acquisition

Microscopy was performed on a Nikon Eclipse Ti2 C2+confocal microscope (Nikon, Amsterdam, The Netherlands) and this system included an automated xy-stage, an integrated Perfect Focus System (PFS) and 408 and 561 lasers. The system was controlled by Nikon's NIS software. All images were acquired using a 20x objective with 0.75 NA at a resolution of 1024x1024 pixels. The acquisition of 9 fields of view per well was done automatically using the NIS Jobs functionality. Representative images are shown in the figure and were created by using OMERO.[46]

Quantification

CellProfiler (version 2.2.0) was used to create a binary image of the DAPI channel and to propagate the cytoplasmic area based on the DAPI binary. An overlay of the binary cytoplasm/TAMRA channel was generated to quantify per segmented pixel the TAMRA intensity. The sum of these intensities in the cytoplasm mask is referred to as the integrated TAMRA intensity in the cytoplasm. Segmentation results were further processed using Excel while GraphPadPrism 9 was used for data visualization and statistics.

Flow Cytometry Experiments

Click reaction between LUF7960 and Cy5-N_3

Click mix was freshly prepared by combining in a 2 mL Eppendorf tube: 250 µL of 100 mM $CuSO_4$ in MilliQ, 150 µL of 1 M NaAsc in MilliQ, 50 µL of 100 mM THPTA in MilliQ and 50 µL of 50 µM Cy5-N_3 in DMSO, in the same respective order. Next, 500 µL of 2 µM LUF7960 in 1% DMSO in MilliQ was added and the mixture was incubated for 1 h at rt while shaking (1000 rpm). The mixture was desalted using a Waters Sep-Pak C18 column (WAT054945). Briefly, the mixture was loaded on the column and washed three times with 1 mL MilliQ. The product (LUF7960-Cy5) was then eluted using 1 mL of acetonitrile. The solvent was removed using an Eppendorf Concentrator Plus and the residue was dissolved in DMSO to obtain the stock concentrations of LUF7960-Cy5.

Flow cytometry experiments using CHO cells

CHOhA_3AR and CHO-K1 cells were cultured as mentioned above. The cells were detached using Trypsin and centrifuged (5 min, 1500 rpm). The pellet was dissolved in medium (1 mL), the cells were counted and the solution was diluted to 1.000.000 cells/mL. 100 µL of cell solution was added to each well of a 96-well plate. The plate was centrifuged (5 min, 1500 rpm) and the medium was replaced by medium containing PSB-11 (final concentration: 1 µM) or 1% DMSO (control). Cells were resuspended and incubated for 30 min (37 °C, 5% CO_2). The plate was centrifuged (5 min, 1500 rpm) and the medium was replaced by medium containing pre-clicked LUF7960-Cy5 (final concentration: 50 nM). Cells were resuspended and incubated for 1 h (37 °C, 5% CO_2). The plate was centrifuged (5 min, 1500 rpm), the medium was removed and 1% BSA in PBS containing rabbitαhA_3AR PE conjugate (1:500) was added. Cells were resuspended and incubated for 30 min at 4 °C. The cells were washed with 1% BSA in PBS to remove unbound probe and antibody and resuspended in 1% BSA in PBS. Cells were measured using a Cytoflex S (Beckman and Coulter, USA) and data was analyzed with FlowJo™ v10.0.7 (BD Life Sciences). The gating strategy is shown in Figure S3.

Purification of human granulocytes

Primary cells were isolated from human blood collected from healthy donors. Polymorphonuclear neutrophils (PMNs) were isolated using a Percoll gradient with a density of 1.076 g/ml.[55] Erythrocytes were lysed with isotonic $NH_4Cl/KHCO_3$, washed twice in PBS and resuspended in HEPES buffer (20 mM HEPES, 132 mM NaCl, 6.0 mM KCl, 1.0 mM $CaCl_2$, 1.0 mM $MgSO_4$, 1.2 mM KH_2PO_4, 5.5 mM glucose and 0.5% (w/v) human serum albumin, pH 7.4). Eosinophils were isolated from the PMNs as described before.[56]

Flow cytometry experiments using human granulocytes

100 µL of PMNs or purified eosinophils ($2 \cdot 10^6$ cells/mL) in HEPES buffer was incubated with 50 µL of PSB-11 (final concentration: 1 µM) or 1% DMSO (control) in HEPES buffer for 30 min at rt. 50 µL of pre-clicked LUF7960-Cy5 (final concentration: 50 nM) or 1% DMSO (vehicle) was added and the samples were incubated for 1 h at rt. The samples were then added to a 96 well-plate and centrifuged (5 min, 1500 rpm, 4 °C). The supernatant was removed and the pellet was suspended in a solution containing antibody (Siglec-8 PE conjugate 1:100) in 0.5% HSA in PBS. The samples were incubated for 30 min at 4 °C, centrifuged (5 min, 1500 rpm, 4 °C) and washed once with 0.5% HSA in PBS. The final pellet was suspended in 0.5% HSA in PBS. Cells were measured on a Canto II flow cytometer (BD, Franklin Lakes, NJ, USA) and analyzed with FACSDiva software. The gating strategy is shown in Figure S3.

Data analysis and statistics

Histograms (Figure 7B and D) were created using FlowJo. Further data analysis was performed using Graphpad Prism. MFI values shown are mean ± SEM from three individual experiments performed in duplicate (Figure 7A) or four individual experiments (Figure 7C). Statistical analysis was performed using a one-way ANOVA test with multiple comparisons (**** $p < 0.0001$; *** $p < 0.001$; ** $p < 0.01$; ns = not significant).

Computational Methods

Docking of the affinity-based probes in an hA_3AR homology model

The Alphafold model of the hA_3AR was retrieved from the GPCRdb.[35,36,57] This structure was prepared using the protein preparation wizard in Maestro (version 13.3, 2022-3, Schrödinger, LLC)[58] and the four compounds (compound **5**, **9** and **13** from this work and **17b** (LUF7602) from Yang et al.)[59] were prepared using LigPrep (Schrödinger, LLC).[60] Compound **17b** (LUF7602) was docked in the receptor model using the covalent binding protocol,[61] and consecutively energy minimized using MacroModel (Schrödinger, LLC). The alkyne moiety was introduced on each of the exit vectors in 3D and subsequently subjected to an energy minimization step using MacroModel. Each of the resulting energy minimized structures was visualized using PyMOL (The PyMOL Molecular Graphics System, version 1.2r3pre, Schrödinger, LLC).

Author Contributions

B.L.H.B., I.M.S. and J.S. synthesized compounds. R.L. performed radioligand displacement experiments. B.L.H.B. and J.S. performed SDS-PAGE experiments. W.J. performed molecular docking experiments. B.L.H.B. and S.L.D. performed confocal microscopy experiments. S.L.D. carried out confocal microscopy data analysis. B.L.H.B. and A.T.J.T. performed flow cytometry experiments and carried out flow cytometry data analysis. T.W.K., G.J.P.W., L.H.H., A.P.IJ. and D.v.d.E. supervised the project.

References

[1] B. B. Fredholm, A. P. IJzerman, K. A. Jacobson, K.-N. Klotz, J. Linden, *Pharmacol Rev* **2001**, *53*, 527–552.

[2] B. B. Fredholm, A. P. IJzerman, K. A. Jacobson, J. Linden, C. E. Müller, *Pharmacol Rev* **2011**, *63*, 1–34.

[3] A. P. IJzerman, K. A. Jacobson, C. E. Müller, B. N. Cronstein, R. A. Cunha, *Pharmacol Rev* **2022**, *74*, 340–372.

[4] L. Antonioli, P. Pacher, G. Haskó, *Trends Pharmacol Sci* **2022**, *43*, 43–55.

[5] C. Cekic, J. Linden, *Nat Rev Immunol* **2016**, *16*, 177–192.

[6] C. Mazziotta, J. C. Rotondo, C. Lanzillotti, G. Campione, F. Martini, M. Tognon, *Oncogene* **2022**, *41*, 301–308.

[7] Y. Kohno, J. Xiao-Duo, S. D. Mawhcrter, M. Koshiba, K. A. Jacobson, *Blood* **1996**, *88*, 3569–3574.

[8] B. A. M Walker, M. A. Jacobson, D. A. Knight, C. A. Salvatore, T. Weir, D. Zhou, T. R. Bai, *Am J Respir Cell Mol Biol* **1997**, *16*, 531–537.

[9] M. G. Bouma, T. M. M. A. Jeunhomme, D. L. Boyle, M. A. Dentener, N. N. Voitenok, F. A. J. M. van den Wildenberg, W. A. Buurman, *The Journal of Immunology* **1997**, *158*, 5400–5408.

[10] J. R. Fozard, H.-J. Pfannkuche, H.-J. Schuurman, *Eur J Pharmacol* **1996**, *298*, 293–297.

[11] D. van der Hoeven, T. C. Wan, J. A. Auchampach, *Mol Pharmacol* **2008**, *74*, 685–696.

[12] R. Corriden, T. Self, K. Akong-Moore, V. Nizet, B. Kellam, S. J. Briddon, S. J. Hill, *EMBO Rep* **2013**, *14*, 726–732.

[13] Y. Chen, R. Corriden, Y. Inoue, L. Yip, N. Hashiguchi, A. Zinkernagel, V. Nizet, P. A. Insel, W. G. Junger, *Science (1979)* **2006**, *314*, 1792–1795.

[14] K. F. Alsharif, M. R. Thomas, H. M. Judge, H. Khan, L. R. Prince, I. Sabroe, V. C. Ridger, R. F. Storey, *Vascul Pharmacol* **2015**, *71*, 201–207.

[15] K. A. Jacobson, S. Merighi, K. Varani, P. A. Borea, S. Baraldi, M. Aghazadeh Tabrizi, R. Romagnoli, P. G. Baraldi, A. Ciancetta, D. K. Tosh, Z.-G. Gao, S. Gessi, *Med Res Rev* **2018**, *38*, 1031–1072.

[16] C. T. Leung, A. Li, J. Banerjee, Z.-G. Gao, T. Kambayashi, K. A. Jacobson, M. M. Civan, *Purinergic Signal* **2014**, *10*, 465–475.

[17] C. K. Goth, U. E. Petäjä-Repo, M. M. Rosenkilde, *ACS Pharmacol Transl Sci* **2020**, *3*, 237–245.

[18] M. Jo, S. T. Jung, *Exp Mol Med* **2016**, *48*, e207.

[19] A. J. Vernall, L. A. Stoddart, S. J. Briddon, S. J. Hill, B. Kellam, *J Med Chem* **2012**, *55*, 1771–1782.

[20] E. Kozma, T. S. Kumar, S. Federico, K. Phan, R. Balasubramanian, Z.-G. Gao, S. Paoletta, S. Moro, G. Spalluto, K. A. Jacobson, *Biochem Pharmacol* **2012**, *83*, 1552–1561.

[21] E. Kozma, E. T. Gizewski, D. K. Tosh, L. Squarcialupi, J. A. Auchampach, K. A. Jacobson, *Biochem Pharmacol* **2013**, *85*, 1171–1181.

[22] A. J. Vernall, L. A. Stoddart, S. J. Briddon, H. W. Ng, C. A. Laughton, S. W. Doughty, S. J. Hill, B. Kellam, *Org Biomol Chem* **2013**, *11*, 5673–5682.

[23] L. A. Stoddart, A. J. Vernall, J. L. Denman, S. J. Briddon, B. Kellam, S. J. Hill, *Chem Biol* **2012**, *19*, 1105–1115.

[24] L. A. Stoddart, A. J. Vernall, S. J. Briddon, B. Kellam, S. J. Hill, *Neuropharmacology* **2015**, *98*, 68–77.

[25] S. Federico, E. Margiotta, S. Paoletta, S. Kachler, K.-N. Klotz, K. A. Jacobson, G. Pastorin, S. Moro, G. Spalluto, *Medchemcomm* **2019**, *10*, 1094–1108.

[26] S. Federico, E. Margiotta, S. Moro, E. Kozma, Z.-G. Gao, K. A. Jacobson, G. Spalluto, *Eur J Med Chem* **2020**, *186*, 111886.

[27] K. S. Toti, R. G. Campbell, H. Lee, V. Salmaso, R. R. Suresh, Z. G. Gao, K. A. Jacobson, *Purinergic Signal* **2022**, DOI 10.1007/s11302-022-09873-3.

[28] M. Macchia, F. Salvetti, S. Bertini, V. di Bussolo, L. Gattuso, M. Gesi, M. Hamdan, K.-N. Klotz, T. Laragione, A. Lucacchini, F. Minutolo, S. Nencetti, C. Papi, D. Tuscano, C. Martini, *Bioorg Med Chem Lett* **2001**, *11*, 3023–3026.

[29] D. Greenbaum, K. F. Medzihradszky, A. Burlingame, M. Bogyo, *Chem Biol* **2000**, *7*, 569–581.

[30] Y. Liu, M. P. Patricelli, B. F. Cravatt, *Proceedings of the National Academy of Sciences* **1999**, *96*, 14694–14699.

[31] X. Yang, J. P. D. Van Veldhoven, J. Offringa, B. J. Kuiper, E. B. Lenselink, L. H. Heitman, D. Van Der Es, A. P. IJzerman, *J Med Chem* **2019**, *62*, 3539–3552.

[32] V. V. Rostovtsev, L. G. Green, V. V. Fokin, K. B. Sharpless, *Angewandte Chemie - International Edition* **2002**, *41*, 2596–2599.

[33] C. W. Tornøe, C. Christensen, M. Meldal, *Journal of Organic Chemistry* **2002**, *67*, 3057–3064.

[34] G. Tomasello, I. Armenia, G. Molla, *Bioinformatics* **2020**, *36*, 2909–2911.

[35] J. Jumper, R. Evans, A. Pritzel, T. Green, M. Figurnov, O. Ronneberger, K. Tunyasuvunakool, R. Bates, A. Žídek, A. Potapenko, A. Bridgland, C. Meyer, S. A. A. Kohl, A. J. Ballard, A. Cowie, B. Romera-Paredes, S. Nikolov, R. Jain, J. Adler, T. Back, S. Petersen, D. Reiman, E. Clancy, M. Zielinski, M. Steinegger, M. Pacholska, T. Berghammer, S. Bodenstein, D. Silver, O. Vinyals, A. W. Senior, K. Kavukcuoglu, P. Kohli, D. Hassabis, *Nature* **2021**, *596*, 583–589.

[36] M. Varadi, S. Anyango, M. Deshpande, S. Nair, C. Natassia, G. Yordanova, D. Yuan, O. Stroe, G. Wood, A. Laydon, A. Žídek, T. Green, K. Tunyasuvunakool, S. Petersen, J. Jumper, E. Clancy, R. Green, A. Vora, M. Lutfi, M. Figurnov, A. Cowie, N. Hobbs, P. Kohli, G. Kleywegt, E. Birney, D. Hassabis, S. Velankar, *Nucleic Acids Res* **2022**, *50*, D439–D444.

[37] D. K. Tosh, M. Chinn, L. S. Yoo, D. W. Kang, H. Luecke, Z.-G. Gao, K. A. Jacobson, *Bioorg Med Chem* **2010**, *18*, 508–517.

[38] P. N. H. Trinh, D. J. W. Chong, K. Leach, S. J. Hill, J. D. A. Tyndall, L. T. May, A. J. Vernall, K. J. Gregory, *J Med Chem* **2021**, *64*, 8161–8178.

[39] B. L. H. Beerkens, Ç. Koç, R. Liu, B. I. Florea, S. E. Le Dévédec, L. H. Heitman, A. P. IJzerman, D. Van Der Es, *ACS Chem Biol* **2022**, *17*, 3131–3139.

[40] X. Yang, T. J. M. Michiels, C. de Jong, M. Soethoudt, N. Dekker, E. Gordon, M. van der Stelt, L. H. Heitman, D. van der Es, A. P. IJzerman, *J Med Chem* **2018**, *61*, 7892–7901.

[41] E.-M. Priego, J. von Frijtag Drabbe Kuenzel, A. P. IJzerman, M.-J. Camarasa, M.-J. Pérez-Pérez, *J Med Chem* **2002**, *45*, 3337–3344.

[42] W. Jespers, A. C. Schiedel, L. H. Heitman, R. M. Cooke, L. Kleene, G. J. P. van Westen, D. E. Gloriam, C. E. Müller, E. Sotelo, H. Gutiérrez-de-Terán, *Trends Pharmacol Sci* **2018**, *39*, 75–89.

[43] C. E. Müller, M. Thorand, R. Qurishi, M. Diekmann, K. A. Jacobson, W. L. Padgett, J. W. Daly, *J Med Chem* **2002**, *45*, 3440–3450.

[44] T. M. Palmer, J. L. Benovic, G. L. Stiles, *J Biol Chem* **1995**, *270*, 29607–29613.

[45] T. M. Palmer, G. L. Stiles, *Mol Pharmacol* **2000**, *57*, 539–545.

[46] C. Allan, J.-M. Burel, J. Moore, C. Blackburn, M. Linkert, S. Loynton, D. MacDonald, W. J. Moore, C. Neves, A. Patterson, M. Porter, A. Tarkowska, B. Loranger, J. Avondo, I. Lagerstedt, L. Lianas, S. Leo, K. Hands, R. T. Hay, A. Patwardhan, C. Best, G. J. Kleywegt, G. Zanetti, J. R. Swedlow, *Nat Methods* **2012**, *9*, 245–253.

[47] J. J. Reeves, C. A. Harris, B. P. Hayes, P. R. Butchers, M. J. Sheehan, *Inflammation Research* **2000**, *49*, 666–672.

[48] L. M. Gazoni, D. M. Walters, E. B. Unger, J. Linden, I. L. Kron, V. E. Laubach, *Journal of Thoracic and Cardiovascular Surgery* **2010**, *140*, 440–446.

[49] Y. Inoue, Y. Chen, M. I. Hirsh, L. Yip, W. G. Junger, *Shock* **2008**, *30*, 173–177.

[50] T. Amelia, J. P. D. van Veldhoven, M. Falsini, R. Liu, L. H. Heitman, G. J. P. van Westen, E. Segala, G. Verdon, R. K. Y. Cheng, R. M. Cooke, D. van der Es, A. P. IJzerman, *J Med Chem* **2021**, *64*, 3827–3842.

[51] P. K. Smith, R. I. Krohn, G. T. Hermanson, A. K. Mallia, F. H. Gartner, M. D. Provenzano, E. K. Fujimoto, N. M. Goeke, B. J. Olson, D. C. Klenk, *Anal Biochem* **1985**, *150*, 76–85.

[52] Y.-C. Cheng, W. H. Prusoff, *Biochem Pharmacol* **1973**, *22*, 3099–3108.

[53] A. Kourounakis, C. Visser, M. De Groote, A. P. IJzerman, *Biochem Pharmacol* **2001**, *61*, 137–144.

[54] A. Vlachodimou, H. de Vries, M. Pasoli, M. Goudswaard, S.-A. Kim, Y.-C. Kim, M. Scortichini, M. Marshall, J. Linden, L. H. Heitman, K. A. Jacobson, A. P. IJzerman, *Biochem Pharmacol* **2022**, *200*, 115027.

[55] A. J. Verhoeven, M. L. J. van Schaik, D. Roos, R. S. Weening, *Blood* **1988**, *71*, 505–507.

[56] L. Koenderman, P. T. M. Kok, M. L. Hamelink, A. J. Verhoeven, P. L. B. Bruijnzeel, *J Leukoc Biol* **1988**, *44*, 79–86.

[57] J. Caroli, A. Mamyrbekov, A. A. Kermani, **2023**, *51*, 395–402.

[58] G. Madhavi Sastry, M. Adzhigirey, T. Day, R. Annabhimoju, W. Sherman, *Journal of Computer-Aided Molecular Design* **2013**, *27*, 221–234.

[59] X. Yang, J. P. D. Van Veldhoven, J. Offringa, B. J. Kuiper, E. B. Lenselink, L. H. Heitman, D. Van Der Es, A. P. IJzerman, *J Med Chem* **2019**, *62*, 3539–3552.

[60] J. R. Greenwood, D. Calkins, A. P. Sullivan, J. C. Shelley, *Journal of Computer-Aided Molecular Design* **2010**, *24*, 591–604.

[61] K. Zhu, K. W. Borrelli, J. R. Greenwood, T. Day, R. Abel, R. S. Farid, E. Harder, *Journal of Chemical Information and Modeling* **2014**, *54*, 1932–1940.

Chapter 6

Development of a Ligand-Directed Probe to Label the Adenosine A_{2B} Receptor

Bert L.H. Beerkens, Vasiliki Andrianopoulou, Rongfang Liu, Laura H. Heitman, Adriaan P. IJzerman and Daan van der Es.

Abstract

Ligand-directed labeling is a biochemical technique that utilizes chemical probes to selectively conjugate protein targets to a detection moiety. Contrary to other probe molecules, e.g. covalent ligands and affinity-based probes, the pharmacophore of a ligand-directed probe does not bind covalently to the binding pocket of the target protein. Instead, during the labeling event, the directing-ligand acts as a leaving group, allowing novel methods to study protein activity. Recently, ligand-directed probes have been reported for multiple types of GPCRs, such as the adenosine A_{2A} receptor, cannabinoid receptor type 2 and metabotropic glutamate receptor 1. In this work, we show the development and evaluation of the first ligand-directed probes for the adenosine A_{2B} receptor (A_{2B}AR). Two probe molecules were synthesized, pharmacologically characterized and biologically evaluated, of which one showed selective labeling of the A_{2B}AR in SDS-PAGE experiments. Interestingly, activation of the A_{2B}AR has been linked to the proliferation of cancer cells, among other hallmarks of cancer. Targeting the A_{2B}AR with ligand-directed probes might therefore offer new opportunities to investigate A_{2B}AR activity in cancer cell lines and tissues.

Introduction

The Adenosine A_{2B} Receptor (A_{2B}AR) is a class A G Protein-Coupled Receptor (GPCR) that is activated through binding of the endogenous signaling molecule adenosine.[1] The A_{2B}AR belongs to the subfamily of Adenosine Receptors (ARs), other members being the Adenosine A_1, A_{2A} and A_3 receptors (A_1AR, A_{2A}AR and A_3AR).[2] The ARs are widely expressed throughout the human body and activation of an individual receptor is strongly dependent on cell and tissue type. In recent years, the A_{2A}AR and A_{2B}AR have attracted attention due to their immunosuppressive role in the tumor micro-environment, leading to the proliferation of cancerous cells.[3–5] Antagonizing of the A_{2A} and A_{2B} receptors is therefore an interesting new strategy to target the tumor micro-environment. In fact, multiple clinical trials are currently ongoing using either selective or dual antagonists to target A_{2A} and A_{2B} receptors in cancer pathologies.[2]

The A_{2A}AR has been extensively studied: the receptor has been purified and crystallized as one of the first GPCRs and therefore became a prototypical GPCR for structure-based studies.[6] The A_{2B}AR on the other hand, has been relatively poorly studied. Due to the low affinity of adenosine for the A_{2B}AR, the receptor has been presumed to be of less importance in physiological and pathological conditions. This idea is changing however, as more and more research is being carried out to decipher the function of the A_{2B}AR. The increase in popularity is reflected in the recent elucidation of the A_{2B}AR three-dimensional structure,[7,8] as well as the surge of chemical tools to study the A_{2B}AR, such as PET tracers,[9–11] fluorescent ligands,[12–14] and covalent ligands.[15,16]

A wide variety of chemical and biological probe molecules has been developed to selectively target and detect GPCRs. Besides PET tracers, fluorescent ligands and covalent ligands, these include antibodies and affinity-based probes.[17–19] Of our particular interest are the affinity-based probes, that contain both an electrophilic and a reporter group on the same molecular scaffold. Together, these groups allow detection of GPCRs in an extended amount of biochemical assay types, as we recently have shown for the A_1AR, A_{2A}AR and A_3AR.[20–22] Next to affinity-based probes, also 'ligand-directed probes' are being developed as novel interrogators of GPCR function.

The idea behind ligand-directed chemistry, developed in the lab of Hamachi, is to selectively donate a functional group to a protein target of interest (POI) using mild electrophiles.[23–25] In brief, a high affinity ligand is conjugated to an electrophile and a reporter group, e.g. a fluorophore, biotin or a click handle. Upon binding of the ligand into the binding pocket of the POI, a nucleophilic amino acid residue in close proximity will attack the electrophilic group, leading to cleavage of the molecule and substitution of the reporter group onto the POI (Figure 1). A big advantage of this technique, as compared to fluorescent ligands and affinity-based probes, is that the ligand itself can leave the binding pocket after covalent donation of the reporter group. This allows new ways to study native proteins, e.g. by activating or blocking the POI after labeling by the probe.

Multiple GPCR-targeting ligand-directed probes have been developed over the past few years, e.g. for the bradykinin B_2 receptor (B_2R),[27] A_{2A}AR,[28,29] metabotropic glutamate receptor 1 ($mGlu_1$R),[30] μ opioid receptor (MOR),[31] cannabinoid receptor type 2 (CB_2R),[32] dopamine D1 receptor (D_1R),[33] and smoothened receptor (SMOR).[34] Most interestingly, one of the ligand-directed probes for the A_{2A}AR has been used to selectively label the A_2AR in a breast cancer cell line,[29] while other ligand-directed probes have already been used to label endogenous $mGlu_1$R and MOR in rodent brain slices.[30,31]

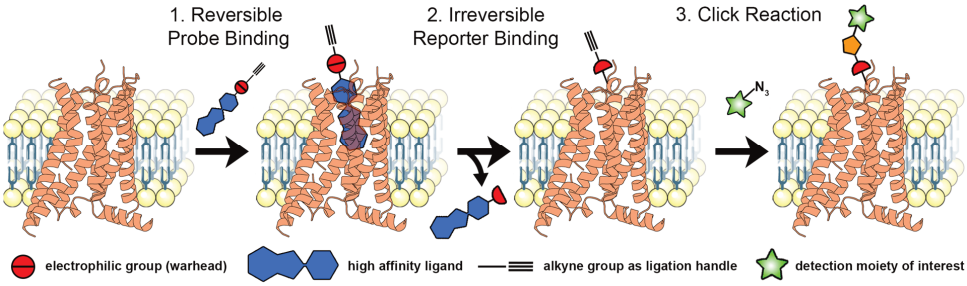

Figure 1. Labeling of GPCRs with ligand-directed probes. First, the probe binds to the receptor through its conjugated high affinity ligand. A nucleophilic amino acid residue then attacks the electrophilic group of the probe, inducing cleavage between the ligand and the reporter. The reporter group, e.g. a fluorophore, biotin or click handle, is now covalently bound to the receptor, while the ligand is allowed to leave the binding pocket (reversible mode of binding). This figure was partly created with Protein Imager,[26] using the structure of the A_{2B}AR (PDB: 8HDO).

In this study, we aim to expand the toolbox of ligand-directed probes for GPCRs by the development of A_{2B}AR-targeting probes. We show the synthesis and evaluation of ligand-directed probes for the A_{2B}AR, as well as labeling of the receptor in SDS-PAGE experiments. Altogether this will allow future investigations towards the detection of native A_{2B}AR in a multitude of biochemical assay types.

Results and Discussion

Design of the A_{2B}AR ligand-directed probes

In chapter 3 we reported on a xanthine-based compound, LUF7982, that covalently binds to the A_{2B}AR through a reaction of the attached fluorosulfonyl group with presumably a lysine residue (Scheme 1A).[15,16] The location of the fluorosulfonyl group on the xanthine scaffold thus is a valid position for the implementation of an electrophilic group for ligand-directed chemistry. Next to that, Tamura *et al.* have recently reported on the use of an *N*-acyl *N*-alkyl sulfonamide (NASA) group for the selective alkylation of a lysine residue on the folate receptor (Scheme 1B).[25] As the NASA group is based around the sulfonyl moiety, we envisioned that transforming the fluorosulfonyl group of LUF7982 into a NASA group would yield the first candidate A_{2B}AR ligand-directed probes (Scheme 1C). To increase the electrophilicity of the acyl group, Tamura *et al.* substituted various electron withdrawing groups onto the sulfonamide moiety (R_2-position),[25] of which the cyano group showed to be superior in terms of reaction kinetics. Therefore we also incorporated a cyano group into the design of our A_{2B}AR-targeting probes. For detection of the receptor, we chose to introduce an alkyne group at the R_3-position. This allows the usage of copper-catalyzed click chemistry to 'click' any reporter group of interest onto the alkylated receptor, without having to incorporate a bulky fluorophore in the design of the ligand.[35,36] Lastly, we varied the length of the alkyl linker between the NASA and the alkyne group, as linker length might influence affinity, reactivity and stability of the compounds. We have therefore synthesized probes containing either a 'short' 3-carbon linker, or a 'long' 8-carbon linker.

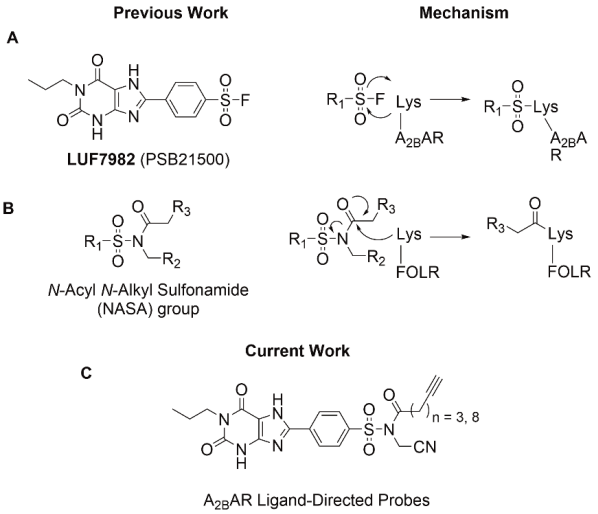

Scheme 1. (A) Molecular structure of the previously synthesized covalent antagonist LUF7982 (PSB21500) and its presumable mode of action at the A_{2B}AR; (B) Molecular structure of the *N*-acyl *N*-alkyl sulfonamide (NASA) group and its mode of action at the Folate Receptor (FOLR); (C) Design of the compounds synthesized in this work.

Synthesis of the A_{2B}AR ligand-directed probes

Synthesis of the two ligand-directed probes started with nitrosylated uracil **1**, synthesized as described in chapter 3.[15] The nitroso group was reduced with PtO_2 and H_2 (g) to obtain amine **2**,[37] which was used directly in a peptide coupling with 4-fluorosulfonyl benzoic acid and EDC·HCl to form amide **3** (Scheme 2). Trimethyl polyphosphate (PPSE) was used as condensating agent for the cyclization of uracil **3** to xanthine **4** (LUF7982),[38] and the fluorosulfonyl group was transformed into a sulfonamide group using aqueous ammonium hydroxide (28-30%). Sulfonamide **5** was used in the subsequent peptide couplings without further purifications and coupled to either 5-hexynoic acid or 10-undecynoic acid using EDC·HCl, DMAP and DIPEA to yield sulfonamides **6** and **8**. Up until this step crystallization was the purification method of preference, as the poor solubility of the xanthine compounds hindered purification by column chromatography. Lastly, the cyano moiety was introduced. Iodoacetonitrile, as used in other syntheses,[25] showed to be too reactive for this step, resulting in oversubstitution at the secondary amines of **6** and **8**. Therefore the milder bromoacetonitrile was used, yielding ligand-directed probes **7** (LUF8019) and **9** (LUF8023).

Stability of the synthesized compounds

Prior to investigating labelling of the A_{2B}AR by the synthesized ligand-directed probes, we investigated the stability of the compounds in aqueous buffer, as well as standard cell culture medium. Probes **7** (LUF8019) and **9** (LUF8023) were added to the buffer or medium, shaken and measured at different time points by LC-MS. Probes **7** (LUF8019) and **9** (LUF8023) were not susceptible towards hydrolysis, as only minor degradation was observed upon incubation in PBS buffer (Figure 2A). This corresponds to the previously observed hydrolytic stability of the NASA group.[25] However, upon incubation in cell culture medium, both **7** (LUF8019) and **9** (LUF8023) were eventually degraded to a compound with an m/z of 389 $[M+H]^+$ (Figure 2B), corresponding to the molecular weight of dealkylated product **10**. The observed bond cleavage is presumably the result of a reaction between the electrophilic NASA group and nucleophiles within the cell culture medium. Other teams have not reported on the susceptibility of the NASA

group towards nucleophiles other than the target proteins.[25,32] This might be due to a lack of investigation or differences in molecular structure. To prevent such unwanted side-reactions, we avoided the use of cell culture medium in all the subsequent experiments.

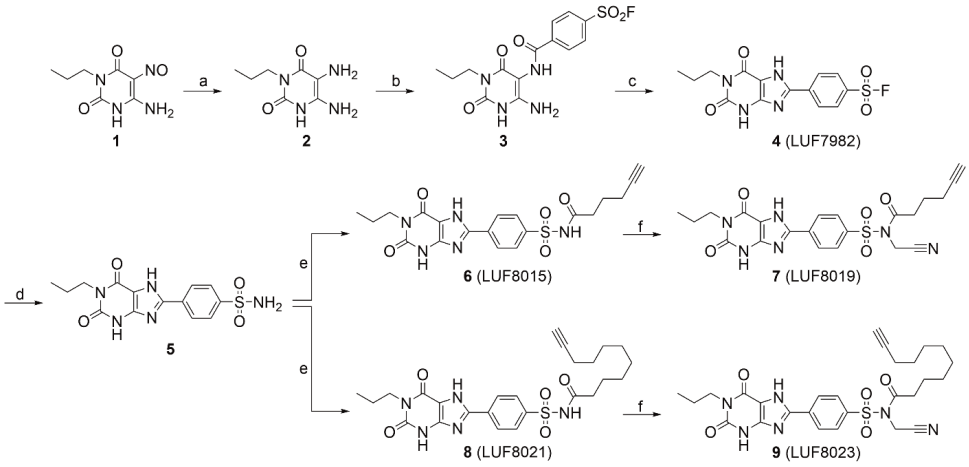

Scheme 2. (A) Molecular structures of the previously synthesized covalent A_{2B}AR antagonist LUF7982 (PSB21500), the NASA warhead, and the design of our ligand-directed probes. (B) Reagents and conditions. (a) PtO_2, H_2 (g), MeOH, RT, 1 h; (b) EDC·HCl, dry DMF, RT, 3 h, 62%; (c) PPSE, 180 °C, 3 h, 87%; (d) NH_4OH (28-30%), RT, 2 h, 75%; (e) EDC·HCl, respective benzoic acid, DMAP, DIPEA, dry DMF, RT, overnight, 41-64%; (f) Bromoacetonitrile, DIPEA, RT, 6-8 days, 12-41%.

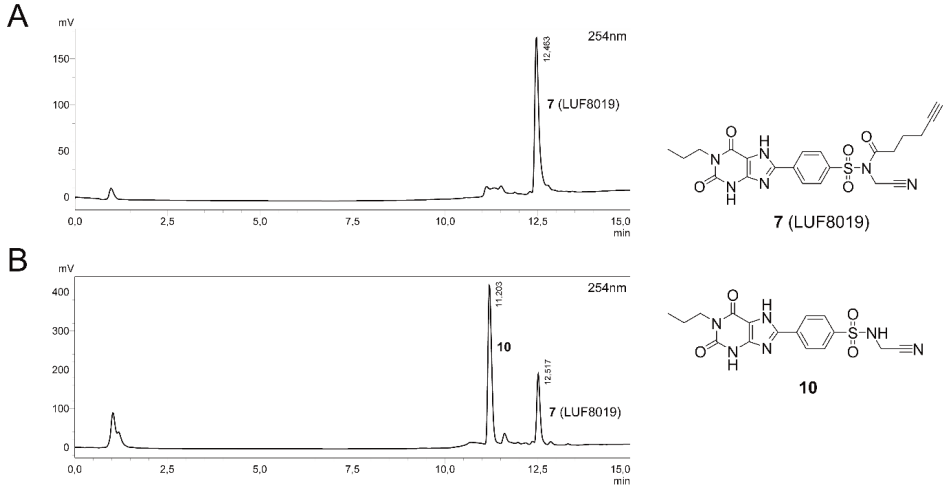

Figure 2 Investigation of probe stability in buffer and medium. Probe **7** (LUF8019) and **9** (LUF8023) were added to (A) PBS buffer or (B) DMEM/F12 medium containing 10% (v/v) newborn calf serum. Samples were shaken for 2 h at rt and afterwards measured by LC-MS. The LC-MS spectra of **7** (LUF8019) are shown as example.

Affinity towards the A_{2B}AR

First, to investigate the ability of the synthesized probes to bind to the A_{2B}AR, radioligand displacement assays were carried out. Control compounds **6** and **8**, lacking the cyano moiety, were included in these assays and a concentration range from 0.1 to 1000 nM of probe was chosen. Two different conditions were investigated: with and without 4 hours of pre-incubation between A_{2B}AR and ligand, prior to addition of radioligand. Using this assay setup, we have observed in chapters 3,4 and 5 that a time-dependent increase in affinity (pre-0h to pre-4h) is a strong indication of a covalent mode of binding.[15,20,39] All synthesized probes showed a decent to good affinity towards the A_{2B}AR, ranging from sub-micromolar (**6**) to double- (**7**-**8**) and single- (**9**) digit nanomolar values at pre-0h (Table 1). Of the four ligands, only **9** (LUF8023) showed to bind with similar strong affinity as **4** (LUF7982). However, contrary to covalent antagonist **4** (LUF7982), none of the synthesized ligands showed a significant time-dependent increase in affinity upon four hours of pre-incubation. This corresponds to the general idea of the ligand-directed probes, being able to leave the binding pocket after donation of the reporter group. Interestingly, compound **9** (LUF8023) showed a decrease in affinity upon 4 hours of pre-incubation. There are multiple possible explanations for this, for example, **9** (LUF8023) might have a higher affinity towards the A_{2B}AR than its cleaved product (**10**), or the donated alkyl group might influence binding of the ligand or radioligand to the A_{2B}AR. To investigate subtype selectivity of the synthesized probes, single point radioligand displacement experiments were carried out on the other adenosine receptors (Table 1). Most of the synthesized compounds showed poor binding to the other ARs (<50% displacement), while only control compound **8** (LUF8021) showed a strong displacement (82%) at the A_1AR. The actual ligand-directed probes **7** (LUF8019) and **9** (LUF8023) thus are selective towards the A_{2B}AR over the other ARs.

Table 1. Radioligand displacement of the synthesized ligand-directed probes on the four adenosine receptors.

	pK_i (pre-0h)[a]	pK_i (pre-4h)[b]	Displacement at 1 µM (%)		
Compound	A_{2B}AR	A_{2B}AR	A_1AR[c]	A_{2A}AR[d]	A_3AR[e]
4 (LUF7982)[f]	8.10 ± 0.06	9.17 ± 0.12**	29 (28, 30)	52 (59, 46)	7 (11, 3)
6 (LUF8015)	6.44 ± 0.06	6.60 ± 0.10	19 (21, 17)	9 (6, 12)	-5 (-8, -2)
7 (LUF8019)	7.31 ± 0.05	7.44 ± 0.12	34 (30, 38)	40 (35, 45)	-2 (-8, 5)
8 (LUF8021)	7.26 ± 0.07	7.51 ± 0.06	82 (82, 81)	0 (-3, 3)	6 (-2, 14)
9 (LUF8023)	8.22 ± 0.10	7.75 ± 0.08*	46 (46, 46)	27 (15, 38)	-9 (-14, -3)

[a] Apparent affinity determined from displacement of specific [^{3}H]PSB-603 binding on CHO-spap cell membranes stably expressing the hA_{2B}AR at 25 °C after 0.5 h of co-incubating probe and radioligand. [b] Apparent affinity determined from displacement of specific [^{3}H]PSB-603 binding on CHO-spap cell membranes stably expressing the hA_{2B}AR at 25 °C after 4 h of pre-incubation with the respective probe, followed by an additional 0.5 h of co-incubation with radioligand. [c] % specific [^{3}H]DPCPX displacement by the respective probe on CHO cell membranes stably expressing the hA_1AR at 25 °C after 0.5 h of co-incubating probe and radioligand; [d] % specific [^{3}H]ZM241385 displacement by the respective probe on HEK293 cell membranes stably expressing the hA_{2A}AR at 25 °C after 0.5 h of co-incubating probe and radioligand; [e] % specific [^{3}H]PSB11 displacement by the respective probe on CHO cell membranes stably expressing hA_3AR at 25 °C after 0.5 h of co-incubating probe and radioligand. [f] Values obtained from previous experiments.[15] Data represent the mean ± SEM of three individual experiments performed in duplicate [a-b] or the mean of two individual experiments performed in duplicate [c-e]. *$p < 0.05$, **$p < 0.01$ compared to the pKi values at pre-0h, determined by a two-tailed unpaired Student's t-test.

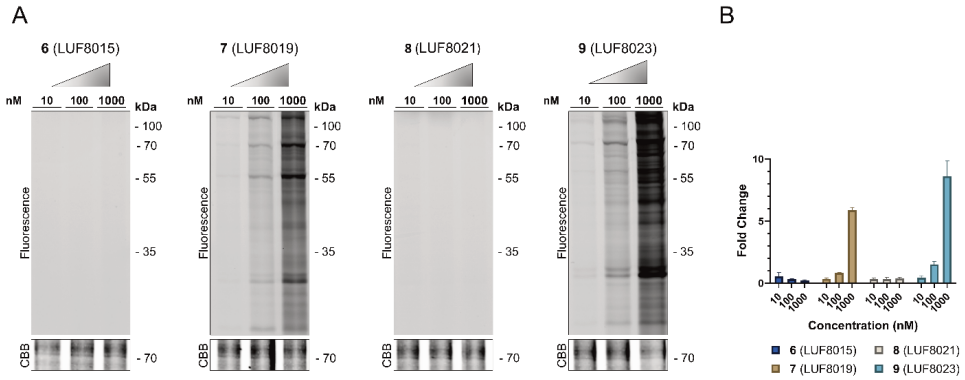

Figure 3 Ligand-directed labelling of the respective ligand-directed probes in CHO-A_{2B}AR-spap membrane fractions. CHO-spap membrane fractions with stable expression of the A_{2B}AR were incubated for 2 h with probes **6** (LUF8015), **7** (LUF8019), **8** (LUF8021) or **9** (LUF8023). Probe-bound proteins were clicked to Cy5-N_3, denatured and resolved by SDS-PAGE. Gels were imaged by in-gel fluorescence. Coomassie Brilliant Blue (CBB) staining was used as loading control. (B) Quantification of the lane intensities. The lane intensities were taken and corrected for the observed amount of protein per lane upon Coomassie staining. The PageRuler Plus ladder (not shown) was used as reference lane and fold changes were calculated relative to this lane (adjusted intensity lane/adjusted intensity reference lane). The mean values ± SEM of three individual experiments are shown.

Labelling of the A_{2B}AR in SDS-PAGE experiments

Finally, the probes were evaluated for their ability to label the A_{2B}AR in SDS-PAGE experiments. In an initial screen probes **7** (LUF8019) and **9** (LUF8023) as well as control compounds **6** (LUF8015) and **8** (LUF8021) were investigated for their ability to label proteins in membrane fractions derived from A_{2B}AR-expressing Chinese hamster ovary (CHO) cells. The membrane fractions were incubated with 10, 100 or 1000 nM of the respective probes, clicked to a Cy5 fluorophore, denatured and resolved by SDS-PAGE. Ligand-directed probes **7** (LUF8019) and **9** (LUF8023) labelled multiple proteins at concentrations ≥10 nM (Figure 3A), while no labelling was observed for control compounds **6** (LUF8015) and **8** (LUF8021), indicating that the cyano substitution is necessary to enhance the electrophilicity of the *N*-acyl group. Additionally, probes **7** (LUF8019) and **9** (LUF8023) show unwanted off-target labelling. In case of the electrophilic probes for the A_1AR and the A_3AR (chapters 4 and 5), we also observed off-target labelling in membrane-derived samples, however not in cellular assays.[20,22] We therefore moved towards cellular assays in our endeavors to label the A_{2B}AR. For these experiments, we chose a probe concentration of 100 nM as a balance between a low (10 nM) and high (1000 nM) degree of protein labeling (Figure 3B).

Live CHO cells with and without stable expression of the A_{2B}AR were first pre-incubated with 1 µM competing ligand and then incubated with 100 nM of ligand-directed probe **7** (LUF8019) or **9** (LUF8023) in Hank's Balanced Salt Solution (HBSS). Non-bound probe was washed away and membrane fractions were collected. Probe-bound proteins were clicked to Cy5-N_3. Samples were then denatured, loaded on SDS-PAGE and the gels were visualized using in-gel fluorescence. Probe **7** (LUF8019) showed clear labelling of one protein, visible as a smear at about 60 kDa (Figure 4A). This protein was absent in the control lanes (without A_{2B}AR or probe) and therefore presumably the A_{2B}AR. Removal of N-glycans through PNGase showed a strong reduction in molecular weight of the observed band, towards a molecular weight that more closely resembles the weight of the A_{2B}AR (36 kDa). A similar pattern of bands has also been observed in western blot experiments and characterized as being the A_{2B}AR.[40–42] Upon pre-incubation with covalent antagonist **4** (LUF7982) the observed fluorescent signal was

significantly reduced (Figure 4B). The partial agonist BAY60-6583 and antagonist PSB1115 however did not significantly reduce A_{2B}AR labelling by probe **7** (LUF8019). Presumably their reversible mode of binding, in combination with sub-micromolar affinities for the A_{2B}AR (212 and 53 nM respectively)[43,44] allow occasional binding of the ligand-directed probe and subsequent labeling of the receptor. Contrary to probe **7** (LUF8019), ligand-directed probe **9** (LUF8023) did not show any specific labelling of the A_{2B}AR (Figure 4C). An increased reactivity of the probe, resulting in faster cleavage of the NASA group, may be the reason for this observation.

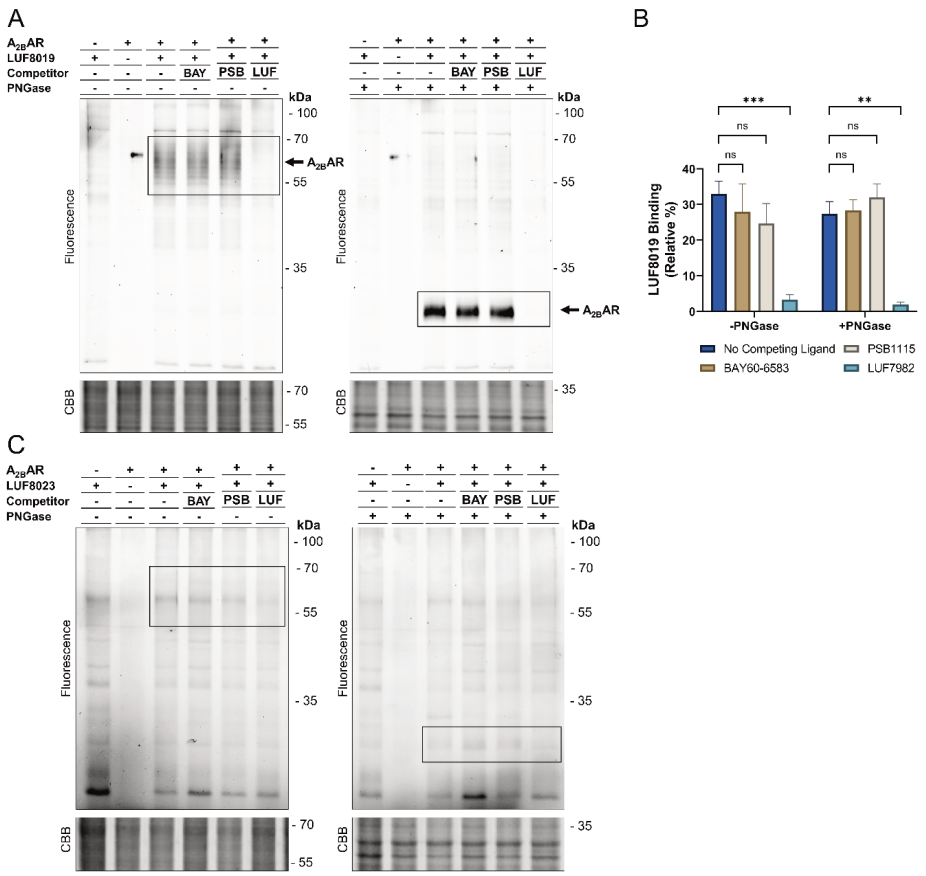

Figure 4 Ligand-directed labelling of the A_{2B}AR in and live CHO cells. CHO-spap cells with or without (lane 1) stable expression of the A_{2B}AR were pre-incubated for 30 min with 1 µM antagonist in medium (BAY60-6583 (BAY), PSB1115 (PSB) or **4** (LUF7982; LUF) and subsequently incubated for 2 h with 100 nM probe (LUF8019 or LUF8023) in HBSS. Cells were washed with PBS and membranes were collected. N-glycans were removed using PNGase (5 U) and alkyne moieties were clicked to 1 µM Cy5-N_3. The samples were then denatured using Laemmli buffer and resolved by SDS-PAGE. Gels were imaged by in-gel fluorescence. Coomassie Brilliant Blue (CBB) staining was used as loading control. (A) Protein labeling by LUF8019. (B) Quantification of A_{2B}AR labelling by LUF8019. The band intensities were taken and corrected for the observed amount of protein per lane upon Coomassie staining. The band at 55 kDa of the PageRuler Plus ladder (not shown) was set to 100% for each gel and band intensities were calculated relative to this band. The mean values ± SEM of three individual experiments are shown. Significance was calculated using a two-way ANOVA test with multiple comparisons; (C) Protein labeling by LUF8023. All shown gels are representatives of the experiments performed with n=3.

Altogether, of the two synthesized ligand-directed probes **7** (LUF8019) was able to selectively label the A_{2B}AR in CHO cells. Looking at the ligand-directed probes developed for the A_{2A}AR, slight differences in molecular structure already seem to cause different modes of binding. Probes bearing a 2-nitrophenyl ester fully blocked the orthosteric binding pocket in radioligand displacement assays, likely occupying the A_{2A}AR in a covalent fashion.[28] On the contrary, a 2-fluorophenyl ester-containing probe successfully labelled endogenous A_{2A}AR.[29] The latter probe was studied in functional assays to measure receptor activation after labelling. Activation of the A_{2A}AR was achieved after 16 h of incubation, indicating full dissociation of the released ligand. The 2-fluorophenyl ester probe thus seems to bind and label the A_{2A}AR in a ligand-directed manner, although with slow binding kinetics. To overcome such long incubation times, the NASA group has been developed and implemented as electrophile with fast kinetics.[25] This strategy yielded successful ligand-directed probes for the CB_2R, as shown in flow cytometry and confocal microscopy experiments.[32] However, dissociation of the released ligands from their binding pockets has not been confirmed in these studies. Such experiments would therefore be a first step towards further characterization of the herein presented ligand-directed probes for the A_{2B}AR.

Conclusion

In summary, we show here the development of the first ligand-directed probe for the A_{2B}AR. Two probes and two control compounds were synthesized, all showing a good affinity and selectivity towards the A_{2B}AR in radioligand displacement assays. Both ligand-directed probes labelled proteins upon incubation in CHO membrane fractions, while only one of the two probes, **7** (LUF8019), showed specific labelling of the A_{2B}AR in live CHO cells. Labelling of the A_{2B}AR could be prevented by pre-incubation with a covalent antagonist, but not by reversible A_{2B}AR ligands. Changing the assay conditions, e.g. by increasing the amount of competing ligand, increasing the competing ligand incubation time or decreasing the probe incubation time, might lead to a stronger competition by the reversible ligands for the A_{2B}AR binding pocket. Probe **9** (LUF8023) on the other hand, did not label the A_{2B}AR in live CHO cells. Altogether, this data suggests ligand-directed probe **7** (LUF8019) to be a valid tool to “tag” the A_{2B}AR.

The ability to click a fluorophore or a biotin moiety onto the receptor, together with the ability of the ligand to dissociate after donation of the reporter group, allows the investigation of agonist-induced activation of the receptor. For example, internalization and subcellar localization of the receptor might be studied with aid of ligand-directed probe **7** (LUF8019). We are currently investigating the optimal assay conditions that allow us to perform such experiments with probe **7** (LUF8019).

Experimental

Chemistry

General

All reactions were performed using commercially available chemicals and solvents, purchased via Sigma-Aldrich (Merck), VWR chemicals and Thermo Scientific. All reactions were carried out under an N_2 atmosphere and at room temperature, unless noted otherwise. Thin layer chromatography (TLC) was carried out using TLC Silica Gel 60 F254 (Merck) and visualized using UV irradiation at wavelengths of 254 and 366 nM. ^{1}H, ^{13}C and ^{19}F NMR spectra were recorded on a Bruker AV-400 (400 MHz) or Bruker AV-500 (500 MHz) spectrometer. Chemical shift values are reported in parts per million (ppm) and designated by δ. Tetramethylsilane or solvent resonance was used as internal standard. Coupling constants (J) are reported in Hertz (Hz) and multiplicities are indicated by s (singlet), bs (broad singlet), d (doublet), t (triplet), td (triplet of doublets), p (pentuplet), h (hexuplet) or m (multiplet). Compound purity was determined by HPLC-MS, using a LCMS-2020 system coupled to a Gemini® 3 µm C18 110Å column (50 x 3 mm). Samples were dissolved in H_2O:MeCN:*t*-BuOH 1:1:1, injected onto the column and eluted with a gradient of H_2O:MeCN 9:1 + 1% formic acid to H_2O:MeCN 1:9 + 1% formic acid over the course of 15 minutes. High-resolution mass spectrometry (HRMS) measurements were done on a X500R QTOF mass spectrometer (SCIEX).

Synthesis of ligand-directed probes

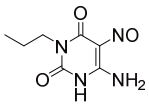

6-Amino-5-nitroso-3-propylpyrimidine-2,4(1H,3H)-dione (1)
Compound **1** was synthesized as described in chapter 3.

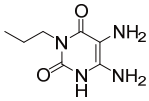

5,6-Diamino-3-propylpyrimidine-2,4(1*H*,3*H*)-dione (2)[37]
Uracil derivative **1** (2.00 g, 10.09 mmol, 1.0 eq) was dissolved in MeOH (80 mL) and PtO_2 (40 mg) was added to the flask. The flask was flushed once with N_2 (g), twice with H_2 (g) and then kept under H_2 (g) for hydrogenation. After 1 h, a gray solid was formed. DCM (500 mL) was added to the flask and the mixture was filtered over Celite. The filtrate was concentrated under reduced pressure to yield quantitative **2** as orange/brown solid. To prevent degradation, compound **2** was used in the next steps without further purifications.

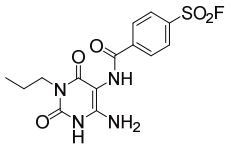

4-((6-Amino-2,4-dioxo-3-propyl-1,2,3,4-tetrahydropyrimidin-5-yl)carbamoyl)benzenesulfonyl fluoride (3)

EDC·HCl (2.01 g, 10,5 mmol, 1.2 eq) was added to a solution of diamine **2** (1.97 g, 9.63 mmol, 1.1 eq) in dry DMF (44 mL). After stirring for 3 h, EtOAc (250 mL) was added and the organic layer was washed with H_2O (250 mL), dried over $MgSO_4$, filtered and concentrated under reduced pressure. The compound was recrystallized overnight using MeOH/EtOAc to yield **3** as an orange solid (2.30 g, 6.20 mmol, 62%). **^{1}H NMR** (500 MHz, $(CD_3)_2SO$) δ [ppm] = 10.55 (s, 1H), 9.30 (s, 1H), 8.27 (s, 4H), 6.26 (s, 2H), 3.66 (t, *J* = 7.3 Hz, 2H), 1.50 (h, *J* = 7.5 Hz, 2H), 0.84 (t, *J* = 7.5 Hz, 3H). **^{19}F NMR** (471 MHz, $(CD_3)_2SO$) δ [ppm] = 66.0.

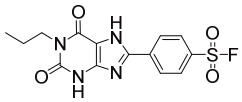

4-(2,6-Dioxo-1-propyl-2,3,6,7-tetrahydro-1*H*-purin-8-yl)benzenesulfonyl fluoride (4)

Trimethylsilyl polyphosphate (PPSE) (31 mL) was added to compound **3** (2.30 g, 6.20 mmol, 1.0 eq) and the mixture was brought to 180 °C under reflux conditions. The formed solution was stirred for 3 h and afterwards cooled down to room temperature, followed by cooling on ice. MeOH (200 mL) was added and the mixture was stirred for 5 min. The mixture was filtered and the residue was washed with MeOH (100 mL), collected and dried under vacuum to yield **4** (1.90 g, 5.39 mmol, 87%) as an off-white powder. **^{1}H NMR** (500 MHz, $(CD_3)_2SO$) δ [ppm] = 14.24 (s, 1H), 12.04 (s, 1H), 8.44 (d, *J* = 8.7 Hz, 2H), 8.28 (d, *J* = 8.7 Hz, 2H), 3.91 – 3.77 (m, 2H), 1.58 (h, *J* = 7.5 Hz, 2H), 0.88 (t, *J* = 7.5 Hz, 3H). **^{19}F NMR** (471 MHz, $(CD_3)_2SO$) δ [ppm] = 66.2.

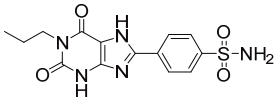

4-(2,6-Dioxo-1-propyl-2,3,6,7-tetrahydro-1*H*-purin-8-yl)benzenesulfonamide (5)

Sulfonyl fluoride **4** (1.6 g, 4.54 mmol, 1.0 eq) was dissolved in 28-30% ammonia solution (23 mL) and stirred for 2 h. The reaction mixture was then quenched and acidified by dropwise addition of 6 M HCl (60 mL). The product was crystallized overnight and the residue was collected by vacuum filtration. To remove impurities, the residue was dissolved in 0.5 M NaOH (75 mL) and the aqueous mixture was washed using 100 mL of 5% MeOH in $CHCl_3$. The pH was then brought to ~2 using 6 M HCl and the product was allowed to crystallize overnight. The residue was collected by vacuum filtration and dried under vacuum to yield **5** (1.19 g, 3.40 mmol, 75 %) as a purple solid, which was used in the next steps without further purification. **^{1}H NMR** (400 MHz, $(CD_3)_2SO$) δ [ppm] = 11.78 (bs, 1H), 8.21 (d, *J* = 8.6 Hz, 2H), 7.87 (d, *J* = 8.3 Hz, 2H), 7.41 (s, 2H), 3.81 (t, *J* = 7.5 Hz, 2H), 1.56 (h, *J* = 7.6 Hz, 2H), 0.87 (t, *J* = 7.4 Hz, 3H).

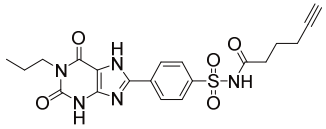

***N*-((4-(2,6-Dioxo-1-propyl-2,3,6,7-tetrahydro-1*H*-purin-8-yl)phenyl)sulfonyl)hex-5-ynamide (6) (LUF8015)**

5-hexynoic acid (98 µL, 0.89 mmol, 1.6 eq), EDC·HCl (316 mg, 1.65 mmol, 3.0 eq), DMAP (20 mg, 0.17 mmol, 0.3 eq) and DIPEA (290 µL, 1.66 mmol, 3.0 eq) were added to a solution of sulfonamide **5** (192 mg, 0.55 mmol,1.0 eq) in dry DMF (6 mL) and the mixture was stirred overnight. EtOAc (50 mL) was added and the organic layer was washed with H_2O (3 x 50 mL). As the product resided in the aqueous layer, the aqueous layers were combined and the pH was brought to ~2 using 6 M HCl. The product was allowed to crystallize overnight and collected by vacuum filtration. The filtrate was recrystallized and the second residue was collected by vacuum filtration. The residues were combined and purified using column chromatography (DCM:MeOH 98:2→93:7) to yield **6** (101 mg, 0.03 mmol, 41%) as an off-white solid. **^{1}H NMR** (500 MHz, $(CD_3)_2SO$) δ [ppm] = 14.03 (s, 1H), 11.99 (s, 1H), 8.28 (d, *J* = 8.7 Hz, 2H), 8.00 (d, *J* = 8.7 Hz, 2H), 3.82 (t, *J* = 7.3 Hz, 2H), 2.76 (t, *J* = 2.6 Hz, 1H), 2.32 (t, *J* = 7.4 Hz, 2H), 2.08 (td, *J* = 7.1, 2.7 Hz, 2H), 1.61 – 1.53 (m, 4H), 0.88 (t, *J* = 7.4 Hz, 3H). **^{13}C NMR** (126 MHz, DMSO) δ 172.2, 155.5, 151.5, 148.6, 148.1, 141.0, 133.7, 128.7, 127.2, 109.1, 84.2, 72.3, 42.0, 34.9, 23.4, 21.4, 17.5, 11.7. **HRMS** (ESI, m/z): $[M+H]^+$, calculated: 444.1336, found: 444.1308. **HPLC** 97%, RT 8.797 min.

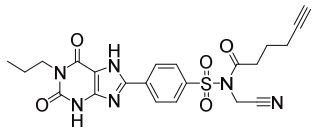

***N*-(Cyanomethyl)-*N*-((4-(2,6-dioxo-1-propyl-2,3,6,7-tetrahydro-1*H*-purin-8-yl)phenyl)sulfonyl)hex-5-ynamide (7) (LUF8019)**

Bromoacetonitrile (8 µL, 0.11 mmol,1.2 eq) was added to a solution of **6** (43 mg, 0.10 mmol, 1.0 eq) in dry DMF (3 mL) and the mixture was stirred overnight. A small conversion of starting material was observed and therefore extra bromoacetonitrile (4 µL, 0.06 mmol, 0.05 eq) was added. The mixture was further stirred for 8 days during which DIPEA (14 µL, 0.08 mmol, 0.8 eq) was added gradually. The reaction was then stopped to prevent overalkylation. EtOAc (50 mL) was added and the organic layer was washed with H_2O (3 x 50 mL), dried using $MgSO_4$, filtered and concentrated under reduced pressure. The residue was purified using column chromatography (DCM: MeOH 99.5:0.5→ 97.5:2.5) to yield **7** (20 mg, 0.04 mmol, 41%) as white solid. **^{1}H NMR** (500 MHz, $(CD_3)_2SO$) δ [ppm] = 14.10 (s, 1H), 12.01 (s, 1H), 8.35 (d, *J* = 8.6 Hz, 2H), 8.16 (d, *J* = 8.7 Hz, 2H), 4.98 (s, 2H), 3.82 (t, *J* = 7.4 Hz, 2H), 2.81 (t, *J* = 7.2 Hz, 2H), 2.77 (t, *J* = 2.6 Hz, 1H), 2.16 (td, *J* = 7.0, 2.7 Hz, 2H), 1.65 (p, *J* = 7.1 Hz, 2H), 1.57 (h, *J* = 7.4 Hz, 3H), 0.88 (t, *J* = 7.4 Hz, 3H). **^{13}C NMR** (126 MHz, $(CD_3)_2SO$) δ [ppm] = 172.2, 155.5, 151.5, 148.1, 148.1, 138.7, 134.9, 129.1, 127.6, 116.9, 109.4, 84.0, 72.5, 42.1, 34.7, 34.5, 23.4, 21.4, 17.3, 11.7. **HRMS** (ESI, m/z): $[M+H]^+$, calculated: 483.1445, found: 483.1423. **HPLC** 96%, RT 9.721 min.

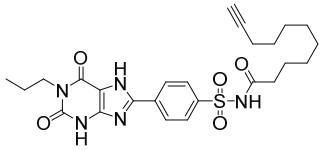

***N*-((4-(2,6-Dioxo-1-propyl-2,3,6,7-tetrahydro-1*H*-purin-8-yl)phenyl)sulfonyl)undec-10-ynamide (8) (LUF8021)**

10-Undecynoic acid (328 mg, 1.80 mmol,1.6 eq), EDC·HCl (656 mg, 3 mmol, 3 eq), DMAP (42 mg, 0.34 mmol, 0.3 eq) and DIPEA (600 µL, 3.44 mmol, 3.0 eq) were added to a solution of **5** (400 mg, 1.14 mmol, 1.0 eq) in dry DMF (12 mL) and the mixture was stirred overnight. EtOAC (100 mL) was then added and the organic layer was extracted with H_2O (3 x 100 mL). As the product resided in the aqueous layer, the aqueous layers were combined and the pH was brought to ~2 using 6 M HCl. The product was allowed to crystallize overnight and was collected by filtration. The product was further purified by recrystallization in a 1:4 mixture of H_2O:EtOAc to yield compound **8** as a pink-white solid (376 mg, 0.73 mmol, 64%). **^{1}H NMR** (400 MHz, $(CD_3)_2SO$) δ [ppm] = 14.05 (s, 1H), 12.16 (s, 1H), 11.99 (s, 1H), 8.29 (d, *J* = 8.6 Hz, 2H), 8.00 (d, *J* = 8.6 Hz, 2H), 3.82 (t, *J* = 7.4 Hz, 2H), 2.69 (t, *J* = 2.6 Hz, 1H), 2.20 (t, *J* = 7.2 Hz, 2H), 2.06 (td, *J* = 7.0, 2.7 Hz, 2H), 1.57 (h, *J* = 7.5 Hz, 2H), 1.43 – 1.28 (m, 4H), 1.27 – 1.18 (m, 2H), 1.17 – 1.02 (m, 6H), 0.88 (t, *J* = 7.4 Hz, 3H). **^{13}C NMR** (101 MHz, $(CD_3)_2SO$) δ [ppm] = 172.3, 155.4, 151.4, 148.4, 148.1, 140.5, 133.8, 128.7, 127.1, 109.0, 84.9, 71.5, 42.0, 35.8, 29.0, 28.8, 28.6, 28.5, 28.4, 24.4, 21.3, 18.1, 11.7. **HRMS** (ESI, m/z): $[M+H]^+$, calculated: 514.2119, found: 514.2089. **HPLC** 100%, RT 10.459 min.

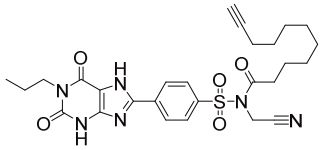

***N*-(Cyanomethyl)-*N*-((4-(2,6-dioxo-1-propyl-2,3,6,7-tetrahydro-1*H*-purin-8-yl)phenyl)sulfonyl)undec-10-ynamide (9) (LUF8023)**

Bromoacetonitrile (21 µL, 0.30 mmol, 1.2 eq) was added to a solution of **8** (130 mg, 0.25 mmol, 1.0 eq) in dry DMF (8 mL). DIPEA (14 µL, 0.08 mmol, 0.3 eq) was added gradually over a period of six days. The reaction was then stopped to prevent overalkylation. EtOAc (100 mL) was added and the organic layer was washed using H_2O (3 x 100mL), dried over $MgSO_4$ and concentrated under reduced pressure. The residue was purified using column chromatography (DCM: MeOH 99.5:0.5→98:2) to yield **9** (16 mg, 0.02 mmol, 12%) as a white solid. **^{1}H NMR** (500 MHz, $(CD_3)_2SO$) δ [ppm] = 14.11 (s, 1H), 12.00 (s, 1H), 8.35 (d, *J* = 8.8 Hz, 2H), 8.15 (d, *J* = 8.7 Hz, 2H), 5.00 (s, 2H), 3.82 (t, *J* = 7.3 Hz, 2H), 2.67 (t, *J* = 2.7 Hz, 1H), 2.64 (t, *J* = 7.2 Hz, 2H), 2.06 (td, *J* = 7.0, 2.7 Hz, 2H), 1.58 (h, *J* = 7.4 Hz, 2H), 1.47 – 1.40 (m, 2H), 1.38 – 1.29 (m, 2H), 1.25 – 1.20 (m, 2H), 1.17 – 1.09 (m, 6H), 0.88 (t, *J* = 7.5 Hz, 3H). **^{13}C NMR** (126 MHz, $(CD_3)_2SO$) δ [ppm] = 172.7, 155.5, 151.5, 148.1, 148.0, 139.0, 134.8, 129.1, 127.5, 117.0, 109.3, 85.0, 71.5, 42.1, 35.6, 34.5, 29.0, 28.8, 28.6, 28.5, 28.4, 24.4, 21.4, 18.1, 11.7. **HRMS** (ESI, m/z): $[M+H]^+$, calculated: 553.2228, found: 553.2218. **HPLC** 98%, RT 11.300 min.

Biology

Materials

[^{3}H]PSB-603 (specific activity 79 Ci/mmol) was purchased from Quotient Bioresearch, [^{3}H]DPCPX, (specific activity 137 Ci/mmol) and [^{3}H]-ZM241385 (specific activity 50 Ci/mmol) were purchased from ARC, Inc. and [^{3}H]PSB-11 (specific activity 56 Ci/mmol) was kindly donated by Prof. C.E. Müller (University of Bonn, Germany). 5'-(N-Ethylcarboxamido)adenosine (NECA), N^6-Cyclopentyladenosine (CPA), EDTA-free protease inhibitor cocktail (cat# P8340) and all click reagents $CuSO_4$, (+)-sodium L-ascorbate (NaAsc), Tris((1-hydroxy-propyl-1H-1,2,3-triazol-4-yl)methyl)amine (THPTA) and Cy5-N_3, were purchased from Sigma-Aldrich (Merck). ZM241385 was a gift of Dr. S.M. Poucher (Astra Zeneca, Manchester, UK) and CGS21680 was purchased from Ascent Scientific. PSB 1115 potassium salt was purchased from Tocris Bioscience and BAY60-6583 and LUF7982 were synthesized in-house as reported before.[15] Adenosine Deaminase (ADA) was purchased from Sigma-Aldrich (Merck) and PNGase F (10 u/µL, cat# V4831) was purchased from Promega. Laemmli buffer was purchased from Bio-Rad and Hank Buffered Saline Solution (HBSS) (cat# 1402550) was purchased from Thermo Fischer. All other reagents were purchased from standard commercial sources and of analytical grade.

Stability assays

5 µL of a 7.5 mM stock solution of probe was added to an LC-MS vial containing 95 µL of PBS buffer or CHO-hA_{2B}AR-spap culture medium (DMEM/F12 1:1, 10% (v/v) Newborn Calf Serum (NCS), 100 mg/mL penicillin/streptomycin, 1 mg/mL G418 and 0.4 mg/mL hygromycin). The samples were constantly shaken at 1000 rpm (rt or 37 °C) to prevent the probes from crystallizing. Samples were measured by LC-MS after 2 h of incubation, using the method described above.

Cell culture and membrane preparation

Chinese Hamster Ovary (CHO)-spap cells stably expressing the human adenosine A_{2B} receptor (CHO-spap-hA_{2B}AR) were kindly provided by S.J. Dowell (GlaxoSmithKline, Stevenage, UK), CHO cells stably expressing the human adenosine A_1 receptor (CHO-hA_1AR) were kindly provided by Prof. S.J. Hill (Nottingham, UK), Human Embryonic Kidney (HEK) 293 cells stably expressing the human adenosine A_{2A} receptor (HEK293-hA_{2A}AR) were kindly provided by Dr. J. Wang (Biogen, Cambridge, Massachusetts USA) and CHO cells stably expressing the human adenosine A_3 receptor (CHO-hA_3AR) were kindly provided by Dr. K.N. Klotz (University of Würzburg, Germany). All cells were cultured and membranes were prepared as reported before.[45]

Radioligand displacement assays

Full curve radioligand displacement experiments using CHO-hA_{2B}AR-spap membranes and single point displacement assays using CHO-hA_1AR, HEK293-hA_{2A}AR and CHO-hA_3AR membranes were carried out as previously reported.[15] Data was analyzed using GraphPad Prism 9.0 (Graphpad Software Inc., San Diego, California USA). IC_{50} values were obtained by non-linear regression curve fitting and converted to pIC_{50} values using the Cheng-Prusoff equation.[46] The KD values of 1.7 nM of [^{3}H]PSB-603 at CHO-spap-hA_{2B}AR membranes and 1.6 nM of [^{3}H]DPCPX at CHO-hA_1AR membranes were taken from previous experiments.[47,48] The KD values of 1.0 nM of [^{3}H]ZM241385 at HEK293-hA_{2A}AR membranes and 17.3 nM of [^{3}H]PSB11 at CHO-hA_3AR membranes were taken from in-house determinations. All pK_i values shown are mean values ± SEM of three individual experiments performed in duplicate.

Single point displacement values are the mean percentages of two experiments performed in duplicate. Statistical analysis was performed using a two-tailed unpaired student's T-test.

SDS-PAGE using CHO-hA_{2B}AR-spap membrane fractions

CHO-hA_{2B}AR-spap membrane fractions were collected as previously reported.[45] Protease inhibitor cocktail (1:100) was added, the membrane fractions were diluted to a concentration of 1 mg/mL and 19 µL was taken per sample. 1 µL of probe LUF8015, LUF8019, LUF8021 or LUF8023 (final concentration: 100 nM) was added and the samples were incubated for 1 h at rt. Click mix was freshly prepared by combining 5 parts 100 mM $CuSO_4$, 3 parts 1 M NaAsc, 1 part 100 mM THPTA and 1 part 100 µM Cy5-N_3. 2.22 µL of the prepared click mix was added per sample and the samples were incubated for 1 h at rt. Proteins were denatured by addition of 7.41 µL of Laemmli buffer (x4) and incubation for at least 1 h at rt. The samples were then loaded on gel (12.5% acrylamide) and run (180 V, 100 min). Gels were imaged on a Bio-Rad Universal Hood III using in-gel fluorescence. Pageruler prestained protein ladder was used as molecular weight marker. Coomassie Brilliant Blue (CBB) staining was carried out as control.

SDS-PAGE using live CHO-hA_{2B}AR-spap cells

CHO-hA_{2B}AR-spap cells were cultured as previously reported.[45] Upon reaching ~90% confluency, medium was removed and competing ligand PSB1115, BAY60-6583 or LUF7982 (final concentration: 1 µM) or 1% DMSO (vehicle) in medium was added, followed by a 30 min incubation (37 °C, 5% CO_2). Medium was then removed and probe LUF8019 or LUF8023 (final concentration: 100 nM) or 1% DMSO (vehicle) in HBSS was added, followed by incubation for 2 h (37 °C, 5% CO_2). HBSS was removed, non-bound probe was washed away with PBS and membranes were prepared as previously reported.[45] Protease inhibitor cocktail (1:100) was added, the membrane fractions were diluted to a concentration of 1 mg/mL and 20 µL was taken per sample. Click mix was freshly prepared by combining 5 parts 100 mM $CuSO_4$, 3 parts 1 M NaAsc, 1 part 100 mM THPTA and 1 part 100 µM Cy5-N_3. 2.22 µL of click mix was added per sample and the samples were incubated for 1 h at rt. 0.5 µL PNGase (5U) was added by which the samples were deglycosylated for 1 h at rt. The samples were denatured by addition of 7.57 µL Laemmli buffer (x4) and incubating for at least 1 h at rt. Samples were then loaded on gel (12.5% acrylamide) and run (180 V, 100 min). Gels were imaged using a Bio-Rad Universal Hood III and in-gel fluorescence. CBB staining was carried out as protein control.

SDS-PAGE data analysis

Gels were analyzed with ImageLab software version 6.0.1 (Bio-Rad). The adjusted volumes of the selected bands were determined using the 'Lane Profile' tab and corrected for the amount of protein per lane, using the adjusted total lane volumes of the CBB stained gels. The adjusted volume of the band at 55 kDa in the molecular weight marker (Pageruler prestained protein ladder) was set to 100% and the other bands were normalized to this value. Further data analysis was carried out using Graphpad Prism. All given percentages are the mean values ± SEM of three individual experiments. Statistical analysis was performed using a one- or two-way ANOVA test with multiple comparisons.

Author Contributions

V.A. synthesized compounds. R.L. performed radioligand displacement experiments. B.L.H.B. and V.A. performed SDS-PAGE experiments. L.H.H., A.P.IJ. and D.v.d.E. supervised the project.

References

[1] B. B. Fredholm, A. P. IJzerman, K. A. Jacobson, K.-N. Klotz, J. Linden, *Pharmacol Rev* **2001**, *53*, 527–552.

[2] A. P. IJzerman, K. A. Jacobson, C. E. Müller, B. N. Cronstein, R. A. Cunha, *Pharmacol Rev* **2022**, *74*, 340–372.

[3] C. Cekic, J. Linden, *Nat Rev Immunol* **2016**, *16*, 177–192.

[4] Z. G. Gao, K. A. Jacobson, *Int J Mol Sci* **2019**, *20*, 5139.

[5] B. Allard, D. Allard, L. Buisseret, J. Stagg, *Nat Rev Clin Oncol* **2020**, *17*, 611–629.

[6] V.-P. Jaakola, M. T. Griffith, M. A. Hanson, V. Cherezov, E. Y. T. Chien, J. R. Lane, A. P. IJzerman, R. C. Stevens, *Science (1979)* **2008**, *322*, 1211–1217.

[7] Y. Chen, J. Zhang, Y. Weng, Y. Xu, W. Lu, W. Liu, M. Liu, T. Hua, G. Song, *Sci Adv* **2022**, *8*, eadd3709.

[8] H. Cai, Y. Xu, S. Guo, X. He, J. Sun, X. Li, C. Li, W. Yin, X. Cheng, H. Jiang, H. E. Xu, X. Xie, Y. Jiang, *Cell Discov* **2022**, *8*, 140.

[9] D. Petroni, C. Giacomelli, S. Taliani, E. Barresi, M. Robello, S. Daniele, A. Bartoli, S. Burchielli, S. Pardini, P. A. Salvadori, F. da Settimo, C. Martini, M. L. Trincavelli, L. Menichetti, *Nucl Med Biol* **2016**, *43*, 309–317.

[10] M. Lindemann, S. Hinz, W. Deuther-Conrad, V. Namasivayam, S. Dukic-Stefanovic, R. Teodoro, M. Toussaint, M. Kranz, C. Juhl, J. Steinbach, P. Brust, C. E. Müller, B. Wenzel, *Bioorg Med Chem* **2018**, *26*, 4650–4663.

[11] M. Lindemann, R. P. Moldovan, S. Hinz, W. Deuther-Conrad, D. Gündel, S. Dukic-Stefanovic, M. Toussaint, R. Teodoro, C. Juhl, J. Steinbach, P. Brust, C. E. Müller, B. Wenzel, *Int J Mol Sci* **2020**, *21*, 3197.

[12] M. Köse, S. Gollos, T. Karcz, A. Fiene, F. Heisig, A. Behrenswerth, K. Kieć-Kononowicz, V. Namasivayam, C. E. Müller, *J Med Chem* **2018**, *61*, 4301–4316.

[13] E. Barresi, C. Giacomelli, S. Daniele, I. Tonazzini, M. Robello, S. Salerno, I. Piano, B. Cosimelli, G. Greco, F. da Settimo, C. Martini, M. L. Trincavelli, S. Taliani, *Bioorg Med Chem* **2018**, *26*, 5885–5895.

[14] J. Barbazán, M. Majellaro, A. L. Martínez, J. M. Brea, E. Sotelo, M. Abal, *Biomedicine and Pharmacotherapy* **2022**, *153*, 113408.

[15] B. L. H. Beerkens, X. Wang, M. Avgeropoulou, L. N. Adistia, J. P. D. van Veldhoven, W. Jespers, R. Liu, L. H. Heitman, A. P. IJzerman, D. van der Es, *RSC Med Chem* **2022**, *13*, 850–856.

[16] A. Temirak, J. G. Schlegel, J. H. Voss, V. J. Vaaßen, C. Vielmuth, T. Claff, C. E. Müller, *Molecules* **2022**, *27*, 3792.

[17] D. Weichert, P. Gmeiner, *ACS Chem Biol* **2015**, *10*, 1376–1386.

[18] Y. Wu, B. Zhang, H. Xu, M. He, X. Deng, L. Zhang, Q. Dang, J. Fan, Y. Guan, X. Peng, W. Sun, *Coord Chem Rev* **2023**, *480*, 215040.

[19] L. Dahl, I. B. Kotliar, A. Bendes, T. Dodig-Crnković, S. Fromm, A. Elofsson, M. Uhlén, T. P. Sakmar, J. M. Schwenk, *bioRxiv* **2022**, 2022.11.24.517810.

[20] B. L. H. Beerkens, Ç. Koç, R. Liu, B. I. Florea, S. E. Le Dévédec, L. H. Heitman, A. P. IJzerman, D. van der Es, *ACS Chem Biol* **2022**, *17*, 3131–3139.

[21] X. Yang, T. J. M. Michiels, C. de Jong, M. Soethoudt, N. Dekker, E. Gordon, M. van der Stelt, L. H. Heitman, D. van der Es, A. P. IJzerman, *J Med Chem* **2018**, *61*, 7892–7901.

[22] B. L. H. Beerkens, I. M. Snijders, J. Snoeck, R. Liu, A. T. J. Tool, S. E. Le Dévédec, W. Jespers, T. W. Kuijpers, G. J. P. van Westen, L. H. Heitman, A. P. IJzerman, D. van der Es, *ChemRxiv* **2023**, DOI 10.26434/chemrxiv-2023-6g59z.

[23] S. Tsukiji, M. Miyagawa, Y. Takaoka, T. Tamura, I. Hamachi, *Nat Chem Biol* **2009**, *5*, 341–343.

[24] S. H. Fujishima, R. Yasui, T. Miki, A. Ojida, I. Hamachi, *J Am Chem Soc* **2012**, *134*, 3961–3964.

[25] T. Tamura, T. Ueda, T. Goto, T. Tsukidate, Y. Shapira, Y. Nishikawa, A. Fujisawa, I. Hamachi, *Nat Commun* **2018**, *9*, 1870.

[26] G. Tomasello, I. Armenia, G. Molla, *Bioinformatics* **2020**, *36*, 2909–2911.

[27] T. Miki, S. H. Fujishima, K. Komatsu, K. Kuwata, S. Kiyonaka, I. Hamachi, *Chem Biol* **2014**, *21*, 1013–1022.

[28] S. M. Moss, P. S. Jayasekara, S. Paoletta, Z. G. Gao, K. A. Jacobson, *ACS Med Chem Lett* **2014**, *5*, 1043–1048.

[29] L. A. Stoddart, N. D. Kindon, O. Otun, C. R. Harwood, F. Patera, D. B. Veprintsev, J. Woolard, S. J. Briddon, H. A. Franks, S. J. Hill, B. Kellam, *Commun Biol* **2020**, *3*, 722.

[30] H. Nonaka, S. Sakamoto, K. Shiraiwa, M. Ishikawa, T. Tamura, K. Okuno, S. Kiyonaka, E. A. Susaki, C. Shimizu, H. R. Ueda, W. Kakegawa, I. Arai, M. Yuzaki, I. Hamachi, *bioRxiv* **2023**, 2023.01.16.524180.

[31] S. Arttamangkul, A. Plazek, E. J. Platt, H. Jin, T. F. Murray, W. T. Birdsong, K. C. Rice, D. L. Farrens, J. T. Williams, *Elife* **2019**, *8*, e49319.

[32] M. Kosar, D. A. Sykes, A. E. G. Viray,] Rosa, M. Vitale, R. C. Sarott, R. L. Ganzoni, D. Onion, J. M. Tobias, P. Leippe, C. Ullmer, E. A. Zirwes, W. Guba, U. Grether, J. A. Frank, D. B. Veprintsev, E. M. Carreira, *ChemRxiv* **2022**, DOI 10.26434/chemrxiv-2022-z58fd.

[33] X. Gómez-Santacana, M. Boutonnet, C. Martínez-Juvés, J. L. Catena, E. Moutin, T. Roux, E. Trinquet, L. Lamarque, J. Perroy, L. Prézeau, J. M. Zwier, J.-P. Pin, A. Llebaria, *ChemRxiv* **2022**, DOI 10.26434/chemrxiv-2022-mqqtz-v2.

[34] D. Xue, L. Ye, J. Zheng, Y. Wu, X. Zhang, Y. Xu, T. Li, R. C. Stevens, F. Xu, M. Zhuang, S. Zhao, F. Zhao, H. Tao, *Org Biomol Chem* **2019**, *17*, 6136–6142.

[35] C. W. Tornøe, C. Christensen, M. Meldal, *Journal of Organic Chemistry* **2002**, *67*, 3057–3064.

[36] V. V. Rostovtsev, L. G. Green, V. V. Fokin, K. B. Sharpless, *Angew. Chem. Int. Ed.* **2002**, *41*, 2596–2599.

[37] C. E. Müller, J. Sandoval-Ramirez, *Synthesis (Stuttg)* **1995**, 1295–1299.

[38] C. E. Müller, D. Shi, M. Manning, J. W. Daly, *J. Med. Chem* **1993**, *36*, 3341–3349.

[39] X. Yang, J. P. D. van Veldhoven, J. Offringa, B. J. Kuiper, E. B. Lenselink, L. H. Heitman, D. van der Es, A. P. IJzerman, *J Med Chem* **2019**, *62*, 3539–3552.

[40] R. Liu, N. J. A. Groenewoud, M. C. Peeters, E. B. Lenselink, A. P. IJzerman, *Purinergic Signal* **2014**, *10*, 441–453.

[41] R. Liu, D. Nahon, B. le Roy, E. B. Lenselink, A. P. IJzerman, *Biochem Pharmacol* **2015**, *95*, 290–300.

[42] X. Wang, W. Jespers, B. J. Bongers, M. C. C. Habben Jansen, C. M. Stangenberger, M. A. Dilweg, H. Gutiérrez-de-Terán, A. P. IJzerman, L. H. Heitman, G. J. P. van Westen, *Eur J Pharmacol* **2020**, *880*, 173126.
[43] S. Hinz, S. K. Lacher, B. F. Seibt, C. E. Müller, *Journal of Pharmacology and Experimental Therapeutics* **2014**, *349*, 427–436.
[44] A. M. Hayallah, J. Sandoval-Ramírez, U. Reith, U. Schobert, B. Preiss, B. Schumacher, J. W. Daly, C. E. Müller, *J Med Chem* **2002**, *45*, 1500–1510.
[45] T. Amelia, J. P. D. Van Veldhoven, M. Falsini, R. Liu, L. H. Heitman, G. J. P. Van Westen, E. Segala, G. Verdon, R. K. Y. Cheng, R. M. Cooke, D. Van Der Es, A. P. IJzerman, *J Med Chem* **2021**, *64*, 3827–3842.
[46] C. Yung-Chi, W. H. Prusoff, *Biochem Pharmacol* **1973**, *22*, 3099–3108.
[47] A. Kourounakis, C. Visser, M. de Groote, A. P. IJzerman, *Biochem Pharmacol* **2001**, *61*, 137–144.
[48] A. Vlachodimou, H. de Vries, M. Pasoli, M. Goudswaard, S.-A. Kim, Y.-C. Kim, M. Scortichini, M. Marshall, J. Linden, L. H. Heitman, K. A. Jacobson, A. P. IJzerman, *Biochem Pharmacol* **2022**, *200*, 115027.

Chapter 7

Conclusions and Future Prospects

Conclusions

On the development of covalent probes to target adenosine receptors

This thesis summarizes the development of various types of covalent probes to target the adenosine A_1, A_{2B} and A_3 receptors. As discussed in **chapter 2**, the use of covalent small molecules in GPCR labelling studies has several benefits, one being the opportunity to target *endogenous* receptors, another the possibility to use *denaturing* assay conditions. However, several aspects have to be taken into account upon developing a *valid* covalent probe for GPCR labelling studies:

1. Selectivity

First of all, covalent probes should bear sufficient selectivity towards their target GPCR, in order to prevent covalent binding to off-target proteins. Due to the low expression levels of GPCRs, off-target labelling can easily hamper the detection of target GPCRs (**chapters 4-6**). A selective pharmacophore should therefore be included in the design of covalent probes. Fortunately, over the past two decades, selective ligands have been developed for all four of the adenosine receptors. In **chapters 3** and **6** probe design was based on the A_{2B}AR antagonist PSB 1115.[1] In **chapter 3** we observed a drop in selectivity upon substitution of the prime scaffold with a 'mere' propyl group, indicating that small changes to the molecular scaffold can have a big influence on the selectivity of the probe. In **chapter 4** probe design was based on the covalent A_1AR agonist LUF7746, in turn derived from the clinical candidate Capadenoson.[2,3] In this study, we observed a loss in affinity for three out of four of the alkyne-substituted probes, indicating that location of the substitution also drastically effects the on-target affinity of the probe. In **chapter 5** probe design was based on the covalent A_3AR antagonist LUF7602.[4] Contrary to the previous chapters, three different locations of the alkynyl substituent did not decrease affinity nor selectivity towards the A_3AR. Nevertheless, on- and off-target selectivity is greatly dependent on the selected molecular scaffold and thus should be investigated per case.

2. Reactivity

Secondly, a reactive warhead should be chosen that covalently binds the target nucleophilic amino acid residue, but not amino acid residues on unrelated proteins present in the sample. Thus, reactivity of the warhead also has a strong influence on overall selectivity of the probe. Besides that, the warhead should bear hydrolytic stability under standard biochemical assay conditions. **Chapter 2** lists the various types of warheads that have been implemented in covalent GPCR probes. In **chapter 3** we investigated three lysine-targeting warheads: fluorosulfonyl, fluorosulfonate and isothiocyanate groups, to covalently bind the A_{2B}AR. In this study the fluorosulfonyl group showed optimal reactivity, while the fluorosulfonate group was not reactive enough, presumably due to an unstable reaction product, and the isothiocyanate group was too reactive, as observed in the increased binding towards other adenosine receptors. The fluorosulfonyl group was therefore our electrophile of choice, also in **chapters 4** and **5**. In **chapter 6** we implemented the electrophilic *N*-acyl-*N*-alkyl sulfonamide (NASA) group as warhead in a ligand-directed probe. Although labelling of the A_{2B}AR was observed in SDS-PAGE experiments, the probe showed to be highly reactive under standard cell culture conditions. Changing the substituents of the NASA group, e.g. replacing the cyano moiety with a less electron withdrawing substituent, might decrease off-target reactivity and result in a more selective probe.[5] Taken together, the fluorosulfonyl group shows a well-balanced reactivity, and new types of electrophiles should be thoroughly investigated prior and after their implementation in covalent probes.

3. Detectability

Lastly, binding of the covalent probe to the GPCR should lead to a measurable signal in biochemical assays. In **chapter 2** the various detection moieties are listed that have been used to covalently functionalize GPCRs. A distinction can be made between one-step (direct) and two-step (via click chemistry) labelling strategies.[6–8] The affinity-based and ligand-directed probes from chapters **4**, **5** and **6** all contain an alkyne group that allows the substitution of an azide-conjugated detection moiety via the copper-catalyzed alkyne-azide cycloaddition (CuAAC).[9,10] This two-step labelling strategy allows the choice between different detection moieties, while using the same stock of probe, in various biochemical assays. This prevents the need for the time-consuming synthesis of one-step probes individually functionalized with detection moieties, such as fluorescent ligands. A drawback of this strategy is the need for cytotoxic click reagents during additional incubation and washing steps, making the probes largely incompatible with live-cell experiments. Bioorthogonal strategies have been developed to overcome the use of cytotoxic reagents, using different click handles such as strained alkynes or tetrazines.[11–13] However, alkyne groups are synthetically accessible, relatively stable and due to their small size more attractive to implement in pharmacological scaffolds than strained alkynes or tetrazines. Therefore we have limited ourselves to the use of alkyne groups as click handles within our experiments. Nevertheless, in **chapter 5** we managed to overcome the aforementioned drawbacks by performing the click reaction and subsequent purification prior to addition of the covalent probe to live cells. A similar strategy might be used in the future to functionalize other two-step probes targeting ARs prior to their use in live-cell experiments.

In the following paragraphs, a closer look is provided on the detectability of GPCRs, in particular the adenosine receptors, in the various biochemical assay types that have been performed as part of this thesis.

A. SDS-PAGE

Throughout **chapters 4**, **5** and **6** SDS-PAGE experiments have been performed to detect labelled A_1AR, A_3AR and A_{2B}AR. SDS-PAGE has been successfully used in the past as a technique to detect the presence of adenosine receptors, especially the A_1AR and A_{2A}AR, in various tissue types, by making use of radiolabeled photo-affinity probes as tool compounds.[14–22] In our experiments, detection of the respective AR was most clearly visible upon performing the experiment in overexpressing cell lines, prior to membrane fractionation, click reaction and protein separation. Interestingly, endogenous N-glycosylation of the receptors hampered their initial detection, as the receptor bands appeared as ‘smear’ over a range of molecular weights.[23–26] In each instance, incubation with PNGase resulted in clear bands at roughly the expected molecular weights. Similar enzymatic incubation steps might also be used in the future to study other post-translational modifications (PTMs). Performing the experiments in membrane fractions, however, resulted in an increase in off-target binding for all of the probes and even prevented detection of the A_{2B}AR with LUF8019 (**chapter 6**). As speculated in **chapters 4** and **5**, we presume the increase in off-target labelling to be caused by a combination of the low expression levels of the respective receptor, the electrophilic character of probes, the high density of other proteins as compared to live cell assays and the presence of intracellular membrane proteins in our membrane fractions. Detection of adenosine receptors in non-overexpressing cell lines showed to be even more cumbersome. Attempts have been done using LUF7909 (A_1AR) in adipocytes (**chapter 4**), but also using LUF7487 (A_{2A}AR) and LUF7960 (A_3AR) in various cancerous cell lines with detectable mRNA expression levels of the respective receptor (data not included). In the latter two experiments, no labelling of the respective AR was observed, while labelling of off-targets was evident. Thus, it seems that the low expression levels of the ARs hinder proper detection in SDS-PAGE experiments, partly due to the inherent reactivity of the electrophilic groups. Taken together,

the herein developed covalent probes should be used in SDS-PAGE experiments to verify binding of ligands, probes and other tool molecules to purified, overexpressed or highly expressed ARs, but not as a technique to detect expression levels of endogenous receptors on cells and tissues.

B. Fluorescent Microscopy

In **chapters 4** and **5** fluorescent microscopy has been used as a technique to detect probe labelled ARs. A considerable amount of fluorescent ligands for ARs has already been developed in the past,[27] yet it still is a lively topic of research.[28–33] These studies deviate from our work by developing one-step and reversible probes, thereby requiring extensive synthetic steps and limiting the number of applications. The herein reported experiments on the A_1AR and A_3AR have been *proof of concept* studies to showcase selective labelling of the respective receptors in microscopy experiments. A drawback of the used experimental setup is the need for a fixation step, prior to incubation with click reagents. However, this hurdle might be overcome by performing the click reaction *a priori* to the first cellular incubation steps, as has been done in case of the flow cytometry experiments in **chapter 5**. Although selective labelling of the A_1ARs and A_3ARs was observed on overexpressing CHO cells, future work should unveil whether selective labelling of the ARs can also be detected in native/primary cells and tissues. Interestingly, selective labelling of the A_{2A}AR on a breast cancer cell line has recently been performed using a ligand-directed probe, showing the future potential of covalently binding probes.[34] Next to that, labelling by the partial agonist probe LUF7909 (**chapter 4**) yielded information on internalization of the A_1AR. Taken together, the use of affinity-based probes in fluorescent microscopy experiments is thus a valid strategy to study (sub)cellular receptor localization in overexpressing cell lines and potentially receptor expression in non-overexpressing cells.

C. Flow Cytometry

In **chapter 5** flow cytometry has been used as technique to detect probe labelled A_3ARs. Instead of fixing cells, as has been done throughout the microscopy assays, covalent probe LUF7960 was clicked to a Cy5 fluorophore prior to the addition to live cells. The pre-click step yielded a probe, LUF7960-Cy5, that had a ~20-fold lower affinity towards the A_3AR (data not included), but allowed us to circumvent an additional incubation step with cytotoxic click reagents. Gratifyingly, the pre-clicked probe showed A_3AR-selective labelling in A_3AR-overexpressing CHO cells, as well as native eosinophils. Fluorescent ligands for the A_{2A}AR, A_{2B}AR and A_3AR have been used in flow cytometry experiments before, however mostly for competition binding experiments.[30,33,35–37] To the best of our knowledge, utilization of chemical probes for the detection of AR expression on native cells has thus far been reported only once.[37] In our experiments, commercial A_3AR antibodies did not show selective labelling of the A_3AR, presumably due to off-target activity.[38] As opposed to antibodies, chemical probes compete with agonists and antagonists for a ligand binding pocket on their respective receptor target. Competition experiments can therefore be used as control to verify selective labeling of the receptor, while such control experiments are not possible for the often poorly selective antibodies.[38–40] Altogether, covalent probes are interesting tool molecules for the detection of AR expression on native cells and tissues in flow cytometry experiments and show more promise than AR-targeting antibodies. The combination of covalent probes and flow cytometry is therefore an interesting strategy to map expression of the ARs in pathological and physiological conditions.

D. Chemical Proteomics

In **chapter 4** biotin-click and subsequent proteomic pull-down experiments have been performed to detect the A_1AR using LC-MS/MS. Gratifyingly, almost 50% of the A_1AR peptide sequence was detected, an amount that is remarkably high for a GPCR. Detection of non-purified GPCRs by LC-MS/MS techniques is often hampered by the low expression levels of GPCRs, even in overexpressing cell lines. The use of covalent probes to pull-down target GPCRs from a complex protein mixture, thereby strongly reducing background noise, is therefore a path forward for detection in LC-MS/MS experiments. Next to that, we found the type of digestion enzyme (e.g. trypsin vs. chymotrypsin) to play an important role in the successful detection of the resulting peptides. Remarkably, pull-down experiments on GPCRs are often carried out using trypsin as digestion enzyme,[41–47] while the seven transmembrane helices contain little to zero sites that are susceptible to trypsin cleavage. In an ideal situation, multiple digestion enzymes are screened to find the optimal conditions for peptide formation. Next to the experiments on the A_1AR, we also performed pull-down experiments with LUF7960 (**chapter 5**) as a tool for the detection of the A_3AR on overexpressing CHO cells. Unfortunately, we were not able to reliably detect the receptor. There are multiple possible reasons for this, such as the low expression of A_3AR as compared to the A_1AR on CHO cells, the poor solubility of the receptor due to its relatively small extracellular regions, or poor compatibility with the digestion enzyme chymotrypsin. It is therefore still questionable whether the current assay setup allows successful pull-down experiments on cells endogenously expressing ARs. However, we think that optimizing the aforementioned problems of solubility and digestion, as well as further reducing the background noise, will lead to an improved detection of the ARs. Ultimately, the detection of ARs in pull-down experiments will yield information that is difficult to obtain in SDS-PAGE, flow cytometry and fluorescent microscopy experiments, such as the presence of PTMs and interactions with other (non-defined) proteins. Taken together, using covalent probes in pull-down proteomics has the promise to be an important strategy for future studies on the ARs.

Altogether, the herein developed covalent probes are promising tool molecules to detect and study the ARs in a multitude of biochemical assays. Each of the abovementioned biochemical assays bears its own challenges, ranging from off-target labelling to lack of sensitivity. The work described in this thesis addresses these issues, bringing the application of covalent AR probes one step further towards general usage. Having this ‘toolbox’ of covalent probes allows investigations towards many interesting aspects of AR signaling, that differ from the applications of reversible probes, antibodies and genetic techniques.

Future Prospects

Detection of endogenous adenosine receptor expression

The first application of covalent AR probes that one might think of is the detection of AR expression levels in pathophysiological conditions, e.g. using cell lines, tissues or disease models. Examples would be the investigation of A_1AR expression in fat tissue under various lipolytic conditions,[48] the investigation of A_{2A}AR and A_{2B}AR expression in tumor models,[49] and the investigation of A_3AR expression during inflammatory conditions.[50] The first steps towards covalent endogenous AR detection have been taken in **chapters 4** and **5**, as well as recent work on the A_{2A}AR.[34] As mentioned in the conclusions, flow cytometry as a technique has, in our view, shown the highest potential to study endogenous expression levels of the ARs. Flow cytometry has already been used to verify binding of covalent probes to other GPCRs.[44,51–55] For example, experiments on the μ opioid receptor (MOR) showed that the fluorescence intensity after probe labeling was similar to the fluorescent intensity upon antibody staining.[55] Next to that, experiments on the Cannabinoid Receptor 2 (CB_2R) revealed good correlations between the observed fluorescence intensity and mRNA levels in various leukocytes.[44] Covalent AR probes therefore have the potential to be used complementarily to mRNA techniques, as tool molecules to quantify relative receptor expression between various cell lines. Ideally, both non- and overexpressing cell lines are included in flow cytometry experiments to determine a binding window for thorough quantifications. In the future, such experiments might be performed to determine the total receptor expression level per cell type, as an alternative to the expensive radioligand binding experiments currently used for these purposes.

A glimpse of other possible future applications of covalent GPCR probes has already been given in the outlook of **chapter 2**. These applications will be further elaborated in the paragraphs below.

Investigation of (sub)cellular receptor localization

Upon agonist-induced activation and G protein dissociation, the intracellular regions of GPCRs are prone to phosphorylation and subsequent arrestin binding, in turn leading to internalization of the GPCR via endosomal vesicles. According to current understanding, the fate of internalized GPCRs is dependent on multiple factors, such as PTMs, protein-protein interactions (PPIs) and protein-lipid interactions.[56,57] The most well-studied consequences of internalization are proteolytic degradation of the GPCR in lysosomes, recycling of the GPCR to the plasma membrane and intracellular signaling via arrestin. All of the former lead to a reduced response (desensitization) towards extracellular ligand binding. Over the past decade, a great amount of work has been carried out to unravel signaling activity of GPCRs upon internalization into cellular vesicles, exemplified by recent crystallographic work on the adrenergic receptors.[58,59] In case of the adenosine receptors, various extents of desensitization have been observed between cell- and tissue types.[57,60] However, receptor presence and/or activity via intracellular vesicles is still uncertain. Covalent functionalization of adenosine receptors with fluorescent groups may give answers to these questions, as covalent probes allow fluorescently labelled receptors to be traced in confocal microscopy experiments. Unfortunately agonist-induced internalization cannot be studied by an antagonist AfBP (LUF7960; **chapter 5**), though agonist AfBPs (LUF7909; **chapter 4**) and ligand-directed probes (LUF8019; **chapter 6**) can be suitable tools for this purpose.

Taking the A_1AR as an example, internalization of the receptor has been studied by genetically engineering a yellow fluorescent protein (YFP),[61] or a HiBiT tag onto the receptor,[62] or by using anti-A_1AR antibodies.[63–66] This has yielded valuable insights into receptor half-life time, endocytosis and PPIs of the A_1AR, yet requires the use of engineered receptors or 'large', often poorly selective, antibodies. Functionalization of the A_1AR by a small alkyne group for click chemistry is therefore an interesting opportunity to study internalization of native A_1ARs. Taking the A_3AR as another example, localization and clustering has been detected at the leading edge and on specific microdomains of membranes from activated neutrophils.[67,68] Most interestingly, a covalent ligand-directed probe has recently been used in imaging flow cytometry experiments to measure CB_2R localization on cells.[54] Studying location-dependent signaling of the A_3AR via imaging flow cytometry might therefore be an interesting case study for the use of the herein developed covalent probes.

Lastly, a large number of GPCRs has also been found to signal from the membranes of intracellular organelles, such as the mitochondria, nucleus, endoplasmic reticulum (ER) and Golgi apparatus.[69] This has thus far not been observed for the four ARs. However, covalent probes may contribute to the discovery of novel intracellular signaling 'hotspots' through functionalization of the receptor with fluorescent groups and detection by confocal microscopy. One requirement for such assays would be proper membrane permeability of the probe, which therefore should be investigated *a priori*.

Characterization of post-translational modifications

All GPCRs are predicted to contain one or more PTMs of which the functions range from altering signaling pathways to intracellular trafficking from and to the plasma membrane.[70] Phosphorylation is the most well-studied PTM and, as mentioned above, plays a role in the internalization and desensitization of GPCRs. Phosphorylation of GPCRs takes place on the intracellular domain and is mediated by the protein family of GPCR Kinases (GRKs). More recently, specific phosphorylation patterns ('barcodes') have been found to induce specific downstream signaling pathways that vary from other phosphorylation barcodes.[71,72] Thus, the amount and pattern of phosphorylation are of physiological importance. In case of the ARs, for example the A_1AR, phosphorylation has been studied by using radioactive phosphorous isotopes in SDS-PAGE experiments.[73,74] More recent experiments on other GPCRs avoid the use of radioactive isotopes and have moved to antibodies in SDS-PAGE experiments and purified GPCRs in mass spectrometry experiments.[71,72,75] The herein reported covalent probes may offer a more sophisticated approach to study phosphorylation of ARs. First of all, covalent probes can be used in SDS-PAGE experiments *in tandem* with phospho-specific antibodies to investigate presence of phosphorylated residues. This, however, will not yield information about the phosphorylation barcode itself. Instead, using covalent probes to pull-down the respective AR for phosphoproteomics experiments can yield quantitative information on the exact peptides and/or residues that have been phosphorylated,[76] avoiding the need for extensive purification procedures.

Besides phosphorylation, all GPCRs are predicted to contain one or more glycosylated asparagine residue(s) (*N*-glycosylation) in the extracellular region, necessary for trafficking of the GPCR from the ER and Golgi to the plasma membrane.[70,77] Next to that, *N*-glycosylation might have an effect on ligand binding and (biased) signaling.[70] Glycosylation of serine or threonine residues (*O*-glycosylation) has also been observed for a number of GPCRs. Most interestingly, it has been proposed that *O*-glycosylation, together with tyrosine sulfonylation, may dictate a barcode that regulates signaling of GPCRs, case of study being the Chemokine Receptor 5 (CCR5).[78] Contrary to the chemokine receptors, the ARs contain short intra- and extracellular regions and are therefore not predicted to be *O*-glycosylated. However, as observed in **chapters 4-6**, *N*-glycosylation of ARs is evident and can be studied with the herein

developed covalent probes. Utilization of the covalent probes in SDS-PAGE and pull-down proteomics experiments may yield information on the presence and location of the *N*-glycosylated residues, e.g. by combining with site-directed mutagenesis experiments or sophisticated proteomics analyses. An interesting development is the field of glycoproteomics, in which the glycan chains on specific proteins are analyzed on their sequence and structure by LC-MS/MS techniques.[79] In the future, such experiments might be combined with pull-down steps to enrich probe-bound GPCRs from native samples. However, detection problems that arise from the low expression levels of GPCRs first have to be overcome.

Further than that, other PTMs have been observed on GPCRs, examples being ubiquitination, palmitoylation, SUMOylation, S-nitrosylation and methylation.[70,77] While palmitoylation of ARs has been observed in early studies,[80,81] it is still questionable whether any other PTMs are present on the ARs. Covalent probes may help to elucidate the presence/absence of PTMs in a manner as mentioned before: through labelling in SDS-PAGE experiments, e.g. in combination with antibodies or labels specific towards the target PTM, or through pull-down experiments with subsequent LC-MS/MS analysis.

Lastly, endogenous GPCRs can be prone to proteolytic cleavage. As example, cleavage of the *N*-terminus of the β1-Adrenergic receptor resulted in a population of cleaved and non-cleaved receptors, that both regulated their own signaling pathways *in vivo*.[82] In our studies, we also observed two populations of A_{2A}AR upon labelling in SDS-PAGE experiments (data not included), although this is most likely due to the presence of proteases in the used membrane fractions. Nevertheless, covalent probes may be used to decipher the possible physiological impact of proteolytic cleavage.

Unravelment of protein-protein interactions

The most well-known protein interaction partners of GPCRs are the G protein subunits and arrestin variants. Classically, GPCRs have been found to signal via either G protein or arrestin. However, recent findings hint towards the formation of 'megacomplexes' in endosomal vesicles: signaling units that consists of a GPCR bound to both G protein and arrestin.[83] More interestingly, signaling 'nanodomains' of the glucagon-like peptide 1 receptor (GLP1R), as well as β_2-adrenergic receptor (β_2AR) have been observed on the plasma membranes of model cell lines.[84] Within these so-called receptor-associated independent cAMP nanodomains ('RAINS'), agonist-induced cAMP formation was only observed within a few nanometers of the respective GPCR. Taken together, this indicates the presence of GPCR-signaling compartments in and near the plasma membrane, as well as on intracellular vesicles.[84] In fact, modern electron microscopy experiments reveal cells to be highly packed with vesicles, organelles and proteins.[85,86] It is therefore highly likely that GPCRs, even prior to agonist-binding, reside in close proximity to the proteins that are involved in their signal transduction pathways.

The ARs have been found to interact with multiple types of G proteins,[87] β-arrestins, GRKs and clathrin, among other proteins.[57] Next to that, interactions between ARs and the same (homodimers) or other (heterodimers) GPCRs have been observed,[88] mostly through co-immunoprecipitation or FRET-based assays. Interestingly, the C-terminus tail of the A_{2A}AR is significantly longer than the C-terminus of other ARs and has been found to interact with various proteins such as actinin,[89] calmodulin,[90,91] and Cathepsin D.[92] Multiple factors, e.g. state of the receptor, cell type, point in time, and molecular composition of the 'nanodomain', presumably influence protein binding towards the A_{2A}AR, since it is unlikely that all of the reported proteins simultaneously occupy the receptor.[93] It would therefore be very interesting, also from a physiological perspective, to be able to map all the PPIs of ARs at specific points in space and time. Covalent probes may be the right tool molecules for this purpose.

First, dual labelling of the respective AR and its PPI might be studied in SDS-PAGE experiments, similar to co-immunoprecipitation studies. However, this requires predetermined knowledge about the nature of the PPI, as well as verified probes to label each protein interaction partner. More promising would be the detection of PPIs in a high throughput fashion, e.g. in chemical proteomics experiments. As an example, peroxidase-catalyzed proximity labelling has shown to be a promising strategy for the MS-based detection of GPCR PPIs, likely requiring the use of genetically altered receptors.[94] Interestingly, after a pull-down of the A_1AR (**chapter 4**) we observed a significant enrichment of the G protein beta-1 subunit, a well-known PPI of the A_1AR. Similarly, presumable PPIs of the dopamine D_2 receptor have recently been mapped using a photo-affinity probe.[47] In both cases however, enrichment of the protein interaction partners has been dependent on the reversible nature of the PPI. Such binding is easily disrupted during one of the many denaturing steps in a pull-down assay protocol and therefore not always reliable. More interestingly, pull-down strategies with covalent probes might be combined with cross-linking proteomics experiments.[95] Within these experiments, a cross-linking agent is added to cross-link proteins that are within a determined range of one another. Subsequent pull-down experiments with a covalent probe will then pull-down the respective AR, as well as all of its cross-linked proteins. This in turn leads to the detection of a whole 'interactome' of signaling proteins, dependent on the 'space and time' of the addition of the crosslinking agent. Altogether, this might lead to the detection of physiologically important PPIs involving the ARs.

Final notes

This thesis describes the development, verification and application of various types of covalent probes to target the adenosine receptors. These include a covalent ligand for the A_{2B}AR, affinity-based probes for the A_1AR and A_3AR and a ligand-directed probe for the A_{2B}AR. The applicability of the covalent probes has been investigated in SDS-PAGE, confocal microscopy, flow cytometry and chemical proteomics experiments, using either membrane fractions, model cell lines or native cells. Altogether, we hope that this thesis offers valuable information on the usage and limitations of covalent probes in various types of biochemical assays. Finally, we hope that the herein developed probes lead to new insights regarding adenosine receptor signaling, ultimately leading to more rational targeting of the adenosine receptors within drug discovery programs.

References

[1] A. M. Hayallah, J. Sandoval-Ramírez, U. Reith, U. Schobert, B. Preiss, B. Schumacher, J. W. Daly, C. E. Müller, *J Med Chem* **2002**, *45*, 1500–1510.

[2] U. Rosentreter, R. Henning, M. Bauser, T. Krämer, A. Vaupel, W. Hübsch, K. Dembowsky, O. Salcher-Schraufstätter, J.-P. Stasch, T. Krahn, E. Perzborn, *SUBSTITUTED 2-THIO-3,5-DICYANO-4-ARYL-6-AMINOPYRIDINES AND THE USE THEREOF AS ADENOSINE RECEPTOR LIGANDS*, **2001**, WO 01/25210 A2.

[3] X. Yang, M. A. Dilweg, D. Osemwengie, L. Burggraaff, D. van der Es, L. H. Heitman, A. P. IJzerman, *Biochem Pharmacol* **2020**, *180*, 114144.

[4] X. Yang, J. P. D. van Veldhoven, J. Offringa, B. J. Kuiper, E. B. Lenselink, L. H. Heitman, D. van der Es, A. P. IJzerman, *J Med Chem* **2019**, *62*, 3539–3552.

[5] T. Tamura, T. Ueda, T. Goto, T. Tsukidate, Y. Shapira, Y. Nishikawa, A. Fujisawa, I. Hamachi, *Nat Commun* **2018**, *9*, 1870.

[6] H. Ovaa, P. F. Van Swieten, B. M. Kessler, M. A. Leeuwenburgh, E. Fiebiger, A. M. C. H. Van den Nieuwendijk, P. J. Galardy, G. A. Van der Marel, H. L. Ploegh, H. S. Overkleeft, *Angew Chem Int Ed* **2003**, *42*, 3626–3629.

[7] A. E. Speers, G. C. Adam, B. F. Cravatt, *J Am Chem Soc* **2003**, *125*, 4686–4687.

[8] J. A. Prescher, C. R. Bertozzi, *Nat Chem Biol* **2005**, *1*, 13–21.

[9] V. V. Rostovtsev, L. G. Green, V. V. Fokin, K. B. Sharpless, *Angew Chem Int Ed* **2002**, *41*, 2596–2599.

[10] C. W. Tornøe, C. Christensen, M. Meldal, *Journal of Organic Chemistry* **2002**, *67*, 3057–3064.

[11] N. J. Agard, J. A. Prescher, C. R. Bertozzi, *J Am Chem Soc* **2004**, *126*, 15046–15047.

[12] M. L. Blackman, M. Royzen, J. M. Fox, *J Am Chem Soc* **2008**, *130*, 13518–13519.

[13] N. K. Devaraj, R. Weissleder, S. A. Hilderbrand, *Bioconjug Chem* **2008**, *19*, 2297–2299.

[14] K.-N. Klotz, G. Cristalliq, M. Grifantiniq, S. Vittoriq, M. J. Lohse, *J Biol Chem* **1985**, *260*, 14659–14664.

[15] G. L. Stiles, D. T. Daly, R. A. Olsson, *Journal of Biological Chemistry* **1985**, *260*, 10806–10811.

[16] M. J. Lohse, K.-N. Klotz, U. Schwabe, *Mol Pharmacol* **1986**, *30*, 403–409.

[17] G. L. Stiles, D. T. Daly, R. A. Olsson, *J Neurochem* **1986**, *47*, 1020–1025.

[18] G. L. Stiles, K. A. Jacobson, *Mol Pharmacol* **1987**, *32*, 184–188.

[19] A. Patel, R. H. Craig, S. M. Daluge, J. Linden, *Mol Pharmacol* **1988**, *33*, 585–591.

[20] W. W. Barrington, K. A. Jacobson, G. L. Stiles, *J Biol Chem* **1989**, *264*, 13157–13164.

[21] W. W. Barrington, K. A. Jacobson, A. J. Hutchison, M. Williams, G. L. Stiles, *PNAS* **1989**, *86*, 6572–6576.

[22] C. Nanoff, K. A. Jacobson, G. L. Stiles, *Mol Pharmacol* **1991**, *39*, 130–135.

[23] H. Nakata, *Journal of Biological Chemistry* **1990**, *265*, 671–677.

[24] Z. Gao, A. S. Robeva, J. Linden, *Biochemical Journal* **1999**, *338*, 729–736.

[25] T. M. Palmer, J. L. Benovic, G. L. Stiles, *J Biol Chem* **1995**, *270*, 29607–29613.

[26] T. M. Palmer, G. L. Stiles, *Mol Pharmacol* **2000**, *57*, 539–545.

[27] E. Kozma, P. Suresh Jayasekara, L. Squarcialupi, S. Paoletta, S. Moro, S. Federico, G. Spalluto, K. A. Jacobson, *Bioorg Med Chem Lett* **2013**, *23*, 26–36.

[28] E. Comeo, P. Trinh, A. T. Nguyen, C. J. Nowell, N. D. Kindon, M. Soave, L. A. Stoddart, J. M. White, S. J. Hill, B. Kellam, M. L. Halls, L. T. May, P. J. Scammells, *J Med Chem* **2021**, *64*, 6670–6695.

[29] E. Comeo, N. D. Kindon, M. Soave, L. A. Stoddart, L. E. Kilpatrick, P. J. Scammells, S. J. Hill, B. Kellam, *J Med Chem* **2020**, *63*, 2656–2672.

[30] M. Köse, S. Gollos, T. Karcz, A. Fiene, F. Heisig, A. Behrenswerth, K. Kieć-Kononowicz, V. Namasivayam, C. E. Müller, *J Med Chem* **2018**, *61*, 4301–4316.

[31] E. Barresi, C. Giacomelli, S. Daniele, I. Tonazzini, M. Robello, S. Salerno, I. Piano, B. Cosimelli, G. Greco, F. Da Settimo, C. Martini, M. L. Trincavelli, S. Taliani, *Bioorg Med Chem* **2018**, *26*, 5885–5895.

[32] J. Barbazán, M. Majellaro, A. L. Martínez, J. M. Brea, E. Sotelo, M. Abal, *Biomedicine and Pharmacotherapy* **2022**, *153*, 113408.

[33] K. S. Toti, R. G. Campbell, H. Lee, V. Salmaso, R. R. Suresh, Z. G. Gao, K. A. Jacobson, *Purinergic Signal* **2022**, DOI 10.1007/s11302-022-09873-3.

[34] L. A. Stoddart, N. D. Kindon, O. Otun, C. R. Harwood, F. Patera, D. B. Veprintsev, J. Woolard, S. J. Briddon, H. A. Franks, S. J. Hill, B. Kellam, *Commun Biol* **2020**, *3*, 722.

[35] E. Kozma, T. S. Kumar, S. Federico, K. Phan, R. Balasubramanian, Z. G. Gao, S. Paoletta, S. Moro, G. Spalluto, K. A. Jacobson, *Biochem Pharmacol* **2012**, *83*, 1552–1561.

[36] E. Kozma, E. T. Gizewski, D. K. Tosh, L. Squarcialupi, J. A. Auchampach, K. A. Jacobson, *Biochem Pharmacol* **2013**, *85*, 1171–1181.

[37] R. Corriden, T. Self, K. Akong-Moore, V. Nizet, B. Kellam, S. J. Briddon, S. J. Hill, *EMBO Rep* **2013**, *14*, 726–732.

[38] L. Dahl, I. B. Kotliar, A. Bendes, T. Dodig-Crnković, S. Fromm, A. Elofsson, M. Uhlén, T. P. Sakmar, J. M. Schwenk, *bioRxiv* **2022**, 2022.11.24.517810.

[39] C. J. Hutchings, M. Koglin, W. C. Olson, F. H. Marshall, *Nat Rev Drug Discov* **2017**, *16*, 787–810.

[40] M. Jo, S. T. Jung, *Exp Mol Med* **2016**, *48*, e207.

[41] A. M. Gamo, J. A. González-Vera, A. Rueda-Zubiaurre, D. Alonso, H. Vázquez-Villa, L. Martín-Couce, Ó. Palomares, J. A. López, M. Martín-Fontecha, B. Benhamú, M. L. López-Rodríguez, S. Ortega-Gutiérrez, *Chemistry - A European Journal* **2016**, *22*, 1313–1321.

[42] J. R. Thomas, S. M. Brittain, J. Lipps, L. Llamas, R. K. Jain, M. Schirle, in *Proteomics for Drug Discovery: Methods and Protocols* (Eds.: I.M. Lazar, M. Kontoyianni, A.C. Lazar), Springer New York, New York, NY, **2017**, pp. 1–18.

[43] C. Blex, S. Michaelis, A. K. Schrey, J. Furkert, J. Eichhorst, K. Bartho, F. Gyapon Quast, A. Marais, M. Hakelberg, U. Gruber, S. Niquet, O. Popp, F. Kroll, M. Sefkow, R. Schülein, M. Dreger, H. Köster, *ChemBioChem* **2017**, *18*, 1639–1649.

[44] M. Soethoudt, S. C. Stolze, M. V. Westphal, L. van Stralen, A. Martella, E. J. van Rooden, W. Guba, Z. V. Varga, H. Deng, S. I. van Kasteren, U. Grether, A. P. IJzerman, P. Pacher, E. M. Carreira, H. S. Overkleeft, A. Ioan-Facsinay, L. H. Heitman, M. van der Stelt, *J Am Chem Soc* **2018**, *140*, 6067–6075.

[45] F. M. Müskens, R. J. Ward, D. Herkt, H. van de Langemheen, A. B. Tobin, R. M. J. Liskamp, G. Milligan, *Mol Pharmacol* **2019**, *95*, 196–209.

[46] R. Miyajima, K. Sakai, Y. Otani, T. Wadatsu, Y. Sakata, Y. Nishikawa, M. Tanaka, Y. Yamashita, M. Hayashi, K. Kondo, T. Hayashi, *ACS Chem Biol* **2020**, *15*, 2364–2373.

[47] S. T. Kim, E. J. Doukmak, R. G. Flax, D. J. Gray, V. N. Zirimu, E. De Jong, R. C. Steinhardt, *ACS Chem Neurosci* **2022**, *13*, 3008–3022.

[48] Y. Yun, J. Chen, R. Liu, W. Chen, C. Liu, R. Wang, Z. Hou, Z. Yu, Y. Sun, A. P. IJzerman, L. H. Heitman, X. Yin, D. Guo, *Biochem Pharmacol* **2019**, *164*, 45–52.

[49] B. Allard, D. Allard, L. Buisseret, J. Stagg, *Nat Rev Clin Oncol* **2020**, *17*, 611–629.

[50] K. A. Jacobson, S. Merighi, K. Varani, P. A. Borea, S. Baraldi, M. Aghazadeh Tabrizi, R. Romagnoli, P. G. Baraldi, A. Ciancetta, D. K. Tosh, Z. G. Gao, S. Gessi, *Med Res Rev* **2018**, *38*, 1031–1072.

[51] D. H. Field, J. S. White, S. L. Warriner, M. H. Wright, *RSC Chem Biol* **2023**, 815–829.

[52] S. T. Kim, E. J. Doukmak, R. G. Flax, D. J. Gray, V. N. Zirimu, E. De Jong, R. C. Steinhardt, *ACS Chem Neurosci* **2022**, *13*, 3008–3022.

[53] A. P. Frei, O. Y. Jeon, S. Kilcher, H. Moest, L. M. Henning, C. Jost, A. Plückthun, J. Mercer, R. Aebersold, E. M. Carreira, B. Wollscheid, *Nat Biotechnol* **2012**, *30*, 997–1001.

[54] M. Kosar, D. A. Sykes, A. E. G. Viray,] Rosa, M. Vitale, R. C. Sarott, R. L. Ganzoni, D. Onion, J. M. Tobias, P. Leippe, C. Ullmer, E. A. Zirwes, W. Guba, U. Grether, J. A. Frank, D. B. Veprintsev, E. M. Carreira, *ChemRxiv* **2022**, DOI 10.26434/chemrxiv-2022-z58fd.

[55] S. Arttamangkul, A. Plazek, E. J. Platt, H. Jin, T. F. Murray, W. T. Birdsong, K. C. Rice, D. L. Farrens, J. T. Williams, **2019**, *8*, e49319.

[56] D. Wootten, A. Christopoulos, M. Marti-Solano, M. M. Babu, P. M. Sexton, *Nat Rev Mol Cell Biol* **2018**, *19*, 638–653.

[57] E. C. Klaasse, A. P. IJzerman, W. J. de Grip, M. W. Beukers, *Purinergic Signal* **2008**, *4*, 21–37.

[58] A. H. Nguyen, R. J. Lefkowitz, *FEBS Journal* **2021**, *288*, 2562–2569.

[59] J. Janetzko, R. Kise, B. Barsi-Rhyne, D. H. Siepe, F. M. Heydenreich, K. Kawakami, M. Masureel, S. Maeda, K. C. Garcia, M. von Zastrow, A. Inoue, B. K. Kobilka, *Cell* **2022**, *185*, 4560-4573.e19.

[60] S. Mundell, E. Kelly, *Biochim Biophys Acta Biomembr* **2011**, *1808*, 1319–1328.

[61] E. C. Klaasse, G. van den Hout, S. F. Roerink, W. J. de Grip, A. P. IJzerman, M. W. Beukers, *Eur J Pharmacol* **2005**, *522*, 1–8.

[62] M. Soave, B. Kellam, J. Woolard, S. J. Briddon, S. J. Hill, *SLAS Discovery* **2020**, *25*, 186–194.

[63] F. Ciruela, C. Saura, E. I. Canela, J. Mallol, C. Lluís, R. Franco, *Mol Pharmacol* **1997**, *52*, 788–797.

[64] C. A. Saura, J. Mallol, E. I. Canela, C. Lluis, R. Franco, *J Biol Chem* **1998**, *273*, 17610–17617.

[65] S. Ginés, F. Ciruela, J. Burgueño, V. Casadó, E. I. Canela, J. Mallol, C. Lluís, R. Franco, *Mol Pharmacol* **2001**, *59*, 1314–1323.

[66] M. Escriche, J. Burgueño, F. Ciruela, E. I. Canela, J. Mallol, C. Enrich, C. Lluís, R. Franco, *Exp Cell Res* **2003**, *285*, 72–90.

[67] R. Corriden, T. Self, K. Akong-Moore, V. Nizet, B. Kellam, S. J. Briddon, S. J. Hill, *EMBO Rep* **2013**, *14*, 726–732.

[68] Y. Chen, R. Corriden, Y. Inoue, L. Yip, N. Hashiguchi, A. Zinkernagel, V. Nizet, P. A. Insel, W. G. Junger, *Science (1979)* **2006**, *314*, 1792–1795.

[69] M. Ali, M. Nezhady, J. C. Rivera, S. Chemtob, *iScience* **2020**, *23*, 101643.

[70] A. Patwardhan, N. Cheng, J. Trejo, *Pharmacol Rev* **2021**, *73*, 120–151.

[71] K. N. Nobles, K. Xiao, S. Ahn, A. K. Shukla, C. M. Lam, S. Rajagopal, R. T. Strachan, T.-Y. Huang, E. A. Bressler, M. R. Hara, S. K. Shenoy, S. P. Gygi, R. J. Lefkowitz, *Cell Biology* **2011**, *4*, ra51.

[72] A. J. Butcher, R. Prihandoko, K. C. Kong, P. McWilliams, J. M. Edwards, A. Bottrill, S. Mistry, A. B. Tobin, *Journal of Biological Chemistry* **2011**, *286*, 11506–11518.

[73] V. Ramkumar, M. E. Olah, K. A. Jacobson, G. L. Stiles, M. P. Author, *Mol Pharmacol* **1991**, *40*, 639–647.

[74] Z. Nie, Y. Mei, V. Ramkumar, *Mol Pharmacol* **1997**, *52*, 456–464.

[75] M. Trester-Zedlitz, A. Burlingame, B. Kobilka, M. von Zastrow, *Biochemistry* **2005**, *44*, 6133–6143.

[76] J. v. Olsen, M. Mann, *Molecular and Cellular Proteomics* **2013**, *12*, 3444–3452.

[77] C. K. Goth, U. E. Petäjä-Repo, M. M. Rosenkilde, *ACS Pharmacol Transl Sci* **2020**, *3*, 237–245.

[78] L. Verhallen, J. J. Lackman, R. Wendt, M. Gustavsson, Z. Yang, Y. Narimatsu, D. M. Sørensen, K. Mac Lafferty, M. Gouwy, P. E. Marques, G. M. Hjortø, M. M. Rosenkilde, P. Proost, C. K. Goth, *Cellular and Molecular Life Sciences* **2023**, *80*, 55.

[79] B. Zhang, S. Li, W. Shui, *Front Chem* **2022**, *10*, 843502.

[80] Z. Gao, Y. Ni, G. Szabo, J. Linden, *Biochem. J* **1999**, *342*, 387–395.

[81] G. Ferguson, K. R. Watterson, T. M. Palmer, *Biochemistry* **2002**, *41*, 14748–14761.

[82] A. E. Hakalahti, M. M. Vierimaa, M. K. Lilja, E. P. Kumpula, J. T. Tuusa, U. E. Petäjä-Repo, *Journal of Biological Chemistry* **2010**, *285*, 28850–28861.

[83] A. R. B. Thomsen, B. Plouffe, T. J. Cahill, A. K. Shukla, J. T. Tarrasch, A. M. Dosey, A. W. Kahsai, R. T. Strachan, B. Pani, J. P. Mahoney, L. Huang, B. Breton, F. M. Heydenreich, R. K. Sunahara, G. Skiniotis, M. Bouvier, R. J. Lefkowitz, *Cell* **2016**, *166*, 907–919.

[84] S. E. Anton, C. Kayser, I. Maiellaro, K. Nemec, J. Möller, A. Koschinski, M. Zaccolo, P. Annibale, M. Falcke, M. J. Lohse, A. Bock, *Cell* **2022**, *185*, 1130-1142.e11.

[85] L. Heinrich, D. Bennett, D. Ackerman, W. Park, J. Bogovic, N. Eckstein, A. Petruncio, J. Clements, S. Pang, C. S. Xu, J. Funke, W. Korff, H. F. Hess, J. Lippincott-Schwartz, S. Saalfeld, A. v. Weigel, R. Ali, R. Arruda, R. Bahtra, D. Nguyen, *Nature* **2021**, *599*, 141–146.

[86] C. S. Xu, S. Pang, G. Shtengel, A. Müller, A. T. Ritter, H. K. Hoffman, S. ya Takemura, Z. Lu, H. A. Pasolli, N. Iyer, J. Chung, D. Bennett, A. v. Weigel, M. Freeman, S. B. van Engelenburg, T. C. Walther, R. v. Farese, J. Lippincott-Schwartz, I. Mellman, M. Solimena, H. F. Hess, *Nature* **2021**, *599*, 147–151.

[87] A. Inoue, F. Raimondi, F. M. N. Kadji, G. Singh, T. Kishi, A. Uwamizu, Y. Ono, Y. Shinjo, S. Ishida, N. Arang, K. Kawakami, J. S. Gutkind, J. Aoki, R. B. Russell, *Cell* **2019**, *177*, 1933-1947.e25.

[88] B. B. Fredholm, A. P. IJzerman, K. A. Jacobson, J. Linden, C. E. Müller, *Pharmacol Rev* **2011**, *63*, 1–34.

[89] J. Burgueño, D. J. Blake, M. A. Benson, C. L. Tinsley, C. T. Esapa, E. I. Canela, P. Penela, J. Mallol, F. Mayor, C. Lluis, R. Franco, F. Ciruela, *Journal of Biological Chemistry* **2003**, *278*, 37545–37552.

[90] G. Navarro, M. S. Aymerich, D. Marcellino, A. Cortés, V. Casadó, J. Mallol, E. I. Canela, L. Agnati, A. S. Woods, K. Fuxe, C. Lluís, J. L. Lanciego, S. Ferré, R. Franco, *Journal of Biological Chemistry* **2009**, *284*, 28058–28068.

[91] H. Piirainen, M. Hellman, H. Tossavainen, P. Permi, P. Kursula, V. P. Jaakola, *Biophys J* **2015**, *108*, 903–917.

[92] A. Skopál, T. Kéki, P. Tóth, B. Csóka, B. Koscsó, Z. H. Németh, L. Antonioli, A. Ivessa, F. Ciruela, L. Virág, G. Haskó, E. Kókai, *Journal of Biological Chemistry* **2022**, *298*, 101888.

[93] I. Gsandtner, M. Freissmuth, *Mol Pharmacol* **2006**, *70*, 447–449.

[94] J. Paek, M. Kalocsay, D. P. Staus, L. Wingler, R. Pascolutti, J. A. Paulo, S. P. Gygi, A. C. Kruse, *Cell* **2017**, *169*, 338-349.e11.

[95] O. Klykov, B. Steigenberger, S. Pektaş, D. Fasci, A. J. R. Heck, R. A. Scheltema, *Nat Protoc* **2018**, *13*, 2964–2990.

Summary

The human body consists of a tremendous number of cells, classified into a wide variety of subtypes. Each individual cell is protected by a membrane bilayer that separates the intracellular compartments from the extracellular environment. Despite this 'barrier', cells must be able to respond towards external stimuli, such as small molecular drugs that float in the bloodstream. There are multiple mechanistic pathways that allow an intracellular response towards extracellular stimuli. One of the most important mechanistic pathways is the activation of G Protein-Coupled Receptors (GPCRs). GPCRs are receptor proteins that reside in the cellular membrane and consist of both an extracellular- and intracellular component. Upon binding towards an extracellular stimulus, e.g. a protein, peptide, small molecule or light, GPCRs will transduce a signal into the cell, 'telling' the cell how to respond to the specific stimulus. Malfunctioning GPCR signaling pathways can lead to severe states of disease. It is therefore no surprise that GPCRs have been of high interest in drug discovery programs of pharmaceutical companies, leading to some 25% of the currently marketed drugs.

A subfamily of GPCRs that has sparked the interest of drug discoverers is the set of Adenosine Receptors (ARs). This subfamily consists of four subtypes of adenosine receptors: the A_1, A_{2A}, A_{2B} and A_3 adenosine receptors (A_1AR, A_{2A}AR, A_{2B}AR and A_3AR, respectively). Activation of the ARs through their natural ligand adenosine induces a wide variety of effects, strongly dependent on cell- and tissue type, but is often immunosuppressive. Caffeine is a famous drug that acts through the ARs, although via inhibition rather than activation. A more elaborated overview of the four ARs and their role in human physiology and pathology is presented in **Chapter 1**. In summary, the four ARs are involved in a plethora of cellular signaling pathways in both physiological and pathological conditions and therefore interesting targets from a drug discovery perspective.

Studying the ARs, however, bears many challenges. As mentioned in **Chapter 1**, there are multiple factors, inherent to GPCRs, that hinder biochemical detection of the ARs. These factors include poor solubility, low expression levels and complex cellular signaling pathways. To overcome, as well as to study the complexities mentioned above, we have put our attention to the development of chemical probes that bind irreversibly (covalently) to either one of the ARs. Covalent probes induce persistent binding to the receptor of interest, requiring the implementation of a reactive group ('warhead') for irreversible binding. Functionalization of covalent probes with reporter groups, e.g. a fluorophore, biotin or click moiety, allows detection of the ARs in a broad range of biochemical assays. Throughout the chapters of this thesis, we have transformed known AR ligands into functionalized and/or covalent probes, for their utilization in biochemical assays.

In **Chapter 2** an overview is given of all the recently reported functionalized covalent probes that target GPCRs. These include affinity-based probes (AfBPs), ligand-directed probes, glycan-targeting probes and metabolically incorporated probes. The warheads of these probes are compared, and their use in biochemical assays is evaluated. In this thesis, we have focused on the development of covalent probes, AfBPs and ligand-directed probes.

Chapter 3 shows the development of a covalent ligand for the A_{2B}AR. In this chapter, different types of warheads were chemically introduced onto a known scaffold for the A_{2B}AR, leading to a set of 12 potential covalent probes. Pharmacological investigation of time-dependent affinity and subtype selectivity showed strong differences between the various substitutions. One of the synthesized compounds, LUF7982, was found to be superior in terms of affinity and selectivity and was therefore further investigated for its possible binding mode towards the receptor.

While covalent ligands are interesting tools to study irreversible blockade of GPCRs, such probes do not allow direct detection of probe-bound receptors in biochemical assays. Therefore, in **Chapters 4** and **5**, we have put our efforts into the development of AfBPs for the A_1AR and A_3AR, respectively. In both chapters, a small set of clickable AfBPs was synthesized based on covalent ligands that had previously been developed in our lab. The potential AfBPs were pharmacologically evaluated on time-dependent affinity, AR selectivity and a covalent mode of binding. The best candidates were evaluated on their ability to fluorescently label the receptor in SDS-PAGE and confocal microscopy experiments. This yielded LUF7909 as AfBP for the A_1AR and LUF7960 as AfBP for the A_3AR.

The possibilities of using LUF7909 and LUF7960 as tools to detect the A_1AR and A_3AR were further explored at the end of the corresponding chapters. We managed to utilize LUF7909 as a tool to 'pull-down' the A_1AR from a complex mixture of proteins, as well as to detect possible protein off-targets using mass spectrometry. Unfortunately, we did not manage to detect the A_3AR in a similar attempt with LUF7960. Presumably the relatively low expression level and hydrophobicity of the A_3AR hinder detection in the current assay setup. Nevertheless, LUF7960 was shown to be a useful tool for the detection of the A_3AR in flow cytometry experiments. Altogether, this led to the detection of the A_1AR on rat adipocytes and the detection of the A_3AR on human granulocytes.

A drawback of AfBPs might be the irreversible occupancy of the receptor binding pocket. Therefore, in **Chapter 6**, we aimed to develop a ligand-direct probe for the A_{2B}AR. Such probes do not irreversibly block the receptor binding pocket and therefore can be used as tool to label to receptor prior to agonist-dependent activation. Two ligand-directed probes were synthesized based on covalent ligand LUF7982. These compounds showed to bind the A_{2B}AR with high affinity in pharmacological assays, but not in a time-dependent fashion, indicating a reversible mode of action. Preliminary SDS-PAGE experiments in A_{2B}AR-overexpressing cells showed labeling of the A_{2B}AR by one of these probes, LUF8019. However, other possible usages of LUF8019 in different biochemical assays and/or cell lines have yet to be explored.

In **Chapter 7**, a critical view is taken at the aspects that are of importance to covalent chemical probes: selectivity, reactivity and detectability. Also the usage of covalently functionalized probes in SDS-PAGE, fluorescent microscopy, flow cytometry and chemical proteomics is discussed, and conclusions are drawn based on the experiments reported in this thesis. Lastly, future prospects are given on possible usages of the herein synthesized probes in future biochemical assays.

Nederlandse Samenvatting

Het menselijk lichaam bestaat uit een enorme hoeveelheid cellen, geclassificeerd in een grote verscheidenheid aan subtypes. Iedere individuele cel is aan de buitenkant beschermd door een membraan dat het binnenste van de cel scheidt van de buitenkant. Ondanks deze beschermende laag moet een cel nog steeds kunnen reageren op hetgeen zich er buiten de cel afspeelt, zoals medicijnen die door de bloedbaan migreren. Hiervoor heeft een cel verschillende mechanismes, maar een van de belangrijkste is de activatie van G eiwit-gekoppelde receptoren (GPCRs). GPCRs zijn receptoreiwitten die zich bevinden in het celmembraan en bestaan uit een intracellulair en extracellulair gedeelte. Wanneer een extracellulaire stimulus, bijvoorbeeld een eiwit, peptide, klein molecuul of licht, bindt aan de GPCR, zendt de GPCR een signaal naar de cel om door te geven hoe de cel hierop moet reageren. Een slecht functionerende GPCR kan leiden tot ernstige ziektebeelden. GPCRs zijn daarom al jaren interessante doeleiwitten voor de ontwikkeling van nieuwe medicijnen. Dit heeft ertoe geleid dat grofweg 25% van de huidige medicijnen een interactie aangaat met een GPCR.

Een subfamilie van GPCRs die de interesse van medicijnontwikkelaars heeft gewekt is die van de Adenosine Receptoren (ARs). Er zijn vier verschillende ARs: de A_1, A_{2A}, A_{2B} en A_3 adenosine receptoren (A_1AR, A_{2A}AR, A_{2B}AR en A_3AR, respectievelijk). Activatie van deze receptoren door het natuurlijke ligand adenosine veroorzaakt een grote verscheidenheid aan effecten, dat sterk afhankelijk is van het cel- en weefseltype, maar veelal een dempende werking heeft op het immuunsysteem. Cafeïne is waarschijnlijk het beroemdste molecuul dat bindt aan de ARs, al zorgt cafeïne voor blokkade van de receptoren in plaats van activatie. Een uitgebreid overzicht van de vier ARs en hun rol in het menselijk lichaam staat in **Hoofdstuk 1**. Samengevat zijn de vier ARs betrokken bij een groot aantal fysiologische omstandigheden en pathologische aandoeningen en hierdoor interessante doeleiwitten voor medicijnonderzoek.

Het bestuderen van de ARs kent echter vele uitdagingen. Zoals uitgelicht in **Hoofdstuk 1** zijn er meerdere factoren, inherent aan GPCRs, die de biochemische detectie van ARs bemoeilijken. Deze factoren zijn o.a. een slechte oplosbaarheid, lage expressielevels en complexe signaalpaden. Om deze problemen niet alleen op te lossen, maar ook dieper te bestuderen, hebben wij onze aandacht gericht op het ontwikkelen van chemische probes die irreversibel (covalent) aan de ARs binden. Een voordeel van covalente probes is de constante binding aan de receptor, maar daarentegen vereisen ze implementatie van een zeer reactieve groep (genaamd ‘warhead’) om de covalente binding mogelijk te maken. Het toevoegen van een extra chemische groep aan zulke covalente probes, bijvoorbeeld een fluorofoor, biotine, of een ‘klik’ groep, maakt detectie van de receptor mogelijk in biochemische analyses. In de verschillende hoofdstukken van dit proefschrift hebben we bekende AR liganden getransformeerd in covalente en/of gefunctionaliseerde probes, om het gebruik hiervan in biochemische analyses mogelijk te maken.

Hoofdstuk 2 geeft een overzicht van de meest recentelijk ontwikkelde gefunctionaliseerde covalente probes. Dit betreft ‘affiniteit-gedreven probes’ (AfBPs), ligand-gestuurde probes, glycaan-gerichte probes en metabolisch geïncorporeerde probes. De verschillende ‘warheads’ van deze probes zijn in dit hoofdstuk vergeleken, alsmede het gebruik in biochemische analyses. Wij hebben ons in dit proefschrift gericht op de ontwikkeling van covalente liganden, AfBPs en ligand-gestuurde probes.

Hoofdstuk 3 beschrijft de ontwikkeling van een covalent ligand voor de A_{2B}AR. Als onderdeel van dit hoofdstuk werden verschillende 'warheads' gesubstitueerd op bekende liganden voor de A_{2B}AR, wat resulteerde in een set van 12 potentiële covalente probes. Farmacologisch onderzoek naar tijdsafhankelijke affiniteit, alsmede selectiviteit, liet sterke verschillen zien tussen de verschillende probes. Een van de gesynthetiseerde stoffen, LUF7982, was superieur wat affiniteit en selectiviteit betreft en werd daardoor verder bestudeerd op mogelijke bindingswijze aan de receptor.

Covalente probes zijn interessante hulpmiddelen om de onomkeerbare blokkade van GPCRs te bestuderen, maar kunnen niet gebruikt worden voor de directe detectie van GPCRs zelf. In **hoofdstukken 4** en **5** hebben we daarom AfBPs ontwikkeld voor respectievelijk de A_1AR en A_3AR. Als onderdeel van beide hoofdstukken werd een kleine set aan 'klikbare' AfBPs gesynthetiseerd, gebaseerd op covalente probes die in het verleden zijn gemaakt in ons lab. Deze potentiële AfBPs werden farmacologisch getest op tijdsafhankelijke affiniteit, AR selectiviteit en mogelijk covalente binding. De beste probes werden vervolgens gebruikt in SDS-PAGE en confocale microscopie experimenten om labeling van de betreffende AR te bestuderen. Dit heeft uiteindelijk twee AfBPs opgeleverd die selectief de A_1AR en A_3AR kunnen labelen: LUF7909 voor de A_1AR en LUF7960 voor de A_3AR.

De verschillende mogelijkheden om LUF7909 en LUF7960 als hulpmiddel te gebruiken voor de detectie van de A_1AR en A_3AR zijn verder onderzocht aan het einde van de corresponderende hoofdstukken. Hierbij zijn we erin geslaagd om LUF7909 te gebruiken om de A_1AR uit een complex eiwitmengsel te isoleren en met massaspectrometrie te detecteren. Dit lukte helaas niet met de A_3AR, gebruikmakende van LUF7960 in een vergelijkbare poging. Waarschijnlijk hinderen de relatief lage expressie en hydrofobiciteit van de A_3AR dit type biochemische analyse. Desondanks is het gelukt om LUF7960 te gebruiken voor de detectie van de A_3AR in flow cytometrie experimenten. Al met al hebben bovenstaande experimenten geleidt tot detectie van de A_1AR op vetcellen van de rat en detectie van de A_3AR op humane granulocyten.

Een potentieel nadeel van het gebruik van AfBPs is de onomkeerbare bezetting van de receptor. In **Hoofdstuk 6** hebben we ons daarom gericht op de ontwikkeling van een 'ligand-gestuurde' probe voor de A_{2B}AR. Een dergelijke probe zorg niet voor onomkeerbare bezetting van de ligand-bindingsplaats van de receptor en kan daarom gebruikt worden om de receptor te labelen vóór activatie. Twee ligand-gestuurde probes werden daarom gesynthetiseerd, gebaseerd op het eerder beschreven covalente ligand LUF7982. Beide stoffen lieten een hoge affiniteit zien ten opzichte van de A_{2B}AR in farmacologische studies. Deze affiniteit was niet tijdsafhankelijk, duidend op een niet-covalent bindingsmechanisme. SDS-PAGE experimenten lieten zien dat één van deze probes de A_{2B}AR kan labelen in cellen met A_{2B}AR-overexpressie. Toekomstig onderzoek moet uitwijzen of dit ook mogelijk is in andere typen experimenten en/of cellijnen.

Hoofdstuk 7 werpt een kritische blik op een aantal aspecten die van belang zijn voor covalente chemische probes, namelijk selectiviteit, reactiviteit en detecteerbaarheid. Daarnaast wordt het gebruik van gefunctionaliseerde probes in SDS-PAGE, fluorescentie microscopie, flow cytometrie en massa spectrometrie experimenten besproken, waarbij conclusies worden getrokken op basis van de in dit proefschrift gedane bevindingen. Tot slot wordt een blik geworpen op toekomstige toepassingen van de gesynthetiseerde probes.

List of Publications

Part of this thesis

B. L. H. Beerkens, X. Wang, M. Avgeropoulou, L. N. Adistia, J. P. D. van Veldhoven, W. Jespers, R. Liu, L. H. Heitman, A. P. IJzerman, D. van der Es. Development of subtype-selective covalent ligands for the adenosine A_{2B} receptor by tuning the reactive group, *RSC Medicinal Chemistry* **2022**, *13*, 850–856.

B. L. H. Beerkens, Ç. Koç, R. Liu, B. I. Florea, S. E. Le Dévédec, L. H. Heitman, A. P. IJzerman and D. van der Es, A Chemical Biological Approach to Study G Protein-Coupled Receptors: Labeling the Adenosine A1 Receptor Using an Electrophilic Covalent Probe, *ACS Chemical Biology* **2022**, *17*, 3131–3139.

B. L. H. Beerkens, I. M. Snijders, J. Snoeck, R. Liu, A. T. J. Tool, S. E. Le Dévédec, W. Jespers, T. W. Kuijpers, G. J. P. van Westen, L. H. Heitman, A. P. IJzerman and D. van der Es, Development of an Affinity-Based Probe to Profile Endogenous Human Adenosine A3 Receptor Expression, *Journal of Medicinal Chemistry* **2023**, *16*, 11399-11413.

Other publications

L.S. den Hollander[§], S. Dekkers[§], **B.L.H. Beerkens**, J.P.D. van Veldhoven, N.V.O. Ortiz-Zacharías, C. van der Horst, I. Sieders, B. de Valk, J. Wang, A.P. IJzerman, D. van der Es, L.H. Heitman. Labeling of endogenously expressed CC chemokine receptor 2 with a versatile intracellular allosteric probe. (manuscript submitted)

K. Bach[§], **B.L.H. Beerkens**[§], P.R.A. Zanon[§], S.M. Hacker. Light-Activatable, 2,5-Disubstituted Tetrazoles for the Proteome-wide Profiling of Aspartates and Glutamates in Living Bacteria, ACS Central Science **2020**, 6, 4, 546–554.

[§]These authors contributed equally

Poster and oral communications

Event	**Location**
LACDR Spring Symposium **2019** (poster)	Leiden, The Netherlands
Figon **2019** (poster)	Leiden, The Netherlands
CHAINS **2019** (poster)	Veldhoven, The Netherlands
LACDR Spring Symposium **2020** (poster)	Online
LACDR Spring Symposium **2021** (poster)	Online
CHAINS **2021** (oral)	Online
LACDR Spring Symposium **2022** (oral)	Leiden, The Netherlands
ULLA Summer School **2022** "*Challenges and opportunities in drug development*" (poster)	Upsala, Sweden
EFMC International Symposium on Medicinal Chemistry **2022** (poster)	Nice, France
EFMC Young Medicinal Chemists Symposium **2022** (oral)	Nice, France
LACDR Spring Symposium **2023** (poster)	Leiden, The Netherlands

Curriculum Vitae

Bert was born in Venray on the 12th of August of 1993, the Netherlands. He graduated from the Bouwens van der Boijecollege in Panningen in 2012. Having a broad interest in chemistry, Bert started the BSc study Molecular Science & Technology at Leiden University and the Technical University of Delft. As part of his studies, Bert also attended a semester at the University of Southern Denmark (SDU) in Odense. From these experiences, Bert gained interest in the use of chemistry to perturbate biological systems. In 2015 he graduated from the BSc Molecular Science and Technology and in the successive year became a fulltime board member of the Chemisch Dispuut Leiden (CDL), the study association for chemistry students. In the meantime Bert started his MSc studies in Chemistry at Leiden University with a specialization in chemical biology. As part of his studies, Bert performed an internship in the group of prof. Mario van der Stelt, where he worked on the synthesis and evaluation of chemical probes for phosphatases. Bert also performed a research internship together with dr. Stephan Hacker at the Technical University of Munich, where he developed photo-activatable probes to site-specifically label bacterial proteins. The latter resulted in a publication in ACS Central Science. Bert obtained his MSc Chemistry degree at the end of 2018 and immediately continued with his PhD studies at the Leiden Academic Centre for Drug Research (LACDR).

Within his PhD studies, Bert continued to develop chemical probes for biologically relevant proteins, now for the four adenosine receptors. This research was carried out under the supervision of prof. Ad IJzerman and dr. Daan van der Es at the division of Drug Discovery and Safety. Altogether, his efforts resulted in the development of a covalent ligand for the adenosine A_{2B} receptor, affinity-based probes for the adenosine A_1 and A_3 receptors and a ligand-directed probe for the adenosine A_{2B} receptor, as described in the individual chapters of this dissertation, as well as published in RSC Medicinal Chemistry, ACS Chemical Biology and Journal of Medicinal Chemistry. Within the various projects, Bert learned how to perform and interpret a broad range of assay types, ranging from chemistry, to biochemistry, to pharmacology and computational experiments. Parts of these chapters have also been presented at (inter)national congresses, such as CHAINS (2019 and 2021), FIGON (2019), the ULLA summer school (2022) and the EFMC International Symposium on Medicinal Chemistry (ISMC) and Young Medicinal Chemists' Symposium (YMCS) (2022).

Bert is currently a post-doctoral researcher at the Division of Drug Discovery and Safety of the LACDR, working together with prof. Laura Heitman and dr. Daan van der Es on the molecular characterization of GPCRs in cancer. This research is being carried out as part of the ONCODE institute.

Acknowledgements

The realization of this PhD thesis could have never been possible without the help and support of many others. For this, I would like to thank some people.

First of all, I would like to thank my promotors, Ad en Daan, for their guidance and endless support. I want to thank both of you for the freedom I got in performing the experiments, letting me be stubborn in the lab from time to time, but also knowing when to either push or unleash the brakes.

Secondly, many thanks to all the MSc students who have joined me on this journey: Çağla, Inge, Maria, Joep, Lisa, Lotte and Vasiliki. Your contributions have been of great importance for the realization of this thesis.

I would like to thank all co-authors that contributed to the various chapters of this thesis. Especially Rongfang: I have always joked that this is also your thesis. Thank you for testing all compounds in radioligand binding assays! Thank you also Xuesong for the nice (ongoing) collaborations on the A_{2B} receptor.

During my PhD, I got acquainted with a broad range of assay types. I would like to thank every person that helped me understand and carry out these assays. Thank you, Bobby, for your help in setting up pull-down experiments, Olivier and Willem for helping with docking experiments, Thomas and Sylvia for your help with microscopy experiments, and Anton and Wieke for helping me understand flow cytometry!

Most crucial to my PhD were the social interactions with my colleagues, from coffee breaks to Science Club Thursdays. I would like to thank Sebastian and Jaco, but also Majlen and Khaled: from the beginning of my PhD studies the chemistry lab felt like home. I am also grateful for the colleagues in my office: Natalia, Chenlin and especially Lisa, for always providing a listening ear. Further thanks to all colleagues from the MolPharm lab: Laura, Huub, Jara, Cas, Tamara and Yao; the Pomplun lab and of course the CDD group. You've all contributed greatly to the nice atmosphere in and outside of the GE4 wing!

I would also like to thank my friends, especially the contacts I had during the COVID lockdowns. These moments were of great value to me and helped me through my PhD studies. Next to that, many thanks to my family members, who have always been a great support.

Finally I would like to thank Sitie, for being there.